Electronic and Transport Properties of Low Dimensional Systems

A thesis submitted in partial fulfilment of the award of the Degree of Doctor of Philosophy in the subject of Physics

by

Debika Debnath

Registration number: 17PHPH01

Supervised by: Prof. Ashok Chatterjee





To
School of Physics
University of Hyderabad
Central University, Gachibowli
Hyderabad-500046
Talangana
India
January 2023

"Fall in love with some activity, and do it! Nobody ever figures out what life is all about, and it doesn't matter. Explore the world. Hearly everything is really interesting if you go into it deeply enough. Work as hard and as much as you want to on the things you like to do the best. Don't think about what you want to be, but what you want to do. Keep up some kind of a minimum with other things so that society doesn't stop you from doing anything at all."

...Richard Feynman







Declaration

I, Debika Debnath hereby declare that the work presented in the thesis is done by me, in the School of Physics, University of Hyderabad, under the supervision of my thesis supervisor Prof. Ashok Chatterjee. This work is authentic and is not previously submitted in part or in full to any university or institute for any degree. The scientific information used during the work has been acknowledged in the text and the list of references is attached at the end of each chapter.

A report on plagiarism from the University Librarian is enclosed herewith.

Place: Hyderabad (Debika Debnath)

Date: 31.01.2023 Registration number: 17PHPH01

Delika Delonath.





Certificate

This is to certify that the thesis entitled "Electronic and Transport Properties of Low Dimensional Systems", submitted by Debika Debnath at School of Physics, University of Hyderabad, in the partial fulfilment for the degree in Doctor of Philosophy in Physics, is legit and the work is done under my supervision and is free of plagiarism.

The work presented in the thesis is genuine and has not been submitted anywhere previously for any degree.

The thesis includes the following articles:

- 1. A semi exact solution for a metallic phase in a Holstein-Hubbard chain at half filling with Gaussian anharmonic phonons, **D Debnath**, MZ Malik, A Chatterjee, Scientific Reports **11** (1), 1-14 (2021).
- 2. A semi-exact study of self-trapping transition in a one-dimensional Holstein-Hubbard model, **D Debnath**, K Bhattacharyya, A Chatterjee, Physica B **646**, 414357 (2022).
- 3. A semi-exact analytical study of the phase diagram of a two dimensional Extended Holstein-Hubbard model, **D Debnath**, K Bhattacharyya, A Chatterjee (communicated).
- 4. Self-trapping transition in a two-dimensional Extended Holstein-Hubbard model: A Mean-field approach, **D Debnath**, A Chatterjee (to be communicated).
- 5. Quantum Transport in a bi-molecular transistor through the Anderson-Holstein-Caldeira-Leggett model, **D** Debnath, K Bhattacharyya, A Chatterjee (to be communicated).

The students is a co-author of the following articles which are not part of this thesis:

- Role of Rashba spin-orbit interaction on polaron Zeeman effect in a twodimensional quantum dot with parabolic confinement, K Bhattacharyya, D Debnath, A Chatterjee, Journal of Magnetism and Magnetic Materials, 166745 (2020).
- 2. Spin filtering by Rashba coupling in a correlated polar dissipative molecular transistor at finite temperature in a magnetic field, K Bhattacharyya, **D Debnath**, A Chatterjee (Under review).

The student has also published the following peer-reviewed articles as the conference proceedings:

- 1. Effect of the hole concentration on the polaronic mobility for the strongly interacting electrons, **D** Debnath, A Chatterjee, IOP Conference Series: Materials Science and Engineering 1221 (1), 012006 (2022).
- 2. Effect of electronic concentration on the self-trapping transition of polaron for the weakly correlated system in the adiabatic limit, **D** Debnath, A Chatterjee, Materials Today: Proceedings, **55** (1), 4-6 (2022).
- 3. Mott-Insulator to Peierls Insulator Transition In The Two-Dimensional Holstein-Hubbard Model, **D Debnath**, A Chatterjee, Materials Today: Proceedings, **66**, 3370-3372 (2022).

The student has attended the international and national conferences and presented her work in the form of oral and poster presentations.

The student has also completed her PhD course-work towards the requirement of the doctoral degree.

She has also worked as a teaching assistant at the School of Physics, University of Hyderabad during her PhD tenure.

Dated: 31.01.2023

Dean

School of Physics University of Hyderabad Hyderabad, 500046

DEAN

School of Physics
University of Hyderabad
HYDERABAD - 500 646.

Prof. Ashok Chatterjee

Supervisor

Prof. ASL OK CHATTERJEE SCHOOL OF PHYSICS UNIVERSITY OF HYDERABAD HYDERABAD - 500 046, INDIA



School of Physics University of Hyderabad

PO: Central University Campus Gachibowli, Hyderabad-500 046, India Phones: (office) 040-23134300/4400 (Direct) 040-23012455

Email: deansp@uohyd.ac.in



Prof. K.C. James Raju Professor & Dean

COURSE WORK CERTIFICATE

This is to certify that Ms. Debika Debnath bearing the enrollment No. 17PHPH01 has carried out the Ph.D. (Physics) research under the supervision of Prof. Ashok Chatterjee, in the School of Physics, University of Hyderabad, Hyderabad.

She passed the following courses which are a pre-requisite for registration to Ph.D. Programme as per UGC norms.

So. No.	Course No.	Title of the Course	Credits
1.	PY801	Research Methodology	4
2.	PY802	Advanced Quantum Mechanics	4
3.	PY803	Advanced Experimental Techniques	4
4	PY804	Advanced Condensed Matter Physics	4

Dated: 11/1/2023

School of Physics

DEAN School of Physics University of Hyderabad HYDERABAD - 500 046



University of Hyderabad

(A Central University under an Act of Parliament)

Prof. K. C. James Raju Dean, School of Physics P. O. Central University, Hyderabad-500 046.

TEACHING ASSISTANTSHIP CERTIFICATE

This is to certify that Ms. Debika Debnath, bearing the enrollment No. 17PHPH01 is pursuing research in the Ph.D. Physics Programme under the supervision of Prof. Ashok Chatterjee in the School of Physics, University of Hyderabad, India.

Ms.Debika Debnath joined the Ph.D. Physics Programme during the academic year 2017-18. She has undertaken the teaching assistantship as per the details given below:

Course No.	Title of the Course	Name of the faculty	Period
PY577	Quantum Theory of Solids	Prof. Ashok Chatterjee	Jan-April 2018
PY804	Advanced Condensed Matter	Prof. Ashok Chatterjee	July - Nov 2018
PY561	Advanced Quantum Mechanics	Prof. Ashok Chatterjee	Jan - April 2019
PY405	Quantum Mechanics	Prof. Anantha Laxmi	Jul - Nov 2019
PY452	Electromagnetic Theory -II	Prof. Ashok Chatterjee	Jan - April 2020
PY802	Advanced Quantum Mechanics	Prof. Ashok Chatterjee	Oct- Feb2021
IPYT351	Statistical Thermodynamics	Prof. Ashok Chatterjee	Feb - July 21
PY802	Advanced Quantum Mechanics	Prof. Ashok Chatterjee	Aug -Feb2022
IPH601	Statistical Thermodynamics	Prof. Ashok Chatterjee	Feb - June 2022

Dated: 14/04/2022

(K. C. James Raju) Professor and Dean DE 1 N

18/4/22

School of Physics University of Lyderabad HYDERABAD - 500 646

List of Papers based on which the thesis has been written

- 1. A semi exact solution for a metallic phase in a Holstein-Hubbard chain at half filling with Gaussian anharmonic phonons, **D Debnath**, MZ Malik, A Chatterjee, Scientific Reports **11** (1), 1-14 (2021).
- 2. A semi-exact study of self-trapping transition in a one-dimensional Holstein-Hubbard model, **D Debnath**, K Bhattacharyya, A Chatterjee, Physica B **646**, 414357 (2022).
- 3. A semi-exact analytical study of the phase diagram of a two dimensional Extended Holstein-Hubbard model, **D Debnath**, K Bhattacharyya, A Chatterjee (communicated).
- 4. Self-trapping transition in a two-dimensional Extended Holstein-Hubbard model: A Mean-field approach, **D Debnath**, A Chatterjee (to be communicated).
- 5. Quantum Transport in a bi-molecular transistor through the Anderson-Holstein-Caldeira-Leggett model, **D** Debnath, K Bhattacharyya, A Chatterjee (to be communicated).

Other publications that are not included in the thesis:

- 6. Role of Rashba spin-orbit interaction on polaron Zeeman effect in a two-dimensional quantum dot with parabolic confinement, K Bhattacharyya, **D Debnath**, A Chatterjee, Journal of Magnetism and Magnetic Materials, **166745** (2020).
- 7. Spin filtering by Rashba coupling in a correlated polar dissipative molecular transistor at finite temperature in a magnetic field, K Bhattacharyya, **D Debnath**, A Chatterjee (Under review).

List of paper published as Conference Proceedings

- 1. Effect of the hole concentration on the polaronic mobility for the strongly interacting electrons, **D** Debnath, A Chatterjee, IOP Conference Series: Materials Science and Engineering 1221 (1), 012006 (2022).
- 2. Effect of electronic concentration on the self-trapping transition of polaron for the weakly correlated system in the adiabatic limit, **D Debnath**, A Chatterjee, Materials Today: Proceedings, **55** (1), 4-6 (2022).
- 3. Mott-Insulator To Peierls Insulator Transition In The Two-Dimensional Holstein-Hubbard Model, **D Debnath**, A Chatterjee, Materials Today: Proceedings, **66** 3370-3372 (2022).

List of Conference and Workshop Attended

2022: QMAT, National Conference on Quantum Condensed Matter, organised at IIT Kanpur. Topic: "Non-equilibrium Transport In a Bi-molecular Transistor: Effect of External Magnetic Field And Temperature" (Poster presentation).

2022: ICFAST, International Conference on Frontier Area of Science and Technology at University of Hyderabad. Topic: "Non-equilibrium Transport In a Bi-molecular Transistor: Effect of External Magnetic Field And Temperature" (Poster presentation).

2021: ICPN, Second International E-Conference on Physics of Materials and Nanotechnology, organised by Mangalore University. Topic: "Effect of the hole concentration on the polaronic mobility for the strongly interacting electrons" (Oral presentation) (online).

2021: CMPA, 9th National Conference on Condensed Matter Physics and Applications, at Manipal Institute of Technology, India. Topic: "Effect of electronic concentration on the self-trapping transition of polaron for the weakly correlated system in the adiabatic limit" (Oral presentation) (online).

2021: QMAT, National Conference on Quantum Condensed Matter, organised at TIFR, Mumbai. Topic: "A semi-exact solution of a metallic phase in the 2D Extended Holstein-Hubbard Model" (Oral presentation, online) (online).

2021: DAE SSPS, 65th DAE Solid State Physics Symposium, organised at BARC, Mumbai. Topic: "Effect of Electron-Hole Concentration on the Self-Trapping Transition of Polaron in the Presence of Strong Coulomb Correlation" (Oral presentation) (online).

2021: CMDAYS, 29th National Conference on Condensed Matter Physics, organised at Central University of Jharkhand. Topic: "A Semi-exact study of the phase diagram of the two-dimensional extended Holstein-Hubbard Model" (Oral presentation) (online).

2020: **Q-MAT**, 3rd Annual Conference on Quantum Condensed Matter, organised at S. N. Bose National Centre for Basic Sciences on "**Metallicity at the Cross-over Region of the Spin Density Wave and the Charge Density Wave in one-dimension**" (Oral presentation) (online).

2018: Attended Summer School on "Collective Behaviour in Quantum Matter", at ICTP, Trieste, Italy.

List of Best Poster/ Oral presentation awards

2022: "Strongly Correlated Matter from Quantum Criticality to Flat Bands", organized at ICTP, Trieste, Italy. Topic: "Non-equilibrium Transport In a Bi-molecular Transistor: Effect of External Magnetic Field and Temperature" (Received Best Poster Presentation Award) (in presence).

2021: ICPS, Virtual International Conference on Physical Sciences, at SVNIT, Surat, India, on "Transition from Large Polaron to Small Polaron at Anti-adiabatic limit" (Received Best Oral Presentation Award) (online presentation).

2020: SPECTRUM, 3rd International Students Conference on Current Advancement in Science and Technology, at IEM Kolkata, on "Metallicity at the Cross-over Region of the SDW & CDW in one-dimensional Holstein-Hubbard model with Gaussian Phonon Anharmonicy" (Received 'Certificate of Best Presentation In the Field of Physics' & 'Certificate of Best Presentation among all stream') (online presentation).

Acknowledgements

The University of Hyderabad has been an incredible experience in my life starting from the very first day of August 3rd, 2017. The campus and the people around me have braced me with knowledge and experience and there are few persons who have been a part of my five and half years' long journey through all sorts of emotions. In this section, I would like to mention and acknowledge them for their support and presence in my life.

To start with, I want to express my sincere gratitude to my supervisor Prof. Ashok Chatterjee. He is the person whom I can mention as the 'friend, philosopher and guide' in my life. As a PhD student of Sir, I get the opportunity to learn the core of the subject exquisitely. I have been fortunate to attend so many of his classes as the teaching assistant. These classes have helped me a lot towards the growth of my knowledge in Physics. I am so much thankful for the freedom he has provided me during the PhD tenure that is quite rare in this field. Here I would like to emphasize the generosity he belongs. He has always extended his support during all my problems (health issues, financial issues, home issues) that I have gone through during these times. His perspective towards life and sense of ethics has always motivated me to be a better version of myself. I shall forever remain grateful to him for considering all my flaws and still giving me so much love and affection. I consider him a father figure in my life and I wish to have his blessing forever.

I am also very much thankful to Dr. Soma Mukhopadhyay Ma'am for all the love and the homely feelings during the visits to their home.

I am sincerely grateful to my doctoral committee members (DRC) Prof. S. Srinath and Prof. Nageswara Rao, for their guidance and comments during the doctoral review meetings. I am glad to express my gratitude to the former deans of the School of Physics, Prof. Bindu Bambah (whom I admire a lot for her grace, style, sense of humour and courage towards life), Prof. V. Seshu Bai, Prof. Ashok Chatterjee, and the present Dean Prof. K. C. James Raju. I am much obliged to the School of Physics (SOP), University of Hyderabad, for providing all the basic amenities during the course.

I acknowledge DST-INSPIRE, India for providing me with the fellowship during my PhD tenure.

I am sincerely thankful to Prof. Ashoka VS for his help in checking the similarity index (plagiarism report) of all my draft papers and thesis before final submission.

I also want to express my gratitude to the former dean Prof. Ashok Chatterjee Sir for the financial help through the departmental fund for my covid treatment. On the same note, I am grateful to Prof. B. V. R Tata and Prof. Sarath Ananthamurthy for their kindness and help during that tough period of covid. I am also thankful to the Deans of Students Welfare (DSW) and Mr. Satish from DSW for providing the university guesthouse to stay in, when I tested covid positive and the health centre of HCU for the medical assistance with ambulance service. When everyone outside was suffering to get an ambulance, I was fortunate to avail that only for being a HCU student.

While working as a teaching assistant of Prof. Ananthalaxmi Ma'am, I started chatting with her. It is her generosity as she has sent me her best wishes during covid and also for my first publication, which made me glad. I am enormously grateful to my Sir for providing me the recommendations to attend the conferences and workshops. Especially, I would like to mention my last visit to ICTP, Italy in 2022. Though it was at the very end of my PhD work, Sir allowed me to attend the conference which turned out to be so much helpful for me to regain my motivation and persistence towards the journey of PhD. I am indebted to ICTP for accepting my application and to the directorate of IOE of HCU for providing me the funds for the travelling expenditure.

I have always received great support from all the non-teaching staff of our school and also from a few administration staff of HCU. I am really thankful to Deepika Ma'am, Vijaylaxmi Ma'am, Shailaja Ma'am, Shashikala Ma'am, Sudarshan Sir, Narshimha Sir and Mr. Mahesh from SOP who have helped me at different times on several administrative works. I would like to express my gratitude to Mr. Sainath Sir and Madhvi Ma'am who have helped me during the fellowship processing times, especially when I was at home during the covid period. My hostel days have been easy as Prasanti Ma'am and Sumalata Ma'am have always extended their help whenever I have asked for it.

I shall be forever indebted to Dr. Bibhas Bhattacharyya and Dr. Molly De Raychaudhury for introducing me to the subject of Condensed Matter Physics. Their teaching has been the only reason for me to join PhD in this field. So this thesis is indeed the result of the inspiration brought by these two incredible teachers during my M.Sc. I feel blessed that I have made the decision to join the Physics department of WBSU to pursue my M.Sc. Here I also want to

mention the impact of Dr. Arunabha Adhikari, Dr. Sunandan Ganguly, Dr. Subhajit Sarkar, Dr. Joydip Mitra and Dr. Anirban Saha. Their teachings were truly my backbone to the knowledge in Physics that helped me during the PhD entrance tests and interviews. Hence I feel I would not be able to join as a research fellow without the teaching and inspiration of these excellent teachers.

Among the teachers of my initial days in college, I would like to mention Dr. Ajay Kumar Maiti (beloved AKM Sir) who has always treated us with love and motivated to do well in life. Because of him only I learned to love the experiments in Physics. The first teacher who inspired me the most in studying Physics was my home tutor Monoranjan Sir who taught me during my 10th class to 12th class and inspired me with several stories from his own Calcutta University days. As a school student, those stories have left a huge impact on my life to choose Physics as my major subject in college. Apart from Physics, I could not complete my thesis without acknowledging one of my most favourite teachers, Krishnendu Sir who has always been there during all my good and tough times. He is the only person who still never misses to call me, once a week, though I always miss to call him from my end. His support in my life and family is incorrigible.

I am also thankful to our group seniors Uma di, Luh Luh di, Zahid vaiya, Manasa di, Hemant vaiya, Pooja di and Kuntal for the warm welcome to the group and their help during different times. We have so many memories of sharing dinners to celebrate teacher's days and Sir's and Ma'am's birthdays, with so much fun. Sometimes the presence of Abhinava has made the get-together excitement at its bests.

I shall forever remain grateful to all who had called and asked me about my health when I stayed in quarantine at the HCU guest house after tested covid positive. Here I would like to express my heartfelt thanks to Sarthak, Nikhil, Avishek Nandan and all the SFI-HCU team for providing us food and water. Without you all, we do not know what would have happened to us! Any 'thank you' is less for all your support and help during that time.

The journey of a PhD student is never smooth, especially at this particular age of life where we have to deal with several issues starting from anxiety, depression, worries about life and future, job, relationship, parent's health, self-health and whatnot! And this sailing towards the doctoral degree needs friends to cope with all the stresses. I was in luck to have a bunch of such good friends during the initial two years of my PhD life. The celebration of birthday parties, cake cutting, JRF treats, jungle picnic and having weekend fun were the best days in

HCU. Our "The Elite group" gang members, Nurul, Sovan, Sushmita, Avishek, Soumen, Suman we had enjoyed a lot during our initial days in HCU. Gradually all became absorbed in their own work and I missed the time that we all had spent together. My cooking skills have given me entrance to the group "Mrittur sathe lorai". I have spent several Saturday weekends cooking delicious foods with Arijit da, Apurba da, Bappa da, Kuntal, and Sudipto da. Staying with them has given me popularity in campus and I made lots of junior and senior friends through them. Though I was very late to make friendship with the amazing "Diva's group" of LH-3, I enjoyed best spending time with Tasnim di, Moumita di, Sneha di, Sabari di, Olivia and Sarada. We had spent some wonderful days during that short tenure. I shall cherish all these moments forever. The celebration of Saraswati pujo, Mahalaya, Diwali are the hearts of "HCU Bong Connection". The festival of "Saraswati puja" in HCU carries a big emotion to all our Bengali community where 'Poojo' is secondary and the main aims are having lots of fun, food, gossip, photo session, games, cultural evening and making new friends ever year. I relish the moments I have spent with all of my seniors, juniors and friends- Soutrick, Shubham, Sumanta, Shampita, Somdatta, Avijit, Arunava, Mainak, Suman, Alam, Anirban da, Avishek da, Saddam da, Olivia di, Subho da, Mou di and all the juniors and seniors with whom I have shared joy and laughter. I would also like to thank my batchmates Aishwarya, Najir, Samir, Rudra, Mitesh and seniors Siva vaiya and Suchismita di for their helps in due times.

The person who deserves all the appreciation for teaching scooty to a person like me, who can't even ride a bicycle, is Sugata da. It was a dream of mine to drive a vehicle someday, which has been physically possible only because of the effort made by him. Learning scooty has made my life so easy in such a huge campus and I shall be endlessly grateful to him for this life lesson.

Last but not least, I can never express my love and indulgence towards this "campus". This campus and its people and life here have played an inevitable part in my mental and philosophical growth. I have started to love trees, insects and animals after spending so much time here. HCU has made me politically sound and emotionally strong. The large community from different states and their cultures and rituals have enriched me a lot. It makes me sad that very soon this ladies hostel-3 is going to be my past address and this is the beauty of life to move on!

There are always a few people whose contribution to life is beyond acknowledgement. But still, I want to mention them as it makes me happy. When I am in Hyderabad, I know, one person in my extended family who will always be there in the need of my mother is "*Rita Kamma*". After ma, she was my first tutor since my nursery days. Another person is my maternal uncle, "*Chotomama*" who has helped me in several steps of my life.

Finally, I would like to express my love and sincere gratitude to my mother whose tremendous dedication, sacrifice and the spirit of fight have led me to what and where I am today. Her love and diligence have always pushed me forward. Whenever I am in trouble physically or emotionally, she is my only strength to overcome the problem. I want to dedicate my thesis to ma for all the fights she has done to protect me and providing me with the best education as far as she could. I wish I could show this thesis to "baba" (father) who would have been the happiest person in the earth to see me getting the doctoral degree. I know he is always sending me his blessings from the heaven, somewhere out there.

At the end of this section, I want to acknowledge each and every person who has made me feel better with their smile, love and kindness.

Debika Debnath

Abbreviations used in the thesis

AHCLH Anderson-Holstein-Caldeira-Leggett Hamiltonian

AFM Anti-ferromagnetic

AFMI Anti-ferromagnetic Mott-insulator

BCH Baker-Campbell-Hausdorff

BMT Bi-molecular transistor

BA Bethe ansatz

CDW Charge density wave

e-e Electron-electron

e-p Electron-phonon

EE Entanglement entropy

GS Ground state

HF Hartree Fock

HH Holstein-Hubbard

HHM Holstein-Hubbard model

HI Hopping integral

KMC Krishna, Mukhopadhyay and Chatterjee

LFT Lang-Firsov transformation

LW Lieb-Wu

MPS Many-phonon state

MF Mean-field

MP Metallic phase

MI Mott-insulator

MIT Mott-insulator transition

MHMP Mott-Hubbard metallicity parameter

NN Nearest neighbour

NNN Next nearest neighbour

QD Quantum dot

ST Self-trapping

SMT Single molecular transistor

SF Spectral function

SDW Spin density wave

TBM Tight binding model

Contents of the thesis

Declaration	1
Certificate	ii
Course-work Certificate	v
Teaching Assistance Certificate	vi
List of papers	vii
List of Conference Proceedings	viii
List of Conference and Workshop Attended	ix
Acknowledgement	xi
Abbreviations used in the Thesis	xvi
Preface	xxi
Introduction	
1.1 Motivation towards the thesis	1
1.2 Tight binding Model	2
1.3 Hubbard Model	5
1.4 Polaron	7
1.4.1 Holstein Model	
1.5 Holstein-Hubbard Model	9
i. Spin-Density-Wave	
ii. Charge-Density-Wave	
1.6 Phase transition in Holstein-Hubbard Model	11
1.6.1 Transition from Spin density wave to Charge density wa	ave
1.6.2 Self-trapping transition of polaron	
1.7 Quantum transport through bi-molecular transistor	14
1.7.1 Single molecular transistor	
1.7.2 Anderson-Holstein-Caldeira-Leggett Model	
1.8 Organisation of the thesis	17
1.9 References.	
	Course-work Certificate Teaching Assistance Certificate List of papers List of Conference Proceedings List of Conference and Workshop Attended Acknowledgement Abbreviations used in the Thesis Preface Introduction 1.1 Motivation towards the thesis. 1.2 Tight binding Model. 1.3 Hubbard Model. 1.4 Polaron 1.4.1 Holstein Model 1.5 Holstein-Hubbard Model. i. Spin-Density-Wave ii. Charge-Density-Wave 1.6 Phase transition in Holstein-Hubbard Model. 1.6.1 Transition from Spin density wave to Charge density wath 1.6.2 Self-trapping transition of polaron 1.7 Quantum transport through bi-molecular transistor. 1.7.1 Single molecular transistor 1.7.2 Anderson-Holstein-Caldeira-Leggett Model

2 A semi exact solution for a metallic phase in a Holstein-Hubbard chain at half filling with Gaussian anharmonic phonons

	2.1 Introduction	22
	2.2 Model and formulation	24
	2.3 Numerical results and Discussion	32
	2.4 Conclusion.	40
	2.5 References.	
3		ed Holstein-
	Hubbard model: The Mean-field approach	
	3.1 Introduction	43
	3.2 Model and formulation	45
	3.2.1 Weak Coulomb correlation	54
	3.2.1.1 Hartree-Fock Approximation	
	3.2.2 Strong Coulomb correlation	56
	3.2.2.1 $t - J$ model	
	3.2.2.2 Gutzwiller Approximation	
	3.2.2.3 Zuberev's Green's function technique	
	3.3 Numerical results and discussions	66
	3.4 Conclusion	74
	3.5 References	75
4	A semi-exact study of self-trapping transition in a one- Holstein-Hubbard model	dimensional
	4.1 Introduction.	78
	4.2Model and formulation	79
	4.3 Numerical results and discussions	
	4.4 Conclusion	89
	4.5 References.	90
5	A semi-exact study of self-trapping transition in a two- Holstein-Hubbard model	dimensional
	5.1 Introduction.	92
	5.2 Model and formulation.	

5.3 Numerical results and discussions	
5.4 Conclusion	108
5.5 References	109
6 Quantum Transport in a bi-molecular tra Anderson- Holstein-Caldeira-Leggett model	nsistor through the
6.1 Introduction	112
6.2 Model and formulation	114
6.2 Model and formulation6.3 Numerical results and discussions	
	128

Preface

This thesis contains two parts. In Part I, we study the phase transitions in the Holstein-Hubbard model and in Part II, we study the quantum transport in a bi-molecular transistor.

We begin **Chapter 1** of the thesis by giving a brief motivation behind our work. We then present an introduction to the tight binding model, the concept of Coulomb correlation and the Hubbard model, the concept of polaron and the Holstein model. We next introduce the Holstein-Hubbard model and the phase transitions that can occur in this model. In this context, we discuss the spin and charge density wave states and the phenomenon of self-trapping transition. Next we introduce the Anderson-Holstein model and the Caldeira-Legette model and the Anderson-Holsrtein-Caldeira-Leggett model and their application to molecular transistors.

Interplay of electron-electron (e-e) and electron-phonon (e-p) interactions in a condensed matter system can lead to interesting ground states. The Holstein-Hubbard (HH) model is one of the most suitable models to study this interplay in a correlated polar material. Depending on the relative strengths of the e-e and e-p interactions, the system can be in a spin-densitywave (SDW) ground state (GS) or in a charge-density-wave (CDW) GS. Variation of the e-e interaction and e-p interaction in the system can change the GS of the system from one insulating state to another insulating state. Though these phases have been quite well known, the nature of the transition has not been very clear. The nature of the SDW-CDW transition has been first studied by Hirsch and Fradkin by a Monte-Carlo calculation and they have shown that the SDW-CDW transition is direct. Takada and Chatterjee (TC) have studied the one-dimensional half-filled HH model analytically to examine more critically the nature of the SDW-CDW transition and have shown for the first time that there exists an intermediate metallic phase between these two insulating phases. This study has thrown a new challenge and received attention from other researchers who also contributed on this problem. Because of these contrary results, it is really very important to study the nature of SDW-CDW phase transition in HH model by more improved analytical calculations. Chatterjee and collaborators have shown, in this context that modifications of the phonon wave function lead to broadening of the width of the intermediate metallic phase. This lends credence to the conjecture of TC regarding the existence of the intervening metallic phase at the cross-over region of the SDW and CDW phases. Considering the anharmonic vibrations of the apex oxygen atoms in the cuprate superconductors, CT [18] have studied the SDW-CDW transition in a 1D HH model taking cubic and quartic phonon anharmonicities. Lavanya et al. have extended this work by considering Gaussian anharmonicity and performed an improved variational calculation. They have supported the existence of the intermediate metallic phase at the cross-over region of the SDW-CDW phases. The metallic phase obtained from their results is also wider than the TC one.

In **Chapter 2** of the thesis, we consider the same HH model in the presence of Gaussian phonon anharmonicity, as studied by Lavanya et al. We study the nature of the SDW-CDW transition within the framework of the above model using a more improved analytical calculation. Following a series of canonical transformations followed by a generalized many-phonon state, we obtain an effective electronic Hamiltonian which we solve exactly using Bethe ansatz to obtain the ground state energy of the system. This calculation can be considered as semi-exact. The transition from the SDW state to CDW state is examined by calculating the effective Hubbard hopping parameter t_{eff} and effective Coulomb correlation strength U_{eff} . The phase diagram of the e-p coupling constant α vs. U shows an intervening region in between the SDW and CDW phases. The nature of the intermediate region is studied by calculating the Mott-Hubbard metallicity criteria, double-occupancy parameter, entanglement entropy and the local spin moment. Our study ensures the metallicity of the intermediate region.

In **Chapter 3**, we study the SDW-CDW phase transition for a two-dimensional (2D) system given by the extended 2D HH Hamiltonian. This work is more realistic in view of the 2D nature of the cuprate superconductors. However, the HH model is not exactly soluble in 2D. So, we solve the extended HH model in two different regions separately, namely in the weak-correlation regime and the strong-correlation regime using two different analytical methods. After eliminating the phonons, the electronic Hamiltonian is solved in weak correlation regime using the mean-field Hartree-Fock (HF) method. In the strong Coulomb correlation regime, the electronic Hamiltonian is first transformed to an effective t-J model and solved by using the Zubarev Green function technique and HF approximation (which becomes valid because of the restriction on the double occupancy). Our result shows that even in 2D there exist an intermediate metallic phase which is wider than that of the 1D case.

The nature of the intermediate region is further studied by calculating the Mott-Hubbard metallicity criteria. Our analytical result matches well with the recent numerical calculations of Wang et al.

In a polar material, an electron forms a polaron because of the e-p interaction that distorts the lattice. If the e-p coupling is weak, the resulting polaron is a large mobile polaron, whereas in the case of strong e-p coupling, the polaron is confined within single lattice spacing and we have what is called a small polaron which is a localized quasi particle. Thus, as the e-p interaction is increased, at a critical value of the e-p coupling constant, one can have a large polaron to small polaron transition. This is known as the self-trapping (ST) transition, as the polarization potential that traps the polaron is created by the electron itself. In the last few decades, extensive investigations have been carried out to study the nature of the ST transition. But, a clear consequence to the nature of this ST transition is still lacking.

In **Chapter 4**, we study the nature of the ST transition in 1D extended HH model. We study this Hamiltonian using a very accurate analytical method. Performing a series of canonical transformations followed by a many-phonon averaging, we obtain an effective electronic Hamiltonian. The effective electronic Hamiltonian is then solved exactly using the Bethe ansatz technique and the ST transition from a large polaron state to the small polaron state is studied.

In **Chapter 5**, we examine the nature of ST transition in 2D extended HH model. In 2D, as the HH model is not exactly soluble, after eliminating the phonons, we deal with the effective electronic Hamiltonian for the weak correlation regime and the strong correlation regime separately by two different analytical methods. The methods employed here to solve the Hamiltonian is similar to the method used in Chapter 3. Our results show that though in 1D HH model, the ST transition is always continuous, in 2D HH model, the ST transition is continuous in the anti-adiabatic regime while it is discontinuous in the adiabatic limit.

Transistors are one of the integral part of modern technology for the fabrication of nanodevices. Of late, single molecular transistors (SMT) have attracted considerable attention for their practical application in transport devices. In 2000, the fabrication of C_{60} molecular transport was first reported by Park et al. with the help of gold electrodes connected with the C_{60} molecules. An SMT device can be used as a switching device as well as a sensor. Dutta has studied electronic transport in mesoscopic systems and subsequently he extended this study to molecular transistors. Lately, extensive studies have been carried out on the double-QD-based molecular transistors as they show many interesting properties like large charge sensibility and more controllable current.

In Chapter 6, we study the transport properties of a bi-molecular transistor where two QDs mounted on an insulating substrate are placed between two metallic electrodes one of which acts as a source (S) and the other as a drain (D). The electrons can be made to flow from the source to the drain through the QDs by applying an external bias-voltage and the energy levels in the QDs can be tuned with a gate voltage applied to the substrate. The QDs are considered to have only single energy levels and onsite e-e and e-p interactions. The e-p interaction is described by the Holstein interaction. The electrons in the source and the drain are considered free and thus they have continuous energy levels. Electrons from the source can tunnel into the QD and from QD to the drain and vice versa. This process is modelled by the Anderson hybridization term. The QD phonon interacts with the phonons of the substrate by a linear coupling which we model by the Caldeira-Leggett (CL) Hamiltonian. This interaction gives rise to dissipation in the phonon dynamics of the QD phonon and increases the tunnelling current. The entire bi-molecular transistor system is thus modelled by the Anderson-Holstein- Caldeira-Leggett (AHCL) Hamiltonian. We first eliminate the interaction between the QD phonon and the substrate phonon (approximately) and then the e-p interaction by the Lang-Firsov transformation. Next we calculate the spectral function, tunnelling current, differential conductance and spin-polarization parameters at different magnetic fields and different temperatures using the non-equilibrium Green function technique of Keldysh.

In **Chapter 7**, we summarize our findings and present our concluding remarks.

1

Introduction

1.1 Motivation

The present thesis contains two parts. In the first part, our aim is to examine the nature of some interesting phase transitions that can occur in correlated polar materials and in the second part we wish to study the quantum transport in a bi-molecular transistor.

Phase transitions in correlated polar materials have continued to remain an interesting subject of research for the last few decades. It is well known that if the electron-electron (e-e) Coulomb repulsive interaction much greater than the electron-phonon (e-p) coupling in a correlated polar system, the ground state (GS) of the system would be a spin-density-wave (SDW) GS. The system behaves as an insulator in this state and is known as a Mott insulator. However, if the e-p coupling is much stronger than the Coulomb correlation, the system is known to be in a charge-density-wave (CDW) GS. This is also an insulating state and we can call it a Peierls insulator. Thus as the e-e interaction increases, a correlated polar material can make an SDW-CDW transition. It is well accepted that there exists such a transition; however, consensus regarding the detailed behaviour of the transition is lacking. The key question that requires an answer is whether the transition from SDW state to CDW state is direct or goes through an intermediate metallic phase. This issue is of profound importance in the context of superconductivity. To attain high T_c superconductivity through e-p interaction, a material has to have large e-p coupling. But, as we have mentioned above, if the system has a strong the e-p coupling, then it would settle into a CDW state which is obviously not a suitable GS state if we are interested in superconductivity. if the SDW to

CDW transition occurs through a conducting metallic phase, then that metallic phase can become superconductive even at large enough e-p interaction strength. In this thesis, we wish to investigate the possibility of such a metallic phase.

Another objective of this thesis is to examine, in detail, the behaviour of self-trapping transition in a polar material. In such a material, e-p interaction distorts the lattice and creates a polarization potential and forms a polaron. For weak e-p coupling, the polarization potential is shallow and the resulting polaron is mobile and is called a large polaron. For strong e-p coupling, the polarization potential is deep and the electron gets trapped in this potential. Such a localized polaron is called a small polaron. Thus, with the increase in the e-p coupling, one expects a large to small polaron transition. Such a transition is called self-trapping (ST) transition, as the potential that traps the electron is created by the electron itself.

Finally, we wish to study the quantum transport in a bi-molecular transistor. It is known that a single molecular transistor can act as a spin filter. Our objective in this thesis is to examine whether the spin-filtering effect can be enhanced in a dissipative bi-molecular transistor with Coulomb correlation and polaronic interaction.

To study correlated materials, the suitable model is the tight-binding model. To study the polaronic coupling, the suitable model is the Holstein model and for the Coulomb correlation, we consider the Hubbard model. To consider tunnelling in the bi-molecular transistor, we shall use the celebrated Anderson model and the dissipation will be taken care of by the Caldeira–Leggett model. In the following section, we shall introduce all these models and discuss the necessary concepts.

1.2 Tight Binding Model (TBM)

The free electron theory proposed by Sommerfeld [1] has been a useful tool to describe the metallic behaviour of elements up to a specific limit. But it fails to explain several other features of the materials. As an improvement on the free electron model, Bloch [21] introduced the linear combination of atomic orbitals (LCAO) method in which the atomic orbitals associated with each lattice site overlap and then it is possible to write the Block function as a linear superposition the atomic states ϕ_n as

$$\psi_{n,k}(\mathbf{r}) = \frac{1}{\sqrt{N}} \sum_{\mathbf{R}_j} e^{i\mathbf{k}\cdot\mathbf{R}_j} \,\phi_n(\mathbf{r} - \mathbf{R}_j),\tag{1.1}$$

where N denotes the number of lattice sites which is a very large number and R_j is the position vector of the atom at the j-th site. The Hamiltonian for a system of electrons interacting with a periodic lattice can be written as

$$H = \frac{\mathbf{p}^2}{2m} + \sum_{\mathbf{R}_i} V_a(\mathbf{r} - \mathbf{R}_j). \tag{1.2}$$

The energy E of the Hamiltonian in Eq. (1.2) can be found using the LCAO state of Eq. (1.1). We obtain

$$E = E_0 + \frac{1}{N} \sum_{\mathbf{R}_i, \mathbf{R}_j} \int d^3 r \, e^{i\mathbf{k} \cdot (\mathbf{R}_i - \mathbf{R}_j)} \phi_n^* (\mathbf{r} - \mathbf{R}_j) V_a(\mathbf{r} - \mathbf{R}_j) \phi_n(\mathbf{r} - \mathbf{R}_i)$$

$$= E_0 + E_{i,j=0} + E_{ij}, \tag{1.3}$$

where $E_0 = \hbar^2 k^2/2m$ is the free-electron kinetic energy, $E_{i,j=0}$ is the on-site potential energy and E_{ij} is the potential energy due to the NN interaction that is given by

$$E_{ij} = -t \sum_{\mathbf{R}_i, \mathbf{R}_i} e^{i\mathbf{k} \cdot (\mathbf{R}_i - \mathbf{R}_j)}, \tag{1.4}$$

where

$$t = \int d^3r \, \phi_n^*(\boldsymbol{r} - \boldsymbol{R_j}) V_a(\boldsymbol{r} - \boldsymbol{R_j}) \phi_n(\boldsymbol{r} - \boldsymbol{R_i}). \tag{1.5}$$

where *i*, *j* refer to the NN sites. The integral in Eq. (1.5) is called the overlap integral that represents the inter-site atomic interaction. Depending upon the interaction involved in the generic Hamiltonian, the overlap integral can be extended to next NN and next to next NN as well.

The lattice Hamiltonian in the tight-binding approximation is easier to deal with when it is written in the second quantized notation. The tight-binding Hamiltonian can be written in second quantization notation as

$$H = -\sum_{\langle ij \rangle} t_{ij} c_{i\sigma}^{\dagger} c_{j\sigma}. \tag{1.6}$$

Here i,j refer to NN sites, <> implies that the sum extends over the NN sites. t_{ij} carries the information of the electron hopping from one site to another, $c_{i\sigma}^{\dagger}$ is the creation operator for a spin- σ electron at site i and $c_{i\sigma}$ is the corresponding annihilation operator. Using the discrete lattice model of tight-binding approximation, the band structures of different materials have been studied. Also, the tight-binding (TB) model (TBM) has been useful to calculate the effective mass m^* of an electron interacting with a lattice. Diagrammatically we can represent different atomic sites with the corresponding wave function in the presence of the lattice potential V_a as the following:

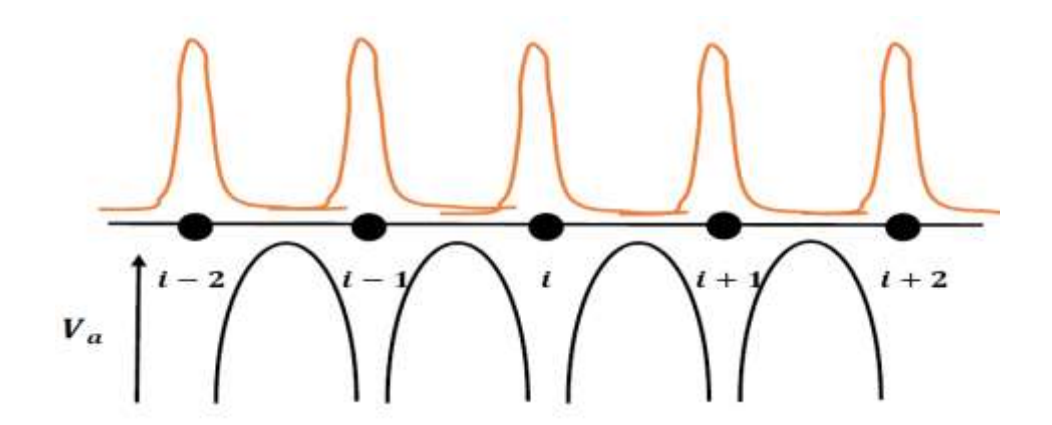


Fig. 1.1: Lattice potential and electronic wave function in tight binding model

The hopping of an electron from one atomic site to another is possible due to the overlap of the electronic wavefunction and this overlap integral can be calculated using the Bloch wavefunction or Wannier wave function. The tight binding formulation is considered under the independent electron approximation and it describes the creation of narrow-band materials. Therefore the theory predicts the d and f-orbital band structure in a more correct way than the s and p-orbital elements.

The conductivity measured in certain materials could be well-established with the help of the TB model [4]. When the atoms are in a closed packed structure with a small lattice constant, the overlap between the atomic orbitals is higher which leads to high conductivity. But as the lattice spacing increases in a lattice, the overlap between the atomic orbitals decreases and as a result, the bandwidth reduces and eventually the conductivity diminishes.

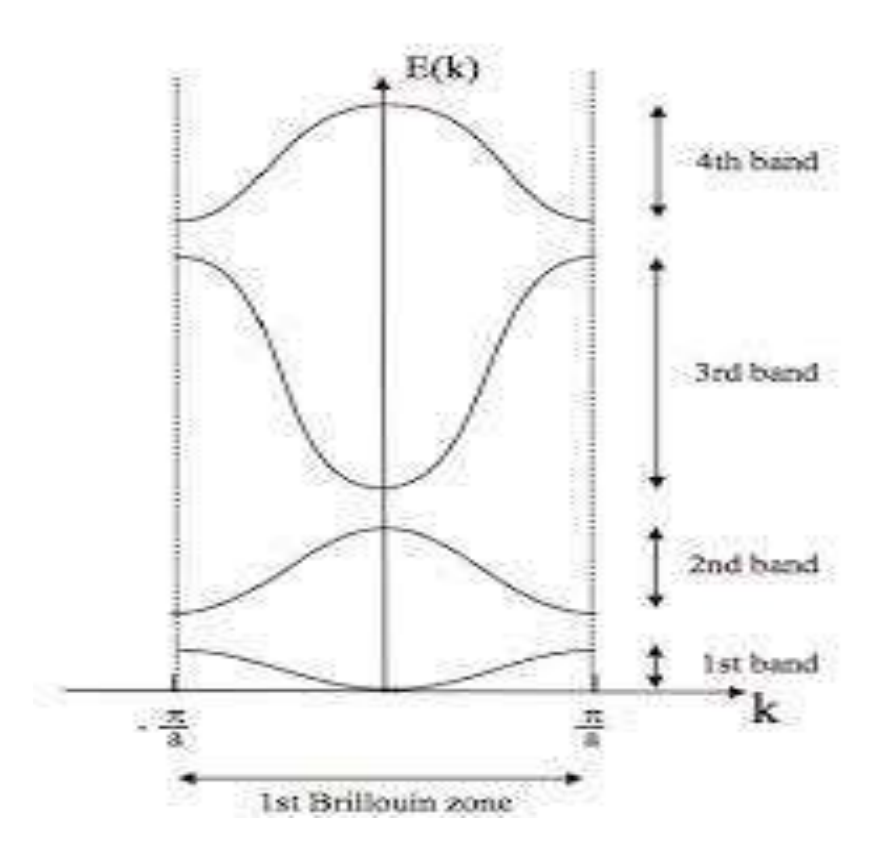


Fig. 1.2: Band structure formulation [Ref. 3].

1.3 Hubbard Model

Certain oxide materials behave as insulators, though according to the band theory they should be conductors. This issue was resolved by Hubbard [5] in 1963. In the case of certain oxides, the number of electrons in the d-orbitals is more than that in the s or the p-orbital. In the tight-binding model, only the overlap of the atomic orbitals is considered. But the presence of several electrons results in a large Coulomb repulsion, which is not incorporated in the tight-binding model. Hubbard introduced this electron-electron (e-e) interaction in the tight-binding model. The Hubbard Hamiltonian is given by

$$H = -\sum_{\langle ij \rangle} t_{ij} c_{i\sigma}^{\dagger} c_{j\sigma} + U \sum_{i} n_{i\uparrow} n_{i\downarrow} , \qquad (1.7)$$

where U is the e-e Coulomb interaction at a particular site and is called the onsite Coulomb correlation energy. In this model, an electron can hop from one site to its neighbouring site which is represented by the first term (hopping term) of the Hamiltonian (1.7) and the second term says it costs an energy U for two anti-parallel-spin electrons to stay at the same lattice site. When the electron density is significantly low in the system, then it is very less likely for two electrons to meet at the same site and hence in that case, the system acts as a weakly correlated system. But if we consider a system in which each site has a single electron in an anti-ferromagnetic order, then it is difficult for the up (down) spin electron of a particular site to hop to the neighbouring down (up) spin electron site, as it will cost an extra energy U. Hence, the motion of the up- (down-) spin electron is correlated with the down- (up-) spin electron. Therefore this system is referred to as a strongly correlated system. We normally assume the t_{ij} is same for all nearest neighbours and write $t_{ij} = t$.

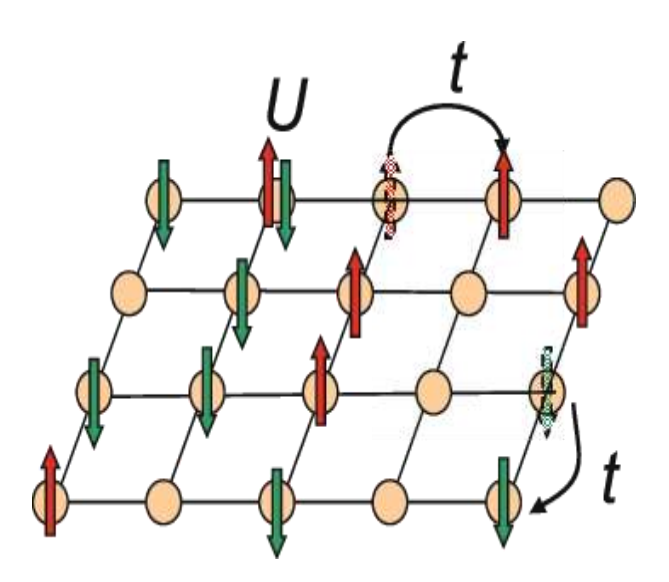


Fig. 1.3: 2D Hubbard model [source Wikipedia]

The competing parameters involved in the Hubbard Hamiltonian are t and U and the ratio U/t can describe the electronic motion involved in the system. Therefore, by varying these two parameters, it is possible to describe a metal-insulator transition. For example, even if a system has a half-filled band, if U/t is much smaller than one, it will be easy for the electrons

to hop from one atom to another and the system would behave as a metal. On the other hand, even for a half-filled band system, if U/t is much larger than one, hopping of an electron from one site to another site will be prohibited and the material would behave as an insulator. These systems are called Mott insulators. Thus, by increasing U, one can have a metal-insulator transition which is known as the Mott-Hubbard transition [6].

For the finite values of the hopping parameter t and Coulomb correlation U, the half-filled Hubbard model was first solved by Lieb and Wu [7] in one dimension using the Bethe ansatz method [8]. The away from half-filling case was first solved by Shiba and collaborators [9]. So far, no exact solution has been found for the Hubbard model in higher dimensions. Therefore, several analytical approximation methods (like the mean-field Hartree-Fock (HF) method, renormalization group (RG) method etc.) and numerical techniques (like Monte Carlo simulation) have been developed to solve the higher dimensional Hubbard model.

1.4 Polaron

An electron in the conduction band of an ionic crystal or a polar semiconductor distorts and polarizes the lattice in its vicinity by the e-p interaction. Such an electron then moves through the crystal together with the distortion (Fig. 1.4). The electron and the distortion together comprise a quasi-particle called polaron. If the e-p interaction is weak, the lattice distortion spreads over many lattice sites and the polarization potential is shallow. Such a polaron is known as a large polaron. If the e-p interaction is strong, the distortion is confined to a single lattice site and the polarization potential is deep and corresponding plaron is called a small polaron. It was Landau [10] who conceived the idea of polaron and term "polaron" was coined by Pekar [11]. The works of Landau and collaborators [12] were essentially semiclassical and dealt with what is now known as the strong-coupling polaron. The quantum mechanical formulation of the polaron problem was first given by Fröhlich in 1954 [13]. He proposed the celebrated Fröhlich Hamiltonian which could give solutions for both the weak and strong coupling regimes within the framework of the continuum model. Later, Holstein proposed an interesting model [14] which is a suitable model for the small polaron in a discrete lattice.

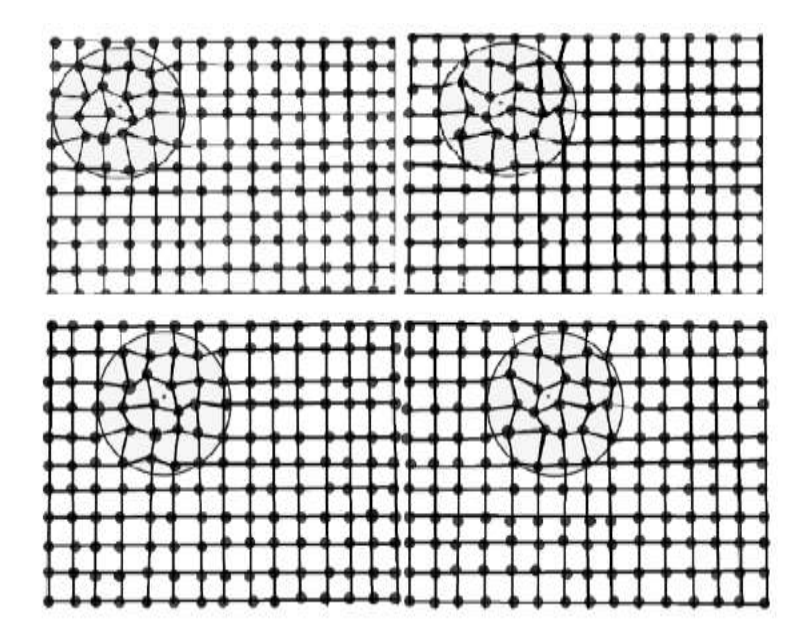


Fig. 1.4: Schematic diagram of polaron [Ref. 15]

1.4.1 Holstein Model

The Holstein Hamiltonian is given by

$$H = -t \sum_{\substack{\langle ij \rangle \\ \sigma}} c_{i\sigma}^{\dagger} c_{j\sigma} + \omega_0 \sum_{i} b_{i}^{\dagger} b_{i} + g \sum_{i\sigma} n_{i\sigma} (b_{i}^{\dagger} + b_{i}), \qquad (1.8)$$

where the first term gives tight-binding Hamiltonian, the next term represents the free phonon Hamiltonian and the third term describes the e-p interaction. Here $n_{i\sigma}(=c_{i\sigma}^{\dagger}c_{i\sigma})$ denotes the electron number operator for electrons at site i with spin σ , $c_{i\sigma}^{\dagger}$ ($c_{i\sigma}$) denoting the creation (annihilation) operator for the corresponding electrons, b_i^{\dagger} is the phonon creation operator at site i with the dispersionless frequency ω_0 , b_i is the corresponding phonon annihilation operator and g refers to the e-p coupling coefficient. The e-p interaction can also be described with the Feynman diagram in the following way:



Fig. 1.5: Feynman diagrams of the e-p interaction in the Holstein model

1.5 Holstein-Hubbard Model

For a correlated system which has a significant e-p interaction, one of the appropriate models is the Holstein-Hubbard model. This is a combination of the Holstein and the Hubbard models and has been employed by several researchers to explain the high temperature superconductivity in cuprates. The interplay between the e-p and the strong Coulomb couplings in a material can be investigated using the Holstein-Hubbard (HH) model (HHM). The HH Hamiltonian (HHH) is given by

$$H = -t \sum_{\substack{\langle ij \rangle \\ \sigma}} t_{ij} c_{i\sigma}^{\dagger} c_{j\sigma} + U \sum_{i} n_{i\uparrow} n_{i\downarrow} + \omega_0 \sum_{i} b_{i}^{\dagger} b_{i} + g \sum_{i\sigma} n_{i\sigma} (b_{i}^{\dagger} + b_{i}), \qquad (1.9)$$

where all the terms have been defined earlier. The ground state (GS) of the HH Hamiltonian can be a spin density wave (SDW) insulator or a charge density wave (CDW) insulator. This will essentially depend on the values of the parameters U and g.

1.5.1 Spin density wave (SDW)

An anti-ferromagnetic (AF) Mott-insulating state can be found as the solution of the HH Hamiltonian if a strong Coulomb correlation is present in the system. When the Hubbard interaction U is much greater than g, the system fails to pay the extra energy cost to keep any two electrons at the same lattice site. Then the electrons stay localized at their respective sites and GS of the system is an AF Mott insulator. This is also known as the SDW state (Fig. 1.6). As the electrons form polarons because of the e-p coupling, this state can also be called a polaronic state. The following diagram represents schematically the AF SDW polaronic Mott insulator:

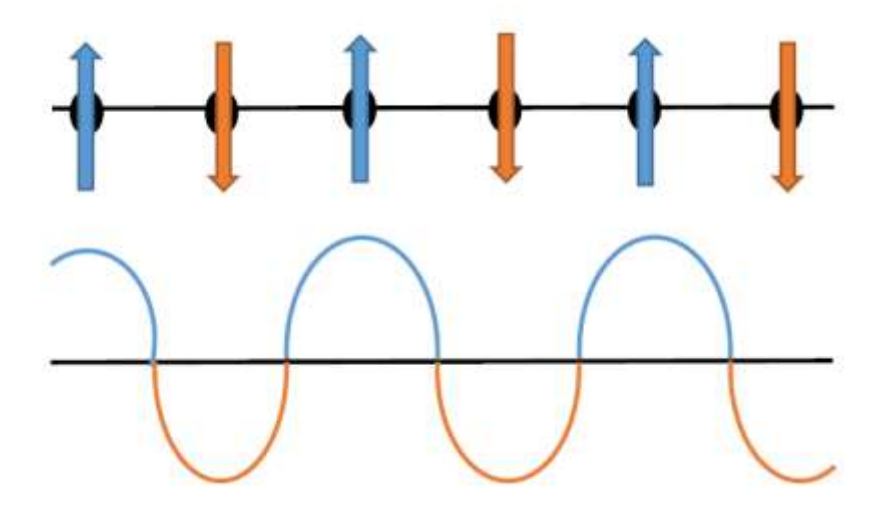


Fig. 1.6: AFMI or SDW

1.5.2 Charge density wave (CDW)

In HH model, if g is so large that the phonon-induced e-e attraction dominates over the repulsive onsite Coulomb correlation, the system prefers to

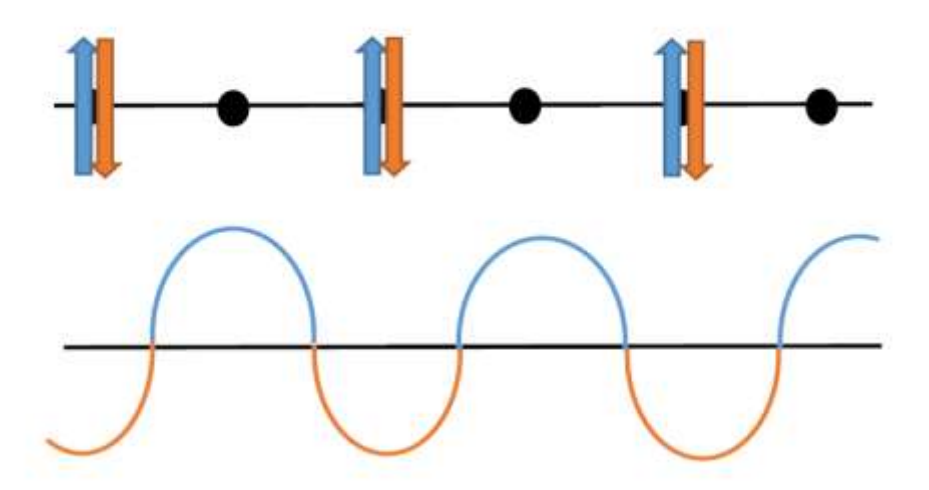


Fig. 1.7: Peierls insulator or CDW

stay in a bipolaronic phase. In this case, each alternating lattice sites are filled with two electrons with opposite spins and the system's GS becomes a paramagnetic CDW state. In this case, the lattice spacing doubles up leading to peierls instability. The lattice is now dimerized and each lattice site is occupied by a bipolaron. Fig. 1.7 shows schematically the CDW state.

1.6 Phase transition in Holstein-Hubbard Model

1.6.1 Transition from Spin density wave to Charge density wave

The HH model is an extremely useful model to study the competing effects of the e-e Coulomb correlation and the e-p interaction. We have already discussed that in the case of $U \gg g$, the GS of the HH Hamiltonian has an AF SDW polaronic Mott insulator, whereas in the case of $g \gg U$, the GS is the paramagnetic CDW bipolaronic Peierls insulator. Thus with the increase in the e-p interaction, one would expect the system to undergo a transition from an SDW phase to CDW phase. In 1983, the SDW-CDW transition has been studied by Hirsch and Fradkin [35] by using a numerical Monte Carlo simulation. Their investigation has suggested that this is a direct transition. An analytical study by Takada and Chatterjee (TC) [17] in 2003 has thrown a challenge in this area. TC have considered the onedimensional (1D) half-filled HH Hamiltonian. Treating the phonon sub-system variationally and employing the Bethe ansatz technique [18-19], TC have shown that the SDW-CDW transition is not a direct rather it goes through an intervening phase which is interestingly metallic. Thus, according to TC, there exists an intermediate metallic phase flanked by the SDW and CDW phases. This result is important in the context of high-T_C superconductivity because it suggests that even at a large e-p interaction, one can have a metallic phase which can become superconductive. Since the apex oxygen atoms in the cuprate superconductors have anharmonic vibration, it is important to consider the phonons to be anharmonic and consider a more realistic HH Hamiltonian with anharmonic phonons. Chatterjee and Takada (CT) [20] have studied the HH model in the presence of cubic and quartic phonon anharmonicity. The results show that width of the metallic phase broadens in the presence of phonon anharmonicity. After the prediction of the intermediate metallic phase in the HH model, several other researchers have examined the same problem using different numerical techniques. The density matrix renormalization group (DMRG) calculation of Clay and Hardikar [21-22] have supported the assertion of TC. DMRG study by Fehske et al. [23] has suggested that the existence of metallic phase for the HH model for large phonon frequencies. Using the exact diagonalization technique and cluster perturbation method, Payeur and Senechal [24] have also observed the metallic state. Quantum Monte-Carlo analyses by Nowadnick et al. [25] and Bourbonnais and Bakrim [26] have further confirmed the presence of the intermediate metallic phase.

There have also been a few studies that disputed the assertion of TC. For example, the studies by Tezuku et al. [27-28] show that the SDW to CDW transition does not require any intermediate phase. Furthermore, the renormalization group (RG) study by Tam et al. [29] also shows a direct transition between the two insulating phases. Therefore, it was important to examine the behaviour of the phase transition by more accurate analytical calculations. With this aim, Chatterjee and collaborators [30-35] have carried out a few improved analytical studies using variational calculations and they have shown that with every improvement of the variational wave function, the width of intermediate metallic phase widens. Recently, Lavanya et al. [33] have studied the HH model in the presence of the Gaussian phonon anharmonicity. The width of metallic phase obtained from their calculation turns out to be broader than that obtained by TC.

In this thesis, we have considered the 1D HH Hamiltonian with the Gaussian anharmonicity at half filling i.e., the same model as considered by Lavanya et al. Using an accurate phonon wave function, we have obtained the effective electronic Hamiltonian which we have solved by the Bethe ansatz method. This calculation can be called semi-exact. We have next considered an extended HH model in two dimensions. We have solved this problem in two different correlation regimes separately. The metallic phases obtained from both our 1D and 2D studies are found to be wider than that obtained by TC.

1.6.2 Self-trapping transition of polaron

In section 1.4, we have discussed the formation of the quasi-particle polarons in a polar semi-conductor or an ionic crystal. The polaron size is dependent on the strength of the e-p interaction strength. In the case of weak e-p coupling, the electron-created polarization potential is shallow and therefore the lattice distortion spreads over several lattice points. In this case, the wave function of the polaron is essentially extended in character and the resulting polaron is known as the large polaron which is delocalized and can wade through the lattice essentially as a free particle with a renormalized effective mass. But as the e-p interaction increases, the lattice deformation potential induced by the electron becomes deeper and the polaron size shrinks. At a sufficiently large e-p interaction, the polarization potential may become so deep that the electron may get confined to a length scale which is of the order of a lattice constant. The resulting complex is known as a small polaron and it

becomes immobile. The small polaron can be described by a localized wave function and has been the subject of the conventional Landau-Pekar problem [12]. The quantum mechanical formulation was first given by Fröhlich [13] who introduced a continuum polaron model and gave the weak-coupling solution. The Frohlich model can also give intermediate coupling [36], strong-coupling [11-12] and all-coupling solutions [37-38]. Alexandrov and Kornilovitch [39] have discussed the possibility of lattice distortion spreading over many sites even for large e-p interaction strength. In this case, the resulting complex is a small Fröhlich polaron i.e., a polaron with a localized wave function, but an extended distortion. It is well known that as the e-p coupling is increased, a polaron undergoes a transformation from a large polaron to a small polaron at a critical e-p coupling constant. This is usually known as the self-trapping (ST) transition because here, the transition occurs because of the trapping of the electron in a potential that is created by the electron itself. Though there is no dispute over the existence of the ST transition, the consensus over the nature of the transition is still lacking. The key question one has to answer here is whether this transition occurs in a continuous fashion or it is accompanied by a discontinuity. Several authors have studied the nature of the ST transition for the single-polaron and the many-polaron systems within the framework of the Fröhlich model. Löwen [40-41] has studied the ST transition for the Fröhlich model and found the transition is continuous. Toyozawa et al. [42-45] have examined the case of an adiabatic small polaron model and Emin [46] has investigated the ST transition in polar insulators using the Holstein molecular crystal model and both the studies have found the ST transition to be discontinuous. Löwen has explained that the discontinuity appearing in some of the studies may be the artefacts of the simplifying mathematical approximations employed in those studies. Raedt and Lagendijk [47] have studied the ST transition problem for both single and multi-polaron systems within the framework of the molecular crystal model of Holstein using a numerical Monte Carlo Technique and have demonstrated the continuous nature of the ST transition. Romero and collaborators [48] have studied the GS of the Holstein molecular crystal of a single electron with the help of a globallocal variational approach and they have found that the small polaron to large polaron transition is smooth until the system approaches the adiabatic limit. Recently, Krishna, Mukhopadhyay and Chatterjee (KMC) [49] have examined the behaviour of the ST transition in an extended HH system using a variational technique. Their calculation shows that ST transition in a 1D correlated polar system is continuous. It should however be mentioned that the analysis of KMC is still approximate because of the approximate treatment of the phonon subsystem.

The issue of ST transition has continued to remain in the focus of attention in the last few decades for its importance in colossal magneto-resistance materials or manganites, semiconductor nanostructures and so on. Therefore, this problem deserves a more accurate solution, preferably analytical, so that the physics of the system can remain transparent. In this thesis, we have made such an attempt. More specifically, we have examined the detailed behaviour of the ST transition in both 1D and 2D extended HH models.

1. 7 Quantum transport through molecular transistors

1.7.1 Single molecular transistor

Transistors are one of the integral parts of modern technology for the fabrication of nanodevices. In a single molecular transistor (SMT), a central molecule or a quantum dot (QD) with discrete energy levels is connected to two metallic leads (source and drain) with continuous energy levels on the two sides and is acted upon by an external bias voltage. The presence of discrete energy levels in the central molecule (i.e. the QD which is also called a tunnelling molecule) is important to study the quantum mechanical effects on the device. The difference in the electronic potential energies of the source and the drain helps the electrons in tunnelling from the source to the drain through the QD. The transfer of electrons through the QD results in a net tunnelling current. The SMT system is mounted on an insulating substrate whose energy is controllable by an external gate voltage. Therefore by applying this gate voltage, the tunnelling current can be manipulated. The fabrication of a single molecular transistor was first reported with C_{60} as the central molecule by Park et al. [50] in 2000 with the help of gold electrodes connected with the C_{60} molecules. The SMT device has shown the properties of a switching device [51] and it can also work as a sensor [52]. Dutta [53] has described the electronic transport in the mesoscopic systems [53] and he has also extended its application to the molecular transistors [54]. The recent review articles by Mickael et al. [55] and Huanyan et al. [56] have reported the mechanisms of the SMT device and its recent developments and applications. Very recently, Pipit and collaborators [57] have experimentally established the Coulomb blockade and Coulomb staircase behaviour for single electron transport at the room temperature. Liang et al. [58] have described the Kondo resonance effect in the SMT device and explained that by tuning the gate voltage, the Kondo phenomena in quantum dot structures can be modified. Later, many other works also have reported the Kondo behaviour in molecular transport [59-61]. Sang and collaborators [62]

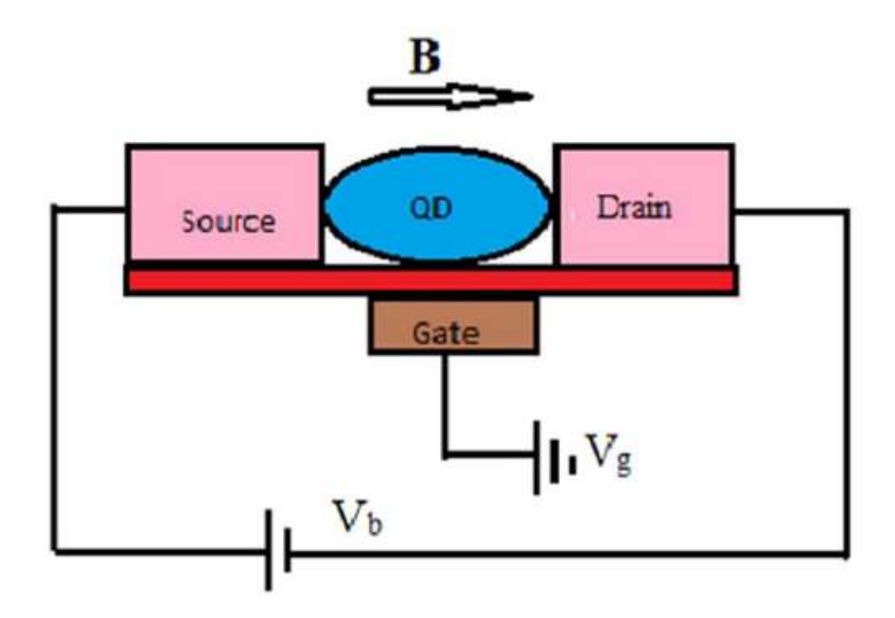


Fig. 1.8: SMT device (Ref. [89])

have investigated the interplay between the e-e and e-p interactions in the Anderson-Holstein model and computed the spectral functions (SF) for the electrons and phonons using the numerical renormalization group technique. Using the Keldysh technique, Chen et al. [63] have shown that the polaronic effect generates side peaks in the SF of an SMT device and modifies the tunnelling current. Extending the work of Chen, Juntao and collaborators [64] have measured the phonon-associated conductance in a SMT device. Raju and Chatterjee [65] have extended the SMT problem to investigate the phonon dissipation-induced tunnelling current by introducing an insulating substrate (Fig. 1.8) and concluded that the dissipation increases the tunnelling current in the single molecular transistor. Chatterjee and collaborators [66] have studied magneto-transport in a dissipative SMT device incorporating the effects of e-e and e-p coupling interactions. Their result shows that the spin-filtering effect is enhanced with the magnetic field. It has been found that the tunnelling current in a SMT reduces with the external temperature [67-68].

1.7.2 Anderson-Holstein-Caldeira-Leggett Model

The electronic, phononic and the tunnelling terms for the SMT device can be described by the Anderson–Holstein [69, 14] Hamiltonian. We consider that the central QD contains a single energy level, a single phonon mode, an onsite e-e interaction strength and an onsite e-p interaction. The source and the drain are considered to have free electrons with continuous energy levels and the electrons from the source can be made to tunnel to the drain through the QD by using a bias voltage. The Hamiltonian for the SMT device can be written as

$$H = \sum_{k,\sigma} \varepsilon_{k\sigma} n_{k\sigma} + \sum_{\sigma} \varepsilon_{d\sigma} n_{d\sigma} + U n_{d\uparrow} n_{d\downarrow} + \omega_0 b^{\dagger} b + g \sum_{\sigma} n_{d\sigma} (b^{\dagger} + b)$$
$$+ \sum_{k} (V_k c_{k\sigma}^{\dagger} c_{d\sigma} + h.c.), \tag{1.9}$$

where $n_{k\sigma}(=c_{k\sigma}^{\dagger}c_{k\sigma})$ is the number operator for the lead electrons, $c_{k\sigma}^{\dagger}(c_{k\sigma})$ denoting the creation (annihilation) operator for a lead electron with wave vector \mathbf{k} , spin σ and energy $\varepsilon_{k\sigma}$, $n_{d\sigma}(=c_{d\sigma}^{\dagger}c_{d\sigma})$ is the number operator for the QD electrons, $c_{d\sigma}^{\dagger}(c_{d\sigma})$ being the creation (annihilation) operator corresponding to the QD electrons with energy $\varepsilon_{d\sigma}$ and spin σ , U is the onsite e-e interaction energy of the QD, $b^{\dagger}(b)$ creates (annihilates) a QD phonon with dispersionless frequency ω_0 , g is onsite e-p coupling coefficient for the QD and V_k gives the hybridization coefficient that gives the strength of tunnelling between the lead and the QD.

For a dissipative system, where a particle of mass m is coupled to a bath of harmonic phonons, the dynamics of the system can be explained through the Caldeira-Leggett (CL) model [70-71] given by the Hamiltonian

$$H = \frac{p_0^2}{2m_0} + \frac{1}{2}m_0\omega_0^2x_0^2 + \sum_{j=1}^N \left[\frac{p_j^2}{2m_j} + \frac{1}{2}m_j\omega_j^2x_j^2\right] - \sum_{j=1}^N C_jx_jx_0,$$
(1.10)

where the particle of mass m with momentum p at position x_0 , interacts with the harmonic oscillators of mass m_j , momentum p_j and the interaction coefficient of the dissipative particle is C_j . The potential $V_0(x)$ can also be written as,

$$\frac{1}{2}m_0\omega_0^2x_0^2 = \left(\sum_{j=1}^N \frac{C_j^2}{2m_j\omega_j^2}\right)x_0^2 + \left(\frac{1}{2}m_0\omega_0^2x_0^2 - \sum_{j=1}^N \frac{C_j^2}{2m_j\omega_j^2}x_0^2\right). \tag{1.11}$$

Using Eq. (1.11), the CL model can be written as,

$$H = \frac{p^2}{2m} + \frac{1}{2}m_0 \left(\omega_0^2 - \sum_{j=1}^N \frac{C_j^2}{2m_j\omega_j^2}\right) x_0^2 + \sum_{j=1}^N \left[\frac{p_j^2}{2m_j} + \frac{1}{2}m_j\omega_j^2 \left(x_j - \frac{C_j}{m_j\omega_j^2}x_0\right)^2\right].$$
(1.12)

Eq. (1.12) shows that the phonon-phonon interaction term of (1.10) reduces the QD phonon frequency as a dissipative effect and thus screens the e-p interaction.

The Anderson-Holstein model combined with the Caldeira-Leggett model can describe the transport in a dissipative SMT device in the presence of e-e and e-p interactions. The combined Hamiltonian is referred as the Anderson-Holstein-Caldeira-Leggett (AHCL) Hamiltonian [72].

Recently, extensive studies have been performed on the double-QD-based molecular transistors [73-75] as they show many useful and interesting properties, like large charge sensibility and more controllable current. We can call such a system as a bi-molecular transistor. In the present thesis, we consider a bi-molecular transistor and calculate the quantum transport in such a system.

1.8 Organisation of the thesis

In the following chapter i.e., in Chapter 2, we consider the 1D HH model with Gaussian anharmonicity and give a semi-exact solution. We treat the phonon subsystem using an accurate wave function and solve the effective electronic Hamiltonian exactly using the Bethe ansatz technique. We study the phase space spanned by the e-e Coulomb interaction (U) and the e-p interaction (U) and show that a metallic phase exists in between the insulating SDW and CDW phases. Our present result demonstrates that the intervening conducting phase is broadened with the consideration of a more accurate phonon wave function.

In Chapter 3, an extended HH model is studied in 2D. For the phonon subsystem a variational wave function is used. As the 2D Hubbard model does not admit an exact solution, we solve the effective electronic problem separately for the weak and strong correlation regimes. In the weak-coupling regime, the effective electronic Hamiltonian is treated by the Hartree-Fock method, while for the strong-coupling regime, the Hamiltonian is

first transformed to the t-J model which is then treated at the mean field level. The phase diagram is obtained by combing the results of the two regimes.

In Chapter 4, The ST transition in the 1D HH model is studied and the nature of the transition is examined using an accurate phonon wave function and the exact Bethe ansatz technique. In Chapter 5, an extended HH model is studied in 2D for weak and strong correlation strengths and the nature of the ST transition is studied using same method that is used to study the SDW-CDW transition for the 2D system in Chapter 3.

In Chapter 6, quantum transport is studied in a dissipative bi-molecular transistor. The effects of bias-voltage, e-p interaction, Coulomb correlation, external magnetic field and temperature are studied on the tunnelling current, conductance and spin-polarization.

In Chapter 7, we present a summary of results and make some concluding remarks.

1.6 References

- [1] A. Sommerfeld, Zeitschrift für Physik (in German), 47 (1–2): 1–3 (1928).
- [2] F. Bloch, Zeitschrift für physik, **52**(7), 555-600 (1929).
- [3] Charles Kittel, Introduction to Solid State Physics. New York: Wiley (1996).
- [4] N. W. Ashcroft and N. D. Mermin, Solid State Physics (Saunders College, 1976).
- [5] J. Hubbard, **276** (1365), 238 257 (1963).
- [6] N. F. Mott., Proceedings of the Physical Society. Section A. IOP Publishing. **62** (7): 416–422 (1949).
- [7] E.H. Lieb and F.Y. Wu, Phys. Rev. Lett. 20, 1445-1448, (1968);
- [8] H. Bethe, Magazine for physics **71**, 205-226 (1931).
- [9] H. Shiba and P. A. Pincus, Phys. Rev. B 5, (1966).
- [10] L. Landau, Z. Phys. 3, 664 (1933).
- [11] S. I. Pekar, ZhETF **16**, 341 (1946).
- [12] L. D. Landau, S. I. Pekar, JETP 18, 341 (1948).
- [13] H. Fröhlich, Adv. Phys. **3**, 11, 325-361, (1954).
- [14] T. Holstein, Ann. Phys. (N.Y.) 8, 325 (1959); 8, 343 (1959).
- [15] A. Chatterje, S. Mukhopadhyay, Polarons and Bipolarons, An introduction, CRC press (2019).

- [16] E. Fradkin and J. E. Hirsch, Phys. Rev. B **27** 4302 (1983).
- [17] Y. Takada and A. Chatterjee, Phys. Rev. B 67 081102 (R) (2003).
- [18] E.H. Lieb and F.Y. Wu, Phys. Rev. Lett. 20, 1445-1448, (1968);
- [19] H. Bethe, Magazine for physics, **71**, 205-226 (1931).
- [20] A. Chatterjee, Y. Takada, J. Phys. Soc. Jap. **73**, 964–969 (2004).
- [21] R. T. Clay, R. P. Hardikar, Phys. Rev. Lett. 95, 096401 (2005).
- [22] R. P. Hardikar, R. T. Clay, Phys. Rev. B. 75, 245103 (2007).
- [23] H. Fehske, G. Hager, E. Jeckelmann, Europhys. Lett. **84**, 57001 (2008).
- [24] A. Payeur, D. Senechal, Phys. Rev. B 83 033104 (2011).
- [25] E. A. Nowadnick, S. Johnston, B. Moritz, R. T. Scalettar, T. P. Devereaux, Phys. Rev. Lett. **109** 246404 (2012).
- [26] H. Bakrim, C. Bourbonnais, Phys. Rev. B **91** 085114 (2015).
- [27] M. Tezuka, R. Arita, H. Aoki, Phys. Rev. Lett. **95** 226401 (2005).
- [28] M. Tezuka, R. Arita, H. Aoki, Phys. Rev. B **76** 155114 (2007).
- [29] K. M. Tam, S. W. Tsai, D. K. Cambell, A. H. C. Neto, Phys. Rev. B **75** *161103* (*R*) (2007).
- [30] P. M. Krishna, A. Chatterjee, Physica C **457**, 55–59 (2007).
- [31] A. Chatterjee, Adv. Con. Matt. Phys. 350787 (2010).
- [32] I. V. Sankar, A. Chatterjee, Physica B **489**, 17–22 (2016).
- [33] C. U. Lavanya, I. V. Sankar, A. Chatterjee, Sci Rep. 7, 3774 (2017).
- [34] Z. M. Malik, S. Mukhopadhyay, A. Chatterjee, Phys. Lett. A 383, 1516–1519 (2019).
- [35] Z. M. Malik, A. Chatterjee, J. Phys. Commun. 4 (2020) 105005.
- [36] M. Gurari, Phil. Mag. 44, 329 (1953).
- [37] T. D. Lee, F. Low, D. Pines, Phys. Rev. 90, 297 (1953).
- [38] A. Chatterjee, Ann. Phys. NY **202**,320 (1990).
- [39] A.S. Alexandrov, P.E. Kornilovitch, Phys. Rev. Lett. **82** (1999) 807.
- [40] H. Löwen, J. Math. Phys. 29, 1498 (1988).
- [41] H. Löwen, Z. Phys. B Condensed Matter 72, 59-64 (1988).
- [42] Y. Toyozawa, Prog. Theor. Phys. **26** (1) (1961);
- [43] K. Cho, Y. Toyozawa, J. Phys. Soc. Jpn. 30 (1971) 1555;
- [44] K. Cho, Y. Toyozawa, J. Phys. Soc. Jpn. **30** (1971) 1555;
- [45] Y. Shinozuka, Y. Toyozawa, J. Phys. Soc. Jpn. 46 (1979) 505.
- [46] D. Emin, Adv. Phys. 22 (1973) 57;
- [47] H. De Raedt, A. Lagendijk, Phys. Rep. 127 (1985) 233.

- [48] A. H. Romero, D. W. Brown, K. Lindenberg, Phys. Rev. B 60 (7) (1999);
- [49] R.P.M. Krishna, S. Mukhopadyay, A. Chatterjee, Phys. Lett. A 327 (2004) 67;
- [50] Park, H. et al. Nature **407**, 57–60 (2000).
- [51] Makoto Yamamoto, Yasuo Azuma, Masanori Sakamoto, Toshiharu Teranishi, Hisao Ishii,

Yutaka Majima & Yutaka Noguchi, Sci. Rep. 7, 1589 (2017).

- [52] N. Abdelghafar, B. Aïmen, H. Bilel, K. assim, K. Adel, IEEE Sens. J. 18, 1558 (2018).
- [53] Datta, S. Electronic Transport in Mesoscopic Systems (Cambridge University Press, 1997).
- [54] S. Datta. Quantum Transport Atom to Transistor (Cambridge University Press, Cambridge, 2005)
- [55] L. P. Mickael, B. Enrique, H. S. van der Zant, J. Chem. Soc. Rev. 44, 902 (2015).
- [56] Huanyan Fu, Xin Zhu, Peihui Li, Mengmeng Li, Lan Yang, Chuancheng Jia and Xuefeng Guo, J. Mater. Chem. C, **10**, 2375 (2022).
- [57] U. V. Pipit, A. Yasuo, S. Masanori, T. Toshiharu, M. Yutaka, Mater. Res. Express 4, 024004 (2017).
- [58] W. Liang, M. P. Shores, M. Bockrath, J. R. Long, H. Park, Nature 417, 725–729 (2002).
- [59] L. H. Yu, D. Natelson, Nano Lett. 4, 79–83 (2003).
- [60] Chen, Z. Z., Lu, H., Lü, R., Zhu, B. F., J. Phys.:Condens. Matter 18, 5435–5446 (2006).
- [61] G. Gonzalez, M. N. Leuenberger, E. R. Mucciolo, Phys. Rev. B 78, 054445–12 (2008).
- [62] G. S. Jeon, T. H. Park, H. Y. Choi, Phys. Rev. B 68, 045106 (2003).
- [63] Chen, Z. Z., Lü, R., Zhu, B. F., Phys, Rev. B. 71, 165324 (2005).
- [64] Song, Sun, J. Gao, X. C. Xie, Phys. Rev B. **75**, 195320 (2007)
- [65] Narasimha Raju, A. Chatterjee, Sci. Rep. 6, 18511 (2016).
- [66] M. Kalla, Narasimha Raju, Ch., Chatterjee, A., Sci. Rep. 9, 16510 (2019).
- [67] Lundin, U., & McKenzie, R. H., Phys. Rev B 66, 075303 (2002).
- [68] M. Kalla, Narasimha Raju, Ch., Chatterjee, A., Sci Rep. 11, 10458 (2021).
- [69] P. W. Anderson, Phys. Rev. **124**, 41 (1961).
- [70] A. O. Caldeira, A. J. Leggett, Physica A, **587** 112(1983).
- [71] A. O. Caldeira, A. J. Leggett, Annals of Physics **149**, 374 (1983).
- [72] Narasimha Raju, A. Chatterjee, Sci. Rep. 6, 18511 (2016).
- [73] V. Khademhosseini, D. Dideban, M.T. Ahmadi, H. Heidari, Molecules, **27**(1):301 (2022).

[74] Faris Abualnaja, Chen Wang, Vlad-Petru Veigang-Radulescu, Jonathan Griffiths,
Aleksey Andreev, Mervyn Jones, and Zahid Durrani, Phys. Rev. Applied 12, 064050 (2019).
[75] E. C. Siqueira *and* G. G. Cabrera, Journal of Applied Physics 111, 113905 (2012).

"Logic will get you from A to B. Smagination will take you everywhere"...Albert Einstein

2

A semi exact solution for a metallic phase in a Holstein-Hubbard chain at half-filling with Gaussian anharmonic phonons

2.1 Introduction

The exotic superconducting behaviour in ceramic Cu-based compounds [1] has continued to elude a convincing theoretical paradigm that could consistently conform to all experimental observations. Though a large number of investigators have posed their faith in the electronic mechanism, there have also been quite a few advocates of the phonon mechanism [2-7] and this tribe has grown with time. The main objection against the phonon mechanism is as follows. In a strongly correlated system, if the e-p interaction is small, the minimum energy state will have the characteristics of a polaronic SDW state that corresponds to an antiferroagnetic Mott insulator. Naturally for the superconductivity to be driven by the phonon-mechanism, the e-p coupling needs to be adequately large compared to the repulsive e-e interaction strength. A study by Plakida [8] has shown that the lattice instability and strong e-p coupling have a pivotal role in inducing high T_C superconductivity. Interestingly, however, if e-p coupling is strong, the GS of the system is described by the bipolaronic CDW which corresponds to a paramagnetic Peierls insulator.

As described in chapter 1, the Holstein-Hubbard (HH) model is a suitable model to study the interplay between e-e and e-p interaction. The interplay between the e-e and e-p interaction

leads to an interesting phase diagram that represents the phase transition from SDW state to the CDW state. In chapter 2, we have explained the results established in this model so far. Though a few studies [9, 10-12] have reported the HH model makes a direct SDW-CDW transition, the Bethe ansatz exact solution by Takada and Chatterjee (TC) [13] in 2003 has thrown a new challenge in the field. The principal premise of the investigation of TC is as follows. With the increase in e-p coupling, both the effective onsite e-e interaction energy (U_{eff}) and the effective hopping energy (t_{eff}) decrease and with U_{eff} approaching zero, the system becomes so sensitive to the interplay between the relative strengths of these two energy scales that instead of going from a SDW phase or to a CDW phase, the system prefers to settle in an intermediate phase which has been shown by TC to be metallic. This interesting observation of TC has sparked off a lot of interest on this issue and naturally a host of investigations [14-17] followed closely on the heels of the work of TC. Using the density matrix renormalization group (DMRG) technique, Clay and Hardikar [14, 15] have not only demonstrated the existence of an intermediate metallic phase (MP) in agreement with the contention of TC but also suggested that this intermediate phase can exhibit superconductivity, which is an exciting result in the context of high-temperature superconductivity. Feshke et al. [16] have also implemented the DMRG method and established the occurrence of the metallic regime between the two insulating phases. They have also proved that IMP widens as the phonon frequency increases. Several other studies using renormalization group (RG) technique [18], Monte- Carlo simulations [19], exact numerical diagonalization and cluster perturbation theory [20] etc. have also shown the evidence of intermediate MP between the SDW and CDW phases.

Chatterjee and Takada (CT) [21] have also examined the problem in the presence of lattice anharmonicity. They have considered cubic and quartic phonon anharmonicities and have shown that intermediate MP becomes broader in the presence of lattice anharmonicity and thus the conjecture on the presence of intermediate MP in the HH system is strengthened in the presence of anharmonic phonons. This work is of much importance because lattice anharmonicity has been found to play a crucial role in high T_c superconductors. In fact, it has been observed that apex oxygen has a substantial anharmonic motion in the cuprates and also the phonon anharmonicity makes a significant impact on the electronic structure of these systems [22-26]. Konior [27] has explained the importance of Gaussian phonon anharmonicity in the context of high $-T_c$ superconductors and have shown that in the presence of Gaussian phonon anharmonicity, the hopping parameter reduces at a slow rate

causing an enhancement in the polaron mobility and the polaron bandwidth, which is a favourable condition for the phonon mechanism to stake claim for inducing pairing. Lavanya et al. [28] have recently re-examined the work of CT with Gaussian anharmonic potential by applying in succession a number of unitary transformations followed by an averaging with a general many-phonon state and the Bethe ansatz technique. This give a wider metallic phase.

The principal aim of the present paper is to further modify the variational wave function of the phonon sub-system used by Lavanya et al. for the anharmonic HH system to obtain a better solution for the GS energy and the SDW-CDW phase diagram. This calculation can be considered as semi-exact as we have included rigorously all possible phonon processes including coherence and correlations while treating the phonon subsystem and solved the effective electronic part exactly with the help of the Bethe ansatz. The GS energy, local spin moment, Von-Newmann entropy, the double occupancy parameter and the phase diagram at the SDW-CDW transition region have been obtained.

2.2 Model and formulation

The one dimensional HH system with Gaussian phonon anharmonicity may be described by the Hamiltonian

$$H = H_e + H_p + H_{ep} \,, \tag{2.1}$$

with

$$H_e = -t \sum_{\langle ij \rangle \sigma} c^{\dagger}_{i\sigma} c_{j\sigma} + U \sum_i n_{i\uparrow} n_{i\downarrow} , \qquad (2.2)$$

$$H_p = \hbar \omega_0 \sum_i b_i^{\dagger} b_i + \lambda_{ap} \sum_i e^{-\gamma \left(b_i^{\dagger} + b_i\right)^2} , \qquad (2.3)$$

$$H_{ep} = g \sum_{i\sigma} n_{i\sigma} \left(b_i^{\dagger} + b_i \right), \tag{2.4}$$

where H_e describes the Hubbard Hamiltonian, H_p is the phonon Hamiltonian and H_{ep} is the Holstein e-p interaction. In Eq. (2.2), the parameter t is the nearest-neighbour hopping integral (HI), the operator $c_{i\sigma}^{\dagger}(c_{i\sigma})$ creates (annihilates) a spin- σ electron at the i-th site,

 $n_{i\sigma}(=c_{i\sigma}^{\dagger}c_{i\sigma})$ being the corresponding electron occupation number and U gives the onsite e-e interaction energy. In Eq. (2.3), $b_i^{\dagger}(b_i)$ represents an operator that creates (annihilates) an optical phonon at site i with dispersionless frequency ω_0 , λ_{ap} and γ measure respectively the strength and range of Gaussian anharmonic phonon. In Eq. (2.4), g is the on-site e-p coupling coefficient which can be written as: $g = \sqrt{\alpha}\omega_0$, where dimensionless α is referred to as the e-p coupling constant.

2.2.1 GS energy

In order to solve the Hamiltonian (2.1) we choose to seek a variational solution. First of all, we apply the modified Lang-Firsov transformation (LFT) [29] with the generator

$$R_1 = \sqrt{\alpha}\eta \sum_{i\sigma} n_{i\sigma} (b_i^{\dagger} - b_i) , \qquad (2.5)$$

where η is the variational parameter that carries the information of the polaronic structure. For strong e-p interaction, $\eta \to 1$, and Eq. (2.5) generates usual LFT and gives a reasonable approximation for the anti-adiabatic region. To deal with the adiabatic regime, we perform the Takada-Chatterjee (TC) transformation [13] with the generator:

$$R_2 = \sum_{i} h_i \ (b_i^{\dagger} - b_i), \tag{2.6}$$

where we assume, $h_i = h$, as all sites are equivalent. The above two transformations together can be generated by:

$$R_{12} = \sum_{i\sigma} \left[h + \eta \sqrt{\alpha} \left(n_{i\sigma} - \frac{h}{\sqrt{\alpha}} \right) \right] \left(b_i^{\dagger} - b_i \right). \tag{2.7}$$

With $\eta=1$, the transformation (2.7) represents the conventional LFT which gives exact results in the anti-adiabatic limit, while for $\eta=0$, it takes care of the adiabatic limit. Thus both the anti-adiabatic and the adiabatic regions can be studied by considering: $0<\eta<1$. Using the Baker-Campbell-Hausdorff (BCH) formula we may calculate the transformed Hamiltonian as,

$$H_{12} = e^{R_{12}}He^{-R_{12}} = H + [R_{12}, H] + \frac{1}{2!}[R_{12}, [R_{12}, H]] + \cdots$$
 (2.8)

$$H_{12} = \frac{\alpha\eta(\eta - 2)}{\hbar\omega_0} \sum_{i\sigma} n_{i\sigma} + \left[U - \left\{ \frac{2}{\hbar\omega_0} \alpha\eta(2 - \eta) \right\} \right] \sum_i n_{i\uparrow} n_{i\downarrow} - t \sum_{\langle ij \rangle \sigma} e^{(x_i - x_j)} c_{i\sigma}^{\dagger} c_{j\sigma}$$

$$+ \hbar\omega_0 \sum_i \left(b_i^{\dagger} - h \right) (b_i - h) + \sqrt{\alpha} (1 - \eta) \sum_{i\sigma} n_{i\sigma} \left(b_i^{\dagger} + b_i - 2h \right)$$

$$+ \lambda_{ap} \sum_i e^{-\gamma \left[\left\{ \left(b_i^{\dagger} + b_i - 2h \right) - \frac{2\sqrt{\alpha}\eta n_i}{\hbar\omega_0} \right\}^2 \right]}$$

$$(2.9)$$

where

$$x_i - x_j = \frac{\sqrt{\alpha \eta}}{\hbar \omega_0} \{ \left(b_i^{\dagger} - b_i \right) - \left(b_j^{\dagger} - b_j \right) \}$$
 (2.10)

To calculate this transformed Hamiltonian we have used the identity, $n_{i\sigma}^2 = n_{i\sigma}$.

It is important to note that Eq. (2.7) assumes that the phonons associated with the electron are in a coherence state. This is essentially a semi-classical approximation in which it is assumed that the phonons in the polaron cloud are independent of each other satisfying a Poissonian distribution. In other words, the phonons emitted or absorbed by the electrons are completely uncorrelated and in that sense, the present transformation is equivalent to Hartree approximation.

The presence of Gaussian anharmonicity in the system introduces anharmonicity to infinite order and results in a finite lifetime of the phonons through phonon-phonon interactions. Furthermore, an electron undergoes a recoil motion while emitting a phonon. While undergoing a recoil motion, if the electron emits another phonon, then these two successively emitted virtual phonons will be correlated. The correlation effects of the phonons and the anharmonicity can be taken into account (to a great extent) by squeezing the phonon vacuum. The squeezing of the phonon vacuum state can be accomplished by the celebrated Bogoliubov transformation with the generator [30]:

$$R_3 = \alpha_s \sum_i (b_i b_i - b_i^{\dagger} b_i^{\dagger}), \qquad (2.11)$$

where the squeeze parameter α_s is to be obtained variationally and this generator transforms the Hamiltonian to,

$$H_3 = e^{R_3} H_{12} e^{-R_3} = H_{12} + [R_3, H_{12}] + \frac{1}{2!} [R_3, [R_3, H_{12}]] + \cdots$$
 (2.12)

The anharmonic term is transformed by the squeezing transformation as follows:

$$e^{R_{3}} \sum_{i} e^{-\gamma \left\{ \left(b_{i}^{\dagger} + b_{i} - 2h\right) - \frac{2\sqrt{\alpha}\eta n_{i}}{\hbar\omega_{0}} \right\}^{2}} e^{-R_{3}}$$

$$= \sum_{i} e^{R_{3}} \left[\sum_{m} \frac{1}{m!} \left(-\gamma \left\{ \left(b_{i}^{\dagger} + b_{i} - 2h\right) - \frac{2\sqrt{\alpha}\eta n_{i}}{\hbar\omega_{0}} \right\}^{2} \right)^{m} \right] e^{-R_{3}}$$

$$= \sum_{i} \sum_{m} \frac{(-\gamma)^{m}}{m!} \left\{ \left[e^{R_{3}} \left\{ \left(b_{i}^{\dagger} + b_{i} - 2h\right) - \frac{2\sqrt{\alpha}\eta n_{i}}{\hbar\omega_{0}} \right\} e^{-R_{3}} \right]^{2} \right\}^{m}$$

$$= \sum_{i} e^{-\gamma \left[\left(b_{i}^{\dagger} + b_{i}\right) e^{2\alpha_{S}} - 2h - \frac{2\sqrt{\alpha}\eta n_{i}}{\hbar\omega_{0}} \right]^{2}}.$$
(2.13)

Using this relation, H_3 of Eq. (2.12) becomes,

$$H_{3} = \frac{\alpha\eta(\eta - 2)}{\hbar\omega_{0}} \sum_{i\sigma} n_{i\sigma} + \left[U - \left\{ \frac{2}{\hbar\omega_{0}} \alpha\eta(2 - \eta) \right\} \right] \sum_{i} n_{i\uparrow} n_{i\downarrow} - t \sum_{\langle ij \rangle \sigma} e^{(x_{i} - x_{j})e^{-2\alpha_{S}}} c_{i\sigma}^{\dagger} c_{j\sigma}$$

$$+ \hbar\omega_{0} \sum_{i} \left[\frac{e^{4\alpha_{S}}}{4} \left(b_{i}^{\dagger} + b_{i} \right)^{2} - \frac{e^{-4\alpha_{S}}}{4} \left(b_{i}^{\dagger} - b_{i} \right)^{2} - \frac{1}{2} - h \left(b_{i}^{\dagger} + b_{i} \right) e^{2\alpha_{S}} + h^{2} \right]$$

$$+ \sqrt{\alpha} (1 - \eta) \sum_{i\sigma} n_{i\sigma} \left[\left(b_{i}^{\dagger} + b_{i} \right) e^{2\alpha_{S}} - 2h \right]$$

$$+ \lambda_{ap} \sum_{i} e^{-\gamma \left[\left(b_{i}^{\dagger} + b_{i} \right) e^{2\alpha_{S}} - 2h - \frac{2\sqrt{\alpha}\eta n_{i}}{\hbar\omega_{0}} \right]^{2}} . \tag{2.14}$$

The variational parameter α_s has been assumed by all investigators to be independent of the electron concentration untill 2019, when Malik-Mukhopadhyay-Chatterjee (MMC) [31] has considered the squeezing of the phonon state to be partly dependent on electron density. According to MMC, the correlation between phonons emitted by the electrons may depend on the number of electrons available at a particular lattice site. Thus, we next apply, a squeezing transformation with the generator:

$$R_4 = \alpha_d \sum_{i\sigma} n_{i\sigma} (b_i b_i - b_i^{\dagger} b_i^{\dagger}), \qquad (2.15)$$

where α_d is the variational parameter. It may be pointed out that in Eq. (2.11), phonon correlation and anharmonicity have been included at a mean-field level while Eq. (2.15) incorporates the fluctuations. Therefore, the transformed Hamiltonian looks like:

$$\mathcal{H} = e^{R_4} e^{R_3} e^{R_2} e^{R_1} H e^{-R_1} e^{-R_2} e^{-R_3} e^{-R_4}. \tag{2.16}$$

The generators transformed the Hamiltonian as

$$\mathcal{H} = \sum_{i\sigma} \left[-\frac{\alpha\eta(\eta - 2)}{\hbar\omega_{0}} + \alpha(1 - \eta) \{ (b_{l}^{\dagger} + b_{l}) e^{2\alpha_{S}} e^{2\alpha_{S}} \Sigma_{\sigma} n_{i\sigma} - 2h \} \right.$$

$$+ \lambda_{ap} e^{-\gamma \left[(b_{l}^{\dagger} + b_{l}) e^{2\alpha_{S}} e^{2\alpha_{S}} \Sigma_{\sigma} n_{i\sigma} - 2h - \frac{2\sqrt{\alpha}\eta n_{l}}{\hbar\omega_{0}} \right]^{2}}$$

$$- \lambda_{ap} e^{-\gamma \left[(b_{l}^{\dagger} + b_{l}) e^{2\alpha_{S}} e^{2\alpha_{S}} \Sigma_{\sigma} n_{i\sigma} - 2h \right]^{2}} \right] n_{l\sigma}$$

$$+ \left[U - \left\{ \frac{2}{\hbar\omega_{0}} \alpha\eta(2 - \eta) \right\} + \lambda_{ap} \sum_{l} e^{-\gamma \left[(b_{l}^{\dagger} + b_{l}) e^{2\alpha_{S}} e^{2\alpha_{S}} \Sigma_{\sigma} n_{i\sigma} - 2h \right]^{2}}$$

$$- \lambda_{ap} \sum_{l} e^{-\gamma \left[(b_{l}^{\dagger} + b_{l}) e^{2\alpha_{S}} e^{2\alpha_{S}} \Sigma_{\sigma} n_{i\sigma} - 2h - \frac{2\sqrt{\alpha}\eta n_{l}}{\hbar\omega_{0}} \right]^{2}} \right.$$

$$+ \lambda_{ap} \sum_{l} e^{-\gamma \left[(b_{l}^{\dagger} + b_{l}) e^{2\alpha_{S}} e^{2\alpha_{S}} \Sigma_{\sigma} n_{i\sigma} - 2h - \frac{4\sqrt{\alpha}\eta n_{l}}{\hbar\omega_{0}} \right]^{2}} \right] \sum_{l} n_{l\uparrow} n_{l\downarrow}$$

$$- t \sum_{l,l > \sigma} e^{(x_{l} - x_{j}) e^{-2\alpha_{S}} e^{-2\alpha_{S}} \Sigma_{\sigma} n_{i\sigma}} e^{(x_{l}' - x_{j}')} c_{l\sigma}^{\dagger} c_{j\sigma}$$

$$+ \hbar\omega_{0} \sum_{l} \left[\frac{e^{4\alpha_{S}}}{4} \left\{ (b_{l}^{\dagger} + b_{l}) e^{2\alpha_{S}} \Sigma_{\sigma} n_{i\sigma} \right\}^{2} - \frac{e^{-4\alpha_{S}}}{4} \left\{ (b_{l}^{\dagger} - b_{l}) e^{-2\alpha_{S}} \Sigma_{\sigma} n_{i\sigma} \right\}^{2} - \frac{1}{2}$$

$$- h(b_{l}^{\dagger} + b_{l}) e^{2\alpha_{S}} e^{2\alpha_{S}} \Sigma_{\sigma} n_{i\sigma} + h^{2} \right] + \lambda_{ap} \sum_{l} e^{-\gamma \left[(b_{l}^{\dagger} + b_{l}) e^{2\alpha_{S}} - 2h \right]^{2}}$$

$$(2.17)$$

where

$$x_{i}' - x_{j}' = \alpha_{d} [(b_{i}b_{i} - b_{i}^{\dagger}b_{i}^{\dagger}) - (b_{j}b_{j} - b_{i}^{\dagger}b_{i}^{\dagger})]$$
 (2.18)

In order to eliminate the phonons, we need to take the expectation value of the Hamiltonian \mathcal{H} in a suitable phonon state. To make the calculation most accurate, we choose the averaging phonon state as:

$$|\Phi_{ph}\rangle = \sum_{n=0}^{M} c_n |\varphi_n(x)\rangle,$$
 (2.19)

where $\varphi_n(x)$ is the n -th excited-state oscillator eigen function in 1D and the coefficients c_n 's are to be obtained variationally. The idea is to start the calculation with M=0 and then keep on increasing the value of M till the energy converges. It may be noted that the canonical transformation procedure followed by the averaging with respect to the phonon state (2.19) described above is same as taking the expectation value of the Hamiltonian (2.1) with respect to the trial variational state

$$|\psi\rangle = e^{-R_1}e^{-R_2}e^{-R_3}e^{-R_4}|\Phi_{nh}\rangle.$$
 (2.20)

We choose units in which $\hbar = \omega_0 = 1$, ω_0 being the dispersionless phonon frequency. The effective electronic Hamiltonian defined by: $H_{eff} = \langle \psi | \mathcal{H} | \psi \rangle$ assumes the following expression:

$$H_{eff} = \varepsilon_{eff} \sum_{i\sigma} n_{i\sigma} - t_{eff} \sum_{\langle ij \rangle \sigma} c_{i\sigma}^{\dagger} c_{j\sigma} + U_{eff} \sum_{i} n_{i\uparrow} n_{i\downarrow} + N \lambda_{ap} E_{1} + N \left(h^{2} - \frac{1}{2} \right)$$

$$+ \frac{N}{4} [S_{2} (1 + 4\alpha_{d} + 12\alpha_{d}^{2}) e^{4\alpha_{s}} - S_{3} (1 - 4\alpha_{d} + 12\alpha_{d}^{2}) e^{-4\alpha_{s}}$$

$$- 4h e^{2\alpha_{s}} S_{1} (1 + 2\alpha_{d} + 3\alpha_{d}^{2})], \qquad (2.21)$$

where

$$\varepsilon_{eff} = -\alpha \eta (2 - \eta) - \sqrt{\alpha} (1 - \eta) [e^{2\alpha_s} S_1 (1 + 2\alpha_d + 3\alpha_d^2) - 2h] + \lambda_{ap} (E_2 - E_1), \quad (2.22)$$

$$t_{eff} = t M_1^2 M_2^2 \,, \tag{2.23}$$

$$U_{eff} = U - 2\alpha\eta(2 - \eta) + \lambda_{ap}(E_1 - 2E_2 + E_3), \tag{2.24}$$

with

$$S_{i} = \sum_{k,l=0}^{M} c_{kl} \int_{-\infty}^{\infty} e^{-y^{2}} \xi_{i}(y) H_{k}(y) H_{l}(y) dy , \qquad (2.25)$$

$$E_{i} = e^{-\gamma \nu_{i}} F \sum_{k,l=0}^{M} c_{kl} \int_{-\infty}^{\infty} e^{(\sqrt{2}\zeta_{i} - y)y} H_{k}(y) H_{l}(y) dy , \qquad (2.26)$$

$$M_1 = \sum_{k,l=0}^{M} c_{kl} e^{-\frac{a^2}{4}} \int_{-\infty}^{\infty} e^{-y^2} H_k \left(y + \frac{a}{2} \right) H_l \left(y - \frac{a}{2} \right) dy , \qquad (2.27)$$

$$M_2 = \sum_{k,l=0}^{M} c_{kl} e^{\alpha_d} \int_{-\infty}^{\infty} e^{-\frac{y^2}{2}(1+\beta^2)} H_k(y) H_l(y\beta) dy, \qquad (2.28)$$

$$F = \sum_{k,l=0}^{M} c_{kl} \int_{-\infty}^{\infty} e^{(2B-1)y^2} H_k(y) H_l(y) dy , \qquad (2.29)$$

where

$$c_{kl} = c_k c_l \sqrt{1/2^{k+l} k! \, l! \, \pi}, \qquad y = \sqrt{x},$$

$$\beta = 1 + 2\alpha_d, \qquad a = \sqrt{2\alpha \eta} e^{-2\alpha_s} (1 - 2\alpha_d + 3\alpha_d^2),$$

$$\xi_1 = \sqrt{2}y, \qquad \xi_2 = 2y^2, \qquad \xi_3 = 2(y^2 - 2l - 1),$$

$$\zeta_i = 2\gamma \nu_i e^{2\alpha_s} (1 + 2\alpha_d + 3\alpha_d^2),$$

$$\nu_1 = 2h, \qquad \nu_2 = 2(h + \sqrt{\alpha}\eta), \quad \nu_3 = 2(h + 2\sqrt{\alpha}\eta),$$

$$B = \gamma e^{4\alpha_s} (1 + 4\alpha_d + 12\alpha_d^2).$$
(2.30)

 ε_{eff} is the renormalized onsite electron energy or in other words the polaron energy, U_{eff} is the renormalized onsite e-e interaction energy and t_{eff} denotes the effective electronic mobility. The GS energy of the system described by the Hamiltonian H_{eff} can be obtained exactly at half-filling with the help of the Bethe ansatz method [32]. The LW solution has however been obtained for $U_{eff} > 0$. We modify the solution to include the results for $U_{eff} \le 0$. To apply the LW result for $U_{eff} < 0$, we may write $U_{eff} = -|U_{eff}|$ and transform the electronic operators as:

$$c_{i\uparrow} \to c_{i\uparrow} \; ; \quad c_{i\downarrow} \to (-1)^i c_{i\downarrow}^{\dagger} \,.$$
 (2.31)

By this transformation, the hopping integral remains same. But the Coulomb interaction term modifies as,

$$U_{eff} \sum_{i} n_{i\uparrow} n_{i\downarrow} \rightarrow -|U_{eff}| \sum_{i} c_{i\uparrow}^{\dagger} c_{i\uparrow} c_{i\downarrow} c_{i\downarrow}^{\dagger} (-1)^{2i}$$

$$= -|U_{eff}| (-1)^{2i} \sum_{i} c_{i\uparrow}^{\dagger} c_{i\uparrow} (1 - c_{i\downarrow}^{\dagger} c_{i\downarrow})$$

$$= -|U_{eff}| \sum_{i} n_{i\uparrow} (1 - n_{i\downarrow})$$

$$= -|U_{eff}| \sum_{i} n_{i\uparrow} + |U_{eff}| \sum_{i} n_{i\uparrow} n_{i\downarrow}$$

$$= -\frac{N}{2} |U_{eff}| + |U_{eff}| \sum_{i} n_{i\uparrow} n_{i\downarrow}. \tag{2.32}$$

Therefore, to consider the attractive e-e interaction contribution, an additional term, $\left(-\frac{u_{eff}}{2}\right)$ is to be added to the GS energy. With this modification, the GS per electron (ε_0) is finally obtained as,

$$\varepsilon_{0} = -J + \frac{1}{4} \left(U_{eff} - \left| U_{eff} \right| \right) + \frac{e^{4\alpha_{s}}}{4} S_{2} (1 + 4\alpha_{d} + 12\alpha_{d}^{2})
- \frac{e^{-4\alpha_{s}}}{4} S_{3} (1 - 4\alpha_{d} + 12\alpha_{d}^{2}) + \left(h^{2} + \lambda_{ap} E_{1} - \frac{1}{2} \right)
- he^{2\alpha_{s}} S_{1} (1 + 2\alpha_{d} + 3\alpha_{d}^{2}) - \int_{0}^{\infty} \frac{4 t_{eff} J_{0}(y) J_{1}(y) dy}{y \left[1 + exp \left(\frac{y \left| U_{eff} \right|}{2 t_{eff}} \right) \right]} ,$$
(2.33)

where

$$J = \alpha \eta (2 - \eta) + \sqrt{\alpha} (1 - \eta) [e^{2\alpha_s} S_1 (1 + 2\alpha_d + 3\alpha_d^2) - 2h] - \lambda_{ap} (E_2 - E_1), \qquad (2.34)$$

and $J_0(y)$ and $J_1(y)$ are the Bessel functions of zeroth order and first order, respectively. ε_0 is finally minimized with respect to the variational parameters to obtain the GS energy.

In order to study the role of the quantum correlation in phase transition, we calculate entanglement entropy for the 1D HH Hamiltonian. Considering a set of four available states $|0\rangle$, $|\uparrow\rangle$, $|\downarrow\rangle$ > and $|\uparrow\downarrow\rangle$, the single-site entanglement entropy is calculated as:

$$E_{\vartheta} = -Tr(\rho_r \log_2 \rho_r), \tag{2.35}$$

where ρ_r is called the reduced density operator given by

$$\rho_r = \omega_e |0\rangle\langle 0| + \omega_\uparrow |\uparrow\rangle\langle \uparrow| + \omega_\downarrow |\downarrow\rangle\langle \downarrow| + \omega_{\uparrow\downarrow} |\uparrow\downarrow\rangle\langle \uparrow\downarrow|, \qquad (2.36)$$

where

$$\omega_{\uparrow\downarrow} = \langle n_{i\uparrow} n_{i\downarrow} \rangle = \omega \quad ; \quad \omega_{\uparrow} = \omega_{\downarrow} = \frac{n}{2} - \omega_{\uparrow\downarrow} \; ; \quad \omega_e = 1 - \omega_{\uparrow} - \omega_{\downarrow} - \omega_{\uparrow\downarrow} \; .$$
 (2.37)

Therefore we obtain the entanglement entropy as,

$$E_{\theta} = -[\omega_e \log_2(\omega_e) + 2\omega_{\uparrow} \log_2(\omega_{\uparrow}) + \omega \log_2(\omega)]. \tag{2.38}$$

Using the Hellmann-Feynman theorem, we get

$$\frac{\partial \varepsilon_0}{\partial U} = \langle n_{i\uparrow} n_{i\downarrow} \rangle. \tag{2.39}$$

Thus all the occupation numbers can be calculated and the corresponding Von-Newman entanglement entropy (E_{ϑ}) is evaluated.

The mean-square spin angular momentum per site (L_0) can be defined as:

$$L_0 = \frac{1}{N} \sum_{i} \langle S_i^2 \rangle , \qquad (2.40)$$

where S_i is the electron spin at site i, $S_i^2 = S_{ix}^2 + S_{iy}^2 + S_{iz}^2$. Using $S_i^{\pm} = S_{ix} \pm iS_{iy}$, $S_i^z = \frac{1}{2}(n_{i\uparrow} - n_{i\downarrow})$, $S_i^+ = c_{i\uparrow}^{\dagger}c_{i\downarrow}$, $S_i^- = c_{i\downarrow}^{\dagger}c_{i\uparrow}$, $S_i^+ \cdot S_i^- = -n_{i\uparrow}n_{i\downarrow}$, $n_{i\uparrow}^2 = n_{i\uparrow}$, $n_{i\downarrow}^2 = n_{i\downarrow}$, we may obtain, $\langle S_i^2 \rangle = \frac{3}{4} - \frac{3}{2} \langle n_{i\uparrow}n_{i\downarrow} \rangle$. Therefore,

$$L_0 = \frac{3}{4} - \frac{3}{2N} \sum_{i} \langle n_{i\uparrow} n_{i\downarrow} \rangle = \frac{3}{4} - \frac{3}{2} \frac{d\varepsilon_0}{dU}.$$
 (2.41)

where use has been made of Eq. (2.39). L_0 gives a measure of the spin magnetic moment and will be loosely referred to as the spin moment. For a completely un-correlated electron gas, we can write: $\langle n_{i\uparrow}n_{i\downarrow}\rangle = \langle n_{i\uparrow}\rangle\langle n_{i\downarrow}\rangle$, and so the average spin moment per site (L_0) is 0.375.

2.3 Numerical results and discussions

2.3.1 Ground State (GS) Energy

The single-site GS energy is determined by varying ε_0 in the space of the variational parameters. The minimum value of ε_0 gives the GS energy. The result (Fig. 2.1) shows that for $\lambda = 0.1$ and $\gamma = 0.05$, though the new transformation (2.15) has only a marginal effect on the GS energy, it has a discernible effect on the phase diagram.

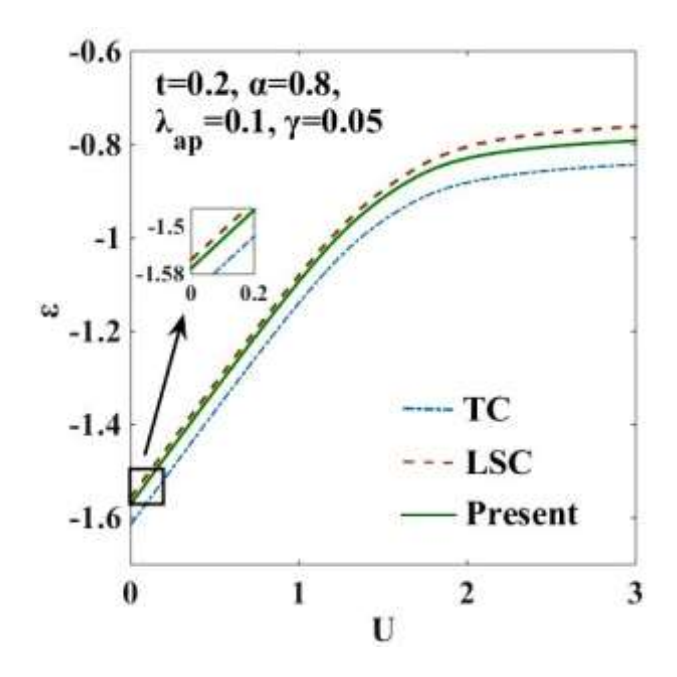


Fig. 2.1: Single-site GS energy (ε) vs. onsite Coulomb energy (U).

The variations of the effective hopping integral (t_{eff}) and the effective onsite e-e interaction energy (U_{eff}) are respectively studied in Figs. 2.2 (a) and 2.2 (b) with respect to the onsite e-e interaction energy (U) for the different strengths of the e-p coupling constant (α) . As expected, for $\alpha=0$, the effective hopping integral, t_{eff} becomes equal to the bare Hubbard hopping parameter t and the U_{eff} becomes equal to the Hubbard U. As e-p coupling constant increases, t_{eff} decreases and with the increase in U, it gradually increases and saturates to the Hubbard value. At small values of the onsite e-e interaction U, the effective attractive e-e interaction induced by e-p interaction overcomes the repulsive e-e interaction U and the effective onsite e-e interaction U_{eff} becomes negative i.e., attractive. The lattice is then unstable against the Peierls transition in which bound states of singlet bipolarons form on every alternate site leading to an insulating phase called the CDW state. On the contrary, when U is larger compared to α , the repulsive U wins, and the polarons cannot hop from one site to the other and consequently the GS of the system is given by the anti-ferromagnetic

mott-insulator state which is also known as SDW. Fig. 2.2(a) shows that in the weak e-p coupling regime, the variation of t_{eff} and U_{eff} with U is continuous. But for higher values of α , discontinuous jumps occur in the behaviour of t_{eff} and U_{eff} . The discontinuous jump corresponds a direct CDW-SDW transition.

In order to examine the nature of the transition between the two phases observed in Figs. 2.2(a) and 2.2(b), the quantity, (dt_{eff}/dU) is plotted in Fig. (2.3) with respect to U for $\alpha = 0.05, 0.08$ and 1.0. The double-peak structure in (dt_{eff}/dU) is clearly evident. One can also observe that the peaks grow in height and shift towards larger values of U with increasing α . Furthermore, the new transformation used in the present calculation broadens the width between the two peaks in Fig. (2.3). Corresponding to the peak values of the (dt_{eff}/dU) vs. U plot, the phase-diagram is drawn in the $(\alpha - U)$ plane. This is shown in Fig. (2.4).

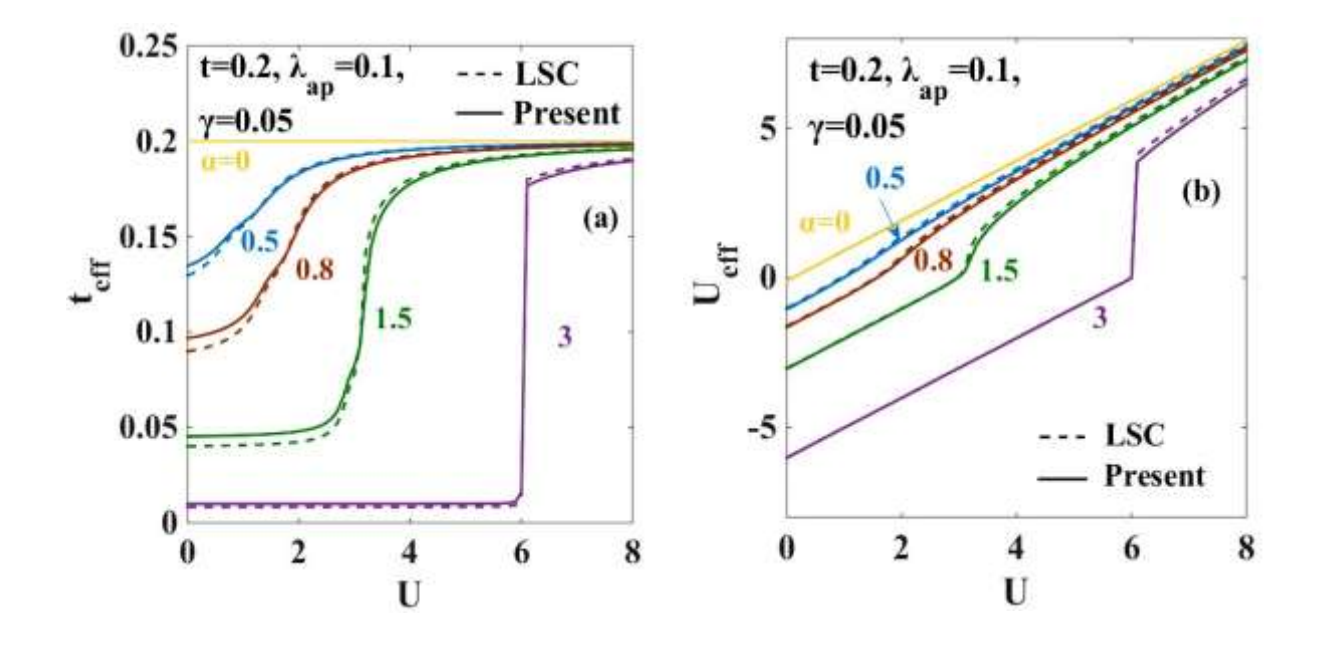


Fig. 2.2: (a) t_{eff} vs U; (b) U_{eff} vs U.

The intermediate phase satisfies the condition: $4t_{eff} \ge U_{eff}$, which is the signature of a metallic or a conducting phase. The metallic phase is flanked by the SDW phase on the left and the CDW phase on the right. The figure shows that intermediate MP appearing at the CDW-SDW cross-over region is now wider compared to that predicted by LSC [28]. It is important to emphasize that it is not important by how much the present modified

variational wave function broadens the width of the intermediate MP, that the improved variational calculation widens intervening MP is itself a result of great significance.

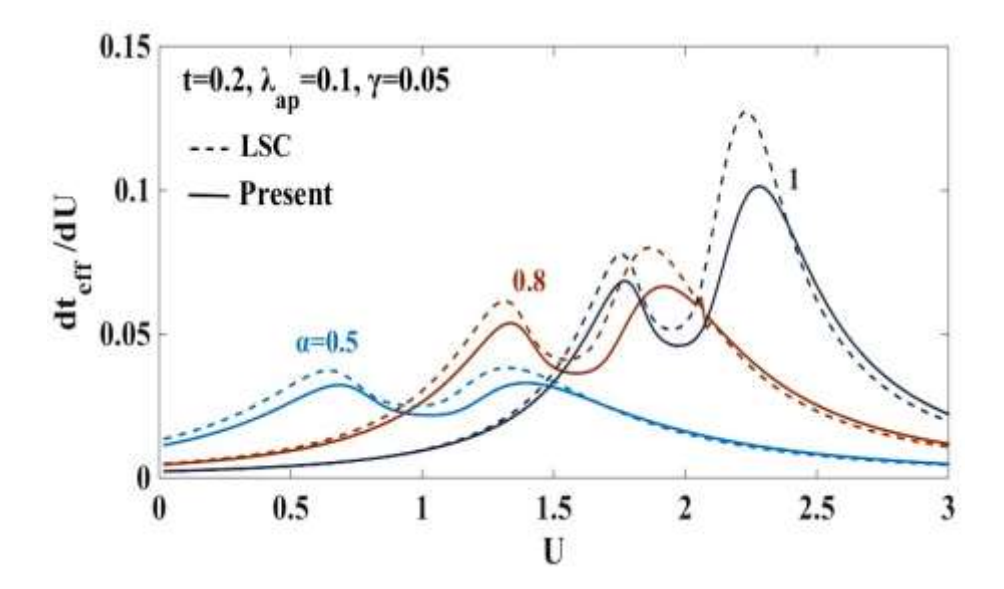


Fig. 2.3: dt_{eff}/dU vs. U for $\alpha = 0.5$, 0.8, 1.0.

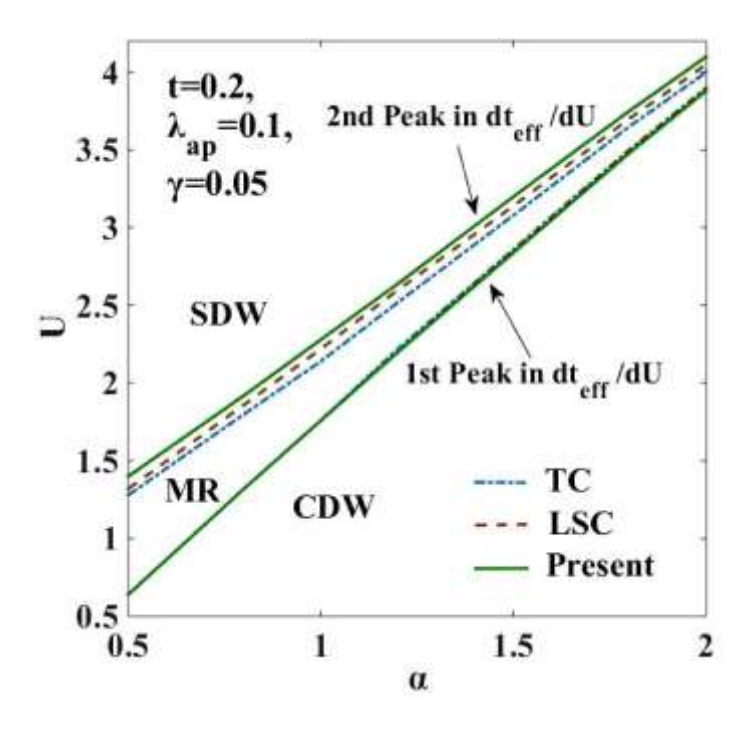


Fig. 2.4: Phase diagram in the $(\alpha - U)$ – plane.

The reason is simple. If a modified variational wave function predicts a narrower intermediate MP, it will have a disastrous effect on the prediction of the existence of

intermediate MP because one may then argue that the MP may as well collapse if a more improved variational calculation is performed. That with every improved variational calculation, the metallic phase widens is indeed an encouraging result.

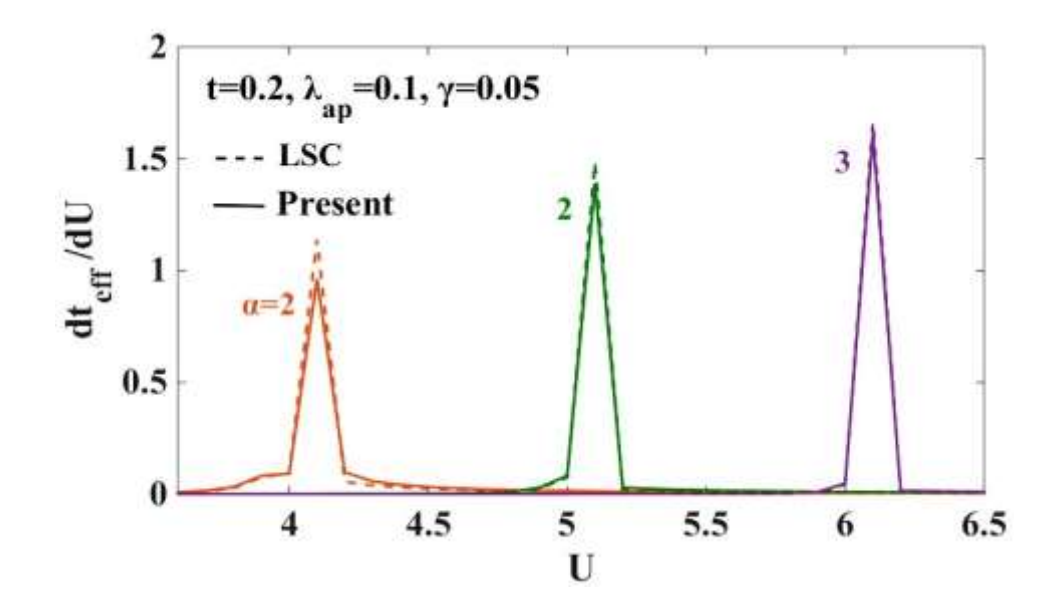


Fig. 2.5: dt_{eff}/dU vs. U for $\alpha = 2.0$, 2.5, 3.0.

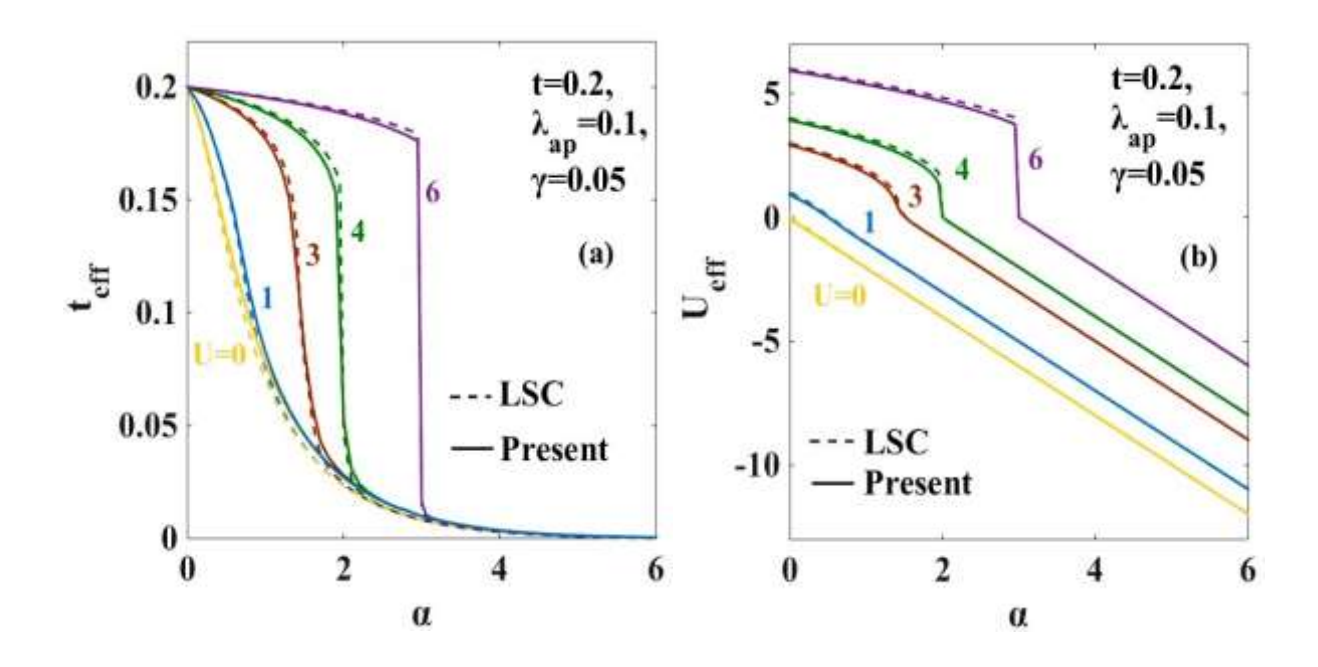


Fig. 2.6: (a) t_{eff} vs. α ; (b) U_{eff} vs α .

In Fig. (2.5), we plot (dt_{eff}/dU) with U for larger values of α . We find that the double peak structure almost disappears as α increases and one can observe from Fig. (2.5) that for

 $\alpha > 2$, only a single peak structure appears. This indicates the absence of any intermediate phase for large α . Figs. 2.6 (a) and 2.6 (b) illustrate respectively the behaviour of t_{eff} and U_{eff} as a function of α . As $\alpha \to 0$, $t_{eff} \to t$. Thus at low α , the system GS is in the SDW phase. As α increases, t_{eff} gradually decreases and finally falls off to zero.

Fig. 2.6(b) tells us that corresponding U_{eff} becomes maximally negative. This indicates the formation of massive singlet bipolarons giving rise to the CDW phase. Here also we see that for large U, SDW-CDW transition is again direct.

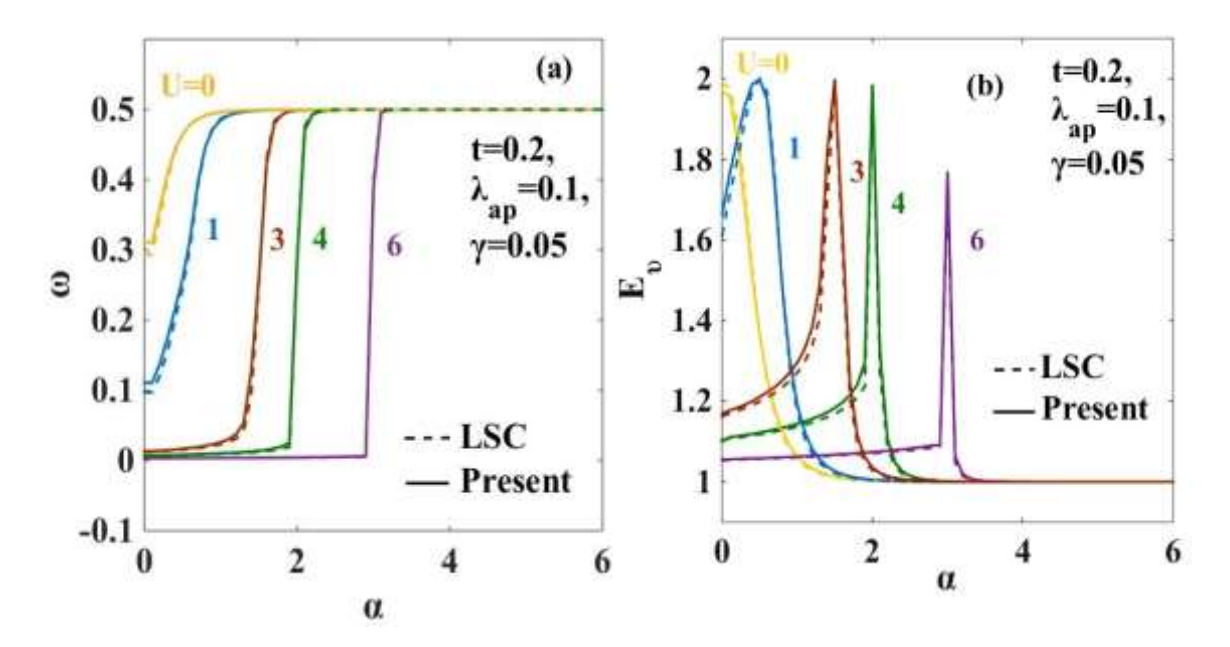


Fig. 2.7: (a) ω vs. α ; (b) entanglement entropy (E_{ν}) vs. α .

In Figs. 2.7(a) and 2.7(b), we plot respectively the double occupancy (ω) and quantum entanglement entropy (E_{ν}) as a function of α . The entanglement entropy (EE) gives a measure of the accessible states the system can have. Obviously then, the maximum in entanglement entropy would correspond to a conducting state. It is observed that for certain combinations of α and U, E_{ν} has maxima and for other values E_{ν} becomes very small. Small values of entanglement entropy correspond to insulating states. When e-p interaction becomes strong compared to the e-e interaction, the electrons form pairs and the double occupancy parameter ω reaches the maximum value 0.5 driving the system to the CDW state. For $\omega < 0.5$, the formation of polaronic SDW state takes place. Similar behaviour is

observed in Figs. 2.8(a) and 2.8(b) when we plot the double occupancy (ω) and quantum entanglement entropy (E_{ν}) with respect to U for different values of e-p interaction (α).

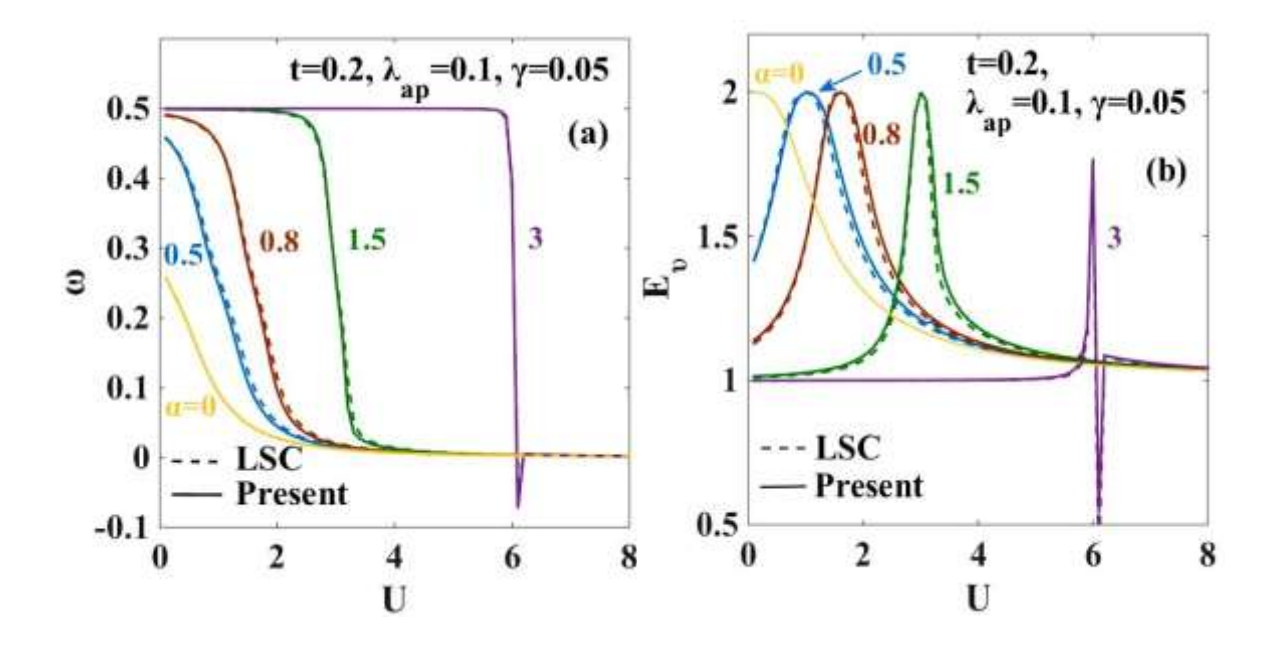


Fig. 2.8: (a) ω vs. α ; (b) E_{ν} vs. α .

In order to unravel the effect of e-e and e-p interaction simultaneously, we plot 3D graphs in Figs. 2.9. Fig. 2.9(a) shows that between the SDW and CDW phases, there lies a region where the value of ω neither corresponds to the SDW region with $\omega=0$ nor to the CDW region with $\omega=0.5$. Therefore, the effect of e-p and e-e interactions has been found simultaneously on ω and E_{ν} . This intermediate cross-over region corresponds to metallic phase. In Fig. 3.9(b), the peak of entanglement entropy (E_{ν}) lies over the metallic region in the $(\alpha-U)$ plane. Therefore, the peak denotes the MP.

We have already emphasized that for a metallic state the bandwidth follows the criterion: $2zt_{eff} \geq U_{eff}$. In Fig. 2.10, we present a 3D representation of $|U_{eff}|$ and $4t_{eff}$ with respect to U and α . The figure displays a region of (α, U) where the condition: $4t_{eff} \geq U_{eff}$ is satisfied. This is the metallic phase. There are two other regions in the $(\alpha - U)$ – plane where this condition is not satisfied and those are insulating phases. Among them the phase where $U_{eff} > 0$ corresponds to the SDW phase and the one where $U_{eff} < 0$ corresponds to the CDW state.

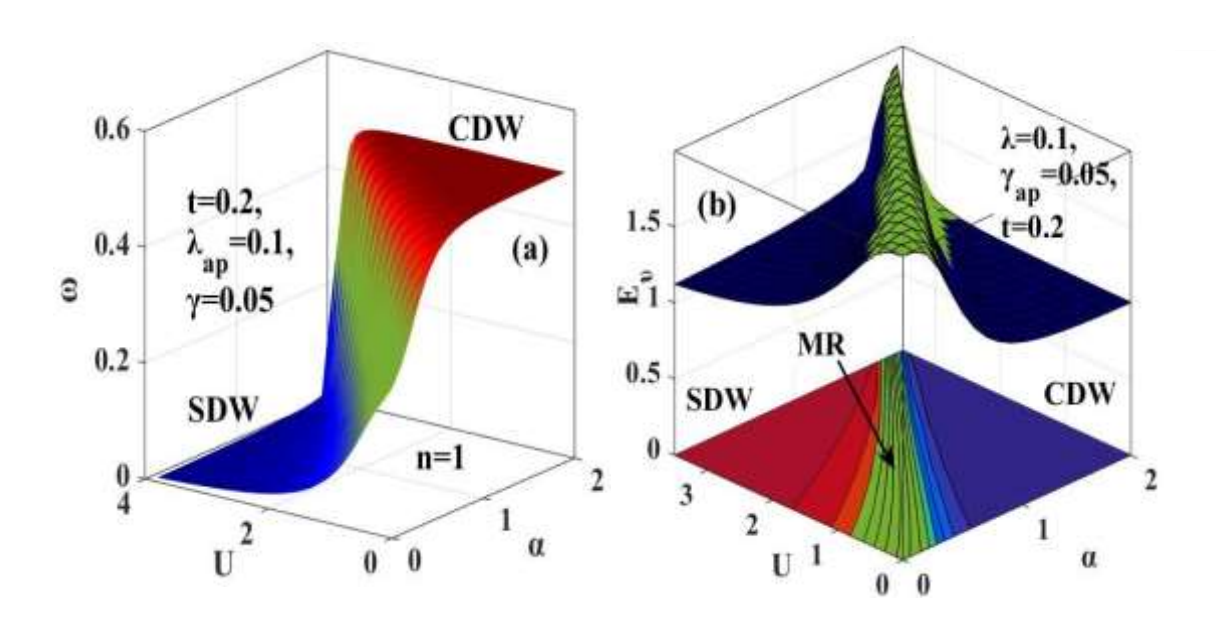


Fig. 2.9 (a) 3D plot of ω with respect ro α and U; (b) 3D plot of E_{ν} with respect to α and U.

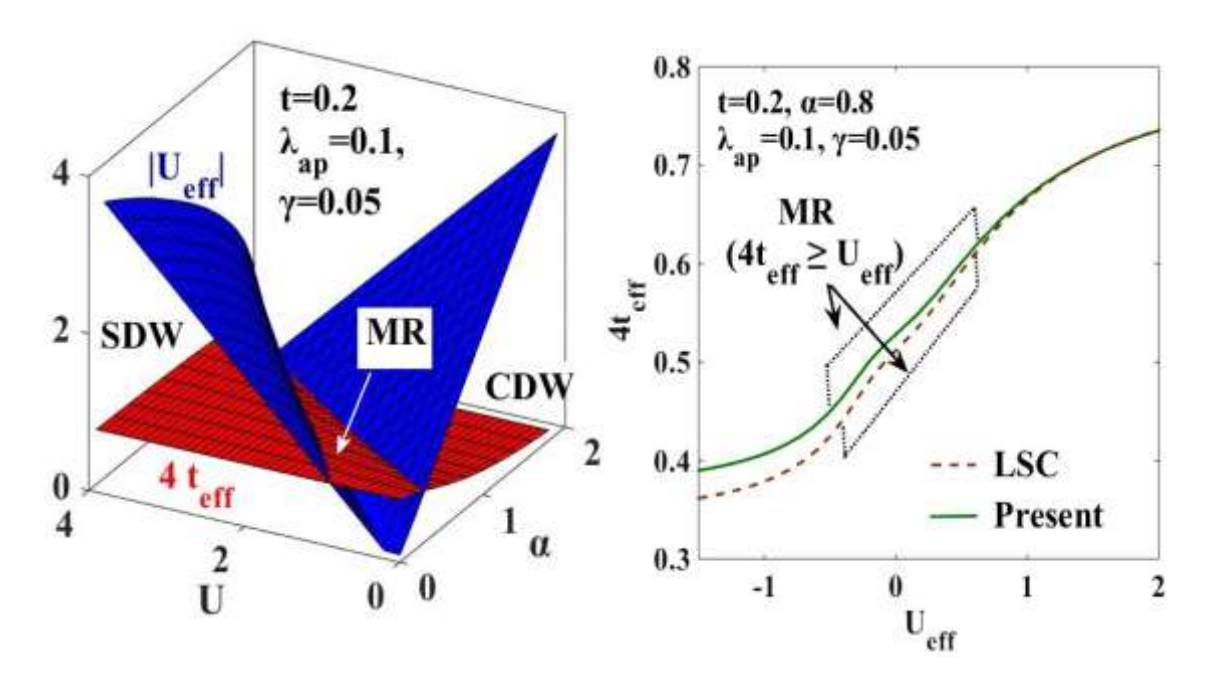


Fig. 2.10: 3D plots of $4t_{eff}$ and $|U_{eff}|$ with respect to α and U.

Fig. 2.11: $4t_{eff}$ vs U_{eff} .

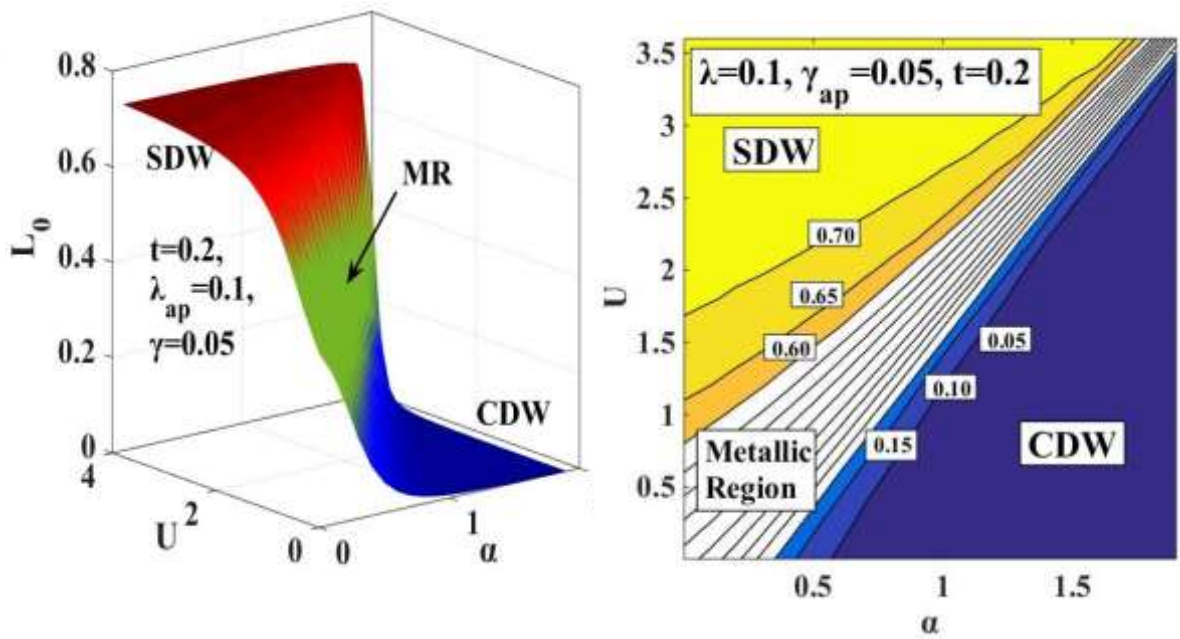


Fig. 2.12 L_0 with respect to α and U.

Fig. 2.13 Contour plot of L_0 in the $(\alpha - U)$ – plane

In order to look into MP by the Mott-Hubbard (MH) criteria more directly, $4t_{eff}$ is plotted in Fig. 2.11, with respect to U_{eff} and the region that satisfies the MH condition is indicated by the dotted line. It is observed that the region satisfying the MH criterion is more extended in the present work than the LSC's result, which again confirms the broadening of the intermediate MP.

The local spin moment (L_0) is calculated using Eq. (2.41) and plotted in Fig. (2.12) with respect to α and U and in Fig. (2.13), the contour plots for constant L_0 are drawn in the ($\alpha - U$) plane. Both the figures indicate the presence of the intermediate MP which is consistent with the phase diagram. The contour plot in LSC's work predicts MP to lie between $L_0 = 0.25$ and $L_0 = 0.50$ while the present calculation shows an extended MP that lies between $L_0 = 0.15$ and $L_0 = 0.60$. One can make the same observation from the local spin moment calculation that re-establishes the broadening of intermediate MP between the CDW and SDW regions.

2.4 Conclusion

The nature of SDW-CDW transition has been studied in a 1D half-filled HH model with Gaussian phonon anharmonicity by improving the variational calculation of Lavanya et al.

[28]. Using a number of unitary transformations performed in succession followed by a generalized many-phonon averaging an effective electronic Hamiltonian is obtained. The phonon-subsystem has been treated in a semi-exact way. The effective electronic Hamiltonian has been solved exactly using the BA technique to obtain the GS energy. The hopping integral and the Coulomb correlation are renormalized by the e-p interaction and phonon anharmonicity. Using the Mott-Hubbard criterion we have shown that the present modified approach broadens the width of intermediate MP reported by Lavanya et al. [28]. The same conclusion has been drawn from the calculation of the local spin moment and double occupancy. Finally a study of quantum entanglement entropy and the double occupancy parameter reconfirms the existence of a wider IMP at the SDW-CDW transition region.

2.5 References

- [1] K. A. Müller, Physica C **341**, 11–18 (2000).
- [2] Y. H. Kim, A. J. Heeger, L. Acedo, G. Stucky, & F. Wudl, Phys. Rev. B **36**, 7252–7255 (1987).
- [3] B. K. Chakraverty, D. Feinberg, Z. Hang, & M. Avignon, Sol. State. Commun. **64**, 1147–1151 (1987).
- [4] A. S. Alexandrov, Phys. Rev. B 38, 925–927 (1988).
- [5] R. Micnas, J. Ranninger, S. Robaszkiewicz, Rev. Mod. Phys. 62 113 (1990).
- [6] S. Sil and A. Chatterjee, Int. J. Mod. Phys. B 4 1879 (1990).
- [7] S. Sil S and A. Chatterjee, Mod. Phys. Lett. B **6** 959 (1992).
- [8] N. M. Plakida, Physica C **162–164**, 1341–1342 (1989).
- [9] E. Fradkin, J. E. Hirsch, Phys. Rev. B 27 4302 (1983).
- [10] M. Tezuka, R. Arita, H. Aoki, Phys. Rev. Lett. 95 226401 (2005).
- [11] M. Tezuka, R. Arita, H. Aoki, Phys. Rev. B 76 155114 (2007).
- [12] K. M. Tam, S. W. Tsai, D. K. Cambell, A. H. C. Neto, Phys. Rev. B **75** 161103 (R) (2007).
- [13] Y. Takada, A. Chatterjee, Phys. Rev. B **67** 081102 (R) (2003).
- [14] R. T. Clay, R. P. Hardikar, Phys. Rev. Lett. **95**, 096401 (2005).
- [15] R. P. Hardikar, R. T. Clay Phys. Rev. B. **75**, 245103 (2007).

- [16] H. Fehske, G. Hager, E. Jeckelmann, Europhys. Lett. **84** 57001(2008).
- [17] Y. Wang, I. Esterlis, T. Shi, C. J. Ignacio, E. Demler, Phys. Rev. Research 2, 043258 (2020).
- [18] H. Bakrim, C. Bourbonnais, Phys. Rev. B 91 085114 (2015).
- [19] E. A. Nowadnick, S. Johnston, B. Moritz, R. T. Scalettar, T. P. Devereaux, Phys. Rev. Lett. **109** 246404 (2012).
- [20] A. Payeur, D. Senechal, Phys. Rev. B 83 033104 (2011).
- [21] A. Chatterjee & Y. Takada, J. Phys. Soc. Jap. **73**, 964–969 (2004).
- [22] D. Mihailovic, C. M. Foster, K. Voss, A. J. Heeger, Phys. Rev. B 42, 7989–7993 (1990).
- [23] S. D. Conradson, I. D. Raistrick, A. R. Bishop, Science **248**, 1394–1398 (1990).
- [24] J. M. de Leon, S. D. Conradson, I. Batistic, A. Bishop, Phys. Rev. Lett. **65**, 1675–1678 (1990).
- [25] H. A. Mook, B. C. Chakoumakos, M. Mostoller, Phys. Rev. Lett. 69, 2272–2275 (1992).
- [26] H. A. Mook, M. Mostoller, J. A. Harvey, N. W. Hill, B. C. Chakoumakos, B. C. Sales, Phys. Rev. Lett. **65**, 2712–2715 (1990).
- [27] J. Konior, Phys. Rev. B 47, 14425–14433 (1993).
- [28] C. U. Lavanya, I. V. Sankar, A. Chatterjee, Sci Rep. 7, 3774 (2017).
- [29] I. G. Lang & Yu. A. Firsov, **43**, 1843-1860 (1962), Soviet Phys. JETP **16**, 1301–1314 (1963).
- [30] H. Zheng, Phys. Lett. A **131** (1988) 115.
- [31] Z. M. Malik, S. Mukhopadhyay, A. Chatterjee, Phys. Lett. A, 383, 1516-1519 (2019).
- [32] E. H. Lieb, & F. Y. Wu, Phys. Rev. Lett. 20, 1445–1448 (1968).

"I am now convinced that theoretical physics is actual philosophy" . . . Max $\ensuremath{\text{Born}}$

3

An analytical study of the phase diagram of a two-dimensional Extended Holstein-Hubbard model: a mean-field study

3.1 Introduction

Strongly correlated e-p systems exhibit intriguing properties due to the interplay of various interactions. The e-e Coulomb repulsion and the phonon-mediated attractive e-e interaction lead to spin fluctuations and enhance the charge and spin correlations in these systems. These correlations have been studied extensively in the context of phonon mechanism of superconductivity [1-3]. Though the phonon mechanism was advocated by several researchers for inducing pairing in cuprates [4-9], it ran into difficulty because of the following reason. It is well known that in a correlated e-p system, different ground state (GS) phases, known as SDW and CDW states, are possible based on the relative strengths of the different interactions present in the system.

As described in chapter 1, several investigations on the HH model have shown the existence of the SDW-CDW transition. Though a few researchers have claimed the transition to be direct [10], many investigators have reported the existence of an intermediate metallic phase in between the two insulating states [11-21]. All these calculations were however restricted to 1D systems, though the real systems of interest in the context of high– T_C superconductivity are doped cuprate materials [22-24], transition-metal dichalcogenides [25-27] and other correlated systems [28-32] which are essentially two-dimensional.

Berger et al. [28] have extensively studied the one and two-dimensional (2D) HH model to examine of the detailed characteristics of the quantum SDW-CDW transition. Hohenadler and Batrouni [29] have shown through a quantum Monte Carlo (QMC) study of the square lattice that there is a possibility of a strongly correlated region in between the spin-density and charge-density phases, which can be either metallic or superconducting. In a recent investigation of the 2D HH system, Wang et al. [30] have shown using a non-Gaussian exact diagonalization method, the presence of an intermediate phase in between the spin and charge-order states. Here, too, the intermediate phase shows a metallic or superconducting behaviour at weak coupling. Costa et al. [31] have analysed the 2D HH model and obtained a rich phase diagram for a square lattice containing anti-ferromagnetic Mott-insulator and CDW phases. Using auxiliary-field quantum Monte Carlo and finite temperature determinant quantum Monte Carlo techniques, they have observed a correlated metallic phase at the crossover region of the SDW and CDW phases. Very recently, Yirga et al. [32] have considered the 2D Hubbard system with the Holstein phonon modes through the Su-Schrieffer-Heeger model and studied the anti-ferromagnetic Mott-insulator-CDW transition by calculating the renormalized quasi-particle weight using the functional renormalization group technique. Their calculation also suggests the presence of a conducting phase flanked by two insulating phases. Since all the aforementioned investigations of the 2D HH model are numerical, we wish to analytically examine the transition region so that the underlying physics of the system becomes more transparent.

We purport to consider, in the present paper, an extended HH model with the nearest neighbour (NN) and next nearest neighbour (NNN) electronic correlations for a 2D square lattice. The e-p interaction is first eliminated from the system by choosing an appropriate phonon state, which gives rise to an effective electronic Hamiltonian with modified Hubbard parameters namely the effective hopping parameter and effective online Coulomb correlation energy. In the case of the weak effective correlation, the problem is solved by employing the Hartree-Fock (HF) mean-field (MF) technique and for large effective on-site correlation, we transform the effective electronic Hamiltonian to the t-J model and solve the problem using the Zubarev Green function technique. Combining the results of both the regimes, we obtain the phase diagram for the whole range of the interaction strength and analyse the properties of the different phases using the Mott-Hubbard (MH) criterion.

3.2 Model and formulation

An extended HH model can be written in 2D as

$$H = H_e + H_p + H_{ep} \,, \tag{3.1}$$

with

$$H_{e} = -t \sum_{\langle ij \rangle \sigma} c_{i\sigma}^{\dagger} c_{j\sigma} + U \sum_{i} n_{i\uparrow} n_{i\downarrow} + V_{1} \sum_{\langle ij \rangle \sigma\sigma'} n_{i\sigma} n_{j\sigma'} + V_{2} \sum_{i\delta''\sigma\sigma'} n_{i\sigma} n_{i+\delta',\sigma'} + V_{3} \sum_{i\delta''\sigma\sigma'} n_{i\sigma} n_{i+\delta'',\sigma'},$$

$$(3.2)$$

$$H_p = \hbar \omega_0 \sum_i b_i^{\dagger} b_i \,, \tag{3.3}$$

$$H_{ep} = g_1 \sum_{i\sigma} n_{i\sigma} (b_i + b_i^{\dagger}) + g_2 \sum_{i\delta\sigma} n_{i\sigma} (b_{i+\delta} + b_{i+\delta}^{\dagger}). \tag{3.4}$$

Here H_e describes the extended Hubbard Hamiltonian where the parameter t denotes the NN hopping integral, $n_{i\sigma}(=c_{i\sigma}^{\dagger}c_{i\sigma})$ represents the number operator for the spin- σ electron at the i-th site, $c_{i\sigma}^{\dagger}(c_{i\sigma})$ being the corresponding electron creation (annihilation) operator, and U, V_1, V_2 and V_3 give the onsite, nearest neighbour (NN), next nearest neighbour (NNN) and next to next nearest neighbour (NNNN) Coulomb interaction energies respectively, H_p is the phonon Hamiltonian, $b_i^{\dagger}(b_i)$ being the creation (annihilation) operator for an optical phonon at the i-th site with dispersionless frequency ω_0 and H_{ep} is the extended Holstein EPI, g_1 and g_2 being the on-site and NN EPC strengths, respectively. We will write: $g_1 = \sqrt{\alpha}$, where α is the onsite e-p coupling constant.

To disentangle the e-p coupling term, the Lang-Firsov transformation (LFT) [33] has been used extensively in the past. This transformation lowers the energy by displacing the phonon vacuum. The phonon state then becomes a coherent superposition of states with different phonon numbers. Several studies on the HH model [16-21, 34, 35] and the Anderson-Holstein model [36, 37] have shown that the variational LFT (VLFT) method is more useful. We, therefore, employ VLFT to transform the extended HH model with the generator,

$$R_1 = \frac{g_1'}{\omega_0} \sum_{i\sigma} n_{i\sigma} (b_i^{\dagger} - b_i) + \frac{g_2'}{\omega_0} \sum_{i\delta\sigma} n_{i\sigma} (b_{i+\delta}^{\dagger} - b_{i+\delta}) , \qquad (3.5)$$

where $g_1' = \eta_1 \sqrt{\alpha}$ and $g_2' = \eta_2 \sqrt{\alpha}$, η_1 and η_2 being the variational parameters. g_1' gives essentially a measure of the depth of the on-site lattice polarization potential created by the EPI and g_2' represents the width of the polaron potential well. The VLFT transforms the Hamiltonian H to $H_1 = e^{R_1}He^{-R_1}$. Using the Baker-Campbell-Hausdorff (BCH) formula we may calculate the transformed Hamiltonian as,

$$H_1 = H + [R_1, H] + \frac{1}{2!} [R_1, [R_1, H]] + \cdots$$
(3.6)

$$= -t \sum_{\langle ij \rangle \sigma} c_{i\sigma}^{\dagger} c_{j\sigma} e^{(x_{i}-x_{j})} + \widetilde{U} \sum_{i} n_{i\uparrow} n_{i\downarrow} + \widetilde{V}_{1} \sum_{\langle ij \rangle \sigma\sigma'} n_{i\sigma} n_{j\sigma'} + \widetilde{V}_{2} \sum_{i\delta'\sigma\sigma'} n_{i\sigma} n_{i+\delta',\sigma'}$$

$$+ \widetilde{V}_{3} \sum_{i\delta''\sigma\sigma'} n_{i\sigma} n_{i+\delta'',\sigma'} + \omega_{0} \sum_{i} b_{i}^{\dagger} b_{i} + \varepsilon \sum_{i\sigma} n_{i\sigma} + P_{1} \sum_{i\sigma} n_{i\sigma} (b_{i} + b_{i}^{\dagger})$$

$$+ P_{2} \sum_{i\delta\sigma} n_{i\sigma} (b_{i+\delta} + b_{i+\delta}^{\dagger}) , \qquad (3.7)$$

where,

$$x_{i} - x_{j} = \frac{g_{1}'}{\omega_{0}} (b_{i}^{\dagger} - b_{i}) + \frac{g_{2}'}{\omega_{0}} \sum_{\delta'} (b_{i+\delta'}^{\dagger} - b_{i+\delta'}), \tag{3.8}$$

$$\widetilde{U} = U - \frac{2}{\omega_0} [2(g_1 g_1' + z g_2 g_2') - (g_1'^2 + z g_2'^2)], \qquad (3.9)$$

$$\tilde{V}_1 = V_1 - \frac{2}{\omega_0} [(g_1 g_2' + g_1' g_2) - g_1' g_2'], \tilde{V}_2 = V_2 - \frac{1}{\omega_0} [2g_2 g_2' - g_2'^2], \tilde{V}_3 = V_3, \quad (3.10)$$

$$\varepsilon = -\left[\frac{2}{\omega_0}(g_1g_1' + zg_2g_2') - \frac{1}{\omega_0}(g_1'^2 + zg_2'^2)\right],\tag{3.11}$$

$$P_1 = g_1 - g_1', \quad P_2 = g_2 - g_2'.$$
 (3.12)

An electron can be considered as a phonon-source. As an electron makes an emission of a phonon, it undergoes a recoil motion and during its action of recoiling, if it releases another phonon, then these two phonons would have a built-in correlation. This phonon-correlation effect can be incorporated by considering a squeezing transformation (or Bogolubov transformation as it is more commonly referred to in condensed matter physics) with a generator [38]:

$$R_2 = \alpha_s \sum_i (b_i b_i - b_i^{\dagger} b_i^{\dagger}), \qquad (3.13)$$

where α_s gives a measure of the phonon correlation and is called a squeeze parameter and will be treated as a variational parameter. The squeezing transformation transforms H_1 to $H_2 = e^{R_2}H_1e^{-R_2}$. The transformed Hamiltonian is obtained as,

$$H_{2} = -t \sum_{\langle ij \rangle \sigma} c_{i\sigma}^{\dagger} c_{j\sigma} e^{(x_{i} - x_{j})e^{-2\alpha_{S}}} + \widetilde{U} \sum_{i} n_{i\uparrow} n_{i\downarrow} + \widetilde{V}_{1} \sum_{\langle ij \rangle \sigma\sigma'} n_{i\sigma} n_{j\sigma'} + \widetilde{V}_{2} \sum_{i\delta'\sigma\sigma'} n_{i\sigma} n_{i+\delta',\sigma'}$$

$$+ \widetilde{V}_{3} \sum_{i\delta''\sigma\sigma'} n_{i\sigma} n_{i+\delta'',\sigma'} + \varepsilon \sum_{i\sigma} n_{i\sigma}$$

$$+ \omega_{0} \left[\frac{e^{4\alpha_{S}}}{4} \sum_{i} (b_{i} + b_{i}^{\dagger})^{2} - \frac{e^{-4\alpha_{S}}}{4} \sum_{i} (b_{i} - b_{i}^{\dagger})^{2} \right] + P_{1} e^{2\alpha_{S}} \sum_{i\sigma} n_{i\sigma} (b_{i} + b_{i}^{\dagger})$$

$$+ P_{2} e^{2\alpha_{S}} \sum_{i\delta\sigma} n_{i\sigma} (b_{i+\delta} + b_{i+\delta}^{\dagger}) + \frac{N\omega_{0}}{2}.$$

$$(3.14)$$

Since the average phonon correlation in the phonon function is expected to depend on the electron concentration at the lattice sites, Malik, Mukhopadhyay and Chatterjee (MMC) [19] have recently suggested that an increase in the electron concentration would increase the average phonon correlation. This immediately implies that R_2 should at least partially depend on the electron concentration. MMC [19] have introduced a new unitary transformation to incorporate this density-dependent phonon correlation effect. Chatterjee and collaborators have subsequently used this transformation in a more improved work [20] and also in a related problem [21] to lower the GS energy. We apply this density-dependent squeezing transformation to H_2 with the generator

$$R_3 = \alpha_d \sum_i n_{i\sigma} (b_i b_i - b_i^{\dagger} b_i^{\dagger}), \qquad (3.15)$$

where α_d is to be obtained variationally. The new Hamiltonian is now given by: $H_3 = e^{R_3}H_2e^{-R_3}$ which can be written as,

$$\begin{split} H_{3} &= -t \sum_{\langle ij \rangle \sigma} c_{i\sigma}^{\dagger} c_{j\sigma} e^{(x_{i} - x_{j})} e^{-2\alpha_{s} - 2\alpha_{d} \sum_{\sigma} n_{i\sigma}} e^{\left(x_{i}' - x_{j}'\right)} + \widetilde{U} \sum_{i} n_{i\uparrow} n_{i\downarrow} + \widetilde{V}_{1} \sum_{\langle ij \rangle \sigma\sigma'} n_{i\sigma} n_{j\sigma'} \\ &+ \widetilde{V}_{2} \sum_{i\delta'\sigma\sigma'} n_{i\sigma} n_{i+\delta',\sigma'} + \widetilde{V}_{3} \sum_{i\delta''\sigma\sigma'} n_{i\sigma} n_{i+\delta'',\sigma'} + \varepsilon \sum_{i\sigma} n_{i\sigma} \\ &+ \omega_{0} \left[\frac{e^{4\alpha_{s}}}{4} \sum_{i} \left[\left(b_{i} + b_{i}^{\dagger}\right) e^{2\alpha_{d} \sum_{\sigma} n_{i\sigma}} \right]^{2} - \frac{e^{-4\alpha_{s}}}{4} \sum_{i} \left[\left(b_{i} - b_{i}^{\dagger}\right) e^{-2\alpha_{d} \sum_{\sigma} n_{i\sigma}} \right]^{2} \right] \end{split}$$

$$+P_{1}e^{2\alpha_{s}}\sum_{i\sigma}n_{i\sigma}e^{2\alpha_{d}\sum_{\sigma}n_{i\sigma}}\left(b_{i}+b_{i}^{\dagger}\right)+P_{2}e^{2\alpha_{s}}\sum_{i\delta\sigma}n_{i\sigma}e^{2\alpha_{d}\sum_{\sigma}n_{i\sigma}}\left(b_{i+\delta}+b_{i+\delta}^{\dagger}\right)$$

$$+\frac{N\omega_{0}}{2}.$$
(3.16)

Here,
$$x_i' - x_j' = \alpha_d [(b_i b_i - b_i^{\dagger} b_i^{\dagger}) - (b_j b_j - b_j^{\dagger} b_j^{\dagger})].$$

Finally, we consider correlation between phonons at different sites. This can be incorporated by correlated squeezing transformation. However, we consider only NN phonon correlation. Following Lo and Sollie [39], the generator of the correlated squeezing transformation is chosen as,

$$R_4 = \frac{1}{2} \sum_{i \neq j} \beta_{ij} \left(b_i b_j - b_i^{\dagger} b_j^{\dagger} \right). \tag{3.17}$$

Here we choose, $\beta_{ij} = \beta$, when i and j are NN and $\beta_{ij} = 0$, otherwise. The parameter β is obtained variationally. The Hamiltonian after the above transformation becomes: $\mathcal{H} \equiv H_4 = e^{R_4}H_3e^{-R_{4_4}}$. To calculate the transformed Hamiltonian, we have to calculate the transformed phonon operators using BCH formula which gives

$$\begin{split} \tilde{b}_{i} &= e^{R_{4}}b_{i}e^{-R_{4}} = b_{i} + [R_{4}, b_{i}] + \frac{1}{2!}[R_{4}, [R_{4}, b_{i}]] + \cdots \\ &= b_{i} + \sum_{k} \beta_{ik}b_{k}^{\dagger} + \frac{1}{2!}\sum_{kk'} \beta_{ik}\beta_{kk'}b_{k'} + \frac{1}{3!}\sum_{kk'j} \beta_{ik}\beta_{kk'}\beta_{k'j}b_{j}^{\dagger} + \cdots \\ &= \sum_{j} \delta_{ij}b_{j} + \sum_{j} \beta_{ij}b_{j}^{\dagger} + \frac{1}{2!}\sum_{kj} \beta_{ik}\beta_{kj}b_{j} + \frac{1}{3!}\sum_{klj} \beta_{ik}\beta_{kl}\beta_{lj}b_{j}^{\dagger} + \cdots \end{split}$$

$$\tilde{b}_i = \sum_j (\mu_{ij} b_j + \nu_{ij} b_j^{\dagger}). \tag{3.18}$$

Similarly, we may calculate,

$$\tilde{b}_i^{\dagger} = \sum_{j} \left(\mu_{ij} b_j^{\dagger} + \nu_{ij} b_j \right) \tag{3.19}$$

where

$$\mu_{ij} = \delta_{ij} + \frac{1}{2!} \sum_{k} \beta_{ik} \beta_{kj} + \frac{1}{4!} \sum_{klm} \beta_{ik} \beta_{kl} \beta_{lm} \beta_{mj} + \cdots$$
 (3.20)

$$\nu_{ij} = \beta_{ij} + \frac{1}{3!} \sum_{kl} \beta_{ik} \beta_{kl} \beta_{lj} + \frac{1}{5!} \sum_{klmn} \beta_{ik} \beta_{kl} \beta_{lm} \beta_{mn} \beta_{nj} + \cdots$$
 (3.21)

Using this we may obtain,

$$\left(\widetilde{b_i^{\dagger} + b_i}\right) = \sum_{i} \left(\mu_{ij} + \nu_{ij}\right) \left(b_j^{\dagger} + b_j\right) \tag{3.22}$$

and

$$\left(\widetilde{b_i^{\dagger} - b_i}\right) = \sum_{j} \left(\mu_{ij} - \nu_{ij}\right) \left(b_j^{\dagger} - b_j\right) \tag{3.23}$$

Using Eqs. (3.20) and (3.21), we calculate

$$(\mu_{ij} + \nu_{ij}) = \delta_{ij} + \beta_{ij} + \frac{1}{2!} (\beta^2)_{ij} + \dots = (e^{\beta})_{ij}$$
 (3.24)

$$(\mu_{ij} - \nu_{ij}) = \delta_{ij} - \beta_{ij} + \frac{1}{2!} (\beta^2)_{ij} + \dots = (e^{-\beta})_{ij}.$$
 (3.25)

Therefore the transformed Hamiltonian becomes,

$$H_{4} = -t_{eff} \sum_{\langle ij \rangle \sigma} c_{i\sigma}^{\dagger} c_{j\sigma} + \widetilde{U} \sum_{i} n_{i\uparrow} n_{i\downarrow} + \widetilde{V}_{1} \sum_{\langle ij \rangle \sigma\sigma'} n_{i\sigma} n_{j\sigma'} + \widetilde{V}_{2} \sum_{i\delta'\sigma\sigma'} n_{i\sigma} n_{i+\delta',\sigma'}$$

$$+ \widetilde{V}_{3} \sum_{i\delta''\sigma\sigma'} n_{i\sigma} n_{i+\delta'',\sigma'} + \varepsilon_{eff} \sum_{l\sigma} n_{i\sigma}$$

$$+ \omega_{0} \frac{e^{4\alpha_{s}+4\alpha_{d} \sum_{\sigma} n_{i\sigma}}}{4} \sum_{i} \left[\sum_{jj'} (\mu_{ij} + \nu_{ij}) (\mu_{ij'} + \nu_{ij'}) (b_{j}^{\dagger} + b_{j}) \left(b_{j'}^{\dagger} + b_{j'} \right) \right]$$

$$- \omega_{0} \frac{e^{-4\alpha_{s}-4\alpha_{d} \sum_{\sigma} n_{i\sigma}}}{4} \sum_{i} \left[\sum_{jj'} (\mu_{ij} - \nu_{ij}) (\mu_{ij'} - \nu_{ij'}) (b_{j}^{\dagger} - b_{j}) \left(b_{j'}^{\dagger} - b_{j'} \right) \right]$$

$$+ P_{1} e^{2\alpha_{s}+2\alpha_{d} \sum_{\sigma} n_{i\sigma}} \sum_{i\sigma} n_{i\sigma} \sum_{j} (\mu_{ij} + \nu_{ij}) (b_{j}^{\dagger} + b_{j})$$

$$+ P_{2} e^{2\alpha_{s}+2\alpha_{d} \sum_{\sigma} n_{i\sigma}} \sum_{i\sigma} n_{i\sigma} \sum_{j} (\mu_{i+\delta,j} + \nu_{i+\delta,j}) (b_{j}^{\dagger} + b_{j}) + \frac{N\omega_{0}}{2}.$$

$$(3.26)$$

One may notice that the transformation (3.13), incorporates the mean-field part of the phonon correlations while (3.15) includes the deviation from the mean-field part i.e., the fluctuations. The purpose of carrying out a set of unitary transformation is to decouple the electron and phonon variables. However an exact separation of the electron and phonon variables is not possible for the present problem. Therefore we seek a variational solution by taking the average of \mathcal{H} with a suitable phonon state $|\Phi_{ph}\rangle$ so that the phonon variables are eliminated. This entire process is same as making a following choice for the phonon wave function:

$$|\psi_{ph}\rangle = e^{-R_1}e^{-R_2}e^{-R_3}e^{-R_4}|\Phi_{ph}\rangle$$
 (3.27)

We thus write an approximate wave function for the original Hamiltonian in the following product form:

$$|\Psi\rangle = |\psi_{el}\rangle \otimes |\psi_{ph}\rangle,\tag{3.28}$$

so that the total energy of the system can then be written as:

$$E = \langle \Psi | H | \Psi \rangle = \langle \psi_{el} | \langle \psi_{ph} | H | \psi_{ph} \rangle | \psi_{el} \rangle = \langle \psi_{el} | \langle \Phi_{ph} | \mathcal{H} | \Phi_{ph} \rangle | \psi_{el} \rangle. \tag{3.29}$$

For $|\Phi_{ph}\rangle$, we choose a fully general phonon state as:

$$|\Phi_{ph}\rangle = \sum_{n=0}^{M} r_n |\varphi_n(x)\rangle,$$
 (3.30)

where $\varphi_n(x)$ is the n-th eigen function of a harmonic oscillator and r_n 's are variational parameters. Our aim is to begin the numerical computation with the value of M equal to zero and then systematically increase its value till the energy becomes convergent. The effective electronic Hamiltonian becomes

$$\begin{split} H_{eff} &= \left< \psi_{ph} \middle| H \middle| \psi_{ph} \right> = \left< \Phi_{ph} \middle| \mathcal{H} \middle| \Phi_{ph} \right> = \left< \Phi_{ph} \middle| e^{R_4} e^{R_3} e^{R_2} e^{R_1} H e^{-R_1} e^{-R_2} e^{-R_3} e^{-R_4} \middle| \Phi_{ph} \right> \\ &= \varepsilon_{eff} \sum_{i\sigma} n_{i\sigma} - t_{eff} \sum_{\langle ij \rangle \sigma} c^{\dagger}_{i\sigma} c_{j\sigma} + U_{eff} \sum_{i} n_{i\uparrow} n_{i\downarrow} + V_1^e \sum_{\langle ij \rangle \sigma\sigma'} n_{i\sigma} n_{j\sigma'} \\ &+ V_2^e \sum_{i\delta'\sigma\sigma'} n_{i\sigma} n_{i+\delta',\sigma'} \\ &+ \frac{N\omega_0}{4} \left[e^{4\alpha} \left(e^{2\beta} \right)_{00} T_2 \left(1 + 4\alpha_d + 12\alpha_d^2 \right) \\ &- e^{-4\alpha} \left(e^{2\beta} \right)_{00} T_3 \left(1 - 4\alpha_d + 12\alpha_d^2 \right) - 2 \right] \end{split} \tag{3.31}$$

where

$$\varepsilon_{eff} = -\frac{1}{\omega_0} \left[2(g_1 g_1' + z g_2 g_2') - (g_1'^2 + z g_2'^2) \right] + e^{2\alpha} (1 + 2\alpha_d + 3\alpha_d^2) M_1 T_1 \left[(g_1 + z g_2) - (g_1' + z g_2') \right], \tag{3.32}$$

$$t_{eff} = te^{\alpha_d} F_1 F_2 F_3 , \qquad (3.33)$$

$$U_{eff} = U - \frac{2}{\omega_0} \left[2(g_1 g_1' + z g_2 g_2') - (g_1'^2 + z g_2'^2) \right], \tag{3.34}$$

$$V_1^e = V_1 - \frac{2}{\omega_0} [(g_1 g_2' + g_1' g_2) - g_1' g_2'], V_2^e = V_2 - \frac{1}{\omega_0} [2g_2 g_2' - g_2'^2], V_3^e = V_3,$$
 (3.35)

$$F_1 = \sum_{k,l=0}^{M} c_{kl} \int_{-\infty}^{\infty} dy \, e^{-y^2} \, H_k(y) \, H_l(y) \,, \tag{3.36}$$

$$F_2 = \sum_{k,l=0}^{M} c_{kl} \ e^{-\frac{\gamma^2}{4}} \int_{-\infty}^{\infty} dy \ e^{-y^2} \ H_k\left(y + \frac{\gamma}{2}\right) H_l\left(y - \frac{\gamma}{2}\right), \tag{3.37}$$

$$F_3 = \sum_{k,l=0}^{M} c_{kl} \int_{-\infty}^{\infty} dy \, e^{-\frac{y^2}{2}(1+\eta^2)} \, H_k(y) \, H_l(y\eta)$$
 (3.38)

$$T_{i} = \sum_{k,l=0}^{M} c_{kl} \int_{-\infty}^{\infty} e^{-y^{2}} \xi_{i}(y) H_{k}(y) H_{l}(y) dy , \qquad (3.39)$$

$$M_1 = (e^{\beta})_{00} + 2n \sum_{m=1}^{\infty} (e^{\beta})_{0m} , \qquad (3.40)$$

$$\sum_{k} \left(A_{k}^{ij}\right)^{2} = \frac{2g_{1}^{\prime 2}}{\omega_{0}^{2}} \left[\left(e^{2\beta}\right)_{00} - \left(e^{-2\beta}\right)_{01} \right] + \frac{2g_{2}^{\prime 2}}{\omega_{0}^{2}} \sum_{\delta' \delta''} \left[\left(e^{-2\beta}\right)_{i+\delta',i+\delta''} - \left(e^{-2\beta}\right)_{i+\delta',j+\delta''} \right]$$

$$+\frac{4g_1'g_2'}{\omega_0^2} \sum_{\delta'} \left[\left(e^{-2\beta} \right)_{0,i+\delta'} - \left(e^{-2\beta} \right)_{i+\delta,i+\delta'} \right], \tag{3.41}$$

where
$$y = \sqrt{x}$$
 and (3.42)

$$c_{kl} = c_k c_l \sqrt{1/2^{k+l} k! \, l! \, \pi},\tag{3.43}$$

$$\gamma = e^{-2\alpha_s} \sum_k A_k^{ij} (1 - 2\alpha_d + 3\alpha_d^2), \ \eta = 1 + 2\alpha_d, \tag{3.44}$$

$$\xi_1 = \sqrt{2}y, \, \xi_2 = 2y^2, \, \xi_3 = 2(y^2 - 2l - 1).$$
 (3.45)

We calculate $(e^{\pm n\beta})_{0n}$ using the periodic boundary condition. Then the 2D lattice can be viewed as a toroid of N lattice sites with N very large so that the effects of end points do not matter (Fig. 3.1).

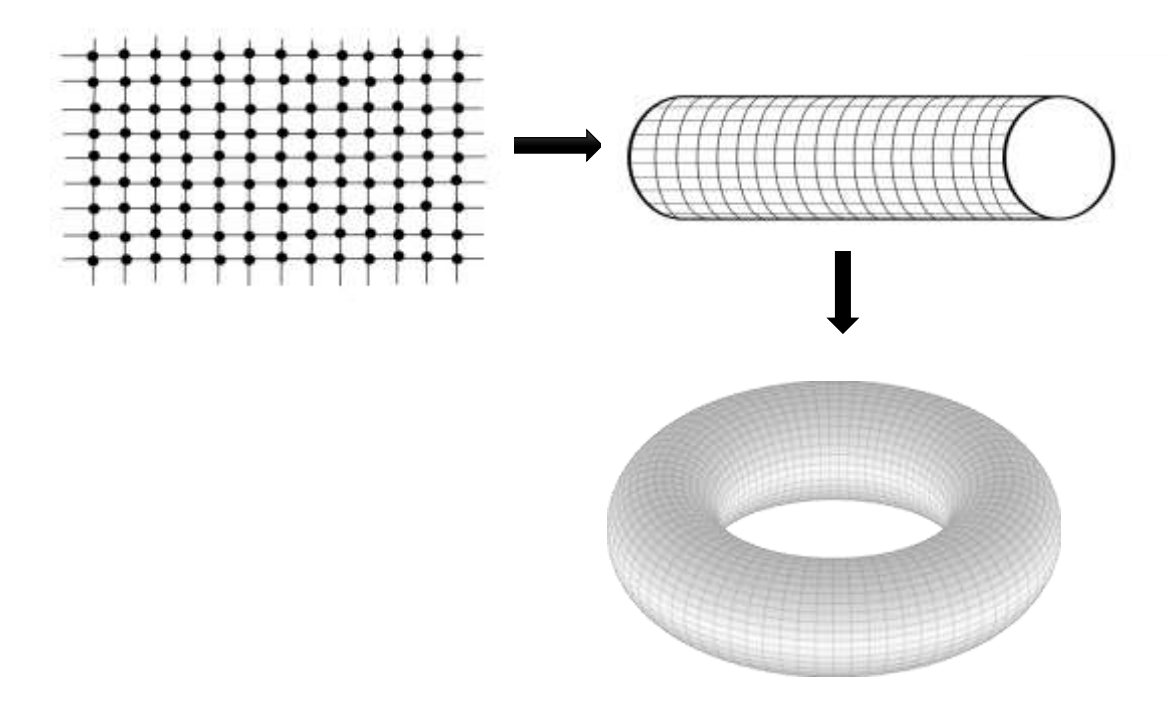


Fig. 3.1: The 2D HH model in the form of a toroid under periodic boundary condition.

The matrix β is given by

$$\boldsymbol{\beta} = \begin{pmatrix} 0 & \beta & 0 & 0 & 0 & \dots & 0 & 0 & \beta \\ \beta & 0 & \beta & 0 & 0 & \dots & 0 & 0 & 0 & 0 \\ 0 & \beta & 0 & \beta & 0 & \dots & 0 & 0 & 0 & 0 \\ \vdots & & & \vdots & & & \vdots & & & \vdots \\ \beta & 0 & 0 & 0 & 0 & & 0 & 0 & 0 & 0 \end{pmatrix}$$

We find that the element $(e^{\pm n\beta})_{0q}$ for the ring structure in Fig. 3.1 can be represented exactly by the following closed form analytical expression:

$$\left(e^{\pm n\beta}\right)_{00} = \sum_{p=0}^{\infty} {2m \choose m} \frac{(\pm n\beta)^{2p}}{p! \, p!} \,, \tag{3.46}$$

$$(e^{\pm n\beta})_{0q} = \sum_{p=0}^{\infty} \left(2p + \left(\frac{q-1}{2} + 1 \right) \right) \frac{(\pm n\beta)^{\left[2p + \left(\frac{q-1}{2} + 1 \right)\right]}}{p! \left[p + \left(\frac{q-1}{2} + 1 \right) \right]!} , \qquad (q = odd)$$
 (3.47)

$$(e^{\pm n\beta})_{0q} = \sum_{p=0}^{\infty} {2p + (\frac{q}{2} + 1) \choose p+1} \frac{(\pm n\beta)^{\left[2p + (\frac{q}{2} + 1)\right]}}{p! \left[p + (\frac{q}{2} + 1)\right]!} . (q = even) (3.48)$$

For the electrons, we assume a square density of states (which is a valid assumption in 2D) and write,

$$\rho(\varepsilon_k) = \frac{1}{2W} \quad ; \quad -W \le \varepsilon_k \le W$$

$$= 0 \quad ; \quad otherwise. \tag{3.49}$$

3.2.1 Weak Coulomb correlation

3.2.1.1 Hartree-Fock Approximation:

In the mean-field theory a four operator term could be decomposed into two-operator form so that the system Hamiltonian can be solved easily in the following way:

$$n_{i}n_{j} = [(n_{i} - \langle n_{i} \rangle) + \langle n_{i} \rangle] [(n_{j} - \langle n_{j} \rangle) + \langle n_{j} \rangle]$$

$$= \langle n_{i} \rangle (n_{j} - \langle n_{j} \rangle) + (n_{i} - \langle n_{i} \rangle) \langle n_{j} \rangle + \langle n_{i} \rangle \langle n_{j} \rangle + (n_{i} - \langle n_{i} \rangle) (n_{j} - \langle n_{j} \rangle)$$
(3.51)

In the HF mean-field theory, we neglect the fluctuations term $(n_i - \langle n_i \rangle)(n_j - \langle n_j \rangle)$ as this approximation does not have any effect on the physics of the problem, to solve the electronic Hamiltonian. Therefore we may write Eq. (3.31) as

$$n_{i}n_{j} = \langle n_{i}\rangle(n_{j} - \langle n_{j}\rangle) + (n_{i} - \langle n_{i}\rangle)\langle n_{j}\rangle + \langle n_{i}\rangle\langle n_{j}\rangle$$

$$= \langle n_{i}\rangle n_{i} + n_{i}\langle n_{i}\rangle - \langle n_{i}\rangle\langle n_{i}\rangle$$
(3.52)

so that

$$\langle n_i n_j \rangle = \langle n_i \rangle \langle n_j \rangle \tag{3.54}$$

Also,

$$\langle n_i \rangle = n = \langle n_{i\uparrow} \rangle + \langle n_{i\downarrow} \rangle$$
 (3.55)

Therefore,

$$\langle n_{i\sigma} \rangle = \frac{n}{2} \tag{3.56}$$

The HF mean-field approximation transforms the many particle average to the product of single particle averages by removing the quartic operator terms. Thus the Hamiltonian becomes soluble. This approximation gives better results at lower electron concentration.

Using the HF mean-field theory we may write the electronic terms of Eq. (3.31) as shown below.

$$V_{1}^{e} \sum_{\langle ij \rangle \sigma\sigma'} n_{i\sigma} n_{j\sigma'} = V_{1}^{e} \sum_{\langle ij \rangle \sigma\sigma'} \left[\langle n_{i\sigma} \rangle n_{j\sigma'} + n_{i\sigma} \langle n_{j\sigma'} \rangle - \langle n_{i\sigma} \rangle \langle n_{j\sigma'} \rangle \right]$$

$$= V_{1}^{e} \left[zn \sum_{j\sigma} n_{j\sigma'} + z \sum_{i\sigma} n_{i\sigma} n - Nzn^{2} \right]$$

$$= V_{1}^{e} \left[2zn \sum_{i\sigma} n_{i\sigma} - Nzn^{2} \right], \qquad (3.57)$$

where $j = i + \delta$, carries the NN information and z is the number of NN in the extended HH model.

Let us consider another term of Eq. (3.31).

$$\begin{split} U_{eff} \sum_{i} n_{i\uparrow} n_{i\downarrow} &= U_{eff} \sum_{i} [\langle n_{i\uparrow} \rangle n_{i\downarrow} + n_{i\uparrow} \langle n_{i\downarrow} \rangle - \langle n_{i\uparrow} \rangle \langle n_{i\downarrow} \rangle] \\ &= U_{eff} \sum_{i} \left[\frac{n}{2} n_{i\downarrow} + n_{i\uparrow} \frac{n}{2} - \frac{n^2}{4} \right] \\ &= U_{eff} \frac{n}{2} \sum_{i\sigma} n_{i\sigma} - N U_{eff} \frac{n^2}{4} \end{split} \tag{3.58}$$

The other two electronic terms can be written with the HF mean-field theory as

$$V_2^e \sum_{i\delta'\sigma\sigma'} n_{i\sigma} n_{i+\delta',\sigma'} = 2z' n V_2^e \sum_{i\sigma} n_{i\sigma} - Nz' n^2 V_2^e, \tag{3.59a}$$

and

$$V_3^e \sum_{i\delta''\sigma\sigma'} n_{i\sigma} n_{i+\delta'',\sigma'} = -Nz'' n^2 V_3^e$$
 (3.59b)

where z' represents the number of the NNN in the extended HH Hamiltonian.

Using these results the effective electronic Hamiltonian of Eq. (3.31) is solved using the mean-field HF approximation. For weak electronic correlation, the mean-field HF decoupling method gives the GS energy (ε_W) (per particle) for the system as

$$\varepsilon_{W} = n \,\varepsilon_{eff} - \frac{1}{2}z \,t_{eff}(2n - n^{2}) + \frac{n^{2}}{4}U_{eff} + zn^{2}V_{1}^{e} + z'n^{2}V_{2}^{e} + z''n^{2}V_{3}^{e}$$

$$+ \frac{N\omega_{0}}{4} \left[e^{4\alpha} \left(e^{2\beta} \right)_{00} T_{2} \left(1 + 4\alpha_{d} + 12\alpha_{d}^{2} \right) - e^{-4\alpha} \left(e^{2\beta} \right)_{00} T_{3} \left(1 - 4\alpha_{d} + 12\alpha_{d}^{2} \right) - 2 \right] , \qquad (3.60)$$

which is finally minimized with respect to g'_1 , g'_2 , α_s , α_d , β and c_n 's.

3.2.2 Strong Coulomb correlation

To investigate the strongly correlated region, the half-filled HH model can be transformed into a Heisenberg model. In this regime, it is assumed that each site is either occupied by a single electron or remains empty, though the presence of virtual fluctuations may result in double occupancies. But in the present case, we consider the system in the subspace of no double occupancy and therefore an effective t-J model can be obtained.

3.2.2.1 t - J model

For the strong Coulomb correlation, i.e. at $U \gg t$, there is no hopping process if t=0 and the ground state of the lattice is degenerate which is a singly occupied lattice chain of electrons. But as t becomes finite, the lattice degeneracy breaks and there could be four possible ways that may have effect on the double occupancy in the chain of lattice. The four probable hopping processes can be explained through the Hamiltonians in the following ways:

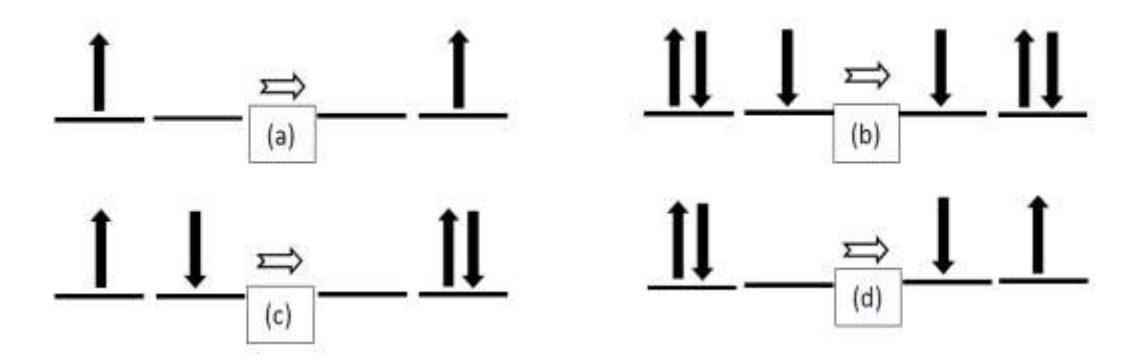


Fig. 3.2: t - J model mechanism

The mechanism (a) represents the process where unoccupied sites are occupied by hopping, that can be presented by the Hamiltonian,

$$H_t^0 = -t \sum_{\langle ij \rangle \sigma} \{ (1 - n_{i,-\sigma}) c_{i\sigma}^{\dagger} c_{j\sigma} (1 - n_{j,-\sigma}) + (1 - n_{j,-\sigma}) c_{j\sigma}^{\dagger} c_{i\sigma} (1 - n_{i,-\sigma}) \}. \quad (4.61)$$

In the mechanism (b), the doubly occupied states hop by one lattice site. This process can be described by the Hamiltonian,

$$H_t^1 = -t \sum_{\langle ij \rangle \sigma} \{ n_{i,-\sigma} c_{i\sigma}^{\dagger} c_{j\sigma} n_{j,-\sigma} + n_{j,-\sigma} c_{j\sigma}^{\dagger} c_{i\sigma} n_{i,-\sigma} \}.$$
 (3.62)

The third process (c) increases the number of doubly occupied sites that can be expressed with the Hamiltonian,

$$H_t^+ = -t \sum_{\langle ij \rangle \sigma} \left\{ n_{i,-\sigma} c_{i\sigma}^\dagger c_{j\sigma} \left(1 - n_{j,-\sigma} \right) + n_{j,-\sigma} c_{j\sigma}^\dagger c_{i\sigma} \left(1 - n_{i,-\sigma} \right) \right\}. \tag{3.63}$$

The fourth process decreases the number of doubly occupied sites that can be presented by the Hamiltonian,

$$H_{t}^{-} = -t \sum_{\langle ij \rangle \sigma} \{ (1 - n_{i,-\sigma}) c_{i\sigma}^{\dagger} c_{j\sigma} n_{j,-\sigma} + (1 - n_{j,-\sigma}) c_{j\sigma}^{\dagger} c_{i\sigma} n_{i,-\sigma} \}.$$
 (3.64)

Considering all the possible hopping mechanisms, the hopping process in the total Hubbard Hamiltonian can be written as,

$$H_t = H_t^0 + H_t^1 + H_t^+ + H_t^-. (3.65)$$

Here as the two processes (c) and (d) change the number of doubly occupied sites, we may write them together as $H_t^+ + H_t^- = H_t^{\pm}$ and this Hamiltonian causes an extra energy U to the system. Therefore in order to eliminate any extra energy cost to the system we apply the Schrieffer-Wolff transformation (SWT) to the total hopping Hamiltonian H_t .

The generator of the canonical SWT is considered as,

$$S = \frac{1}{U}(H_t^+ - H_t^-),\tag{3.66}$$

That transforms the Hubbard Hamiltonian as,

$$\widetilde{H} = e^{S} (H_{t}^{0} + H_{t}^{\pm} + H_{U}) e^{-S}
= H_{t}^{0} + H_{t}^{\pm} + H_{U} + [S, H_{t}^{0}] + [S, H_{U}] + [S, H_{t}^{\pm}] + \frac{1}{2} [S, [S, (H_{t}^{0} + H_{t}^{\pm} + H_{U})]].$$
(3.67)

For a strongly correlated system, as we do not want any change in the doubly occupied sites, the result of the SWT gives,

$$H_t^{\pm} + [S, H_U] = 0. (3.68)$$

Other terms in the transformed Hamiltonian become:

$$[S, H_t^{\pm}] = \frac{1}{U} [H_t^+, H_t^-] = \sigma(t^2/U), \tag{3.69}$$

$$\frac{1}{2}[S,[S,H_U]] = -\frac{1}{U}[H_t^+,H_t^-] = \sigma(t^2/U), \tag{3.70}$$

$$\frac{1}{2} \left[S, \left[S, H_t^0 + H_t^{\pm} \right] \right] = \left[S, H_U \right] + \sigma(t^3/U). \tag{3.71}$$

Therefore collecting all the terms we obtain the transformed Hamiltonian as,

$$\widetilde{H} = H_t^0 + H_U + \frac{2}{U} [H_t^+, H_t^-] + \sigma(t^3/U).$$
 (3.72)

The commutator $[H_t^+, H_t^-]$ contains the terms $H_t^+H_t^-$ and $H_t^-H_t^+$. Here the term $H_t^+H_t^-$ acts on a doubly occupied site. So we may ignore the effect of that term. Also the bare Hubbard correlation term has to be neglected as it contributes the energy og the doubly occupied sites.

The term $H_t^- H_t^+$ acts to creat a doubly occupancy at one site and destroys the same at other site, and $H_t^- H_t^+ = \sigma(t^2)$. This term has the same effect of a spin-flip operator: $S_i^+ S_j^- + S_j^- S_i^+$. $S_i \cdot S_j$ can be written in terms of the spin-flip operator as

$$\mathbf{S}_{i} \cdot \mathbf{S}_{j} = \frac{1}{2} \left(S_{i}^{+} S_{j}^{-} + S_{i}^{-} S_{j}^{+} \right) + S_{i}^{z} S_{i}^{z}, \tag{3.73}$$

with

$$S_i^+ = c_{i\uparrow}^\dagger c_{i\downarrow}$$
, $S_i^- = c_{i\downarrow}^\dagger c_{i\uparrow}$, (3.74)

and S_i^z , the z-component of S_i , is given by

$$S_i^z = \frac{1}{2}(n_{i\uparrow} - n_{i\downarrow}). \tag{3.75}$$

As the flipping of spin happens for the anti-parallel spin configuration and there is no effect of this spin-flip operator on the parallel spin, this may be written as, $(S_i \cdot S_j - \frac{1}{4}n_i n_j)$.

Therefore the two site effective t - J model can be written as,

$$H_{t-J} = -t \sum_{\langle ij \rangle \sigma} \{ (1 - n_{i,-\sigma}) c_{i\sigma}^{\dagger} c_{j\sigma} (1 - n_{j,-\sigma}) + h. c \} + \frac{4t^2}{U} \sum_{\langle ij \rangle} \left(\mathbf{S}_i \cdot \mathbf{S}_j - \frac{1}{4} n_i n_j \right). \quad (3.76)$$

Using this effective t - J model, we may write our effective electronic Hamiltonian (3.13) as

$$\begin{split} \widetilde{\mathcal{H}}_{eff} &= \varepsilon_{eff} \sum_{i\sigma} n_{i\sigma} + t_{eff} \sum_{\langle ij > \sigma} (1 - n_{i\overline{\sigma}}) \, c_{i\sigma}^{\dagger} c_{j\sigma} \, \left(1 - n_{j\overline{\sigma}} \right) + J \sum_{\langle ij \rangle} \left(\mathbf{S}_{i} \cdot \mathbf{S}_{j} - \frac{1}{4} n_{i} n_{j} \right) \\ &+ V_{1}^{e} \sum_{\langle ij > \sigma\sigma'} n_{i\sigma} n_{j\sigma'} \\ &+ \frac{1}{4} N \omega_{0} \left[e^{4\alpha} \left(e^{2\beta} \right)_{00} \, T_{2} \, \left(1 + 4\alpha_{d} + 12\alpha_{d}^{2} \right) \right. \\ &- e^{-4\alpha} \left(e^{2\beta} \right)_{00} \, T_{3} \, \left(1 - 4\alpha_{d} + 12\alpha_{d}^{2} \right) - 2 \right], \end{split}$$
(3.77)

where S_i is the electron spin operator at site i and J represents the NN AFM coupling strength for the electronic interaction which is obtained as

$$J = \frac{4t_{eff}^2}{\left(U_{eff} - V_1^e\right)} \,, \tag{3.78}$$

Because we consider here a strongly correlated electronic system, we neglect the NN and NNN interaction terms V_2 and V_3 .

It is difficult to solve Eq. (3.77) analytically with the double occupancy constraint. Therefore, we replace the actual local constraints by the average double-occupancy constraint using the Gutzwiller approximation (GA) [40, 41].

3.2.2.2 Gutzwiller Approximation

GA is a more improved approximation technique than the mean-field theory where the system with a constraint can be dealt with. In this method, the GS energy of the system is calculated using variational technique with respect to the renormalized GS wave function. Therefore GA can also be described as a variational approximation to the dynamical mean-field theory (DMFT). To estimate the GS energy, the effective renormalized wave function is first written as

$$|\psi\rangle = \hat{P}|\psi_0\rangle,\tag{3.79}$$

where \hat{P} is the projection operator, $|\psi_0\rangle$ is the uncorrelated electronic wavefunction and in case of the GA, this operator is defined as,

$$\hat{P} = \prod_{j} (1 - \hat{n}_{j\uparrow} \hat{n}_{j\downarrow}). \tag{3.80}$$

Using the projected mean-field approximation the double occupancy can be avoided and the expectation values of the operators can be calculated as

$$\langle \hat{O} \rangle = \frac{\langle \psi | \hat{O} | \psi \rangle}{\langle \psi | \psi \rangle} = \frac{\langle \psi_0 | \hat{P} \hat{O} \hat{P} | \psi_0 \rangle}{\langle \psi_0 | \psi_0 \rangle}.$$
 (3.81)

Therefore to solve the t-J Hamiltonian, the renormalized expectation values for the electronic number operator $c_{i\sigma}^{\dagger}c_{j\sigma}$ and the spin projection operator can be written as,

$$\langle c_{i\sigma}^{\dagger} c_{j\sigma} \rangle = \varphi_t \langle c_{i\sigma}^{\dagger} c_{j\sigma} \rangle_0 \tag{3.82}$$

$$\langle \mathbf{S}_i \cdot \mathbf{S}_j \rangle = \varphi_s \langle \mathbf{S}_i \cdot \mathbf{S}_j \rangle_0 , \qquad (3.83)$$

where the coefficients g_t and g_s are the renormalization factors for the corresponding operators' expectation values. In the similar way, the parameters t and J can be replaced in the t-J model with the multiplication factor due to renormalization,

$$t_{eff} = \varphi_t t$$
, and $J_{eff} = \varphi_t J$. (3.84)

Ogawa et al. [42] have applied the GA to the strongly correlated t - J model. Considering the average electron density n and the hole density x = (1 - n), the GA leads to [43],

$$\varphi_t = \frac{2x}{(1+x)} \tag{3.85}$$

and

$$\varphi_J = \frac{4}{(1+x^2)}. (3.86)$$

where φ_t acts as the band reduction factor due to the strong correlation. Using this formalism of GA, we may write the effective hopping term of the Hamiltonian of Eq. (3.77) as

$$(1 - n_{i\overline{\sigma}}) c_{i\sigma}^{\dagger} c_{j\sigma} \left(1 - n_{j\overline{\sigma}} \right) \cong \varphi_t c_{i\sigma}^{\dagger} c_{j\sigma} , \qquad (3.87)$$

Under GA, the antiferromagnetic interaction coefficient J is also renormalized by a factor $\varphi_J = 4/(1+x^2)$, i.e., J transforms to \tilde{J} where $\tilde{J} = \varphi_J J$.

Next we impose the HFA which is now a valid approximation because of the restriction on the double occupancy. The effective Hamiltonian in the Fourier space reads,

$$\widetilde{\mathcal{H}}_{eff} = \sum_{k\sigma} E_{k} c_{k\sigma}^{\dagger} c_{k\sigma} - 2 \left(\widetilde{I} - V_{1}^{e} \right) \Delta_{b} \sum_{k} \gamma_{k} \left(c_{k\uparrow}^{\dagger} c_{-k\downarrow} + c_{-k\downarrow}^{\dagger} c_{k\uparrow} \right)
+ Nz \left[\frac{1}{4} \left(\widetilde{I} - 4V_{1}^{e} \right) n^{2} + \left(\widetilde{I} - V_{1}^{e} \right) \Delta_{b}^{2} + \widetilde{I} p^{2} \right]
+ \frac{N\omega_{0}}{4} \left[e^{4\alpha} \left(e^{2\beta} \right)_{00} T_{2} \left(1 + 4\alpha_{d} + 12\alpha_{d}^{2} \right) - e^{-4\alpha} \left(e^{2\beta} \right)_{00} T_{3} \left(1 - 4\alpha_{d} + 12\alpha_{d}^{2} \right)
- 2 \right]$$
(3.88)

with

$$E_{\mathbf{k}} = \varepsilon_e - \varepsilon_{\mathbf{k}}$$
,

$$\varepsilon_{e} = \varepsilon_{eff} - \frac{1}{2} (\tilde{J} - 4V_{1}^{e}) z n ,$$

$$\varepsilon_{k} = (\varphi_{t} t_{eff} + p\tilde{J})$$

$$\gamma_{k} = W \gamma_{k} ,$$
(3.89)

where γ_k is given by: $\gamma_k = \sum_{j \neq i} e^{i k \cdot R_{ij}}$ which for a square lattice reduces to: $\gamma_k = 2 \left(\cos k_x a + \cos k_y a\right)$, the expression of ε_k may be used to define the band width and the average occupation number per site (n), the Hartree correction to the kinetic energy term (p) and the gap parameter term (Δ_b) are defined as

$$n = \frac{1}{N} \sum_{i\sigma} \langle c_{i\sigma}^{\dagger} c_{i\sigma} \rangle ;$$

$$p = \frac{1}{2zN} \sum_{\langle ij \rangle \sigma} \langle c_{i\sigma}^{\dagger} c_{j\sigma} \rangle ;$$

$$\Delta_b = \frac{1}{zN} \sum_{\langle ij \rangle} \langle c_{i\uparrow}^{\dagger} c_{j\downarrow} \rangle = \frac{1}{zN} \sum_{\langle ij \rangle} \langle c_{i\downarrow}^{\dagger} c_{j\uparrow} \rangle ,$$
(3.90)

which are calculated using the double-time Green function method of Zubarev.

3.2.2.3 Zubarev's Green's function technique

Green function is a very useful mathematical tool to study the many body physics,. Though there are several Green function methods, the double time, temperature dependent Green function method is one of the most useful methods among them. Zubarev has suggested a double time temperature-dependent Green function technique which has been applied to superconductivity, ferromagnetism and also to the electron-lattice interacting system. Here, we also use the Green function method of Zubarev.

The time dependent advanced and retarded Green's functions can be defined as the average value of the time product of operators as,

$$G_{\pm}(t,t') = \langle \langle A(t); B(t') \rangle \rangle_{\pm} = \mp i\theta \{ \pm (t-t') \} \langle [A(t), B(t')]_{n} \rangle, \tag{3.91}$$

where G_+ and G_- represent the retarded (G_r) and advanced (G_a) Green functions respectively and $\langle ... \rangle$ indicates the average over a grand canonical ensemble, $\langle \langle ... \rangle \rangle$ denotes the double time Green function which is of higher order than the initial one and $\eta = +1(-1)$ for bosons (fermions).

Using the equation of motion method we obtain

$$i\frac{d}{dt}\langle\langle A(t),B(t')\rangle\rangle^{\pm} = \delta(t-t')\langle[A(t),B(t')]_{\eta}\rangle + i\theta(t-t')\langle[i\frac{d}{dt}A(t),B(t')]_{\eta}\rangle(3.92)$$

Using the Heisenberg equation of motion method, we finally obtain the equation of motion for the Zubarev Green function as

$$EG(E) = E \langle \langle A(t), B(t^{/}) \rangle \rangle^{\pm} = \frac{1}{2\pi} \langle [A(t), B(t^{/})]_{\eta} \rangle + \langle \langle [A(t), H]; B(t^{/}) \rangle \rangle^{\pm}. \quad (3.93)$$

After calculating the Green functions, the time-dependent correlation functions can be calculated as,

$$\langle B(t^{\prime})A(t)\rangle = i\int_{-\infty}^{\infty} \frac{[G(\omega + i\varepsilon) - G(\omega - i\varepsilon)]}{e^{\beta\omega} - \eta} e^{-i\omega(t - t^{\prime})} d\omega. \tag{3.94}$$

Following Zubarev's formalism and using Eq. (3.94), we have to calculate the Green functions

$$G_{k\uparrow} = \langle \langle c_{k\uparrow}; c_{k\uparrow}^{\dagger} \rangle \rangle, \tag{3.95}$$

and

$$F_{\mathbf{k}\downarrow\uparrow} = \langle \langle c_{-\mathbf{k}\downarrow}^{\dagger}; c_{\mathbf{k}\uparrow}^{\dagger} \rangle \rangle. \tag{3.96}$$

Now considering,

$$\omega_{\mathbf{k}} = \sqrt{E_{\mathbf{k}} + \Delta_{\mathbf{k}}} \quad ; \quad \Delta_{\mathbf{k}} = 2(\tilde{J} - V_1^e) \Delta_b \, \gamma_{\mathbf{k}} \,, \tag{3.97}$$

and using the equation of motion method for the Hamiltonian (3.88), we obtain the following two relations,

$$(\omega - E_{\mathbf{k}})G_{\mathbf{k}\uparrow} = \frac{1}{2\pi} - \Delta_b F_{\mathbf{k}\downarrow\uparrow}, \qquad (3.98)$$

and

$$(\omega + E_{\mathbf{k}})F_{\mathbf{k}\downarrow\uparrow} = -\Delta_b G_{\mathbf{k}\uparrow}. \tag{3.99}$$

Solving these two equations we obtain the Green functions as

$$G_{\mathbf{k}\uparrow} = \frac{1}{2\pi} \frac{(\omega + E_{\mathbf{k}})}{(\omega^2 - \omega_{\mathbf{k}}^2)},\tag{3.100}$$

$$F_{k\downarrow\uparrow} = -\frac{1}{2\pi} \frac{\Delta_k}{(\omega^2 - \omega_k^2)} \,. \tag{3.101}$$

To find the average occupation number per site of Eq. (3.90), we can Fourier transform the operators and using Eq. (3.94) we write

$$\langle c_{\mathbf{k}\uparrow}^{\dagger}(0)c_{\mathbf{k}\uparrow}(t)\rangle = -2\lim_{\varepsilon\to 0}\int_{-\infty}^{\infty} \frac{Im\ G(\omega+i\varepsilon)}{(e^{\beta\omega}+1)}e^{-i\omega t}\ d\omega. \tag{3.102}$$

From Eq. (3.100) we may write

$$G_{k\uparrow}(\omega) = \frac{1}{2\pi} \left[\frac{\omega}{(\omega^2 - \omega_k^2)} + \frac{E_k}{(\omega^2 - \omega_k^2)} \right]$$

$$= \frac{1}{2\pi} \left[\frac{1}{2} \left(\frac{1}{\omega - \omega_k} + \frac{1}{\omega + \omega_k} \right) + \frac{E_k}{2\omega_k} \left(\frac{1}{\omega - \omega_k} - \frac{1}{\omega + \omega_k} \right) \right]$$

$$= \frac{1}{2\pi} \left[\frac{1}{2} \left(1 + \frac{E_k}{\omega_k} \right) \frac{1}{\omega - \omega_k} + \frac{1}{2} \left(1 - \frac{E_k}{\omega_k} \right) \frac{1}{\omega + \omega_k} \right]$$
(3.103)

Therefore, we have

 $\lim_{\varepsilon\to 0} Im \ G(\omega + i\varepsilon)$

$$=\frac{1}{2\pi}\left[\left(\frac{\omega_{k}+E_{k}}{2\omega_{k}}\right)Im\left(\frac{1}{\omega+i\varepsilon-\omega_{k}}\right)+\left(\frac{\omega_{k}-E_{k}}{2\omega_{k}}\right)Im\left(\frac{1}{\omega+i\varepsilon+\omega_{k}}\right)\right]. \tag{3.104}$$

For $t \to 0$, we can use the Eq. (3.104) and calculate the Eq. (3.102) as,

$$\lim_{t\to 0} \langle c_{\mathbf{k}\uparrow}^{\dagger}(0)c_{\mathbf{k}\uparrow}(t)\rangle$$

$$= -2\frac{1}{2\pi} \int_{-\infty}^{\infty} \frac{d\omega}{(e^{\beta\omega} + 1)} \left(-\frac{\pi}{2\omega_k} \right) \left\{ (\omega_k + E_k) \delta(\omega - \omega_k) + (\omega_k - E_k) \delta(\omega + \omega_k) \right\}$$

$$= \frac{1}{2\omega_k} \left[\left(\frac{\omega_k + E_k}{e^{\beta\omega_k} + 1} \right) + \left(\frac{\omega_k - E_k}{e^{-\beta\omega_k} + 1} \right) \right]$$

$$= \frac{\omega_k}{2\omega_k} \left(\frac{1}{e^{\beta\omega_k} + 1} + \frac{1}{e^{-\beta\omega_k} + 1} \right) + \frac{E_k}{2\omega_k} \left(\frac{1}{e^{\beta\omega_k} + 1} - \frac{1}{e^{-\beta\omega_k} + 1} \right)$$

$$= \frac{1}{2} \left(\frac{1}{e^{\beta\omega_k} + 1} + \frac{e^{\beta\omega_k}}{1 + e^{\beta\omega_k}} \right) + \frac{E_k}{2\omega_k} \left(\frac{1}{e^{\beta\omega_k} + 1} - \frac{e^{\beta\omega_k}}{1 + e^{\beta\omega_k}} \right)$$

$$= \frac{1}{2} + \frac{E_k}{2\omega_k} \left(\frac{1 - e^{\beta\omega_k}}{1 + e^{\beta\omega_k}} \right)$$

$$= \frac{1}{2} \left[1 - \frac{E_k}{\omega_k} \tanh \left(\frac{\beta\omega_k}{2} \right) \right]. \tag{3.105}$$

As total $n = n_{\uparrow} + n_{\downarrow}$, we may write for N number of particles,

$$n(T,\Delta) = \frac{1}{N} \sum_{k} \left[1 - \frac{E_k}{\omega_k} \tanh\left(\frac{1}{2}\beta\omega_k\right) \right]. \tag{3.106}$$

Similarly, the number of holes can be calculated as,

$$p(T,\Delta) = \frac{1}{2Nz} \sum_{k} \gamma_{k} \left[1 - \frac{E_{k}}{\omega_{k}} \tanh\left(\frac{1}{2}\beta\omega_{k}\right) \right], \tag{3.107}$$

and the gap parameter is found to be,

$$\Delta_b = \frac{1}{Nz} \sum_{k} \gamma_k \left[\left(\frac{\Delta_k}{2\omega_k} \right) \tanh\left(\frac{1}{2} \beta \omega_k \right) \right]. \tag{3.108}$$

In order to solve the final Hamiltonian Eq. (3.88), consider materials with $\Delta_b = 0$, at $T \to 0$. Under this assumption, the GS energy per site (ε_{SN}) for the system reads

$$\begin{split} \varepsilon_{SN} &= Nn\varepsilon_{e} - \left(\varphi_{t} \, t_{eff} + p\tilde{J}\right) \sum_{\boldsymbol{k}\sigma} \gamma_{\boldsymbol{k}} \theta(-E_{\boldsymbol{k}}) + Nz \left[\frac{1}{4} (\tilde{J} - 4V_{1}^{e}) n^{2} + \tilde{J}p^{2}\right] \\ &+ \frac{N\omega_{0}}{4} \left[e^{4\alpha} \left(e^{2\beta}\right)_{00} T_{2} \left(1 + 4\alpha_{d} + 12\alpha_{d}^{2}\right) - e^{-4\alpha} \left(e^{2\beta}\right)_{00} T_{3} \left(1 - 4\alpha_{d} + 12\alpha_{d}^{2}\right) \\ &- 2 \right], \end{split} \tag{3.109}$$

where $\theta(-E_k)$ is the step function and the correlation functions read,

$$p(0,0) = \frac{1}{4}(1-x^2).$$
 ; $n(0,0) = (1-x) \cong n.$ (3.110)

Therefore, the GS energy per site is given by

$$\varepsilon_{S} = n\varepsilon_{e} - (\varphi_{t} t_{eff} + p\tilde{J}) zp + Nz \left[\frac{1}{4} (\tilde{J} - 4V_{1}^{e})n^{2} + \tilde{J}p^{2} \right]
+ \frac{N\omega_{0}}{4} \left[e^{4\alpha} (e^{2\beta})_{00} T_{2} (1 + 4\alpha_{d} + 12\alpha_{d}^{2}) - e^{-4\alpha} (e^{2\beta})_{00} T_{3} (1 - 4\alpha_{d} + 12\alpha_{d}^{2}) - 2 \right].$$
(3.111)

3.3 Numerical results and discussions

Our primary goal here is to examine the nature of the phase transition from the SDW state to the CDW state for the 2D extended HH model. As the Hamiltonian (3.1) does not admit an exact analytical solution, we deal with the system analytically in two different regimes separately, namely, the weak-correlation regime and the strong-correlation regime for different e-p coupling constants. For low values of U_{eff} , we would use the formulation for weak correlation given in Section 3.2.1 to calculate the effective parameters and for high values of the U_{eff} , we use the formulation for strong correlation presented in Section 3.2.2. We find that for $U_{eff} \lesssim 2.1$, the strong-correlation expressions do not work and lead to divergent results. We therefore use weak-correlation expressions for the region $U_{eff} \gtrsim 2.1$. This critical value of U_{eff} varies a little bit depending on the el-ph coupling strength α . For example, for $\alpha = 0.5$, U = 3, the critical U_{eff} is 2.08, whereas, for $\alpha = 1$, U = 4, $U_{eff} = 2.12$.

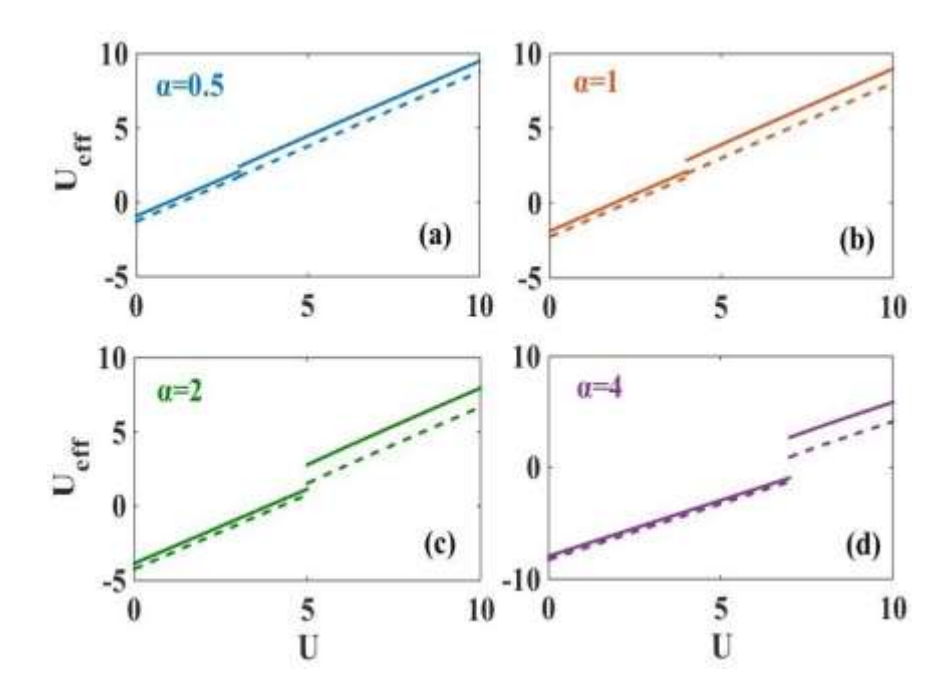


Fig 3.3: Effective onsite e-e interaction (U_{eff}) vs. bare onsite e-e interaction (U) for t = 0.2 and $g_2 = 0$ (solid lines) & $g_2 = 0.2$ (dashed lines) for a few values of on-site e-p coupling coefficient (α) .

In Fig. 3.3, we plot the effective onsite Coulomb correlation (U_{eff}) with respect to the bare onsite e-e interaction strength (U). As we deal with two different regimes of the system by two different mathematical formulations, the graphs of the two regimes meet each other in a discontinuous manner at the correlation boundary. Thus this discontinuity may well be an artefact of the approximation we have used. We however find that this discontinuity does not affect the energy or the phase diagram. Fig. 3.3 shows that at weak correlation i.e., at small U, the phonon-mediated electronic attraction dominates over the onsite bare Coulomb repulsion and the effective e-e interaction U_{eff} becomes negative which implies that at low U, the e-p interaction drives the effective onsite electronic interaction attractive. This leads to the formation of the onsite bipolarons leading to a Peierls insulator that can also be described as the CDW state.

As U increases, U_{eff} increases gradually and turns positive and then the GS is given by an anti-ferromagnetic Mott polaronic SDW state which is also an insulating phase. In other words, as α exceeds a certain strength, the GS of the system undergoes a transformation from

an SDW phase to a CDW phase, both being insulating phases. In both the phases, U_{eff} appears to increase linearly with U which is understandable from Eq. (3.34). One can also find that as α increases, the bipolaronic bound state becomes stronger and localization increases.

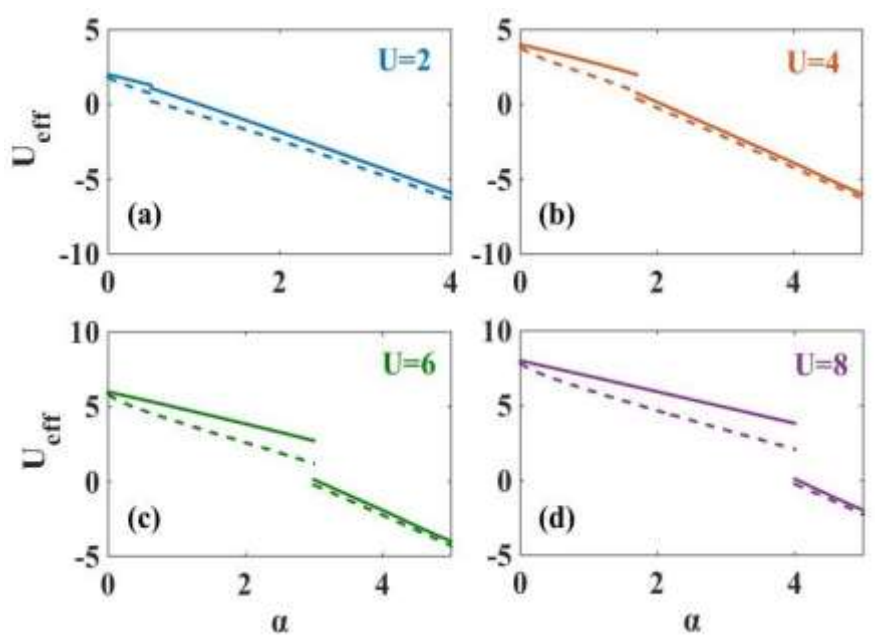


Fig 3.4: U_{eff} versus α for t = 0.2 and $g_2 = 0$ (shown by straight lines) and $g_2 = 0.2$ (shown by dashed lines) for a few values of U.

The behaviour of U_{eff} versus α for a few U values is shown in Fig. 3.4. We find that as α increases, U_{eff} decreases and the decrease is essentially linear, which is again understandable from in Eq. (3.34). This reduction in the value of U_{eff} is caused by the phonon-induced attractive el-el interaction. At low e-p interaction, U_{eff} is positive and the GS is a polaronic Anti-ferromagnetic Mott SDW wave insulator. As the e-p interaction increases, beyond a certain α , U_{eff} becomes negative and the GS transforms into a bipolaronic CDW Peierls insulator. The nature of the intermediate region in between these two insulating states is the focus of our attention in this work. We find that with increasing U, the role of the NN e-p coupling becomes important.

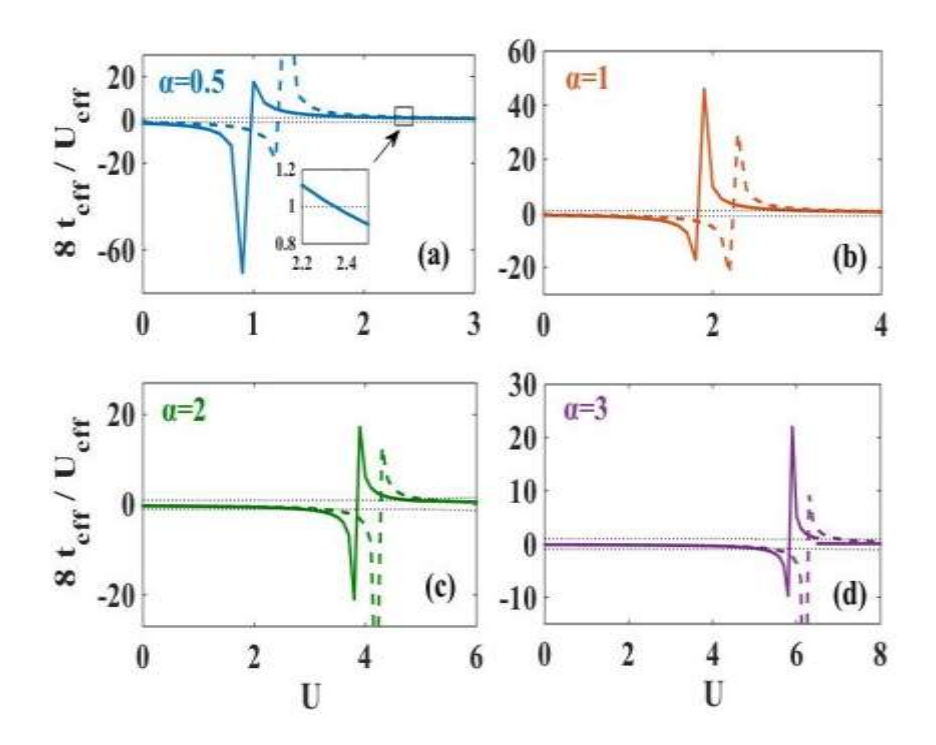


Fig 3.5: Mott-Hubbard metallicity parameter (MHMP) $(8t_{eff}/U_{eff})$ versus U for t=0.2 and $g_2=0$ (shown by the straight lines) & $g_2=0.2$ (shown by the dashed lines) for a few values of α . (The dotted line shows ± 1 value).

According to the Mott-Hubbard (MH) criterion, the condition for metallicity is given by: $(2zt_{eff}/U_{eff}) \ge 1$, where z is the coordination number which for a 2D square lattice is equal to 4. We shall investigate the behaviour of the SDW-CDW transition in the 2D HH system with the help of the above MH metallicity criterion and accordingly draw the phase diagram of the system in the $\alpha-U$ space. The quantity: $8t_{eff}/U_{eff}$ will be referred to as the Mott-Hubbard metallicity parameter (MHMP). In Fig. 3.5, we show the variation of the MHMP with U for a few values of α . The negative values of the Mott-Hubbard parameter correspond to a CDW phase with $-1 < (8t_{eff}/U_{eff}) < 0$. Above a critical value of U, MHMP satisfies $|8t_{eff}/U_{eff}| \ge 1$. Hence this region should have the attributes of a metallic phase. As U increases further, MHMP again becomes less than 1 but positive. In this phase, $U_{eff} > 0$ and $0 < (8t_{eff}/U_{eff}) < 1$, and therefore this corresponds to an SDW phase and the one where $U_{eff} < 0$, i.e. $1 < (8t_{eff}/U_{eff}) < -1$, corresponds to the CDW state. Fig. 3.5 clearly depicts that the intermediate region lying between the CDW and SDW phases is metallic in nature. One can observe that for a finite value of NN e-p interaction coefficient, the intermediate region only shifts towards higher U values. The reason for this is that as the

NN e-p interaction g_2 becomes finite, stronger on-site Coulomb correlation is required to overcome the e-p interaction coefficient to make the transitions.

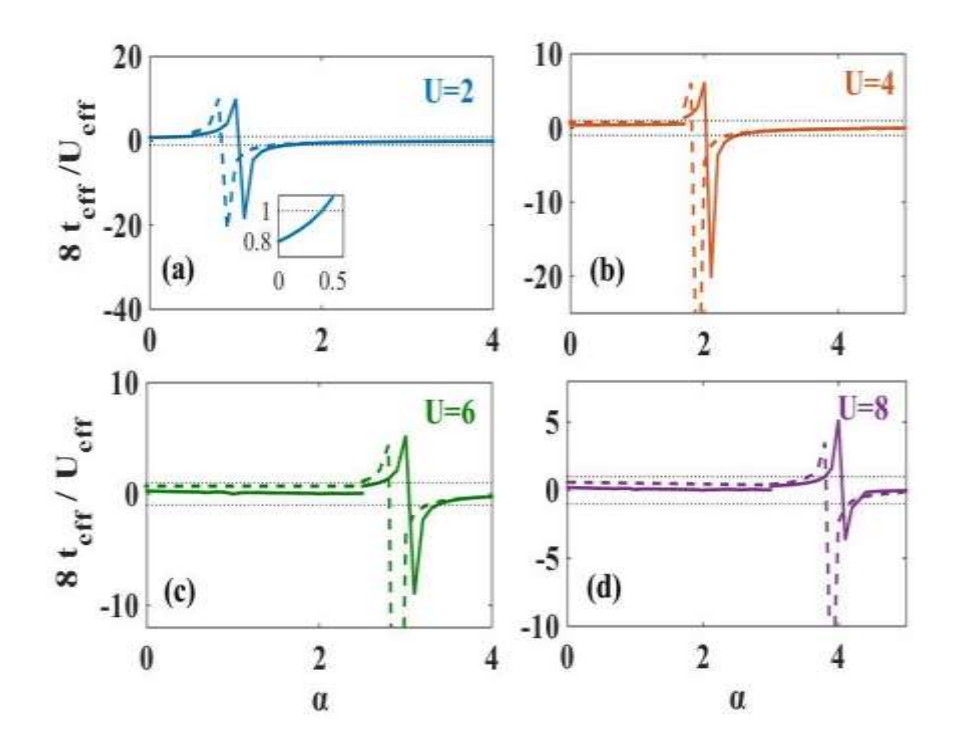


Fig 3.6: MHMP $(8t_{eff}/U_{eff})$ versus α for t=0.2 and $g_2=0$ (shown by the straight lines) & $g_2=0.2$ (shown by the dashed lines) for a few values of U. (The dotted line shows ± 1 value).

The variations of MHMP with α for a few values of U are studied in Fig. 3.6. Here also the behaviour of MHMP in the figure shows an SDW-CDW transition with the cross-over region being a metallic phase. We now observe that for a finite NN e-p interaction coefficient g_2 , the plot shifts towards left i.e., towards the lower values of α . The reason is understandable because at finite g_2 , the polaronic interaction is stronger than that for $g_2 = 0$ and therefore the transition to the CDW phase can take place at a lower value of α for a given U.

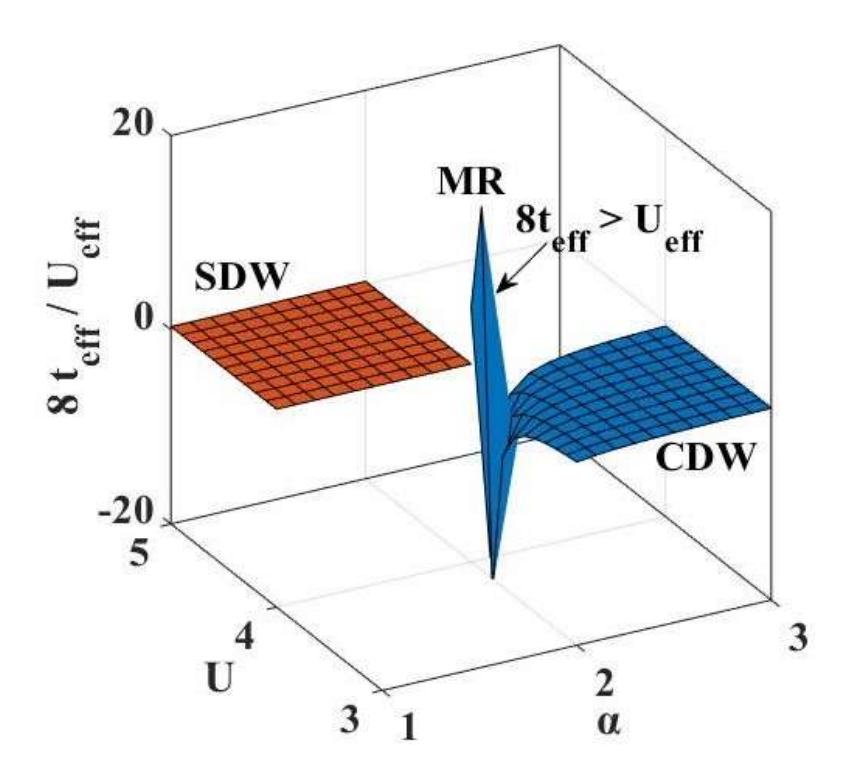


Fig 3.7: 3D plot of MHMP $(8t_{eff}/U_{eff})$ with respect to α and U for t=0.2.

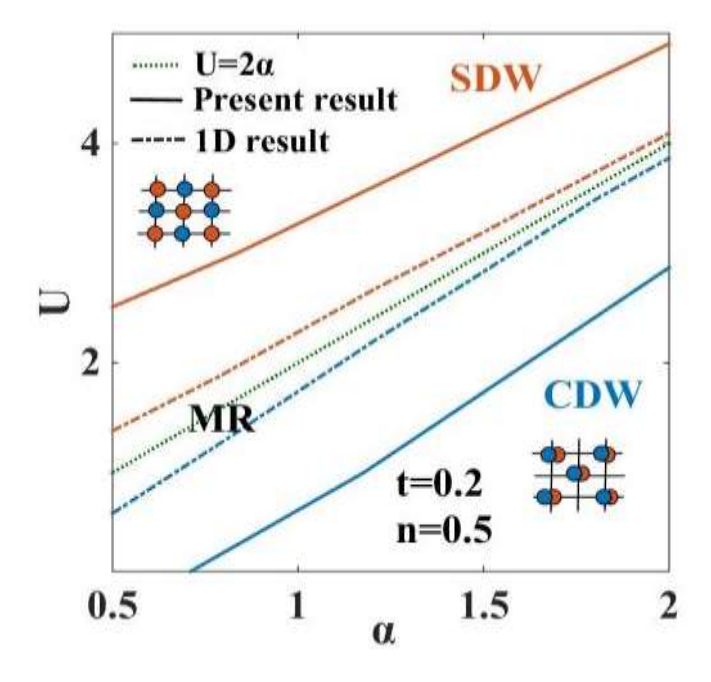


Fig. 3.8: Phase diagram in $(\alpha - U)$ plane: Comparison with results of Wang et al. [30].

In Fig. 3.7, we display the three-dimensional (3D) phase diagram by plotting MHMP in the $(\alpha - U)$ plane. The left side of the graph indicates the SDW phase while the right side shows

the CDW state. The region in between the two phases satisfies the Mott-Hubbard metallicity criterion.

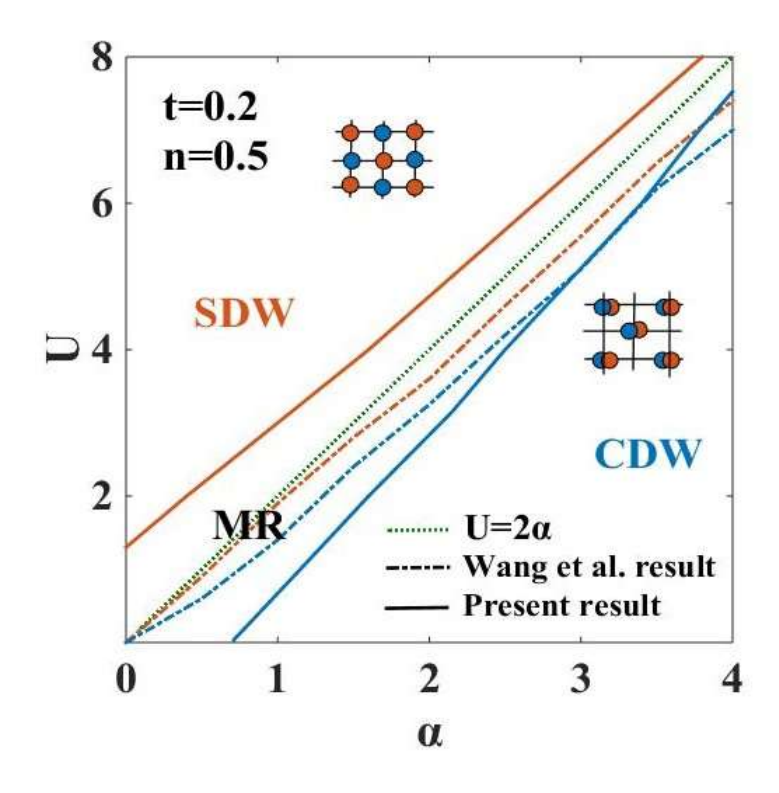


Fig. 3.9: Comparison of 1D and 2D phase diagrams.

We next plot in Fig. 3.8, the SDW-CDW phase diagram for an extended 2D HH system in the $(\alpha - U)$ -plane using the transition-point values of α for each U from Fig. 3.5 and Fig. 3.6. The figure shows a wide intermediate region flanked by the SDW and CDW regions. This intervenng phase satisfies the MH metallicity creterion and is therefore a metallic phase. We have also shown the result of Wang et al. [30] obtained by non-Gaussian exact diagonalization method for the sake of comparison. It is clear that the results of Wang et al. [30] and our results are qualititatively similar though our results predict a wider metallic phase and therefore more appealing from the point of view of superconductivity. In Fig. 3.9, we compare our present 2D phase diagram with that obtained for the 1D HH model [20]. The figure shows that the metallic region is wider in 2D, which is of course an expected result. This result is particularly important because the majority of high temperature superconductors are either two-dimensional or quasi-two dimensional systems.

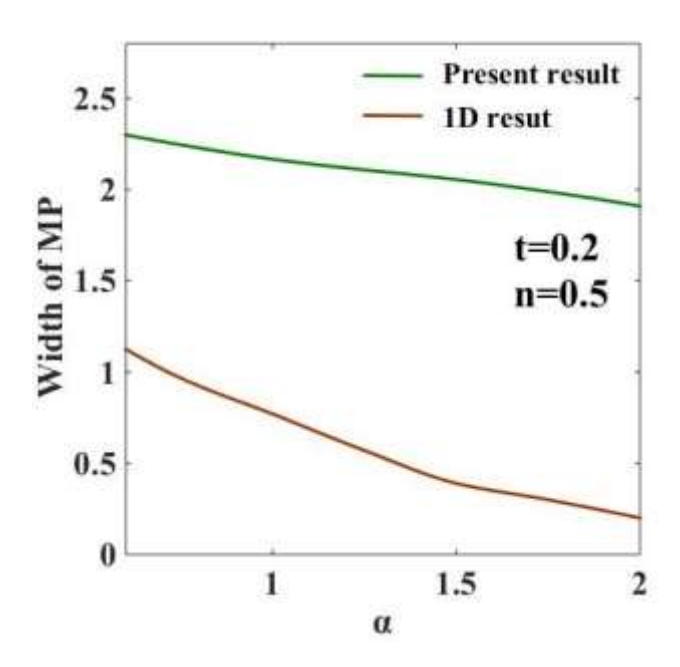


Fig. 3.10: Width of MP vs. α in 1D and 2D HH systems.

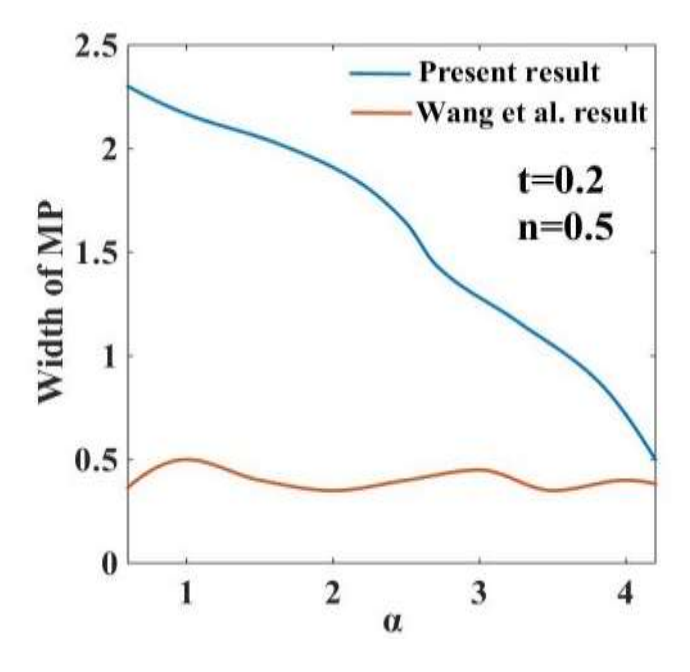


Fig. 3.11: Comparison of present results for the width of MP vs. α with those of Wang et al [30].

We have finally calculated the width of the metallic phase from the Fig. 3.8 and plotted it with respect to α in Fig. 3.10 and Fig. 3.11. At a specific α value, we can find two values of

U from the phase diagram, one corresponding to the transition from CDW phase to MR (say, U_1) and the other corresponding to the transition from MR to the SDW phase (say, U_2). The difference $\Delta U = (U_2 - U_1)$ gives the width of the metallic phase. In Fig 3.10, the 2D metallic width is compared with the 1D system [20].

We see that in 2D, the width of the MP decreases with α more slowly than in 1D. Thus the existence of an intermediate metallic phase is more probable in a 2D system. This is again an interesting result and useful for superconductivity in 2D. In Fig 3.11, in contrast to our result, the result of Wang et al. shows that the width of the metallic phase hardly changes with α even over large range of α . We would normally expect the MP to shrink with increasing α because of the emergence of the CDW phase at large α .

3.4 Conclusion

In this chapter, the CDW-SDW transition is studied in a two-dimensional half-filled extended HH model by employing an analytical method which is variational in nature. A fullygeneralized many-phonon averaging is performed upon the succession of canonical transformations that leads to an effective electronic system which is solved analytically in weak and strong correlation regimes separately using plausible approximations. More specifically, for low values of the Coulomb correlation strength, i.e. in the weak correlation regime, the renormalized electronic system is treated by the method of Hartree-Fock meanfield theory while for the higher values of the on-site Coulomb correlation i.e. in the strong correlation regime, the effective Hamiltonian is first mapped on the t-J model and then simplified, employing the Gutzwiller approximation and finally solved using the Zuberev time dependent Green's function technique followed by the Hartree-Fock method. For both the regimes, we have calculated the effective Hubbard correlation and examined it as a function of the bare Hubbard parameter U for different e-p interaction coefficients. The SDW-CDW transitions are observed at different e-p interaction strengths as the U_{eff} changes its sign. The principal interest in this work has been to unravel the nature of the phase across the SDW-CDW transition. Studies in 1D HH model have almost unequivocally revealed the existence of a metallic phase at the CDW-SDW cross-over region. Few recent investigations have made similar claim for a 2D HH system using numerical methods [31, 32]. An analytical examination of this issue was certainly called for from the point of view of the basic understanding of the physics behind the system. We have therefore investigated the nature the phases around the SDW-CDW transition using the Mott-Hubbard criterion. Calculation of the Mott-Hubbard parameter over different regimes reveal that even in a 2D HH system, an intervening metallic phase exists between the insulating SDW and CDW phases. This result is consistent with what our commonplace notion would justify, as one would normally expect more accessible states in 2D than in 1D and hence more mobility. The comparison of the present results with the 2D non-Gaussian exact diagonalization results of Wang et al. [30] shows that the present results are qualitatively similar to the numerical results of Wang et al. However, our analytical results predict a wider intermediate metallic phase which is more appealing from the view of superconductivity. Comparison of the present results with those of one of our previous works shows that the width of the metallic phase is wider in 2D than 1D. This result is again interesting from the point of view of high-temperature superconductivity in 2D systems.

3.5 References

- [1] N. M. Plakida, Physica C **162–164**, 1341–1342 (1989).
- [2] Y. H. Kim, A. J. Heeger, L. Acedo, G. Stucky, F. Wudl, Phys. Rev. B 36, 7252–7255 (1987).
- [3] B. K. Chakraverty, D. Feinberg, Z. Hang, M. Avignon, Sol. State. Commun. **64**, 1147–1151 (1987).
- [4] A. S. Alexandrov, Phys. Rev. B **38**, 925–927 (1988).
- [5] D. Mihailovic, C. M. Foster, K. Voss, A. J. Heeger, Phys. Rev. B 42, 7989–7993 (1990).
- [6] S. D. Conradson, I. D. Raistrick, A. R. Bishop, Science **248**, 1394–1398 (1990).
- [7] J. M. de Leon, S. D. Conradson, I. Batistic, A. Bishop, Phys. Rev. Lett. **65**, 1675–1678 (1990).
- [8] H. A. Mook, B. C. Chakoumakos, M. Mostoller, Phys. Rev. Lett. 69, 2272–2275 (1992).
- [9] H. A. Mook, M. Mostoller, J. A. Harvey, N. W. Hill, B. C. Chakoumakos, B. C. Sales, Phys. Rev. Lett. 65, 2712–2715 (1990).
- [10] E. Fradkin and J. E. Hirsch, Phys. Rev. B 27 4302 (1983).
- [11] Y. Takada and A. Chatterjee, Phys. Rev. B 67 081102 (R) (2003).
- [12] R. T. Clay, R. P. Hardikar, Phys. Rev. Lett. 95, 096401 (2005).

- [13] R. P. Hardikar, R. T. Clay, Phys. Rev. B. **75**, 245103 (2007).
- [14] H. Fehske, G. Hager, E. Jeckelmann, Europhys. Lett. **84** 57001(2008).
- [15] A. Payeur, D. Senechal, Phys. Rev. B 83 033104 (2011).
- [16] A. Chatterjee, Y. Takada, J. Phys. Soc. Jap. **73**, 964–969 (2004).
- [17] I. V. Sankar, A. Chatterjee, Physica B **489**, 17–22 (2016).
- [18] C. U. Lavanya, I. V. Sankar, A. Chatterjee, Sci Rep. 7, 3774 (2017).
- [19] Z. M. Malik, S. Mukhopadhyay, A. Chatterjee, Phys. Lett. A, 383, 1516-1519 (2019).
- [20] Z. M. Malik, A. Chatterjee, J. Phys. Commun. 4 (2020) 105005.
- [21] D. Debnath, M. Z. Malik, A. Chatterjee, Sci Rep. 11, 12305 (2021).
- [22] O. Cyr-Choinière, D. LeBoeuf, S. Badoux, S. Dufour-Beauséjour, A. D. Bonn et al., Phys. Rev. B 98, 064513 (2018).
- [23] T. Wu, H. Mayaffre, S. Krämer, M. Horvatić, C. Berthier, et al., Nature **477**, 191–194 (2011).
- [24] J. Chang, E. Blackburn, A. T. Holmes, N. B. Christensen, J. Larsen et al., Nat. Phys. 8, 871–876 (2012).
- [25] A. H. Castro Neto, Phys. Rev. Lett. **86**, 4382–4385 (2001).
- [26] K. Rossnagel, J. Phys.: Condens. Matter. 23, 213001 (2011).
- [27] S. Manzeli, D. Ovchinnikov, D. Pasquier, O.V. Yazyev, A. Kis, Nat. Rev. Mater. 2, 17033 (2017).
- [28] E. Berger, P. Valášek, W. L. Vonder, Phys. Rev. B 52, 4806–4814 (1995).
- [29] M. Hohenadler and G. G. Batrouni, Phys. Rev. B **100**, 165114 (2019).
- [30] Y. Wang, I. Esterlis, T. Shi, C. J. Ignacio, E. Demler, Phys. Rev. Research 2, 043258 (2020).
- [31] N. C. Kosta, K. Seki, S. Yunoki, S. Sorella, Communications Physics, 3, 80 (2020).
- [32] N.K. Yirga, K.M. Tam, D.K. Campbell, arXiv: 2206.03981v1 (2022).
- [33] I. G. Lang, Yu. A. Firsov, **43**, 1843-1860 (1962), Soviet Phys. JETP **16**, 1301–1314 (1963).
- [34] H. Fehske, D. Ihle, J. Loos, U. Trapper, and H. Büttner, Z. Phys. B 94, 91 (1994).
- [35] A. Ghosh, S. Kar, and S. Yarlagadda, Eur. Phys. J. B **91**, 205 (2018).
- [36] C. N. Raju and A. Chatterjee, Eur. Phys. J. B 88, 108 (2015).
- [37] P. J. Monisha, I. V. Sankar, S. Sil, and A. Chatterjee, Sci. Rep. 6, 20056 (2016).
- [38] H. Zheng, Phys. Lett. A 131 (1988) 115.
- [39] C.F. Lo, R. Sollie, Phys. Rev. B 48 (1993) 10183.

- [40] M.C. Gutzwiller, Phys. Rev. Lett. 10, 159 (1963).
- [41] M.C. Gutzwiller, Phys. Rev. 137, A1726 (1965).
- [42] T. Ogawa, K. Kanda, T. Mastsubara, Progress of Theoretical Physics, 53, 3 (1975).
- [43] M. Ogata, A. Himeda, arXiv:cond-mat/0003465v1 (2000).

"When you change the way you look at things, the things you look at change"... Max Planck

4

A semi-exact study of self-trapping transition in a one-dimensional Holstein-Hubbard model

4.1 Introduction

In chapter 1, we have described the phenomenon of self-trapping (ST) transition in electronphonon system. The issue of ST transition has continued to remain in the focus of attention in the last few decades for its importance in high- T_C superconductors [4-5], colossal magnetoresistance (CMR) materials or manganites [6] and semiconductor nanostructures [7]. Therefore several authors have studied the nature of ST transition for the single-polaron [8-12] and the many-polaron systems [13] within the framework of the Fröhlich model and for the correlated polar systems using the Holstein-Hubbard (HH) model. However, no clear concord has been established regarding the nature of the ST transition.

Recently, Krishna, Mukhopadhyay and Chatterjee (KMC) [14] have examined the behaviour of the ST transition in an extended HH system including the NN e-p interaction with the help of a variational technique. To incorporate coherence and correlation in the phonon wave function, they have applied a variational Lang-Firsov (LF) transformation [15] and the on-site and inter-site squeezing transformations [16-17] followed by a zero-phonon averaging. The resulting effective electronic problem has been solved using the exact Bethe ansatz technique following Lieb and Wu (LW) [18]. Their calculation shows that ST transition in a one-dimensional correlated polar system is continuous. It should however be

mentioned that the analysis of KMC is approximate because of the approximate treatment of the phonon subsystem. Because of the relevance of the ST transition in systems like manganites etc, a more improved analysis of the ST transition in the HH system may be useful so that a more authentic statement can be made about the continuity or otherwise of the nature of the ST transition. Our main goal in this chapter is to achieve this purpose.

In this work, we study the ST transition in a 1D extended HH model with a more improved variational calculation than the one carried out by KMC. We consider the strength of the onsite Coulomb interaction to be sufficiently large so that the phonon-induced effective correlation coefficient remains positive in order to prevent the formation of bipolaronic charge density wave (CDW) state through Peierls instability. The ST transition is examined by analyzing the relevant parameters both in the adiabatic and anti-adiabatic regimes.

4.2 Model and Formulation

An extended HH Hamiltonian in 1D can be written as

$$H = -t \sum_{\langle ij \rangle \sigma} c_{i\sigma}^{\dagger} c_{j\sigma} + U \sum_{i} n_{i\uparrow} n_{i\downarrow} + \omega_{o} \sum_{i} b_{i}^{\dagger} b_{i} + g_{1} \sum_{i\sigma} n_{i\sigma} (b_{i} + b_{i}^{\dagger})$$

$$+ g_{2} \sum_{i\delta\sigma} n_{i\sigma} (b_{i+\delta} + b_{i+\delta}^{\dagger}), \tag{4.1}$$

where the first and the second terms together constitute the Hubbard model, the third term refers to the free phonon Hamiltonian and the last two terms represent respectively the onsite and nearest-neighbour (NN) electron-phonon (e-p) interactions. Here, t gives the electronic hopping integral, $c_{i\sigma}^{\dagger}(c_{i\sigma})$ creates (annihilates) an electron at site-i with spin σ , $n_{i\sigma}(=c_{i\sigma}^{\dagger}c_{i\sigma})$ represents the number operator for electrons at site i and with spin σ , U refers to the onsite Coulomb correlation strength, $b_i^{\dagger}(b_i)$ stands for the creation (annihilation) operator of an optical phonon at site with Einstein frequency ω_o , g_1 and g_2 indicate respectively the onsite and NN e-p interaction coefficients, δ referring to an NN site.

To deal with the phonon degrees of freedom, we carry out a sequence of unitary

transformations on Hamiltonian (4.1). We first perform on (4.1) a modified LF (MLF) transformation [15] with the generator:

$$R_1 = \frac{g_1'}{\omega_0} \sum_{i\sigma} n_{i\sigma} (b_i^{\dagger} - b_i) + \frac{g_2'}{\omega_0} \sum_{i\delta\sigma} n_{i\sigma} (b_{i+\delta}^{\dagger} - b_{i+\delta}), \tag{4.2}$$

where g_1' and g_2' are the variational parameters. The Hamiltonian transforms to

$$H_1 = e^{R_1} H e^{-R_1} = H + [R_1, H] + \frac{1}{2!} [R_1, [R_1, H]] + \cdots$$
(4.3)

$$= -t \sum_{\langle ij \rangle \sigma} c_{i\sigma}^{\dagger} c_{j\sigma} e^{(x_i - x_j)} + \widetilde{U} \sum_{i} n_{i\uparrow} n_{i\downarrow} + \omega_0 \sum_{i} b_i^{\dagger} b_i + \varepsilon \sum_{i\sigma} n_{i\sigma} + P_1 \sum_{i\sigma} n_{i\sigma} (b_i + b_i^{\dagger})$$

$$+ P_2 \sum_{i\delta\sigma} n_{i\sigma} (b_{i+\delta} + b_{i+\delta}^{\dagger}) , \qquad (4.4)$$

where

$$(x_i - x_j) = \frac{g_1'}{\omega_0} (b_i^{\dagger} - b_i) + \frac{g_2'}{\omega_0} (b_{i+\delta}^{\dagger} - b_{i+\delta}), \tag{4.5}$$

$$\varepsilon = -\left[\frac{2}{\omega_0}(g_1g_1' + 2g_2g_2') - \frac{1}{\omega_0}(g_1'^2 + 2g_2'^2)\right],\tag{4.6}$$

$$\widetilde{U} = U - \frac{2}{\omega_0} [2(g_1 g_1' + 2g_2 g_2') - (g_1'^2 + 2g_2'^2)], \tag{4.7}$$

$$P_1 = g_1 - g_1'$$
 ; $P_2 = g_2 - g_2'$. (4.8)

Physically g_1' plays the role of the depth of the onsite polaron potential and would thus increase with increasing g_1 and be responsible for localization. On the other hand, g_2' gives the length scale over which the lattice is distorted by the e-p interaction and thus it would be responsible for delocalization. In the conventional LF transformation $g_1' = g_1$ and $g_2' = g_2$ which is a good approximation when we consider the e-p interaction as strong. But, for weak and intermediate coupling regime, one can obtain a lower value of the ground state (GS) energy by considering g_1' and g_2' as variational parameters. One may note that the above variational LF transformation takes into account the displacement of the lattice modes caused by the e-p interaction and brings in coherence in the phonon state which is the essential effect

of the e-p interaction. Next, we apply, following Zheng [16], an onsite squeezing transformation with the generator:

$$R_2 = \alpha \sum_i (b_i b_i - b_i^{\dagger} b_i^{\dagger}), \tag{4.9}$$

where α is a variational parameter. The transformed Hamiltonian now becomes,

$$H_2 = e^{R_2} H_1 e^{-R_2} = H_1 + [R_2, H_1] + \frac{1}{2!} [R_2, [R_2, H_1]] + \cdots$$
(4.10)

$$= -t \sum_{\langle ij \rangle \sigma} c_{i\sigma}^{\dagger} c_{j\sigma} e^{(x_i - x_j)e^{-2\alpha}} + \widetilde{U} \sum_{i} n_{i\uparrow} n_{i\downarrow}$$

$$+ \omega_0 \left[\frac{e^{4\alpha}}{4} \sum_{i} (b_i^{\dagger} + b_i)^2 - \frac{e^{-4\alpha}}{4} \sum_{i} (b_i^{\dagger} - b_i)^2 \right] + \varepsilon \sum_{i\sigma} n_{i\sigma} + \frac{N\omega_0}{2}$$

$$+ P_1 e^{2\alpha} \sum_{i\sigma} n_{i\sigma} (b_i + b_i^{\dagger}) + P_2 e^{2\alpha} \sum_{i\delta\sigma} n_{i\sigma} (b_{i+\delta} + b_{i+\delta}^{\dagger})$$

$$(4.11)$$

The above transformation can be identified as the Bogolubov transformation and it normally takes care of some of the higher-order effects. Specifically, it incorporates the correlation between successively emitted virtual phonons at a particular site and also the anharmonic phonon-phonon interaction partially and thus the finite phonon life-time effect to a certain extent. Recently, Malik, Mukhopadhyay and Chatterjee (MMC) [19] have proposed a new electron-density-dependent squeezing transformation that lowers the GS energy further. This transformation is accomplished by the generator:

$$R_{3} = \alpha_{d} \sum_{i} n_{i\sigma} (b_{i}b_{i} - b_{i}^{\dagger}b_{i}^{\dagger}), \tag{4.12}$$

where the parameter α_d is to be obtained variationally. After the transformation with (4.12), the transformed Hamiltonian reads

$$H_3 = e^{R_3} H_2 e^{-R_2} = H_2 + [R_3, H_2] + \frac{1}{2!} [R_3, [R_3, H_2]] + \cdots$$
(4.13)

$$= -t \sum_{\langle ij \rangle \sigma} c_{i\sigma}^{\dagger} c_{j\sigma} e^{(x_{i}-x_{j})e^{-2\alpha}e^{-2\alpha_{d}\Sigma_{\sigma}n_{i\sigma}}} e^{(x_{i}'-x_{j}')} + \widetilde{U} \sum_{i} n_{i\uparrow} n_{i\downarrow}$$

$$+ \omega_{0} \left[\frac{e^{4\alpha}}{4} \sum_{i} \left\{ \left(b_{i}^{\dagger} + b_{i} \right) e^{2\alpha_{d}\Sigma_{\sigma}n_{i\sigma}} \right\}^{2} - \frac{e^{-4\alpha}}{4} \sum_{i} \left\{ \left(b_{i}^{\dagger} - b_{i} \right) e^{-2\alpha_{d}\Sigma_{\sigma}n_{i\sigma}} \right\}^{2} \right]$$

$$+ \varepsilon \sum_{i\sigma} n_{i\sigma} + \frac{N\omega_{0}}{2} + P_{1}e^{2\alpha} \sum_{i\sigma} n_{i\sigma} e^{2\alpha_{d}\Sigma_{\sigma}n_{i\sigma}} \left(b_{i} + b_{i}^{\dagger} \right)$$

$$+ P_{2}e^{2\alpha} \sum_{i\delta\sigma} n_{i\sigma} e^{2\alpha_{d}\Sigma_{\sigma}n_{i\sigma}} \left(b_{i+\delta} + b_{i+\delta}^{\dagger} \right)$$

$$(4.14)$$

where,

$$x_{i}' - x_{j}' = \alpha_{d} [(b_{i}b_{i} - b_{i}^{\dagger}b_{i}^{\dagger}) - (b_{j}b_{j} - b_{j}^{\dagger}b_{j}^{\dagger})]. \tag{4.15}$$

Next we perform the NN correlated squeezing transformation [17] with the generator:

$$\mathcal{R}_4 = \frac{1}{2} \sum_{i \neq j} \beta_{ij} (b_i b_j - b_i^{\dagger} b_j^{\dagger}), \tag{4.16}$$

where $\beta_{ij} = \beta$, if *i* and *j* are NN sites and zero otherwise. The transformed Hamiltonian then becomes

$$H_{4} = e^{R_{4}}H_{3} e^{-R_{4}} = H_{3} + [R_{4}, H_{3}] + \frac{1}{2!}[R_{4}, [R_{4}, H_{3}]] + \cdots$$

$$= -t \sum_{\langle ij \rangle \sigma} c_{i\sigma}^{\dagger} c_{j\sigma} e^{(x_{i} - x_{j})e^{-2\alpha}e^{-2\alpha_{d}\Sigma_{\sigma}n_{i\sigma}}} e^{(x_{i}' - x_{j}')} + \widetilde{U} \sum_{i} n_{i\uparrow} n_{i\downarrow}$$

$$+ \omega_{0} \frac{e^{4\alpha + 4\alpha_{d}\Sigma_{\sigma}n_{i\sigma}}}{4} \sum_{i} \left[\sum_{jj'} (\mu_{ij} + \nu_{ij})(\mu_{ij'} + \nu_{ij'}) (b_{j}^{\dagger} + b_{j}) (b_{j'}^{\dagger} + b_{j'}) \right]$$

$$- \omega_{0} \frac{e^{-4\alpha - 4\alpha_{d}\Sigma_{\sigma}n_{i\sigma}}}{4} \sum_{i} \left[\sum_{jj'} (\mu_{ij} - \nu_{ij})(\mu_{ij'} - \nu_{ij'}) (b_{j}^{\dagger} - b_{j}) (b_{j'}^{\dagger} - b_{j'}) \right]$$

$$+ \varepsilon \sum_{i\sigma} n_{i\sigma} + \frac{N\omega_{0}}{2} + P_{1}e^{2\alpha} \sum_{i\sigma} n_{i\sigma} e^{2\alpha_{d}\Sigma_{\sigma}n_{i\sigma}} \sum_{j} (\mu_{ij} + \nu_{ij})(b_{j}^{\dagger} + b_{j})$$

$$+ P_{2}e^{2\alpha} \sum_{i\delta\sigma} n_{i\sigma} e^{2\alpha_{d}\Sigma_{\sigma}n_{i\sigma}} \sum_{j} (\mu_{i+\delta,j} + \nu_{i+\delta,j})(b_{i+\delta} + b_{i+\delta}^{\dagger})$$

$$(4.18)$$

The Hamiltonian H_4 is to be averaged over a suitable phonon state for which KMC chose the zero-phonon state. In this work, we choose for the averaging phonon state a fully-generalized many-phonon state [20]:

$$\left|\Phi_{ph}\right\rangle = \sum_{n=0,1,2,\dots,M} c_n \left|\varphi_n(x)\right\rangle,\tag{4.20}$$

where $\varphi_n(x)$ represents the n —th excited state eigen function of a simple harmonic oscillator and M is the value of the upper limit of the summation in (4.20) at which the result converges. This is a fully generalized many-phonon state in the sense that it does not set any limit to the phonon occupation for any lattice site i.e., any site can contain any number of phonons. We can also have a less-general many-phonon state in which a particular site can have at most one phonon, which is a Gurari state. Obviously, the state (4.20) is the most general many-phonon state. The effective electronic Hamiltonian is obtained as

$$\begin{split} \mathcal{H}_{eff} &= \varepsilon_{eff} \sum_{i\sigma} n_{i\sigma} - t_{eff} \sum_{\langle ij \rangle \sigma} c_{i\sigma}^{\dagger} c_{j\sigma} + U_{eff} \sum_{i} n_{i\uparrow} n_{i\downarrow} \\ &+ N \omega_{0} \left[\frac{e^{4\alpha}}{4} \left(e^{2\beta} \right)_{00} (1 + 4\alpha_{d} + 12\alpha_{d}^{2}) S_{2} - \frac{e^{-4\alpha}}{4} \left(e^{2\beta} \right)_{00} (1 - 4\alpha_{d} + 12\alpha_{d}^{2}) S_{3} - \frac{1}{2} \right], (4.21) \end{split}$$

where

$$\varepsilon_{eff} = -\left[\frac{2}{\omega_0}(g_1g_1' + 2g_2g_2') - \frac{1}{\omega_0}(g_1'^2 + 2g_2'^2)\right] + \left[e^{2\alpha}(1 + 2\alpha_d + 3\alpha_d^2)M_1S_1\right]\left[(g_1 + 2g_2) - (g_1' + 2g_2')\right],\tag{4.22}$$

$$U_{eff} = U - \frac{2}{\omega_0} [2(g_1 g_1' + 2g_2 g_2') - (g_1'^2 + 2g_2'^2)], \qquad (4.23)$$

$$t_{eff} = te^{\alpha_d} F_1 F_2, \tag{4.24}$$

$$F_{1} = \sum_{k,l=0}^{M} c_{kl} \ e^{-\frac{\gamma^{2}}{4}} \int_{-\infty}^{\infty} dy \ e^{-y^{2}} H_{k} \left(y + \frac{\gamma}{2} \right) H_{l} \left(y - \frac{\gamma}{2} \right), \tag{4.25}$$

$$F_2 = \sum_{k,l=0}^{M} c_{kl} \int_{-\infty}^{\infty} dy \, e^{-\frac{y^2}{2}(1+\eta^2)} \, H_k(y) \, H_l(y\eta), \tag{4.26}$$

$$S_{i} = \sum_{k,l=0}^{M} c_{kl} \int_{-\infty}^{\infty} e^{-y^{2}} \xi_{i}(y) H_{k}(y) H_{l}(y) dy , \qquad (4.27)$$

$$M_1 = (e^{\beta})_{00} + 2n \sum_{m=1}^{\infty} (e^{\beta})_{0m} , \qquad (4.28)$$

$$\sum_{k} (A_{k}^{ij})^{2} = \frac{2g_{1}^{\prime 2}}{\omega_{0}^{2}} \left[(e^{2\beta})_{00} - (e^{-2\beta})_{01} \right] + \frac{2g_{2}^{\prime 2}}{\omega_{0}^{2}} \sum_{\delta' \delta''} \left[(e^{-2\beta})_{i+\delta',i+\delta''} - (e^{-2\beta})_{i+\delta',j+\delta''} \right] + \frac{4g_{1}^{\prime}g_{2}^{\prime}}{\omega_{0}^{2}} \sum_{\delta'} \left[(e^{-2\beta})_{0,i+\delta'} - (e^{-2\beta})_{i+\delta,i+\delta'} \right], \tag{4.29}$$

where

$$c_{kl} = c_k c_l \sqrt{1/2^{k+l} k! \, l! \, \pi}, \quad y = \sqrt{x},$$

$$\gamma = e^{-2\alpha} \sum_k A_k^{ij} \left(1 - 2\alpha_d + 3\alpha_d^2 \right),$$

$$\eta = 1 + 2\alpha_d,$$

$$\xi_1 = \sqrt{2}y, \quad \xi_2 = 2y^2, \quad \xi_3 = 2(y^2 - 2l - 1)$$
(4.30)

We calculate $(e^{\pm n\beta})_{0n}$ using the periodic boundary condition. Then the linear chain can be viewed as a ring of N lattice sites with N very large so that the effects of end points do not matter (Fig. 4.1).

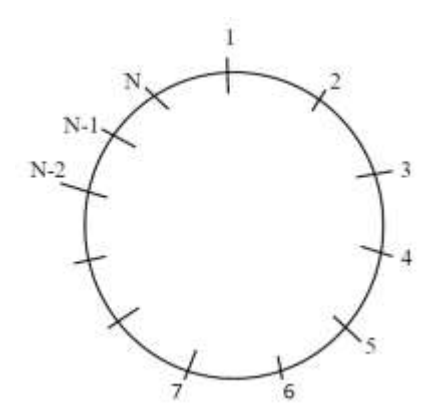


Fig. 4.1: The HH chain in the form of a ring under periodic boundary condition.

The matrix β is given by

$$\boldsymbol{\beta} = \begin{pmatrix} 0 & \beta & 0 & 0 & 0 & \dots & 0 & 0 & \beta \\ \beta & 0 & \beta & 0 & 0 & \dots & 0 & 0 & 0 & 0 \\ 0 & \beta & 0 & \beta & 0 & \dots & 0 & 0 & 0 & 0 \\ \vdots & & \vdots & & \vdots & & \vdots & & \vdots \\ \beta & 0 & 0 & 0 & 0 & 0 & 0 & 0 & 0 & 0 \end{pmatrix}$$

We find that the element $(e^{\pm n\beta})_{0q}$ for the ring structure in Fig. 4.1 can be represented exactly by the following closed form analytical expression:

$$\left(e^{\pm n\beta}\right)_{0q} = \sum_{p=0,1,2...} (\pm 1)^q \frac{(n\beta)^{2p+q}}{p! (p+q)!},\tag{4.31}$$

For a half-filled band, the Hamiltonian (4.21) can be exactly solved using the Bethe ansatz technique [35] and the GS energy per site is obtained (in units of ω_0) as:

$$\varepsilon_{0} = \varepsilon_{eff} + \frac{1}{4} \left[e^{4\alpha} \left(e^{2\beta} \right)_{00} \left\{ (1 + 4\alpha_{d} + 12\alpha_{d}^{2}) S_{2} - e^{-8\alpha} (1 - 4\alpha_{d} + 12\alpha_{d}^{2}) S_{3} \right\} \right] - \frac{1}{2}$$

$$- \int_{0}^{\infty} \frac{4 t_{eff} J_{0}(y) J_{1}(y) dy}{y \left[1 + e^{\frac{y U_{eff}}{2 t_{eff}}} \right]}, \tag{4.32}$$

which is finally minimized with respect to $g'_1, g'_2, \alpha, \alpha_d, \beta$ and c_n 's.

4.3 Numerical results and discussion

We consider here both the adiabatic regime (large t, small ω_0) and the non-adiabatic regime (small t, large ω_0) and examine the nature of the large-polaron to small-polaroron transition as a function of the hopping parameter, the e-p interaction coefficients and the Hubbard correlation. Throughout the analysis, we work with $U_{eff} > 0$ so that the formation of bipolaron is precluded and the only insulating phase that the system can possible in the system is the Mott antiferromagnetic (AFM) spin density wave (SDW) polaron state. We make a comparison of our results for the GS energy with those of KMC to show that the present calculation lowers the GS energy and therefore is expected to predict a more accurate result for the ST transition. Using the Bethe ansatz solution of the effective electronic

problem, KMC have predicted the continuity of the ST transition. As the problem is not exactly soluble, our primary objective here has been to examine whether the scenario changes in the case of an improved calculation.

We find that the present variational calculation does yield an improvement, albeit marginal, in the GS energy which is of course expected because the present work involves an improved phonon wave function. Also, the GS energy is found to decrease as the on-site e-p interaction coefficient g_1 increases. This is also an expected result as an increase in g_1 is expected to lead to a stronger polaron binding. We do not show the results for the GS energy here because the magnitude of the improvement in the GS energy is not so much important for our purpose; what is really important for us is whether or not the improved calculation supports the conclusion of the KMC. To that end, we need to calculate the parameters that can indicate the behaviour of the ST transition unequivocally. The size and depth of the polarization potential, the phonon correlation coefficient and the effective hopping parameter are some of the quantities the behaviour which can clearly demonstrate the character of the ST transition.

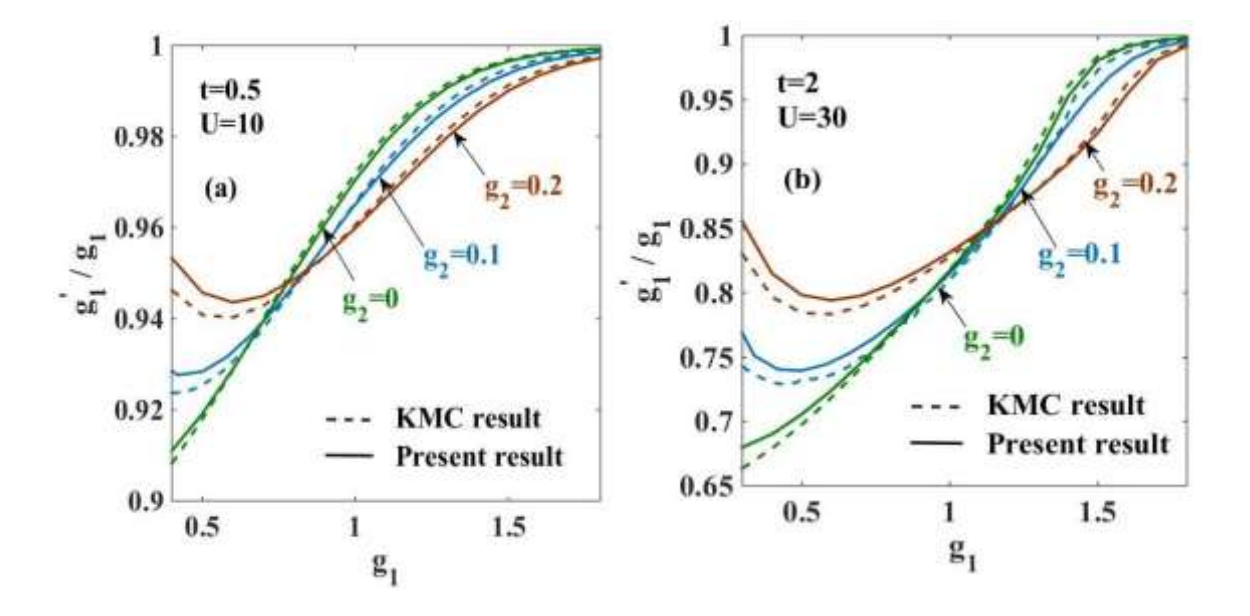


Fig. 4.2 g'_1/g_1 vs g_1 for a few values of g_2 for an: (a) anti-adiabatic case (t = 0.5); (b) adiabatic case (t = 2).

For a small value of the onsite e-p interaction coefficient g_1 , the distortion of the lattice vibration is spread over many lattice sites and a large polaron is created. As g_1 increases, the

spread of the lattice distortion shrinks and the polaron size decreases. In Fig. 4.2, we plot the behaviour of g_1'/g_1 with respect to g_1 for a few values of the NN e-p interaction coefficient g_2 . For the anti-adiabatic case, we have chosen t=0.5 and U=10. These values satisfy the condition: $U_{eff}>0$ for the considered range of g_1 . For the adiabatic case, we have chosen t=2. In this case, we need to consider a stronger Coulomb correlation strength to keep the effective Coulomb correlation strength positive and we have chosen to work with U=30.

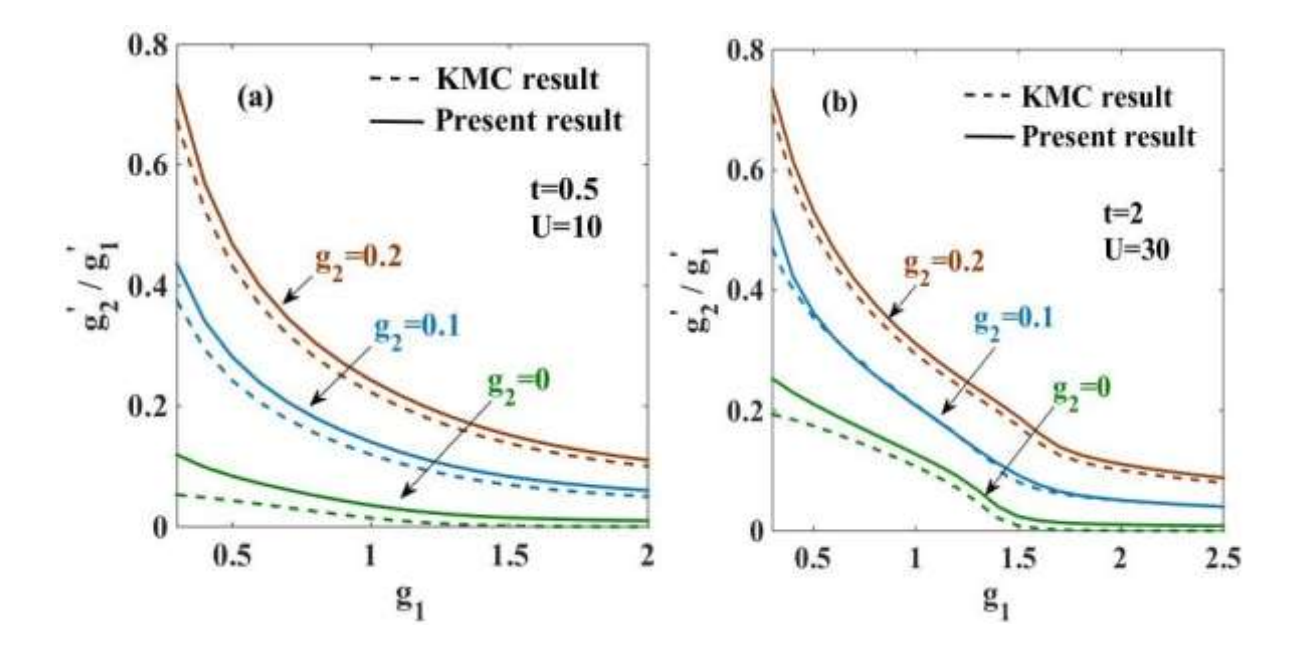


Fig. 4.3: g'_2/g'_1 vs g_1 for different values of g_2 for an (a) anti-adiabatic case (t = 0.5); (b) adiabatic case (t = 2).

Figs. 4.2(a) and 4.2(b) show that as g_1 increases, g'_1/g_1 initially goes through a dip and then increases monotonically and finally g'_1 becomes asymptotically equal to g_1 . In this limit, the depth of the polarization potential becomes maximum leading to the strongest polaronic binding. What we have in this case is a self-trapped small polaron localized in a single lattice state. One can clearly see that Fig. 4.2 suggests that the ST transition is continuous in both the adiabatic and anti-adiabatic cases which is in agreement with the observation of KMC. Since the present calculation is more accurate, it lends more credence in favour of the continuity of the ST transition. One can also see that the present improved calculation predicts a stronger coherence in the phonon cloud of the polaron than the one indicted by KMC, particularly for

weaker e-p coupling constant. We also note that as g_2 increases, a larger value of g_1 is necessary for polaron localization. The reason for such a behaviour is easy to understand. With increasing g_2 , the polaron develops a stronger tendency to remain mobile and therefore, unless the on-site e-p interaction g_1 is made sufficiently large, the polaron cannot be trapped. The spread of the lattice distortion is denoted by g_2' .

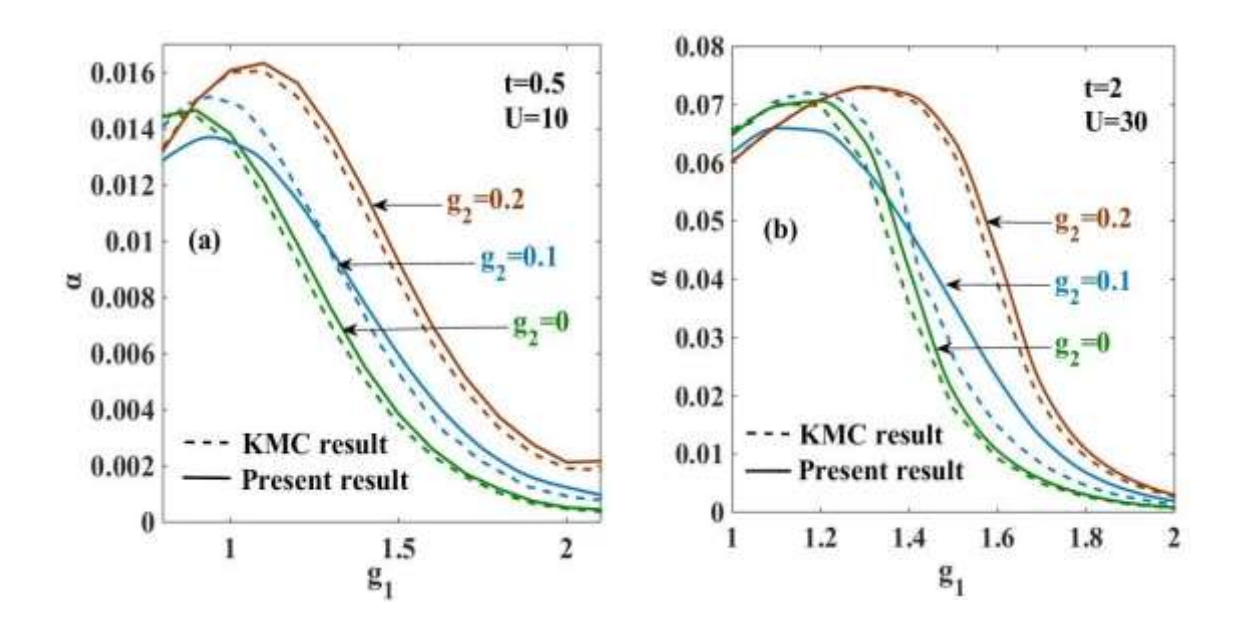


Fig. 4.4: α vs g_1 for different values of g_2 for an (a) anti-adiabatic case (t = 0.5); (b) adiabatic case (t = 2).

In Fig. 4.3, we plot g'_2/g'_1 as a function of g_1 for a few values of g_2 . In Fig. 4.3(a), we plot results for an anti-adiabatic region whereas in Fig. 4.3(b), we give results for an adiabatic region. One can see that g'_2/g'_1 is higher for smaller values of g_1 . This implies that the polaron size is large at small g_1 . As g_1 increases, g'_2/g'_1 decreases and gradually becomes zero, which implies that the polaron reduces its size with increasing g_1 and eventually gets trapped within a single lattice spacing. According to Fig. 4.3, in both adiabatic and anti-adiabatic cases, the ST transition takes place continuously.

Fig. 4.4 suggests the same qualitative behaviour as shown in Fig. 4.3. For example, as the NN EPI becomes stronger, a larger value of g_1 is necessary to localize the polaron. Similarly, with the increase in g_2 , g_2'/g_1' increases as well. This suggests that the polaron becomes more

mobile as g_2 increases. The present result predicts that the ST transition takes place at a higher value of g_1 than the one indicated by the KMC result.

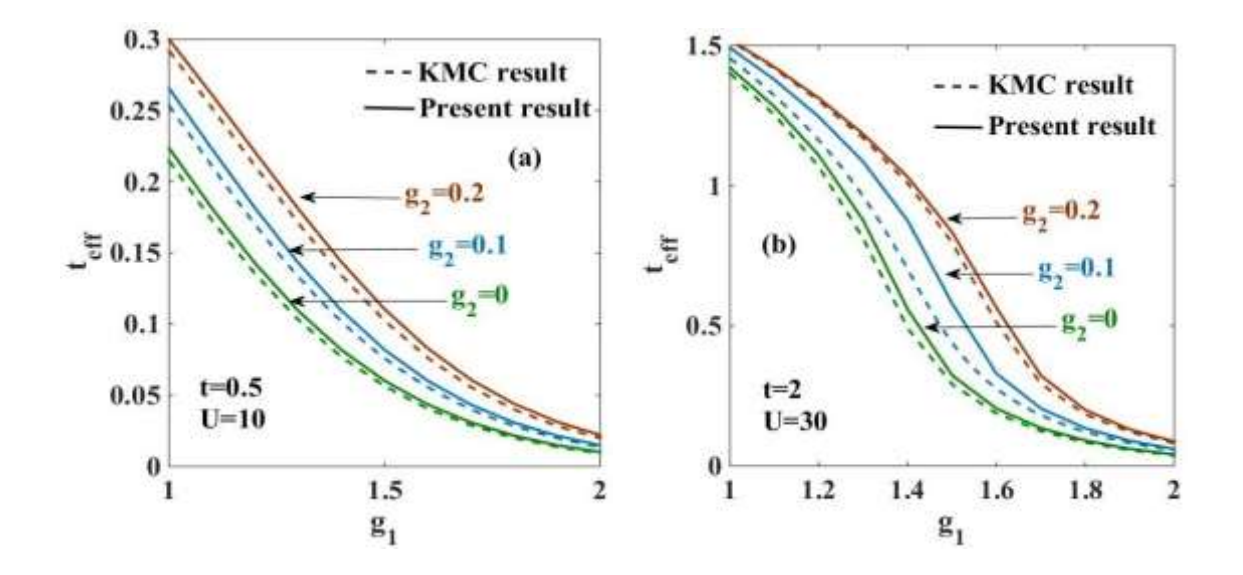


Fig. 4.5 t_{eff} vs g_1 for different values of g_2 for an (a) anti-adiabatic case (t = 0.5); (b) adiabatic case (t = 2).

The effective polaron hopping parameter t_{eff} is plotted with respect to g_1 in Fig. 4.5. We find that in the limit $g_1 \rightarrow 0$, t_{eff} completely loses the shroud of the phononic clouding and turns onto the bare Hubbard parameter t. As g_1 increases, t_{eff} decreases and decreases continuously and finally reduces to zero. The renormalized hopping parameter t_{eff} is linear in the width of the polaron band and is reciprocal to the polaron mass, a quantity that can be measure in the laboratory through optical experiments or magneto-optical experiments. Hence, the continuous transition of a large mobile polaron with finite t_{eff} to an immobile localized small polaron with $t_{eff} = 0$ clearly describes continuity of the ST transition for both non-adiabatic and adiabatic cases. Fig. 4.5 shows that our result for t_{eff} is a little higher than the one obtained by KMC which again implies that according to our results, a higher g_1 than the one predicted by KMC is needed to cause the ST transition.

4.4 Conclusion

In the present work, we have examined the ST transition in a 1D extended HH model by employing a more accurate variational method than the one used by KMC [31]. The phonon

subsystem has been treated by a series of unitary transformations by incorporating all the essential aspects of the phonon mechanisms and the attributes of the e-p interaction. A fully generalized many-body phonon state has been used as the averaging phonon state in place of the zero-phonon state used previously, to get the effective electronic problem which is finally treated exactly by the Bethe ansatz method. Since the total phonon state used in this work can be considered as essentially exact and the Bethe ansatz technique has been used to obtain the effective electron problem exactly, the present calculation can be considered to provide very accurate results.

Our results suggest that a stronger EPI than the one suggested by KMC is required for the ST transition to take place. Also as the NN e-p interaction strength increases, a higher value of the onsite e-p coupling is needed to induce polaronic localization. This is because with the enhancement in the NN e-p interaction, the polaron mobility increases and then naturally we need a higher on-site e-p coupling for polaron trapping. Regarding the nature of the ST transition, our results support the conjecture of KMC i.e., the ST transition is a continuous transition both in the adiabatic regime and also in the anti-adiabatic regime. Since the present calculation is analytical and is based on an essentially exact wave function, it has a few advantages over other calculations. First, since we have an accurate wave function of the system, we have a much clearer understanding of the physics and dynamics of the system. Secondly, we have a clear view of how variables and interactions between variables affect the result. Thirdly and finally, the analytical results are more transparent and trustworthy than those obtained from numerical methods.

4.5 References

- [1] T.K. Mitra, A. Chatterjee, S. Mukhopadhyay, Phys. Rep. **153** (1987) 91;
- [2] J.T. Devreese, A.S. Alexandrov, Rep. Prog. Phys. 72 (2009) 066501.
- [3] A. Chatterjee, S. Mukhopadhyay, Polarons and Bipolarons: An Introduction, Taylor and Francis, 2018.
- [4] A.S. Alexandrov, N.F. Mott, Rep. Prog. Phys. B **57** (1994) 1197.
- [5] R. Micnas, J. Ranninger, S. Robaszkiewicz, Rev. Modern Phys. **62** (1) (1990) 113–171.
- [6] K.H. Kim, J.Y. Gu, H.S. Choi, G.W. Park, T.W. Noh, Phys. Rev. Lett. 77 (1996) 1877.
- [7] M. Califano, G. M. Francisco, Nano Lett. 13, 5, (2013) 2047–2052.

- [8] F. Peeters, J.T. Devreese, et al., Phys. Status Solidi B 112 (1982) 219;
- [9] B. Gerlach, H. Löwen, Phys. Rev. B 35 (1987) 4291;
- [10] B. Gerlach, H. Löwen, Phys. Rev. B 35 (1987) 4297;
- [11] R. Manka, Phys. Stat. Solidi (b) 93, 53 (1979);
- [12] R. Manka, M. Suffczynski, J. Phys. C 13, 6369 (1980);
- [13] A. Chatterjee, S. Sil, Phys. Rev. B **51** (1995) 2223.
- [14] R.P.M. Krishna, S. Mukhopadyay, A. Chatterjee, Phys. Lett. A 327 (2004) 67.
- [15] I. Lang, Y.A. Firsov, Sov. Phys. JETP 16 (1963) 1301.
- [16] H. Zheng, Phys. Lett. A 131 (1988) 115.
- [17] C.F. Lo, R. Sollie, Phys. Rev. B 48 (1993) 10183.
- [18] Lieb, E. H. & Wu, F. Y, Phys. Rev. Lett. 20, 1445–1448 (1968).
- [19] Z.M. Malik, S. Mukhopadhyay, A. Chatterjee, Phys. Lett. A, 383, 1516-1519 (2019).
- [20] D. Debnath, M. Z. Malik & A. Chatterjee, Sci Rep. 11, 12305 (2021).
- [21] H. Bethe, Magazine for Physics, **71**, 205-226 (1931).

5

Self-trapping transition in a twodimensional Holstein-Hubbard model: A Mean-field approach

5.1 Introduction

Though the ST transition of polaron [1-3] has been in the forefront of research due to its several applications, the nature of the transition is still under investigation. In Chapter 4, we have presented our recent work on the ST transition in an extended Holstein-Hubbard (HH) model and have shown using a semi-exact calculation that the ST transition in 1D extended HH model is continuous in both adiabatic and anti-adiabatic regimes. But the real systems of interest in the context of high-temperature curate superconductors [5-7], transition-metal dichalcogenides [8-10] and other correlated systems [11-15] are all essentially two-dimensional. A few ST transition problems have been studied for the excitonic [16] and photonic lattices [17, 18] and perovskite materials [19, 20] in 2D. But these studies have not reported about the nature of the ST transition.

Recently, Sankar, Mukhopadhyay and Chatterjee (SMC) [25] have studied the ST transition in the 2D extended HH Hamiltonin in the weak correlation regime. They have included the phonon coherence and correlations for the phonon sub-system using the modified LF transformation and squeezing transformations and obtained the effective electronic Hamiltonian by averaging with respect to a zero-phonon state. Finally they have solved the effective electronic Hamiltonian using the mean-field Hartree-Fock (HF) method. Their

calculation shows that the ST transition is continuous in the anti-adiabatic regime while it is discontinuous in the adiabatic region. Sankar and Chatterjee (SC) [26] have studied the ST transition in the same 2D extended HH model in the strong correlation regime. They have treated the phonon sub-system in the same way as SMC did, but to treat the effective electric Hamiltonian, they have first transformed it to an effective t - J model and solved it finally using the Zuberev Green function technique. Their conclusions are qualitatively similar to that of SMC.

In this chapter, we study the ST transition in a 2D extended HH model with a more improved variational calculation than the one carried out by Sankar and collaborators [25, 26]. The idea is to examine whether an improved variational calculation with a modified phonon state discounts the conclusion of Sankar and collaborators or reinforces it. The calculation is modified by making the phonon wave function more accurate by performing a newly invented electron-density-dependent correlated squeezing transformation [28] followed by a many-phonon averaging [29]. The variational phonon wave function chosen here can be considered as "essentially" exact. The effective electronic Hamiltonian is solved using the similar method as incorporated by Sankar and his collaborators. Here also we consider the strength of the onsite Coulomb interaction to be sufficiently large so that the phonon-induced effective correlation coefficient remains positive in order to prevent the formation of bipolaronic CDW state through Peierls instability. The ST transition is examined by analyzing the relevant parameters both in the adiabatic and anti-adiabatic regimes for both the strong and weak Coulomb interaction strengths.

5.2 Model and formulation

A 2D EHH model can be described by the Hamiltonian

$$H = H_e + H_p + H_{ep} \,, \tag{5.1}$$

with

$$\begin{split} H_{e} &= -t \sum_{\langle ij \rangle \sigma} c_{i\sigma}^{\dagger} c_{j\sigma} + U \sum_{i} n_{i\uparrow} n_{i\downarrow} + V_{1} \sum_{\langle ij \rangle \sigma\sigma'} n_{i\sigma} n_{j\sigma'} \\ &+ V_{2} \sum_{i\delta' \sigma\sigma'} n_{i\sigma} n_{i+\delta',\sigma'} \,, \end{split} \tag{5.2}$$

$$H_p = \hbar \omega_0 \sum_i b_i^{\dagger} b_i , \qquad (5.3)$$

$$H_{ep} = g_1 \sum_{i\sigma} n_{i\sigma} (b_i + b_i^{\dagger}) + g_2 \sum_{i\delta\sigma} n_{i\sigma} (b_{i+\delta} + b_{i+\delta}^{\dagger}).$$
 (5.4)

Here H_e describes the extended Hubbard Hamiltonian where the parameter t denotes the NN hopping integral, $n_{i\sigma}(=c_{i\sigma}^{\dagger}c_{i\sigma})$ represents the number operator for the spin- σ electron at site i, $c_{i\sigma}^{\dagger}(c_{i\sigma})$ being the corresponding electron creation (annihilation) operator, and U, V₁, and V₂ give the onsite, nearest neighbour (NN) and next nearest neighbour (NNN) Coulomb interaction energies respectively, H_p is the phonon Hamiltonian, $b_i^{\dagger}(b_i)$ being the creation (annihilation) operator for an optical phonon at site i with dispersionless frequency ω_0 and H_{ep} is the extended Holstein e-p interaction, g_1 and g_2 being the on-site and NN e-p coupling strengths, respectively. We will write: $g_1 = \sqrt{\alpha}$, where α is the onsite e-p coupling coefficient.

To disentangle the e-p interaction term, the Lang-Firsov transformation (LFT) [27] has been used extensively in the past. This transformation lowers the energy by displacing the phonon vacuum. The phonon state then becomes a coherent superposition of states with different phonon numbers. Several studies on the HH model [26, 30, 32, 49-52] and the Anderson-Holstein model have shown that the variational LFT (VLFT) method is more useful. We, therefore, employ VLFT to transform the EHH model with the generator

$$R_1 = \frac{g_1'}{\omega_0} \sum_{i\sigma} n_{i\sigma} (b_i^{\dagger} - b_i) + \frac{g_2'}{\omega_0} \sum_{i\delta\sigma} n_{i\sigma} (b_{i+\delta}^{\dagger} - b_{i+\delta}) , \qquad (5.5)$$

where $g_1' = \eta_1 \sqrt{\alpha}$ and $g_2' = \eta_2 \sqrt{\alpha}$, η_1 and η_2 being the variational parameters. g_1' gives essentially a measure of the depth of the on-site lattice polarization potential created by the epinteraction and g_2' represents the width of the polaron potential well. The VLFT transforms the Hamiltonian H to $H_1 = e^{R_1}He^{-R_1}$. An electron can be considered as a phonon-source. As an electron makes an emission of an optical phonon, it undergoes a recoil motion and during its action of recoiling, if it releases another phonon, then these two phonons would have a built-in correlation. This phonon-correlation effect can be incorporated by considering a Bogolubov transformation with a generator [28]:

$$R_2 = \alpha_s \sum_i (b_i b_i - b_i^{\dagger} b_i^{\dagger}), \tag{5.6}$$

where α_s which gives a measure of the phonon correlation is called a squeeze parameter and will be treated as a variational parameter. The squeezing transformation transforms H_1 to $H_2 = e^{R_2}H_1e^{-R_2}$. Since the average phonon correlation in the phonon function is expected to depend on the electron number at the lattice sites, Malik et al. (MMC) [19] have recently suggested that an increase in the electron concentration would increase the average phonon correlation. This immediately implies that R_2 should at least partially depend on the electron concentration. MMC [30] have introduced a new unitary transformation to incorporate this density-dependent phonon correlation effect. Chatterjee and collaborators have subsequently used this transformation in a more improved work [32] and also in a related problem [52] to lower the GS energy. We apply this density-dependent squeezing transformation to H_2 with the generator

$$R_3 = \alpha_d \sum_i n_{i\sigma} (b_i b_i - b_i^{\dagger} b_i^{\dagger}), \tag{5.7}$$

where α_d is a trial parameter to be determined variationally. The new Hamiltonian reads $H_3 = e^{R_3}H_2e^{-R_3}$. Finally, we consider intersite phonon correlations. This can be incorporated by correlated squeezing transformation. However, we consider only NN phonon correlation. Following Lo and Sollie [29], the generator of the correlated squeezing transformation is chosen as

$$\mathcal{R}_4 = \frac{1}{2} \sum_{i \neq j} \beta_{ij} \left(b_i b_j - b_i^{\dagger} b_j^{\dagger} \right). \tag{5.8}$$

Here we choose, $\beta_{ij} = \beta$, when i and j are NN and $\beta_{ij} = 0$, otherwise. The parameter β is obtained variationally. The Hamiltonian after the above transformation becomes: $\mathcal{H} \equiv H_4 = e^{R_4}H_3e^{-R_4}$. One may notice that the transformation (6), incorporates the mean-field part of the phonon correlations while (8) includes the deviation from the mean-field part i. e., the fluctuations. The purpose of carrying out a set of unitary transformation is to decouple the electron and phonon variables. However an exact separation of the electron and phonon variables is not possible for the present problem. We therefore seek a variational solution by taking the average of \mathcal{H} with a suitable phonon state $|\Phi_{ph}\rangle$ so that the phonon variables are eliminated. This entire process is same as making the following choice for the variational phonon wave function:

$$|\psi_{vh}\rangle = e^{-R_1}e^{-R_2}e^{-R_3}e^{-R_4}|\Phi_{vh}\rangle$$
 (5.9)

We thus write an approximate wave function for the original Hamiltonian in the following product form:

$$|\Psi\rangle = |\psi_{el}\rangle \otimes |\psi_{ph}\rangle,\tag{5.10}$$

so that the total energy of the system can then be written as:

$$E = \langle \Psi | H | \Psi \rangle = \langle \psi_{el} | \langle \psi_{ph} | H | \psi_{ph} \rangle | \psi_{el} \rangle = \langle \psi_{el} | \langle \Phi_{ph} | \mathcal{H} | \Phi_{ph} \rangle | \psi_{el} \rangle. \tag{5.11}$$

For $|\Phi_{ph}\rangle$, we choose a fully general phonon state as:

$$|\Phi_{ph}\rangle = \sum_{n=0}^{M} r_n |\varphi_n(x)\rangle,$$
 (5.12)

where $\varphi_n(x)$ is the n-th eigen function of a harmonic oscillator and r_n 's are variational parameters. Our aim is to begin the numerical computation with the value of M equal to zero and then systematically increase its value till the energy becomes convergent. The effective electronic Hamiltonian becomes

$$H_{eff} = \langle \psi_{ph} | H | \psi_{ph} \rangle = \langle \Phi_{ph} | \mathcal{H} | \Phi_{ph} \rangle = \langle \Phi_{ph} | e^{R_4} e^{R_3} e^{R_2} e^{R_1} H e^{-R_1} e^{-R_2} e^{-R_3} e^{-R_4} | \Phi_{ph} \rangle$$

$$= \varepsilon_{eff} \sum_{i\sigma} n_{i\sigma} - t_{eff} \sum_{\langle ij \rangle \sigma} c^{\dagger}_{i\sigma} c_{j\sigma} + U_{eff} \sum_{i} n_{i\uparrow} n_{i\downarrow} + V_1^e \sum_{\langle ij \rangle \sigma\sigma'} n_{i\sigma} n_{j\sigma'}$$

$$+ V_2^e \sum_{i\delta'\sigma\sigma'} n_{i\sigma} n_{i+\delta',\sigma'}$$

$$+ \frac{N\omega_0}{4} \left[e^{4\alpha} (e^{2\beta})_{00} T_2 (1 + 4\alpha_d + 12\alpha_d^2) - e^{-4\alpha} (e^{2\beta})_{00} T_3 (1 - 4\alpha_d + 12\alpha_d^2) - 2 \right], \qquad (5.13)$$

where

$$\varepsilon_{eff} = -\frac{1}{\omega_0} [2(g_1 g_1' + z g_2 g_2') - (g_1'^2 + z g_2'^2)] + e^{2\alpha} (1 + 2\alpha_d + 3\alpha_d^2) M_1 T_1 [(g_1 + z g_2) - (g_1' + z g_2')],$$
 (5.14)

$$t_{eff} = te^{\alpha_d} F_1 F_2 F_3 , \qquad (5.15)$$

$$U_{eff} = U - \frac{2}{\omega_0} \left[2(g_1 g_1' + z g_2 g_2') - (g_1'^2 + z g_2'^2) \right], \tag{5.16}$$

$$V_1^e = V_1 - \frac{2}{\omega_0} [(g_1 g_2' + g_1' g_2) - g_1' g_2'], \quad V_2^e = V_2 - \frac{1}{\omega_0} [2g_2 g_2' - g_2'^2], \quad (5.17)$$

$$F_1 = \sum_{k,l=0}^{M} c_{kl} \int_{-\infty}^{\infty} dy \, e^{-y^2} \, H_k(y) \, H_l(y) \,, \tag{5.18}$$

$$F_2 = \sum_{k,l=0}^{M} c_{kl} \ e^{-\frac{\gamma^2}{4}} \int_{-\infty}^{\infty} dy \ e^{-y^2} \ H_k\left(y + \frac{\gamma}{2}\right) H_l\left(y - \frac{\gamma}{2}\right), \tag{5.19}$$

$$F_3 = \sum_{k,l=0}^{M} c_{kl} \int_{-\infty}^{\infty} dy \ e^{-\frac{y^2}{2}(1+\eta^2)} H_k(y) H_l(y\eta) , \qquad (5.20)$$

$$T_{i} = \sum_{k,l=0}^{M} c_{kl} \int_{-\infty}^{\infty} e^{-y^{2}} \xi_{i}(y) H_{k}(y) H_{l}(y) dy , \qquad (5.21)$$

$$M_1 = (e^{\beta})_{00} + 2n \sum_{m=1}^{\infty} (e^{\beta})_{0m}$$
 , (5.22)

$$\sum_{k} \left(A_{k}^{ij}\right)^{2} = \frac{2g_{1}^{\prime 2}}{\omega_{0}^{2}} \left[\left(e^{2\beta}\right)_{00} - \left(e^{-2\beta}\right)_{01} \right] + \frac{2g_{2}^{\prime 2}}{\omega_{0}^{2}} \sum_{\delta' \delta''} \left[\left(e^{-2\beta}\right)_{i+\delta',i+\delta''} - \left(e^{-2\beta}\right)_{i+\delta',j+\delta''} \right]$$

$$+\frac{4g_1'g_2'}{\omega_0^2}\sum_{\delta'}\left[\left(e^{-2\beta}\right)_{0,i+\delta'}-\left(e^{-2\beta}\right)_{i+\delta,i+\delta'}\right],\tag{5.23}$$

where
$$y = \sqrt{x}$$
 (5.24)

and
$$c_{kl} = c_k c_l \sqrt{1/2^{k+l} k! \, l! \, \pi},$$
 (5.25)

$$\gamma = e^{-2\alpha_s} \sum_k A_k^{ij} (1 - 2\alpha_d + 3\alpha_d^2), \ \eta = 1 + 2\alpha_d, \tag{5.26}$$

$$\xi_1 = \sqrt{2}y, \, \xi_2 = 2y^2, \, \xi_3 = 2(y^2 - 2l - 1),$$
 (5.27)

 $(e^{\pm n\beta})_{0n}$ is to be calculated for a 2D square lattice as explained in chapter 3.

$$(e^{\pm n\beta})_{00} = \sum_{p=0}^{\infty} {2m \choose m} \frac{(\pm n\beta)^{2p}}{p! \, p!} \,,$$
 (5.28)

$$(e^{\pm n\beta})_{0q} = \sum_{p=0}^{\infty} \left(2p + \left(\frac{q-1}{2} + 1 \right) \right) \frac{(\pm n\beta)^{\left[2p + \left(\frac{q-1}{2} + 1 \right)\right]}}{p! \left[p + \left(\frac{q-1}{2} + 1 \right) \right]!} , \qquad (q = odd)$$
 (5.29)

$$(e^{\pm n\beta})_{0q} = \sum_{p=0}^{\infty} {2p + (\frac{q}{2} + 1) \choose p+1} \frac{(\pm n\beta)^{\left[2p + (\frac{q}{2} + 1)\right]}}{p! \left[p + (\frac{q}{2} + 1)\right]!} . (q = even) (5.30)$$

For the electrons, we assume a square density of states (which is a valid assumption in 2D) and write

$$\rho(\varepsilon_k) = \frac{1}{2W} \quad ; \quad -W \le \varepsilon_k \le W \tag{5.31}$$

= 0 : otherwise.

(a) Weak Correlation:

For weak correlation, we use the HF approximation and the GS energy (ε_W) (per particle) for the system is obtained as

$$\varepsilon_{W} = n \, \varepsilon_{eff} - \frac{1}{2} z \, t_{eff} (2n - n^{2}) + \frac{n^{2}}{4} U_{eff} + z n^{2} V_{1}^{e} + z' n^{2} V_{2}^{e}$$

$$+ \frac{N \omega_{0}}{4} \left[e^{4\alpha} \left(e^{2\beta} \right)_{00} T_{2} \left(1 + 4\alpha_{d} + 12\alpha_{d}^{2} \right) - e^{-4\alpha} \left(e^{2\beta} \right)_{00} T_{3} \left(1 - 4\alpha_{d} + 12\alpha_{d}^{2} \right) - 2 \right] , \qquad (5.32)$$

which is finally minimized with respect to $g_1', g_2', \alpha_s, \alpha_d, \beta$ and c_n 's.

(b) Strong Correlation

In the strong correlation regime we solved the electronic Hamiltonian in the same way as explained in chapter 3, section 3.2.2. The GS energy per site (ε_{SN}) for the system reads

$$\varepsilon_{S} = n\varepsilon_{e} - \left(\varphi_{t}\;t_{eff} + p\tilde{J}\right)zp + Nz\left[\frac{1}{4}\left(\tilde{J} - 4(V_{1}^{e} + V_{2}^{e})\right)n^{2} + \tilde{J}p^{2}\right]$$

$$+\frac{N\omega_0}{4} \left[e^{4\alpha} \left(e^{2\beta} \right)_{00} T_2 \left(1 + 4\alpha_d + 12\alpha_d^2 \right) - e^{-4\alpha} \left(e^{2\beta} \right)_{00} T_3 \left(1 - 4\alpha_d + 12\alpha_d^2 \right) - 2 \right]. \tag{5.33}$$

5.2 Numerical Results

5.3.1 Weak Correlation results

We have considered both the non-adiabatic (large ω_0 , small t) and adiabatic (small ω_0 , large t) cases by taking two different values of t (0.5 and 2). We have also compared our results with those of Sankar et al. [50] by choosing $V_1 = V_2 = 0$.

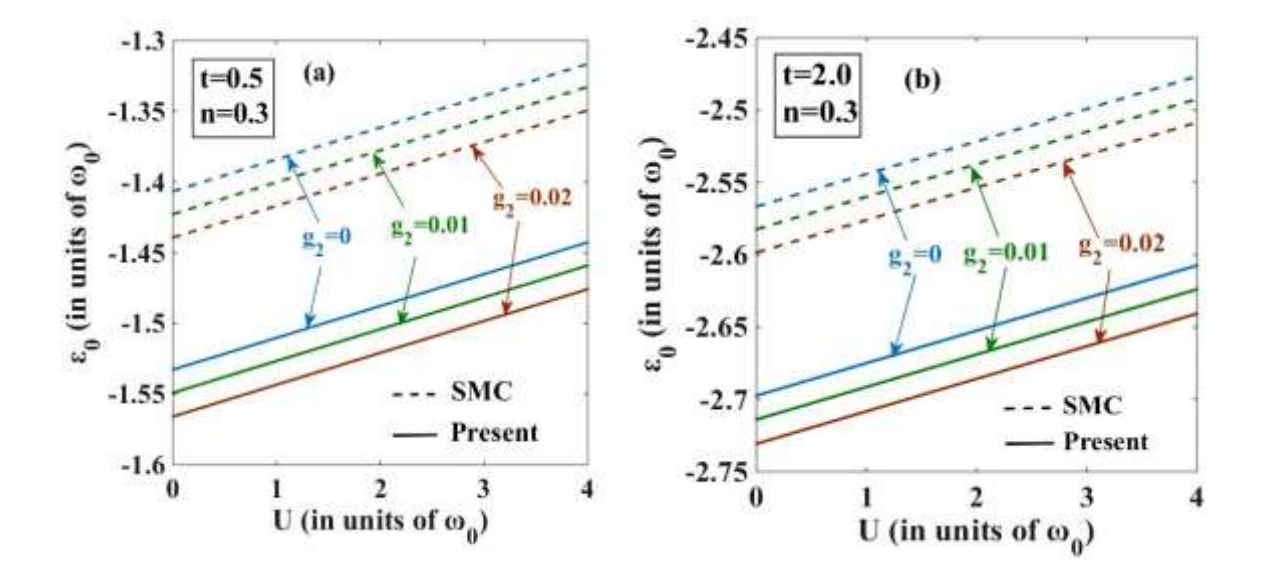


Fig. 5.1: GS energy (ε_0) vs. Coulomb correlation (U) for (a) anti-adabatic case; (b) adiabatic case.

Fig 5.1 shows how NN e-p interaction influences the $\varepsilon_0 - U$ plots. It is clearly visible that the NN e-p interaction lowers the GS energy further. Also the present method provides a lower GS than the ones obtained by Sankar et al. [50], as expected from an improved variational calculation. In Fig. 5.2, g_1'/g_1 is plotted with respect to g_1 for both adiabatic and

non-adiabatic cases. At small g_1 , g_1' is small. This is because at small g_1 , the lattice deformation spreads over several sites and one has a large polaron. As g_1 increases, g_1' also increases and above a critical g_1 , g_1' equals g_1 . This is the small polaron phase. With the increase in g_1 , the onsite polarization potential becomes deep and consequently the polaron gets confined and loses its mobility resulting in the formation of a small polaron. Thus, an increase in g_1 leads to a ST transition. In Fig. 5.2(a), g_1'/g_1 gradually increases with g_1 and finally saturates to $g_1' = g_1$ in a continuous way. Thus ST transition turns out to be continuous in this case. For the adiabatic case (Fig. 5.2(b)), g_1'/g_1 sharply reaches 1 at a critical g_1 implying that the transition is discontinuous here. In the present analysis, the polaron localization takes place at a higher value of g_1 compared to that in [50].

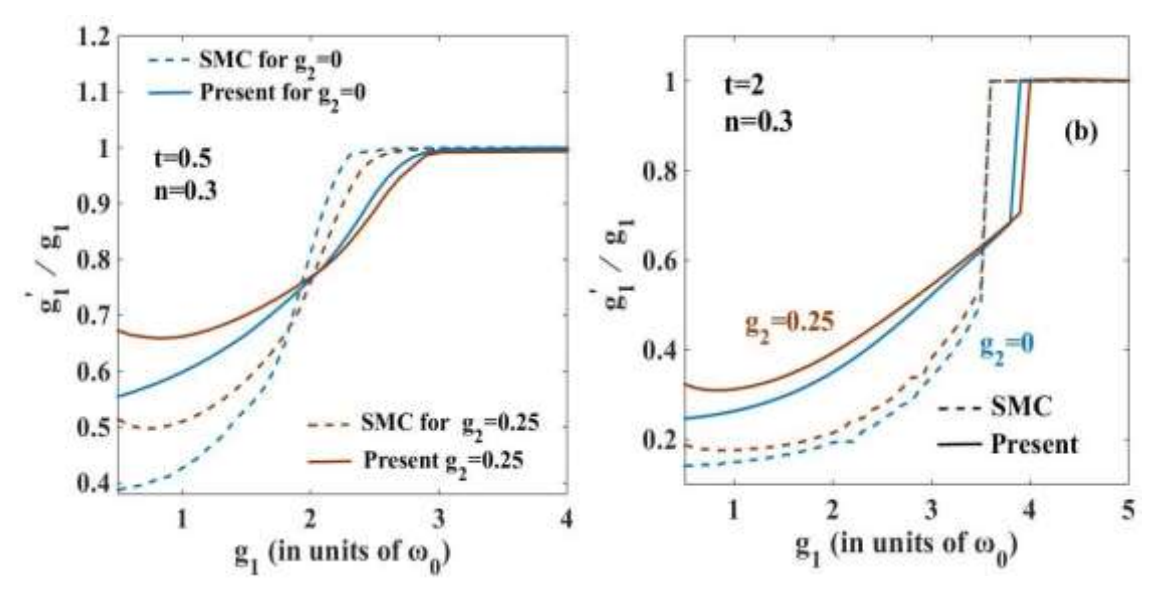


Fig. 5.2 g'_1/g_1 vs. g_1 for different values of g_2 for: (a) anti-adiabatic case; (b) adiabatic case, with U=3 at less than half-filling.

The variations of g'_2/g'_1 with respect to g_1 is studied in Fig. 5.3 for t=0.5 and 2. As g_1 increases, g'_2 decreases and eventually reduces to zero. This implies that as g_1 increases, the width of the polarization potential shrinks and eventually ST transition takes place. Here again, we see that the transition is continuous for t=0.5 whereas it is discontinuous for t=2. g'_2/g'_1 is now lower compared to [50], in the case of weak coupling. This implies that in the present analysis ST transition requires a stronger e-p interaction strength.

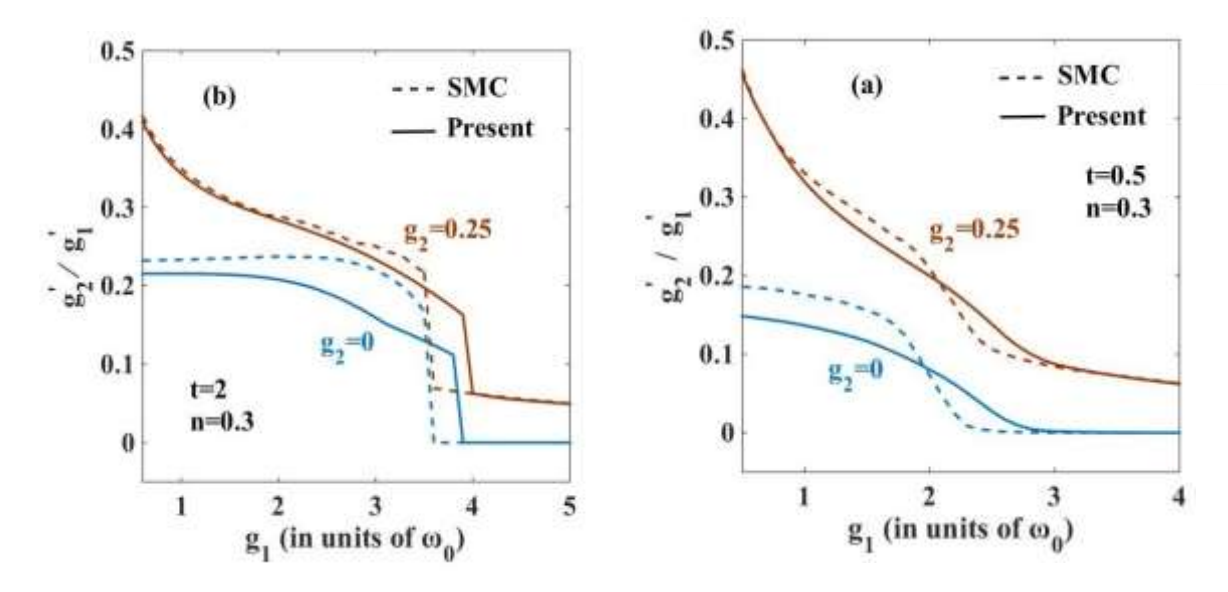


Fig. 5.3: g'_2/g'_1 vs. g_1 for different values of g_2 for: (a) anti-adabatic case; (b) adiabatic case with U=3 at less than half-filling

We study the behaviour of α_s with g_1 in Fig. 5.4; the anti-adiabatic case in Fig. 5.4 (a) and the adiabatic case in Fig. 5.4(b). One can observe that as g_1 increases, α_s also increases, attains a peak and then decreases to zero in a continuous manner for t=0.5 and in a discontinuous manner at t=2. Thus the phonon correlation is maximum at a certain critical g_1 , above which it reduces to zero. In the anti-adiabatic case, the phonon correlation becomes maximum at a lower value of g_1 than in the adiabatic case.

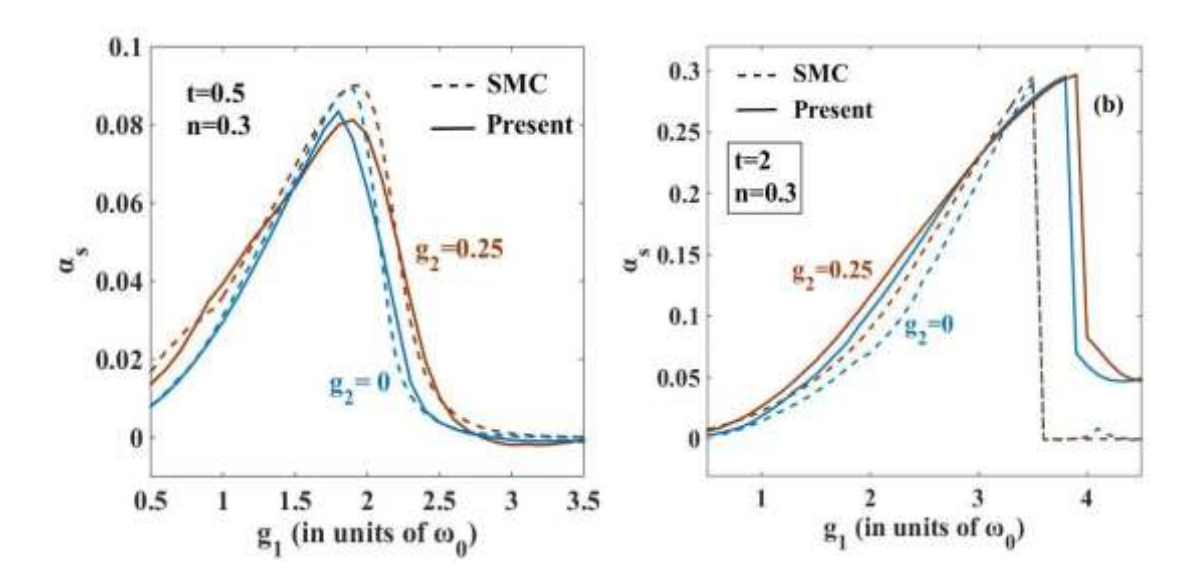


Fig. 5.4: α_s vs. g_1 for different values of g_2 : (a) for anti-adabatic case; (b) for adiabatic case, with U=3 at less than half-filling.

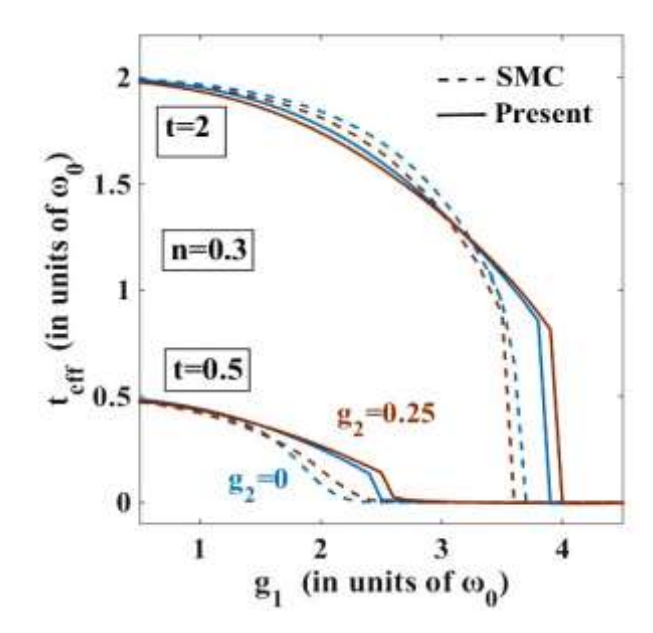


Fig. 5.5: t_{eff} vs. g_1 for different values of g_2 at t = 0.5 (anti-adiabatic case) and t = 2 (adiabatic case) with U = 3 at less than half-filling.

To examine the ST transition through the hopping parameter, we plot t_{eff} versus g_1 in Fig. 5.5. We expect: $t_{eff} \propto m_p$, where the polaron mass m_p is a measurable quantity. One can observe that t_{eff} decreases with g_1 and becomes zero in both adiabatic and the anti-adiabatic regimes. Thus the system shows ST transition in both cases. One can see that ST transition is continuous in the ant-adiabatic regime and discontinuous in the adiabatic limit. Furthermore, we observe that in the adiabatic case, discontinuous jumps in t_{eff} are observed at higher g_1 values. Thus, a stronger e-p interaction is required to localize the polaron in the adiabatic case.

5.3.2 Strong Correlation results

Here we will look into a strongly correlated system both in adiabatic and anti-adiabatic regimes. In Fig. 5.6, we plot the variational GS energy as a function of U and compare our present results with those of SC [51]. It is clear that the present results are more accurate than the results of SC in general. In Fig. 5.7, we study the variation of g'_1 with g_1 for a strongly correlated system. One can observe that g'_1 in general increases with g_1 . At small values of g_1 , g'_1 however remains small which implies the presence of a shallow on-site polarization

potential and consequently a large polaron in both the adiabatic and anti-adiabatic regimes. At some critical g_1 , g_1' becomes equal to g_1 indicating a small-polaron formation. Thus we observe an ST transition here.

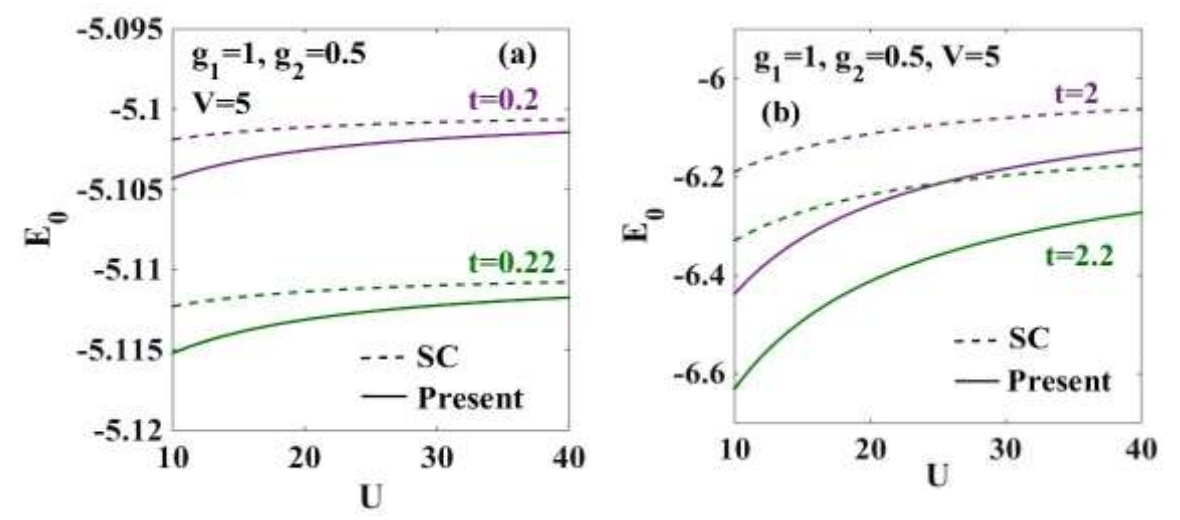


Fig. 5.6: E_0 vs. U for different values of hopping parameter t in: (a) anti-adiabatic regime; (b) adiabatic regime.

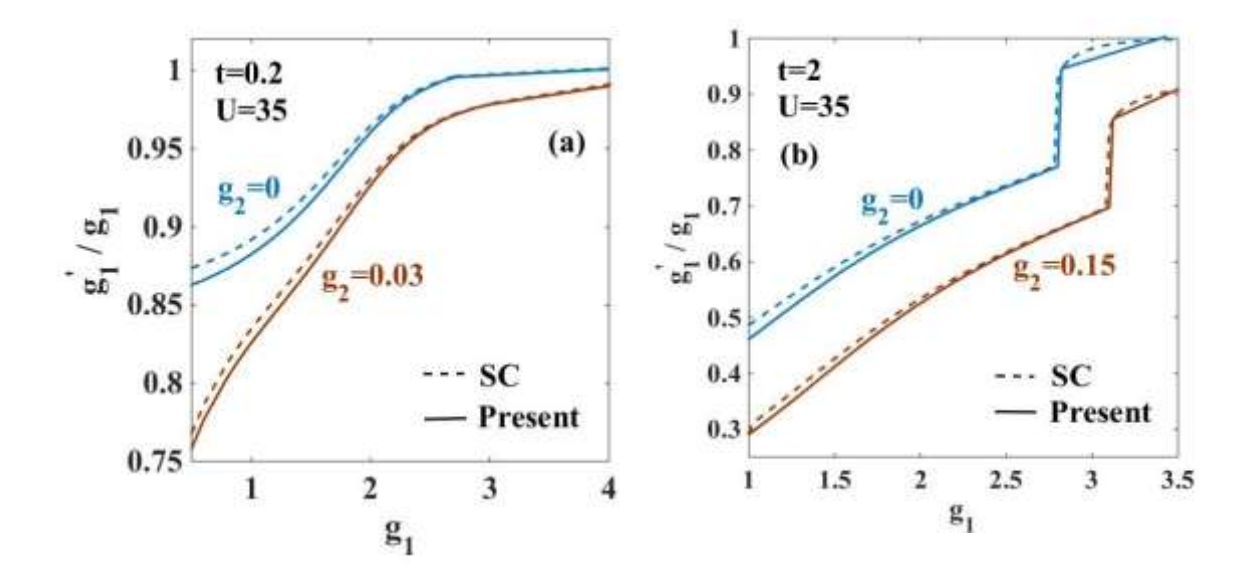


Fig. 5.7: Depth of the polarisation potential (g_1'/g_1) vs. g_1 with $g_2 = 0$ and 0.03: (a) for anti-adiabatic regime; (b) for adiabatic regime.

In Fig. 5.7(a), i.e., in the anti-adiabatic regime, ST transition is continuous, but in Fig. 5.7(b), i.e., in the adiabatic regime, a finite discontinuity is accompanied with ST transition. For non-zero g_2 , the polarization potential becomes shallower as compared to the one in the case of

 $g_2 = 0$ and the polaron remains mobile till a higher critical g_1 . In this case, a stronger on-site e-p interaction strength is required to trap the polaron. One can also observe from the figure that in the adiabatic regime, ST transition occurs at a higher value of g_1 than in the anti-adiabatic case.

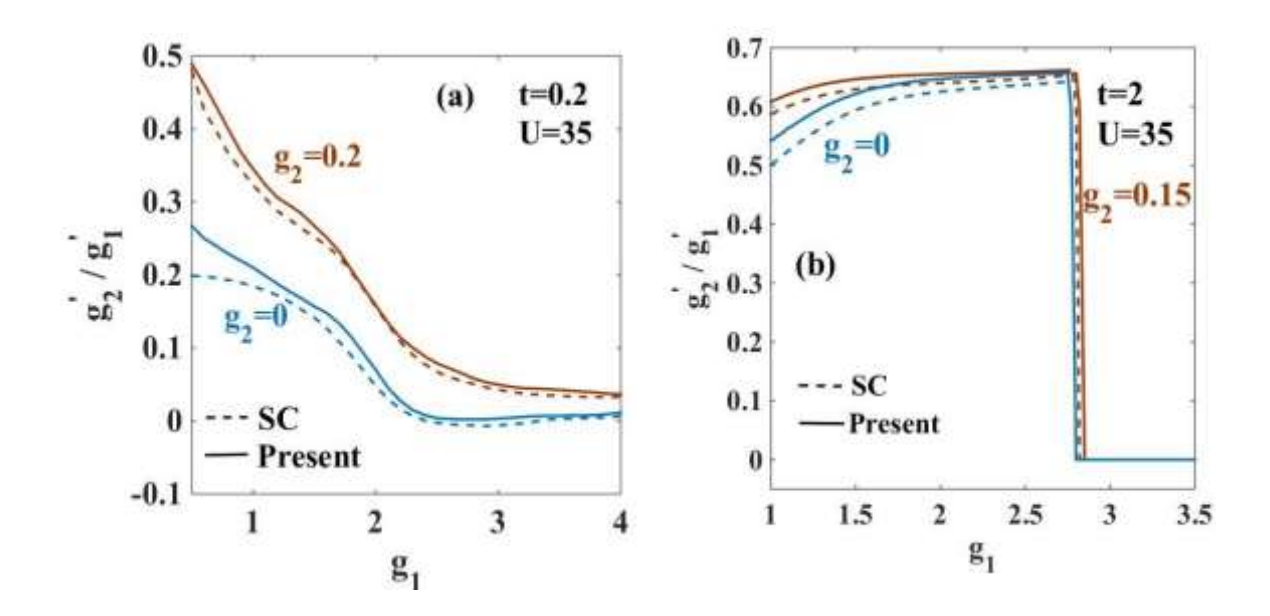


Fig. 5.8: Spread of the polarisation potential (g'_2/g'_1) vs. g_1 with with $g_2 = 0$ and 0.2 for: (a) anti-adiabatic regime; (b) for adiabatic regime.

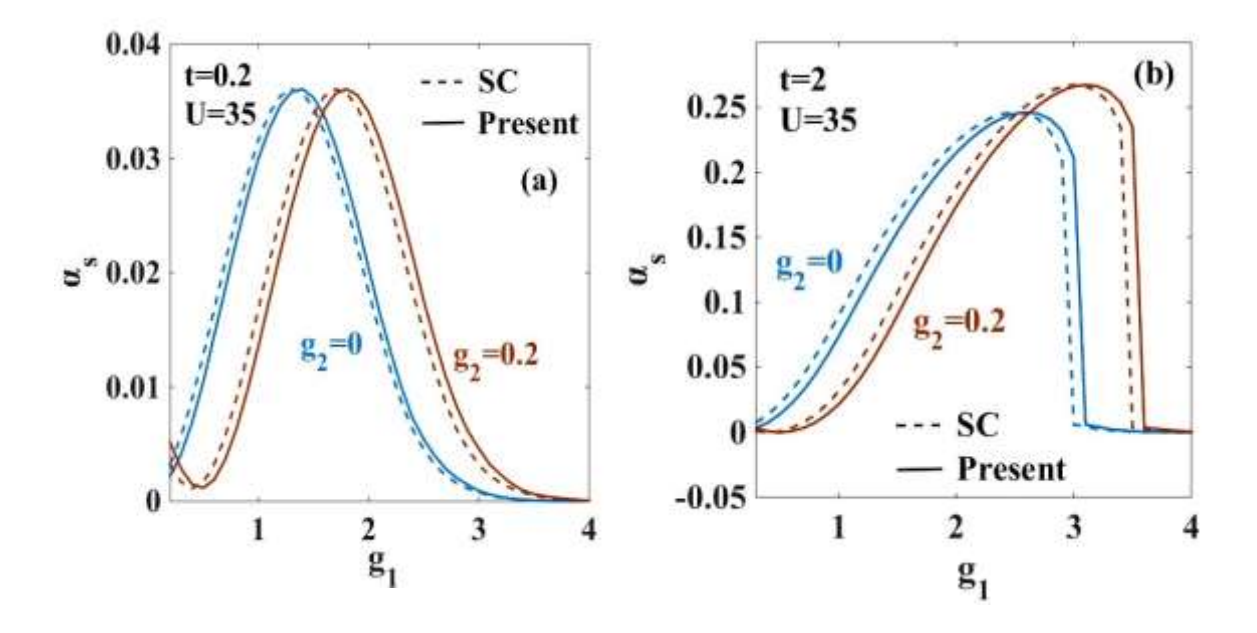


Fig. 5.9: α_s vs. g_1 with $g_2 = 0$ and 0.2 for: (a) ant-adiabatic regime; (b) adiabatic regime.

The variation of (g'_2/g'_1) with respect to g_1 is plotted in Fig. 5.8. g'_2 decreases gradually with g_1 and eventually becomes zero at some critical value of g_1 . At $g'_2 = 0$, the width of the polarization potential vanishes and the polaron becomes small and localized. One can clearly see from Fig. 5.8 that for t = 0.2, g'_2 falls off to zero in a continuous way, whereas in the adiabatic case, it goes to zero in a discontinuous manner. Thus this result also confirms the continuity of ST transition in the non-adiabatic regime and the discontinuity of ST transition in the adiabatic case.

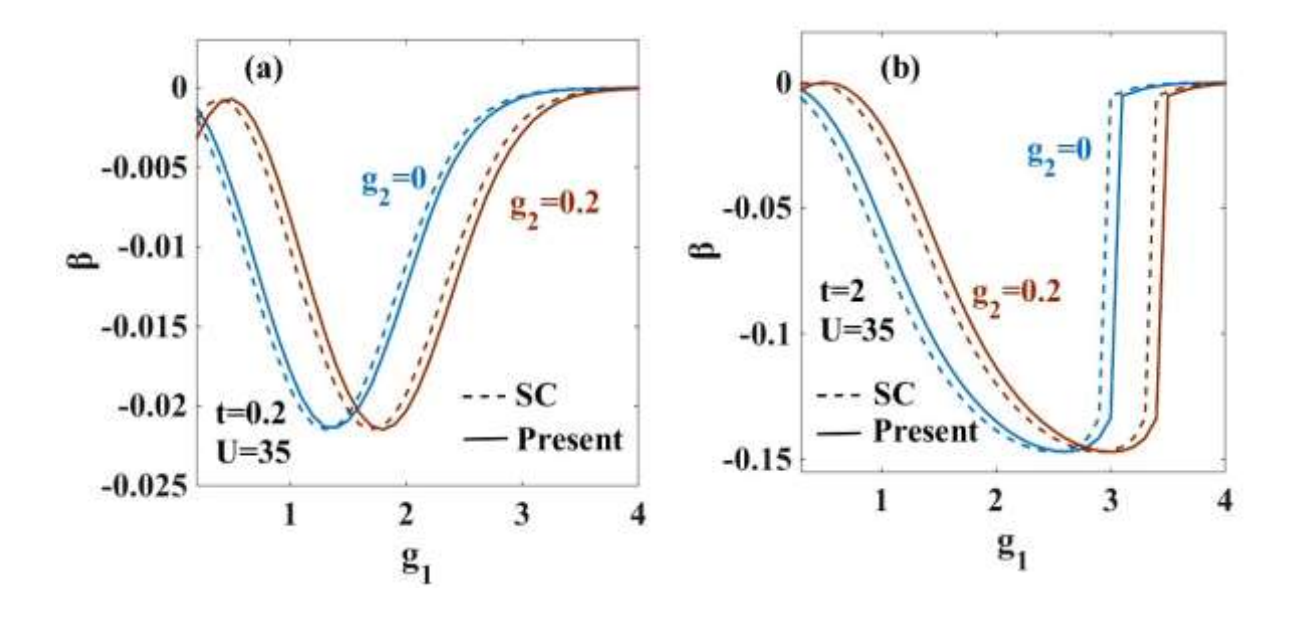


Fig. 5.10: β vs. g_1 with $g_2=0$ and 0.2 for (a) anti-adiabatic regime; (b) adiabatic regime.

The variations of the phonon correlation parameters (α_s, β) with respect to g_1 are also studied to investigate the nature of STT. In Fig. 9, α_s is plotted with respect to g_1 . Fig. 5.9(a) shows the anti-adiabatic scenario whereas the adiabatic case is plotted in Fig. 5.9(b). In both cases, the onsite phonon correlation is largest at certain critical value of g_1 . One may notice that the present modified calculation indicates a marginally higher polaron mobility than the one suggested by SC. Again, the nature of the transition is found to be continuous in the anti-adiabatic regime and discontinuous in the adiabatic case. Also, in the presence of a finite NN e-p interaction, a larger value of g_1 is required to trap the delocalized polaron both in the adiabatic and the anti-adiabatic cases. Similar behaviour is exhibited by β versus g_1 figures in Fig. 5.10. Fig. 5.10(a) shows that in the non-adiabatic regime, β as a function of g_1 goes to zero through a symmetric minimum continuously and smoothly while in the adiabatic regime (Fig. 5.10(b)), we see that β go to zero through an asymmetric minimum in a discontinuous

way making the ST transition sharp. Fig. 5.11(b) shows that in the adiabatic case, ST transition occurs at a marginally higher g_1 value than the one predicted from the SC calculation [51].

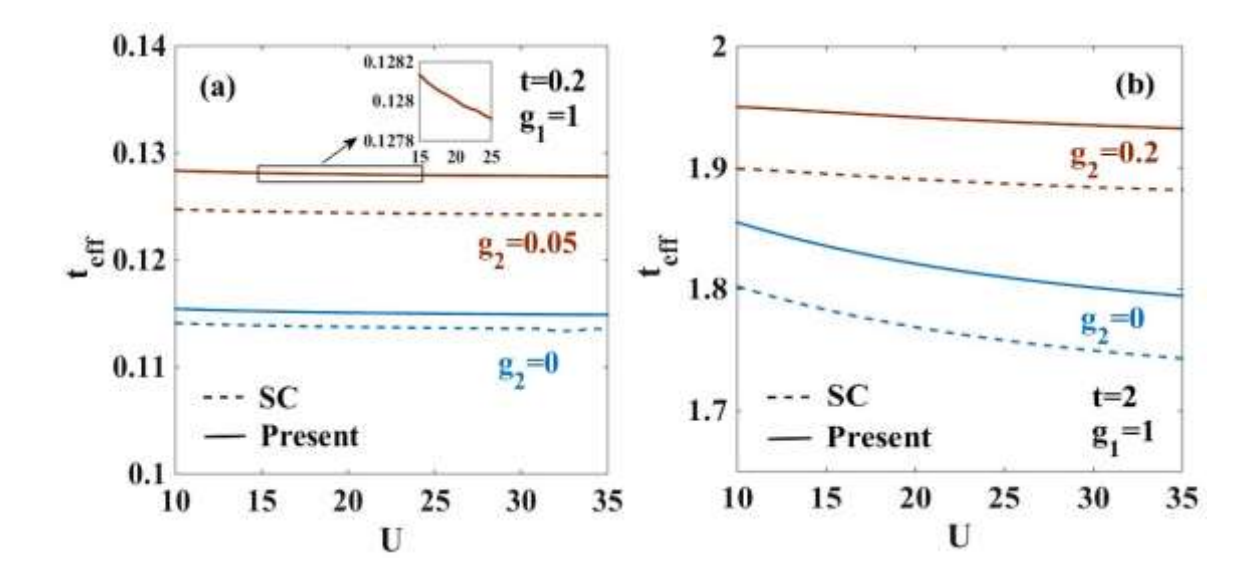


Fig. 5.11 t_{eff} vs. U with $g_2 = 0$ and 0.2 (a) anti-adiabatic regime and (b) adiabatic regime

Fig. 5.11 shows the change in the effective electronic hopping parameter with respect U. Our present modified variational calculation shows that it is higher than the SC result [51]. This is quite reassuring as a higher value of t_{eff} implies a higher polaron mobility which is always useful from the point of view of polaronic transport. For small (=0.2), the variation of t_{eff} with U is much slower that for large t (=2). It is also observed that effective polaron mobility decreases as U becomes stronger.

In Fig. 5.12, we show the behaviour of t_{eff} with respect to g_1 . It is found that the effective polaron mobility decreases with increasing g_1 than the Hubbard hoping parameter t value and it reaches to zero. The condition: $t_{eff} = 0$ indicates that the polaron is localized. The delocalization-localization transition is clearly visible in Fig. 5.12. The present modified calculation shows that a stronger e-p coupling is required for ST transition to occur. Also in the presence of the NN e-p interaction, the effective electronic hopping is larger. Fig. 5.12(a) and 5.12(b) also establish that the nature of ST transition is continuous in the anti-adiabatic regime and discontinuous at the adiabatic case.

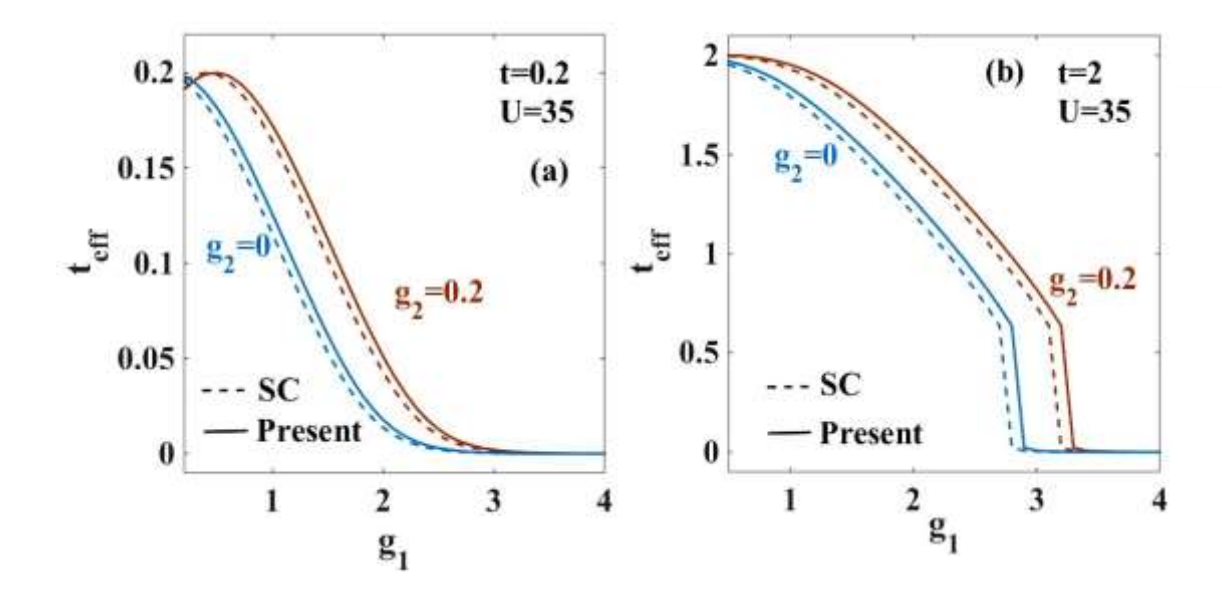


Fig. 5.12: t_{eff} vs. g_1 with with $g_2 = 0$ and 0.2 for: (a) anti-adiabatic regime and (b) adiabatic regime.

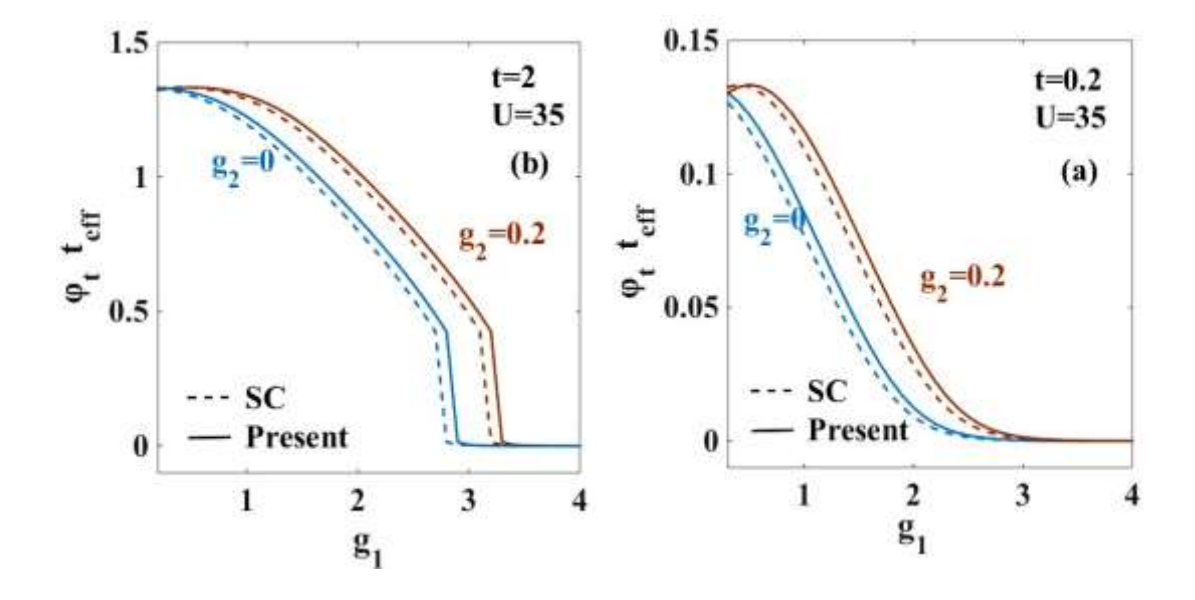


Fig. 5.13: Band reduction factor (φt_{eff}) vs. g_1 for (a) anti-adiabatic regime and (b) adiabatic regime.

The effective electronic hopping parameter gives us the information about the polaron mobility, and it also helps us to calculate the band-width and polaron mass. The band reduction factor (φt_{eff}) gives the physical effect of the presence of impurities in the system. We plot φt_{eff} with respect to the g_1 in Fig. 5.13. Though the behaviour of φt_{eff} is

qualitatively similar to t_{eff} , the effective polaron mobility gets suppressed by the parameter σ

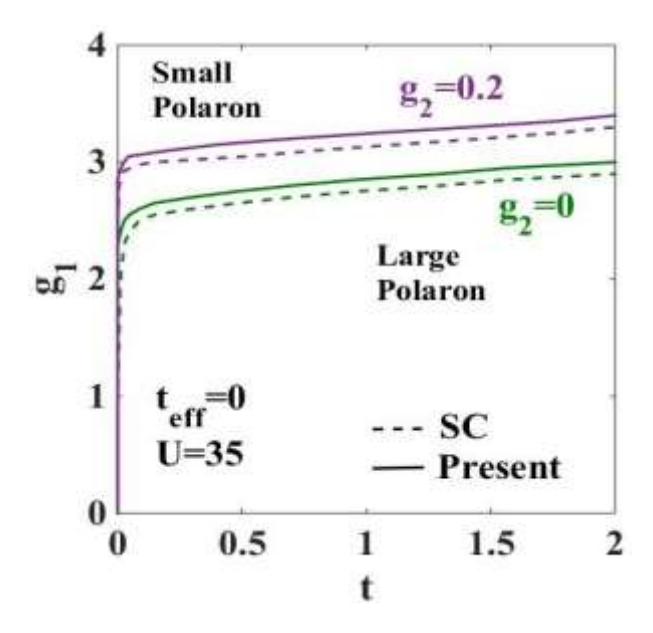


Fig. 5.14: Self-trapping transition line.

In Fig. 5.14, we plot the ST transition line and compare with the results of SC [51]. The ST transition line is plotted for the sets of (g_1, t) that give $t_{eff} = 0$. We call them (g_{1c}, t_c) . The curves give the large polaron-small polaron phase diagram. It is found that as t_c increases, g_{1c} also increases. Below a certain g_1 , one cannot have a small polaron. Compared to SC, the present result provides a little broader phase for the large polaron.

5.4 Conclusion

In conclusion, we have explored in this work, the nature of ST transition in a 2D extended HH model. For the phonon subsystem, we have used a very acute wave function incorporating all the important characteristics of the phonon dynamics and the e-p interaction. The effective electronic system is solved analytically in the weak and strong correlation regimes separately using plausible approximations. More specifically, in the weak-correlation regime, the renormalized electronic system is treated by the Hartree-Fock mean-filed theory

and in the strong correlation regime, the effective Hamiltonian is first mapped on the t-J model and then simplified employing the Gutzwiller approximation and finally solved by the Hartree-Fock method using the restriction that double occupancy is not allowed. For both the regimes, the GS energy is calculated variationally. The ST transition is examined by studying the depth and spread of the polarization potential as a function of the e-p coupling constants. The effective polaron hopping also indicates the nature of the ST transition for the entire range of the Coulomb correlation strength. Our results confirm that the ST transition occurs in a continuous way in the anti-adiabatic case while in the adiabatic regime it is accompanied with a finite discontinuity.

5.4 References

- [1] T.K. Mitra, A. Chatterjee, S. Mukhopadhyay, Phys. Rep. **153** (1987) 91;
- [2] J.T. Devreese, A.S. Alexandrov, Rep. Prog. Phys. **72** (2009) 066501.
- [3] A. Chatterjee, S. Mukhopadhyay, Polarons and Bipolarons: An Introduction, Taylor and Francis, 2018.
- [4] L. D. Landau, S. I. Pekar, Zh. Eksp. Teor. Fiz. 18, 419 (1948).
- [5] A.S. Alexandrov, P.E. Kornilovitch, Phys. Rev. Lett. 82 (1999) 807.
- [6] F. Peeters, J.T. Devreese, et al., Phys. Status Solidi B 112 (1982) 219;
- [7] B. Gerlach, H. Löwen, Phys. Rev. B 35 (1987) 4291;
- [8] B. Gerlach, H. Löwen, Phys. Rev. B 35 (1987) 4297;
- [9] R. Manka, Phys. Stat. Solidi (b) **93**, 53 (1979);
- [10] R. Manka, M. Suffczynski, J. Phys. C 13, 6369 (1980);
- [11] A. Chatterjee, S. Sil, Phys. Rev. B **51** (1995) 2223.
- [12] Y. Toyozawa, Prog. Theor. Phys. 26 (1) (1961);
- [13] K. Cho, Y. Toyozawa, J. Phys. Soc. Jpn. 30 (1971) 1555;
- [14] K. Cho, Y. Toyozawa, J. Phys. Soc. Jpn. 30 (1971) 1555;
- [15] Y. Shinozuka, Y. Toyozawa, J. Phys. Soc. Jpn. 46 (1979) 505.
- [16] A.S. Alexandrov, N.F. Mott, Rep. Prog. Phys. B **57** (1994) 1197.
- [17] R. Micnas, J. Ranninger, S. Robaszkiewicz, Rev. Modern Phys. **62** (1) (1990) 113–171.
- [18] K.H. Kim, J.Y. Gu, H.S. Choi, G.W. Park, T.W. Noh, Phys. Rev. Lett. 77 (1996) 1877.
- [19] M. Califano, G. M. Francisco, Nano Lett. 13, 5, (2013) 2047–2052.

- [20] D. Emin, Adv. Phys. 22 (1973) 57;
- [21] H. De Raedt, A. Lagendijk, Phys. Rep. 127 (1985) 233.
- [22] P.O.J. Scherer, E.W. Knapp, S.F. Fischer, Chem. Phys. Lett. **106** (1984) 191;
- [23] H. Löwen, Phys. Rev. B 37 (1988) 8661;
- [24] H. Löwen, Z. Phys. B Condensed Matter **71**, 219-224 (1988);
- [25] A. H. Romero, D. W. Brown, K. Lindenberg, Phys. Rev. B 60 (7) (1999);
- [26] R.P.M. Krishna, S. Mukhopadyay, A. Chatterjee, Phys. Lett. A 327 (2004) 67;
- [27] I. Lang, Y.A. Firsov, Sov. Phys. JETP 16 (1963) 1301.
- [28] H. Zheng, Phys. Lett. A 131 (1988) 115.
- [29] C.F. Lo, R. Sollie, Phys. Rev. B 48 (1993) 10183.
- [30] Z.M. Malik, S. Mukhopadhyay, A. Chatterjee, Phys. Lett. A, **383**, 1516-1519 (2019).
- [31] Lieb, E. H. & Wu, F. Y, Phys. Rev. Lett. 20, 1445–1448 (1968).
- [32] D. Debnath, K. Bhattacharyya, A. Chatterjee, Physics B, **646**, 414357 (2022).
- [33] O. Cyr-Choinière, D. LeBoeuf, S. Badoux, S. Dufour-Beauséjour, & A. D. Bonn et al., Phys. Rev. B **98**, 064513 (2018).
- [34] T. Wu, H. Mayaffre, S. Krämer, M. Horvatić, & C. Berthier, et al., Nature **477**, 191–194 (2011).
- [35] J. Chang, E. Blackburn, A. T. Holmes, N. B. Christensen, & J. Larsen et al., Nat. Phys. **8**, 871–876 (2012).
- [36] J.G. Bednorz, K.A. M"uller, Z. Phys. B 64, 189 (1986).
- [37] A. H. Castro Neto, Phys. Rev. Lett. **86**, 4382–4385 (2001).
- [38] K. Rossnagel, J. Phys.: Condens. Matter. 23, 213001 (2011).
- [39] S. Manzeli, D. Ovchinnikov, D. Pasquier, O.V. Yazyev, A. Kis, Nat. Rev. Mater. 2, 17033 (2017).
- [40] K.H. Kim, J.Y. Gu, H.S. Choi, G.W. Park, T.W. Noh, Phys. Rev. Lett. 77, 1877 (1996).
- [41] S. Jin et al., Science **264**, 413 (1994).
- [42] Yu Zhang, Xingyi Liu, Huaiyang Sun, Jinxia Zhang, Xiaowen Gao, Chuang Yang, Prof. Dr.
- Qi Li,Prof. Dr. Hong Jiang,Prof. Dr. Juan Wang,Prof. Dr. Dongsheng Xu, Angew. Chem. Int. Ed. **60**, 7587–7592 (2021).
- [43] Junze Li, Haizhen Wang, Dehui Li, Front. Optoelectron., **13** (3) 225-234 (2020).
- [44] Akimasa Ohnishi, Ken-ichi Tanaka, and Takehisa Yoshinari, J. Phys. Soc. Jpn. **68**, pp. 288-290 (1999)
- [45] Ziad H. Musslimani and Jianke Yang, Journal of the Optical Society of America B, **21** (5), 973-981 (2004).

- [46] Anton S. Desyatnikov, Nina Sagemerten, Robert Fischer, Bernd Terhalle, Denis Träger, Dragomir N. Neshev, Alexander Dreischuh, Cornelia Denz, Wieslaw Krolikowski, and Yuri S. Kivshar, Optics Express, **14** (7), 2851-2863 (2006).
- [47] Hou Jun-Hua, Liang Xi-Xia, Chinese Phys. 16 3059 (2007).
- [48] Junhua Hou, Journal of Luminescence, **152**, 247-249 (2014).
- [49] A.N. Das, S. Sil, J. Phys.: Condens. Matter. 5, 8265 (1993).
- [50] I.V. Sankar, S. Mukhopadhyay, A. Chatterjee, Physica C, 480 (2012) 55-60.
- [51] I.V. Sankar, A. Chatterjee, Eur. Phys. J. B (2014) 87: 154
- [52] D. Debnath, M. Z. Malik and A. Chatterjee, Sci Rep. 11, 12305 (2021).
- [53] M.C. Gutzwiller, Phys. Rev. Lett. **10**, 159 (1963).
- [54] M.C. Gutzwiller, Phys. Rev. **137**, A1726 (1965).

"It is no good to try to stop knowledge from going forward. Ignorance is never better than knowledge"...Enrico Fermi

6

Quantum Transport in a bi-molecular transistor through the Anderson-Holstein-Caldeira-Leggett model

6.1 Introduction

Transistors are one of the integral parts of modern technology for the fabrication of nanodevices. Of late, single molecular transistors have attracted considerable attention for their practical application in nano-devices. In a single molecular transistor (SMT), a central molecule or a quantum dot (QD) with discrete energy levels is connected to two metallic leads (source and drain) with continuous energy levels on the two sides and is acted upon by an external bias voltage. The presence of discrete energy levels in the central molecule which is also called a tunnelling molecule is important to have pure quantum mechanical effects on the device properties. The difference in the electronic potential energies of the source and the drain helps the electrons to tunnel from one lead to the other through the QD and from the QD to the other lead. The transfer of electrons through the QD results in a net tunnelling current. The SMT system is mounted on an insulating substrate which can be attached to a gate. Then by applying a gate voltage, the tunnelling current can be manipulated. In late 90s scientists have been interested in studying the electronic transport in nano-materials using molecules, nanotubes, nanocrystals etc. In 2000, the fabrication of C_{60} molecular transistor was reported by Park et al. [1] with the help of gold electrodes connected with the C_{60} molecules. Using a single-electron hopping mechanism they have shown the conduction

properties in the transistor with respect to the applied bias-voltage. In 2002, Liang et al. [2] have studied the Kondo effect on SMT following the works by Goldhaber-Gordon et al. [3] and Yu et al. [4]. Liang et al. have studied the Kondo resonance effect on the SMT device and examined how the gate voltage can influence the Kondo phenomenon in quantum dot structures. Later, many other works have unravelled the Kondo behaviour in molecular transport [5-7]. Another important low-temperature property that shows up in electronic transport is the effect of Coulomb blockade. Very recently, Pipit and his collaborators [8] have experimentally established the Coulomb blockade and Coulomb staircase behaviour for single electron transport at the room temperature. This work has a great significance for the molecular transport at room temperature. The three-terminal device has found potential use in the study of fine-structure of single-molecule magnets [9] and in magnetic anisotropy in SMT [10-11]. The SMT device can be used as a switching device [12] and also a sensor [13]. Dutta has discussed the electronic transport in the mesoscopic systems [14] and also explained the quantum transport in a molecular transistor [15]. The recent review articles by Mickael et al. [16] and Huanyan et al. [17] have reported the mechanisms involved in the SMT device and its recent developments and applications.

In an SMT system, QD electrons can interact with the phonons through the Holstein e-p interaction leading to the creation of quasi-particles called polarons. The Coulomb correlation and the e-p interaction are likely to influence different molecular characteristics like transition and vibrational energy levels of different spin-states, quantum interference, transport properties and other interesting phenomena [18-24]. The fabrication of different molecular devices and their theoretical and experimental study constitute a new area of research called moletronics [25, 26] which has attracted a great deal of attention in recent times.

In 2003, Sang and collaborators [27] have investigated the interplay of the e-e and e-p interaction for the Anderson-Holstein Hamiltonian and computed the electron and phonon spectral function (SF) using the numerical renormalization group technique. Using Keldysh Green function method, Chen et al. [28] have shown that the polaronic effect generates side peaks in the SF of an SMT device and modifies the tunnelling current. Extending the work of Chen, Juntao and collaborators [29] have measured the phonon assisted conductance in a SMT device. Raju and Chatterjee [30] have extended the SMT problem to investigate the dissipation-induced tunnelling current by introducing an insulating substrate. They have reported that the interaction between the substrate phonons and the QD phonon introduces

dissipation in the phonon dynamics of the QD phonon and enhances the tunnelling current in the molecular transistor. Very recently, Khedri et al. [31-33] have considered the spinless Anderson-Holstein impurity model and investigated the phonon-assisted linear thermoelectric tunnelling transport in molecular QDs. Chatterjee and collaborators [33] have studied the SMT in the presence of e-e and e-e interactions, quantum dissipation and an external magnetic field. Their result shows that the spin-filtering effect increases with the magnetic field. They have subsequently shown that the tunnelling current in an SMT device reduces with increasing temperature [34, 35]. Kuntal et al. [36] have studied the combined effect of temperature and magnetic field on tunnelling current and differential conductance in an SMT device in the presence of phonon dissipation. It has been shown that the tunnelling current and the spin-polarization coefficient can be controlled by the bias-voltage, e-p interaction coefficient, external magnetic field and the temperature.

Several theoretical techniques have been implemented to study the molecular devices. The Anderson model has been studied using the slave-boson mean-field method by Meir et al. [37] and by non-crossing approximation method by Wingreen and Meir [38]. The molecular transistor has also been treated by using the rate equation approach [39]. To solve the single impurity Anderson model, the numerical renormalization group technique [31, 32, 40] has been found to be very useful, as this is applicable for the entire parameter regime. Another celebrated method to study the quantum transport in the molecular device is the non-equilibrium Green function approach [28, 30, 33, 35, 41].

More recently extensive studies have been performed on the double-QD (DQD) based molecular transistors [42-44] as they show many useful practical applications. In the present chapter, we study a double-QD-based molecular transistor which we refer to as a bimolecular transistor (BMT). In a BMT, we introduce an extra QD in the SMT system i.e., we place two QDs in series between the source (S) and the drain (D) and the whole system is embedded on an insulating substrate. The system is represented by the Anderson-Holstein-Caldeira-Leggett (AHCL) model [46-49] as discussed in Chapter 1 and the spectral function, tunnelling current, differential conductance and spin-polarization are studied in the BMT in the presence of an external magnetic field, finite temperature and phonon dissipation.

6.2 Model and formulation

In our present work, we place two QDs in series in the central region of the molecular transistior. One of the QDs is connected to the source and another QD is connected to the drain. This whole system is placed on an insulating substrate. The two metallic leads are connected to an external voltage source so that electrons can tunnel from S to first QD and from the second QD to D. The schematic diagram of the BMT device is shown in Fig. 6.1. Here the QDs are considered to have single energy levels and the conducting leads have free electrons with continuous energy levels. Electrons in an individual QD can interact with themselves with the onsite Hubbard interaction. Electrons from the first QD can go to the second QD by hopping. This interacting system is modelled by the Anderson-Holstein model [45, 46]. The insulating substrate works as a heat bath and its phonons interact with the QD phonon through the linear Caldeira Leggett model [47, 48]. An external magnetic field is also introduced so that the electron spin degeneracy is lifted.

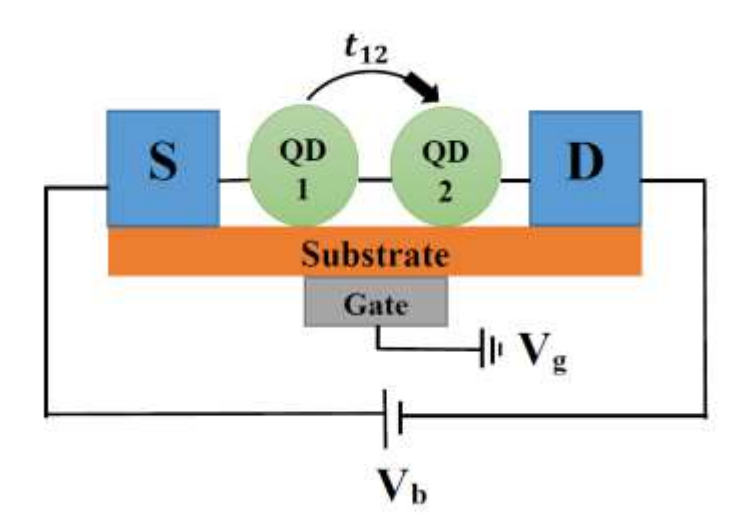


Fig. 6.1: Schematic diagram of the Multi-molecular transistor (MMT).

The Hamiltonian for the BMT system can be written as

$$H = H_L + H_{ODD} + H_S + H_{DS} + H_T + H_t, (6.1)$$

Here, the first term represents the lead Hamiltonian (H_L) , L = S referring to the source and L = D to the drain. The second term represents the Hamiltonian of the two-QD systems (H_{QDD}) which we call a QD dimer (QDD). The insulating substrate Hamiltonian is described by H_S . The interaction between the substrate phonons and the phonons of the QDD is

described by H_{DS} . The electronic hopping from the QD1 to QD2 is described by the Hamiltonian H_T , and the last term of (6.1) describes the tunnelling of electrons from S to QD 1 and from QD2 to D. The different terms of (6.1) are given by

$$H_L = \sum_{k\sigma} \varepsilon_k \left(c_{kS,\sigma}^{\dagger} c_{kS,\sigma} + c_{kD,\sigma}^{\dagger} c_{kD,\sigma} \right), \tag{6.2}$$

$$H_{\text{QDD}} = \sum_{i=1, \sigma}^{2} (\varepsilon_{i} - eV_{g}) n_{i,\sigma} + U \sum_{i=1}^{2} n_{i,\sigma} n_{i,-\sigma} + \hbar \omega_{0} \sum_{i=1}^{2} b_{i}^{\dagger} b_{i} + \hbar \omega_{0} \sum_{i=1}^{2} g_{i} n_{i,\sigma} (b_{i}^{\dagger} + b_{i})$$

$$+\frac{1}{2}\sum_{i=1}^{2}g\mu_{B}BS_{z},\tag{6.3}$$

$$H_S = \sum_{j=1}^{N} \hbar \omega_j b_j^{\dagger} b_j, \tag{6.4}$$

$$H_{t} = V_{r} \sum_{k\sigma} (c_{kS,\sigma}^{\dagger} c_{1\sigma} + c_{1\sigma}^{\dagger} c_{kS,\sigma}) + V_{r} \sum_{k\sigma} (c_{kD,\sigma}^{\dagger} c_{2\sigma} + c_{2\sigma}^{\dagger} c_{kD,\sigma}).$$
 (6.5a)

$$H_{DS} = \sum_{i=1}^{2} \sum_{j=1}^{N} \beta_j x_i x_j = \sum_{j=1}^{N} \beta_j (x_1 + x_2) x_j,$$
 (6.5b)

$$H_T = t_{12} \sum_{\sigma} \left(c_{1\sigma}^{\dagger} c_{2\sigma} + c_{2\sigma}^{\dagger} c_{1\sigma} \right) \tag{6.6}$$

In H_L , $n_{kS(D),\sigma}(=c_{kS(D),\sigma}^{\dagger}c_{kS(D),\sigma})$ is the number operator for the lead (S, D) electrons, $c_{kS(D),\sigma}^{\dagger}(c_{kS(D),\sigma})$ being the creation (annihilation) operator for an S(D) electron with wave vector \mathbf{k} , spin σ and energy ε_k . In H_{QDD} , $n_{i,\sigma}(=c_{i,\sigma}^{\dagger}c_{i,\sigma})$ denotes is the number operator for the QD electrons, $c_{i,\sigma}^{\dagger}(c_{i,\sigma})$ being the creation (annihilation) operator for the electron of the ith QD (i=1,2) with energy ε_i , V_g is the gate voltage, U is the onsite Coulomb interaction, $b_i^{\dagger}(b_i)$ denotes the creation (annihilation) operator for the QD phonon of frequency ω_0 , g_i gives the on-site e-p interaction coefficient for the i-th QD, i0 is the external magnetic field applied in the z-direction, i1 is the z-component of spin of the QD electron, i2 is the gryo-magnetic ratio and i3 is the Bohr magneton. In i4 is the gives a measure

of the strength of electron tunnelling from the lead to the QD and vice versa. In H_S , $b_j^{\dagger}(b_j)$ denotes the creation (annihilation) operator for the j –th substrate phonon with frequency ω_j . In H_{DS} , β_j gives the coupling strength for the interaction of the QD phonons with j –th substrate phonon. In H_t , t_{12} is the coefficient for hopping between the two quantum dots.

 H_S and H_{DS} can be combined together and may be written as

$$H_S + H_{DS} \equiv \sum_{j=1}^{N} \left[\frac{p_j^2}{2m_j} + \frac{1}{2} m_j \omega_j^2 x_j^2 \right] + \sum_{j=1}^{2} \sum_{j=1}^{N} \beta_j x_i x_j , \qquad (6.7)$$

where we have written the phonon energy in the form of Harmonic oscillator Hamiltonian as,

$$\sum_{j=1}^{N} \hbar \omega_j b_j^{\dagger} b_j = \sum_{j=1}^{N} \left[\frac{p_j^2}{2m_j} + \frac{1}{2} m_j \omega_j^2 x_j^2 \right]. \tag{6.8}$$

In Eq. (6.7), the coupling between the QDD phonons and the substrate phonons can be decoupled by the following transformations:

$$\tilde{x}_{j} = x_{j} + \frac{\beta_{j}}{m_{j}\omega_{j}^{2}} \left(\sum_{i=1}^{2} x_{i} \right),$$

$$\tilde{p}_{j} = -i\hbar \frac{\partial}{\partial \tilde{x}_{j}} . \tag{6.9}$$

Using these transformations, we may write the Eq. (6.7) as,

$$H_{S} + H_{DS} = \sum_{j=1}^{N} \left[\frac{\tilde{p}_{j}^{2}}{2m_{j}} + \frac{1}{2} m_{j} \omega_{j}^{2} \left(\tilde{x}_{j} - \frac{\beta_{j} \sum_{i=1}^{2} x_{i}}{m_{j} \omega_{j}^{2}} \right)^{2} \right] + \sum_{i=1}^{2} \sum_{j=1}^{N} \beta_{j} \left(\tilde{x}_{j} - \frac{\beta_{j} x_{i}}{m_{j} \omega_{j}^{2}} \right) x_{i}$$

$$= \sum_{j=1}^{N} \left[\frac{\tilde{p}_{j}^{2}}{2m_{j}} + \frac{1}{2} m_{j} \omega_{j}^{2} \tilde{x}_{j}^{2} - \frac{\beta_{j}^{2} \sum_{i} x_{i}^{2}}{2m_{j} \omega_{j}^{2}} \right]. \tag{6.10}$$

Combining the phonon energy for the QDD with the Eq. (6.10), we may write the combined terms as,

$$\sum_{i=1}^{2} \left[\frac{p_i^2}{2m_i} + \frac{1}{2} m_i \omega_i^2 x_i^2 \right] + \sum_{j=1}^{N} \left[\frac{\tilde{p}_j^2}{2m_j} + \frac{1}{2} m_j \omega_j^2 \tilde{x}_j^2 - \frac{\beta_j^2 \sum_i x_i^2}{2m_j \omega_j^2} \right]$$

$$= \sum_{i=1}^{2} \left[\frac{p_i^2}{2m_i} + \frac{1}{2} m_i \tilde{\omega}_i^2 x_i^2 \right] + \sum_{j=1}^{N} \left[\frac{\tilde{p}_j^2}{2m_j} + \frac{1}{2} m_j \omega_j^2 \tilde{x}_j^2 \right]$$
(6.11)

Therefore, the transformed phonon frequencies become modified and the renormalized frequency becomes,

$$\widetilde{\omega}_i = \left[\omega_i^2 - \Delta \omega^2\right]^{1/2},\tag{6.12}$$

where,

$$\Delta\omega^{2} = \sum_{j=1}^{N} \frac{\beta_{j}^{2}}{m_{i}m_{j}\omega_{j}^{2}}.$$
(6.13)

In the large N limit, $\Delta\omega^2$ can be cast in an integral form through the spectral density function $J(\omega)$ of the bath-phonon over ω as,

$$\Delta\omega^2 = 2\int_0^\infty \left(\frac{J(\omega)}{m_0\omega}\right) d\omega,\tag{6.14}$$

where

$$J(\omega) = \sum_{i=1}^{N} \left(\frac{\beta_i^2}{2m_i \omega_i} \right) \delta(\omega - \omega_i)$$
 (6.15)

which at large-N limit can be written in the Lorentz-Drude form as

$$J(\omega) = \frac{2m_0\gamma\omega}{\left[1 + (\omega/\omega_c)^2\right]},\tag{6.16}$$

where γ is the rate of quantum dissipation and ω_c is the cut-off frequency. As ω_c is considerably larger than other SMT frequencies, the deviation in the QD phonon frequency essentially becomes: $\Delta\omega^2 = 2\pi\gamma\omega_c$. With the modified phonon frequency, the transformed Hamiltonian becomes,

$$\widetilde{H} = \sum_{k\sigma} \varepsilon_{k} \left(c_{kS,\sigma}^{\dagger} c_{kS,\sigma} + c_{kD,\sigma}^{\dagger} c_{kD,\sigma} \right) + \sum_{i=1,\sigma}^{2} \widetilde{\varepsilon}_{i} n_{i,\sigma} + U \sum_{i=1}^{2} n_{i,\sigma} n_{i,-\sigma} + \sum_{i=1}^{2} \hbar \widetilde{\omega}_{i} b_{i}^{\dagger} b_{i}$$

$$+ g \mu_{B} B S_{z} + \sum_{i=1}^{2} g_{i} n_{i,\sigma} \left(b_{i}^{\dagger} + b_{i} \right) \hbar \widetilde{\omega}_{i} + V_{r} \sum_{k\sigma} \left(c_{kS,\sigma}^{\dagger} c_{1\sigma} + c_{1\sigma}^{\dagger} c_{kS,\sigma} \right)$$

$$+ t_{12} \sum_{\sigma} \left(c_{1\sigma}^{\dagger} c_{2\sigma} + c_{2\sigma}^{\dagger} c_{1\sigma} \right)$$

$$+ V_{r} \sum_{k\sigma} \left(c_{kD,\sigma}^{\dagger} c_{2\sigma} + c_{2\sigma}^{\dagger} c_{kD,\sigma} \right). \tag{6.17}$$

Now in order to decouple the e-p interaction in Eq. (6.17), the Lang-Firsov (LF) transformation [51] is applied. The generator for the LF transformation is

$$S = \sum_{i=1}^{2} g_i (b_i^{\dagger} - b_i) n_i . \tag{6.18}$$

where $n_i = \sum_{\sigma} n_{i,\sigma}$. Using the Baker-Campbell-Hausdorff (BCH) formula we calculate the transformed Hamiltonian as,

$$\widetilde{\widetilde{H}} = e^{S} H e^{-S} = \widetilde{H} + \left[S, \widetilde{H} \right] + \frac{1}{2!} \left[S, \left[S, \widetilde{H} \right] \right] + \cdots$$
 (6.19)

Thus, we obtain,

$$\widetilde{\widetilde{H}} = \sum_{k\sigma} \varepsilon_k \left(c_{kS,\sigma}^{\dagger} c_{kS,\sigma} + c_{kD,\sigma}^{\dagger} c_{kD,\sigma} \right) + \sum_{i=1,\sigma}^{2} \widetilde{\varepsilon}_i \, n_{i,\sigma} + \widetilde{U} \sum_{i=1}^{2} n_{i,\sigma} n_{i,-\sigma} + \sum_{i=1}^{2} \hbar \widetilde{\omega}_i \, b_i^{\dagger} b_i
+ \widetilde{V}_r \sum_{k\sigma} \left(c_{kS,\sigma}^{\dagger} c_{1\sigma} + c_{1\sigma}^{\dagger} c_{kS,\sigma} \right) + \widetilde{t} \sum_{\sigma} \left(c_{1\sigma}^{\dagger} c_{2\sigma} + c_{2\sigma}^{\dagger} c_{1\sigma} \right)
+ \widetilde{V}_r \sum_{k\sigma} \left(c_{kD,\sigma}^{\dagger} c_{2\sigma} + c_{2\sigma}^{\dagger} c_{kD,\sigma} \right),$$
(6.20)

where

$$\tilde{\varepsilon}_i = \varepsilon_i - eV_q - \hbar \widetilde{\omega}_0 g_i^2 - \mu_B B\sigma \,, \tag{6.21}$$

$$\widetilde{U} = U - 2\hbar \widetilde{\omega}_0 g_i^2, \tag{6.22}$$

$$\tilde{V}_r = V_r e^{-g_i(b_i^{\dagger} - b_i)},\tag{6.23}$$

$$\tilde{t} = t_{12} e^{\left[g_1(b_1^{\dagger} - b_1) - g_2(b_2^{\dagger} - b_2)\right]}. \tag{6.24}$$

The tunnelling current in a molecular transistor is defined as,

$$J_{S(D)} = \langle \frac{dQ}{dt} \rangle = \langle \frac{d(-eN_{S(D)})}{dt} \rangle = -ie \langle \left[\widetilde{H}, N_{S(D)} \right] \rangle$$
 (6.25)

where Q is the total charge transported and $N_{s(D)} = \sum_{k\sigma} c_{kS(D),\sigma}^{\dagger} c_{kS(D),\sigma}$ represents the total number of particles in the source(drain).

Using the transformed Hamiltonian of Eq. (6.20) we obtain the commutation relation,

$$\left[\widetilde{\widetilde{H}}, N_{S}\right] = \sum_{k\sigma} \widetilde{V}_{r} \left(c_{1,\sigma}^{\dagger} c_{kS,\sigma} - c_{kS,\sigma}^{\dagger} c_{1,\sigma}\right), \tag{6.26}$$

and,

$$\left[\widetilde{\widetilde{H}}, N_D\right] = ie \sum_{k\sigma} \widetilde{V}_r \left(c_{2,\sigma}^{\dagger} c_{kD,\sigma} - c_{kD,\sigma}^{\dagger} c_{2,\sigma}\right). \tag{6.27}$$

Using the results of the commutation relations we calculate the tunnelling current as the following:

The current from the source to the first QD is denoted as,

$$J_{S} = -ie \sum_{k\sigma} \overline{\tilde{V}}_{r} \left[\langle c_{1,\sigma}^{\dagger} c_{kS,\sigma} \rangle - \langle c_{kS,\sigma}^{\dagger} c_{1,\sigma} \rangle \right]. \tag{6.28}$$

The current from the first QD to the second QD is denoted as,

$$J_{12} = -ie \sum_{k\sigma} \overline{\tilde{V}}_r \left[\langle c_{1,\sigma}^{\dagger} c_{2,\sigma} \rangle - \langle c_{2,\sigma}^{\dagger} c_{1\sigma} \rangle \right]. \tag{6.29}$$

The current from the drain to the second QD is found as,

$$J_D = -ie \sum_{k\sigma} \overline{\tilde{V}}_r \left[\langle c_{2,\sigma}^{\dagger} c_{kD,\sigma} \rangle - \langle c_{kD,\sigma}^{\dagger} c_{2,\sigma} \rangle \right]. \tag{6.30}$$

Here, $\overline{\tilde{V}}_r = \langle \tilde{V}_r \rangle$, is the expectation value of \tilde{V}_r with respect to the phonon state.

The Keldysh lesser (greater) Green function $G_{d\sigma,kS(D)}^{<(>)}$ and the retarded (r) and the advanced (a) Green's functions are calculated to find the transport current for the BMT. By definition, the retarded (advanced) Green function for the coupling of the first (second) QD to the source (drain) is calculated as,

$$G_{d\sigma,kS(D)}^{r(a)}(t,t') = \mp i\theta(\pm t \mp t')\langle 0|\{\tilde{c}_{d\sigma}(t), c_{kS(D),\sigma}^{\dagger}(t')\}|0\rangle. \tag{6.31}$$

Here, 'd' denotes the QDs and using the LFT and the BCH formula the electronic operator $c_{i\sigma}$ transforms as

$$\tilde{c}_{i\sigma}(t) = c_{i\sigma}(t)e^{-g_i(b_i^{\dagger} - b_i)}, \tag{6.32}$$

and, therefore we may write the retarded and advanced Green functions for the QDs as

$$G_{d\sigma,d\sigma}^{r(a)}(t,t') = \mp i\theta(\pm t \mp t')\langle 0 | \{ \tilde{c}_{d\sigma}(t), \tilde{c}_{d,\sigma}^{\dagger}(t') \} | 0 \rangle.$$
 (6.33)

The Green function for the leads is defined as,

$$g_{kS(D)}^{r(a)}(t,t') = \mp i\theta(\pm t \mp t') \langle \{c_{kS(D)}(t), c_{kS(D)}^{\dagger}(t')\} \rangle,$$
 (6.34)

and, the lesser and greater Green functions for the leads are defined as,

$$g_{kS}^{<(>)}(t-t') = \langle c_{kS(D)}^{\dagger}(t')c_{kS(D)}(t) \rangle$$
 (6.35)

Following the work of Chen et al. [28], the tunnelling current through BMT can be calculated using the Keldysh non-eqilibrium Green function (KNGF) technique as,

$$J_{\sigma} = \frac{J_{S} - J_{D}}{2} = \frac{e}{\hbar} \int \frac{d\omega}{2\pi} Re \left\{ \sum_{k} \langle \tilde{V}_{r} \rangle G_{1\sigma,kS\sigma}^{<}(\omega) - \sum_{k} \langle \tilde{V}_{r} \rangle G_{2\sigma,kD\sigma}^{<}(\omega) \right\}. \quad (6.36)$$

Using the equation of motion method, we may calculate the relation between the Green functions:

$$-\frac{\partial}{\partial t'} \left[G_{d\sigma,kS(D)}^{r(a)}(t,t') \right] = -\frac{\partial}{\partial t'} \left[\mp i\theta(\pm t \mp t') \langle 0 | \{ \tilde{c}_{d\sigma}(t), c_{kS(D),\sigma}^{\dagger}(t') \} | 0 \rangle \right]$$

$$= -i \left[\mp i(\mp) \delta(\pm t \mp t') \langle 0 | \{ \tilde{c}_{d\sigma}(t), c_{kS(D),\sigma}^{\dagger}(t') \} | 0 \rangle \right]$$

$$+ (-i) \left[\mp i\theta(\pm t \mp t') \langle 0 | \{ \tilde{c}_{d\sigma}(t), \frac{\partial}{\partial t'} \left(c_{kS(D),\sigma}^{\dagger}(t') \right) \} | 0 \rangle \right]$$
(6.37)

Using the Ehrenfest's theorem we may write,

$$\frac{\partial}{\partial t'} \left(c_{kS(D),\sigma}^{\dagger}(t') \right) = -\frac{i}{\hbar} \left[c_{kS(D),\sigma}^{\dagger}(t'), \widetilde{\widetilde{H}} \right]. \tag{6.38}$$

Considering the transformed Hamiltonian of Eq. (6.20), we calculate the commutation relation of Eq. (6.39) which gives (considering $\hbar = 1$),

$$\left[c_{kS(D),\sigma}^{\dagger}(t'), \widetilde{\tilde{H}}\right] = -\varepsilon_k c_{kS(D),\sigma}^{\dagger}(t') - \tilde{V}_r \tilde{c}_{d,\sigma}^{\dagger}(t')$$
(6.39)

Using Eqs. (6.35) and (6.36), on Eq. (6.34) we obtain,

$$-i\frac{\partial}{\partial t'} \left[G_{d\sigma,kS(D)}^{r(a)}(t,t') \right]$$

$$= \varepsilon_k \left[\mp i\theta(\pm t \mp t') \langle 0 | \{ \tilde{c}_{d\sigma}(t), c_{kS(D),\sigma}^{\dagger}(t') \} | 0 \rangle \right]$$

$$+ \tilde{V}_r \left[\mp i \theta(\pm t \mp t') \langle 0 | \{ \tilde{c}_{d\sigma}(t), \tilde{c}_{d,\sigma}^{\dagger}(t') \} | 0 \rangle \right]$$

Using Eq. (6.26) and (6.28), we may write this as,

$$\left(-i\frac{\partial}{\partial t'} - \varepsilon_k\right) G_{d\sigma,kS(D)}^{r(a)}(t,t') = \tilde{V}_r G_{d\sigma,d\sigma}^{r(a)}(t,t') . \tag{6.40}$$

Similarly we calculate the relation between the lead and QD coupling Green's function $(G_{d\sigma,kS(D)}^{r(a)})$ and the QD's Green's function $(G_{d\sigma,d\sigma}^{r(a)})$ and the Green function for the leads $(g_{kS(D)}^{r(a)})$ as,

$$G_{d\sigma,kS(D)}^{r(a)}(t,t') = \tilde{V}_r G_{d\sigma,d\sigma}^{r(a)}(t,t') g_{kS(D)}^{r(a)}(t,t')$$
(6.41)

Eq. (6.41) is known as the Dyson's equation at equilibrium which contains the structure of $C(\tau) = A(\tau)B(\tau)$. Using the analytical continuation rule we may write this explicitly following Langreth theorem as,

$$C(t,t') = \int_{C} dt_1 A(t,t_1) B(t_1,t')$$
 (6.42)

To solve this integral we modify the Keldysh contour in such way that t is on the first half of the contour (in the outward direction) and t' is on the latter half (on the way back).

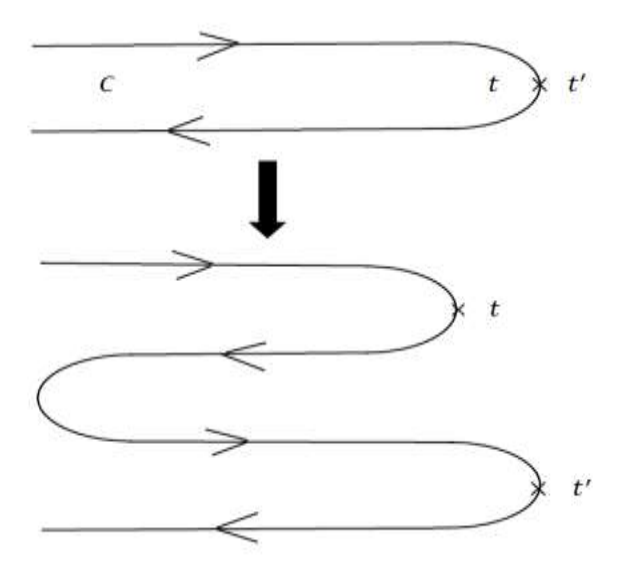


Fig. 6.2: Deformation of Keldysh Contour

For the new configuration of the Keldysh contour we can express Eq. (6.42) as,

$$C^{<}(t,t') = \int_{C_1} dt_1 A(t,t_1) B^{<}(t_1,t') + \int_{C_2} dt_1 A^{<}(t,t_1) B(t_1,t'). \tag{6.43}$$

For the integration on the contour C_1 , the integration variable t_1 is confined on the contour and it must be less than t'. Therefore we may split the first term of the Eq. (6.43) as,

$$\int_{C_1} dt_1 A(t, t_1) B^{<}(t_1, t') = \int_{-\infty}^{t_1} dt A^{>}(t, t_1) B^{<}(t_1, t') + \int_{t_1}^{\infty} dt A^{<}(t, t_1) B^{<}(t_1, t')$$

$$= \int_{-\infty}^{\infty} dt A^{r}(t, t_1) B^{<}(t_1, t')$$
(6.44)

where we have used the definition of the retarded function of Eq. (6.28) and here $A^{r(a)}$ represent the retarded(advanced) function. In the similar way, we may split the second term of the Eq. (6.43) and obtain,

$$\int_{C_2} dt_1 A^{<}(t, t_1) B(t_1, t') = \int_{-\infty}^{\infty} dt A^{<}(t, t_1) B^{a}(t_1, t')$$
 (6.45)

Combining Eqs. (6.44) and Eq. (6.45), we may write Eq. (6.43) as,

$$C^{<}(t,t') = \int_{-\infty}^{\infty} dt [A^{r}(t,t_{1})B^{<}(t_{1},t') + A^{<}(t,t_{1})B^{a}(t_{1},t')]. \tag{6.46}$$

Therefore, in the form of Eq. (6.46), we may write the Dyson equation of Eq. (6.41) as,

$$G_{d\sigma,kS(D)}^{\leq}\left(t,t'\right) = \int dt_{1}\,\tilde{V}_{r}\left[G_{d\sigma,d\sigma}^{r}(t,t')g_{kS(D)}^{\leq}\left(t,t'\right) + G_{d\sigma,d\sigma}^{\leq}(t,t')g_{kS(D)}^{a}\left(t,t'\right)\right]. \tag{6.47}$$

We define $G_{dd}^{\leq}(\omega)$ and $G_{dd}^{\geq}(\omega)$ as the Fourier Transforms of $G_{dd}^{\leq}(\tau=t-t')=i\langle 0|\tilde{c}_{d\sigma}^{\dagger}(t')\tilde{c}_{d\sigma}(t)|0\rangle$ and $G_{dd}^{\geq}(t-t')=i\langle 0|\tilde{c}_{d\sigma}(t)\,\tilde{c}_{d\sigma}^{\dagger}(t')|0\rangle$, which can be written for the QD electrons as follows,

$$G_{dd}^{\leq}(\tau) = i \langle 0 | \tilde{c}_d^{\dagger}(0) \tilde{c}_d(\tau) | 0 \rangle = i \langle 0 | c_d^{\dagger}(0) c_d(\tau) | 0 \rangle_{el} \langle \hat{\chi}^{\dagger} \hat{\chi} \rangle_{ph}$$
(6.48)

$$G_{dd}^{>}(\tau) = -i\langle 0 | \tilde{c}_d(0) \tilde{c}_d^{\dagger}(\tau) | 0 \rangle = -i\langle 0 | c_d(0) c_d^{\dagger}(\tau) | 0 \rangle_{el} \langle \hat{\chi}^{\dagger} \hat{\chi} \rangle_{ph}$$
 (6.49)

where

$$\langle \hat{\chi}^{\dagger} \hat{\chi} \rangle_{ph} = \langle e^{-g_i (b_i^{\dagger} - b_i)} e^{-g_i (b_i^{\dagger} - b_i)} \rangle \tag{6.50}$$

To calculate $\langle \tilde{V}_r \rangle$, we consider the 'n' phonon state as,

$$|n\rangle = \frac{(a^{\dagger})^n |0\rangle}{\sqrt{n!}} \quad . \tag{6.51}$$

Using this phonon state we calculate the following quantities.

$$\langle \tilde{V}_r \rangle = V_r \langle e^{-g_i(b_i^{\dagger} - b_i)} \rangle$$

$$\langle e^{-g_i(b_i^{\dagger} - b_i)} \rangle = \frac{\langle n | \sum_{n=0}^{\infty} e^{-2n\beta\hbar\widetilde{\omega}_0} e^{-g_i(b_i^{\dagger} - b_i)} | n \rangle}{\langle n | \sum_{n=0}^{\infty} e^{-2n\beta\hbar\widetilde{\omega}_0} | n \rangle}$$

$$=\frac{\langle n|\sum_{n=0}^{\infty}e^{-2n\beta\hbar\widetilde{\omega}_{0}}e^{-g_{i}b_{i}^{\dagger}}e^{g_{i}b_{i}}e^{-\frac{g_{i}^{2}}{2}}|n\rangle}{\langle n|\sum_{n=0}^{\infty}e^{-2n\beta\hbar\widetilde{\omega}_{0}}|n\rangle}.$$
(6.52)

Using the n-th phonon state of Eq. (6.51) we calculate,

$$\langle n \left| e^{-g_i b_i^{\dagger}} e^{g_i b_i} \right| n \rangle = \sum_{m=0}^n (-1)^m \frac{n!}{m! (n-m)!} (g_1)^{2m} = \mathcal{L}_n(g_1^2),$$
 (6.53)

where L_n' represents the Laguerre polynomial.

$$\sum_{n=0}^{\infty} e^{-2n\beta\hbar\widetilde{\omega}_0} = \frac{1}{1 - e^{-2\beta\hbar\widetilde{\omega}_0}} = \frac{e^{2\beta\hbar\widetilde{\omega}_0}}{e^{2\beta\hbar\widetilde{\omega}_0} - 1} = e^{2\beta\hbar\widetilde{\omega}_0} N_{ph}, \qquad (6.54)$$

where $N_{ph} = \frac{1}{e^{2\beta\hbar\tilde{\omega}_0} - 1}$ is the number of phonons. Using these results we obtain,

$$\langle e^{-g_i(b_i^{\dagger}-b_i)}\rangle = \frac{e^{-\frac{g_i^2}{2}}\sum_{n=0}^{\infty}\mathcal{L}_n(g_1^2)\,e^{-2n\beta\hbar\widetilde{\omega}_0}}{e^{2\beta\hbar\widetilde{\omega}_0}\,N_{ph}}$$

Considering, $g_1^2 = x$ and $e^{-2\beta\hbar\widetilde{\omega}_0} = y$, we have

$$\sum_{n=0}^{\infty} \mathcal{L}_n(g_1^2) \, e^{-2n\beta\hbar\widetilde{\omega}_0} = \sum_{n=0}^{\infty} \mathcal{L}_n(x) \, y^n$$

$$=\frac{e^{-\frac{xy}{(1-y)}}}{(1-y)}=\frac{e^{-g_1^2}\frac{e^{-2\beta\hbar\widetilde{\omega}_0}}{(1-e^{-2\beta\hbar\widetilde{\omega}_0})}}{(1-e^{-2\beta\hbar\widetilde{\omega}_0})}$$

$$= \frac{e^{-g_1^2 \frac{1}{(e^{2\beta\hbar\widetilde{\omega}_0} - 1)}}}{(1 - e^{-2\beta\hbar\widetilde{\omega}_0})} = e^{-g_1^2 N_{ph}} \cdot \frac{1}{(1 - e^{-2\beta\hbar\widetilde{\omega}_0})}$$
(6.55)

Therefore we may write,

$$\langle e^{-g_{i}(b_{i}^{\dagger}-b_{i})}\rangle = e^{-\frac{g_{i}^{2}}{2}}e^{-g_{1}^{2}N_{ph}} \cdot \frac{1}{(1-e^{-2\beta\hbar\tilde{\omega}_{0}})} \frac{1}{e^{2\beta\hbar\tilde{\omega}_{0}}N_{ph}}$$

$$= e^{-g_{1}^{2}(N_{ph}+\frac{1}{2})} \cdot \frac{1}{(e^{2\beta\hbar\tilde{\omega}_{0}}-1)} \cdot \frac{1}{N_{ph}}$$

$$= e^{-g_{1}^{2}(N_{ph}+\frac{1}{2})}T \cdot N_{ph} \cdot \frac{1}{N_{ph}}$$

$$= e^{-g_{1}^{2}(N_{ph}+\frac{1}{2})}.$$
(6.56)

At temperature $T \to 0$, number of phonons $N_{ph} = 0$. Therefore we may write,

$$\langle e^{-g_i(b_i^{\dagger} - b_i)} \rangle = e^{-\frac{g_1^2}{2}}.$$
 (6.57)

Another term we need to calculate is the phonon average with respect to the n-phonon state to evaluate the Green functions of Eqs. (6.48) and (6.49). Let,

$$\mathcal{F}(t,t') = \langle \hat{\chi}^{\dagger} \hat{\chi} \rangle_{ph}$$

$$= \frac{\langle n | \sum_{n=0}^{\infty} e^{-\beta \hbar \widetilde{\omega}_0} \sum_{i=0}^{2} b_i^{\dagger} b_i \hat{\chi}^{\dagger}(t) \hat{\chi}(t') | n \rangle}{\langle n | \sum_{n=0}^{\infty} e^{-\beta \hbar \widetilde{\omega}_0} \sum_{i=0}^{2} b_i^{\dagger} b_i | n \rangle}$$
 (6.58)

Using the results of Eqs. (6.50) and (6.52), we obtain

$$\mathcal{F}(t,t') = e^{-g_i^2 (2N_{ph}+1)} e^{z\cos\theta}$$
(6.59)

and,

$$e^{z\cos\theta} = \sum_{n=-\infty}^{\infty} I_n(z)e^{-in\hbar\tilde{\omega}_0(t-t')}e^{2n\hbar\tilde{\omega}_0\beta}$$
 (6.60)

So, we can write

$$\mathcal{F}(t,t')=e^{-g_i^2\left(2N_{ph}+1\right)}\sum_{n=-\infty}^{\infty}I_n(z)e^{-in\hbar\widetilde{\omega}_0(t-t')}e^{2n\hbar\widetilde{\omega}_0\beta}$$

$$= \sum_{n=-\infty}^{\infty} I_n(z) e^{n\hbar\widetilde{\omega}_0 \beta} e^{-g_i^2 (2N_{ph}+1)} \cdot e^{-in\hbar\widetilde{\omega}_0(t-t')}$$

$$= \sum_{n=-\infty}^{\infty} L_{\pm n}(z) \cdot e^{-in\hbar\widetilde{\omega}_0 \tau}, \qquad (6.61)$$

where, $z=2g_i^2\big[N_{ph}\big(1+N_{ph}\big)\big]^{\frac{1}{2}}$, $\tau=(t-t')$ and I_n is the nth order Modified Bessel function of the second kind. Here, $L_{\pm n}(z)=\exp\left[-g_i^2\big(2N_{ph}+1\big)+\left(\frac{n\hbar\widetilde{\omega}_0}{k_BT}\right)\right]I_n(z)$, and $L_{\pm n}$ describes the spectral weight of the $\pm n^{th}$ phonon side band [28].

We may now write Eqs. (6.48) and (6.49) as

$$G_{dd}^{\leq}(\tau) = i \langle 0 | c_d^{\dagger}(0) c_d(\tau) | 0 \rangle_{el} \langle \hat{\chi}^{\dagger} \hat{\chi} \rangle_{ph}$$

$$= \tilde{G}_{dd}^{\leq}(\tau) \sum_{n=-\infty}^{\infty} L_n e^{in\hbar \tilde{\omega}_0 \tau}, \qquad (6.62)$$

and,

$$G_{dd}^{>}(\tau) = -i \langle 0 | c_d(0) c_d^{\dagger}(\tau) | 0 \rangle_{el} \langle \hat{\chi}^{\dagger} \hat{\chi} \rangle_{ph}$$

$$= \tilde{G}_{dd}^{>}(\tau) \sum_{n=-\infty}^{\infty} L_n e^{in\hbar \tilde{\omega}_0 \tau}. \tag{6.63}$$

Next, multiplying Eq. (6.40) by $e^{i(\epsilon \mp n\hbar\tilde{\omega}_0)t'}$ on both sides and integrating over t' we obtain,

$$\left[(\epsilon \mp n\hbar\widetilde{\omega}_0) - \sum_k \varepsilon_{kS}\right] \widetilde{G}^{r(a)}_{1\sigma,kS}(\epsilon \mp n\hbar\widetilde{\omega}_0) = \overline{\tilde{V}}_r \widetilde{G}^{r(a)}_{1\sigma,1\sigma}(\epsilon \mp n\hbar\widetilde{\omega}_0)$$

which gives

$$\tilde{G}_{1\sigma,kS}^{r(a)}(\epsilon \mp n\hbar\widetilde{\omega}_{0}) = \frac{\overline{\tilde{V}_{r}}\tilde{G}_{1\sigma,1\sigma}^{r(a)}(\epsilon \mp n\hbar\widetilde{\omega}_{0})}{[(\epsilon \mp n\hbar\widetilde{\omega}_{0}) - \sum_{k} \varepsilon_{kS}]}.$$
(6.64)

Eq. (6.64) represents the relation between the two Green functions of the source and the first QD, i.e. $\tilde{G}_{1\sigma,kS}^{r(a)}(\epsilon \mp n\hbar\widetilde{\omega}_0)$ and $\tilde{G}_{1\sigma,1\sigma}^{r(a)}(\epsilon \mp n\hbar\widetilde{\omega}_0)$.

Similarly, we calculate the following relations,

$$\tilde{G}_{1\sigma,2\sigma}^{r(a)}(\epsilon \mp n\hbar\widetilde{\omega}_{0}) = \frac{\tilde{t} \; \tilde{G}_{1\sigma,1\sigma}^{r(a)}(\epsilon \mp n\hbar\widetilde{\omega}_{0})}{\left[(\epsilon \mp n\hbar\widetilde{\omega}_{0}) - \varepsilon_{k} - \widetilde{U}\langle n_{\sigma}\rangle\right]} + \frac{\overline{\widetilde{V}_{r}} \tilde{G}_{1\sigma,kD}^{r(a)}(\epsilon \mp n\hbar\widetilde{\omega}_{0})}{\left[(\epsilon \mp n\hbar\widetilde{\omega}_{0}) - \varepsilon_{k} - \widetilde{U}\langle n_{\sigma}\rangle\right]}, \quad (6.65)$$

and

$$\tilde{G}_{1\sigma,kD}^{r(a)}(\epsilon \mp n\hbar\widetilde{\omega}_{0}) = \frac{\overline{\tilde{V}_{r}}\tilde{G}_{1\sigma,2\sigma}^{r(a)}(\epsilon \mp n\hbar\widetilde{\omega}_{0})}{[(\epsilon \mp n\hbar\widetilde{\omega}_{0}) - \varepsilon_{k}]}.$$
(6.66)

Using Eqs. (6.65) to Eq. (6.66), we obtain

 $\tilde{G}_{d\sigma,1\sigma}^{r(a)}(\epsilon \mp n\hbar\widetilde{\omega}_0)$

$$= \frac{1}{\left[(\epsilon \mp n\hbar \widetilde{\omega}_0) - \varepsilon_k - \widetilde{U} \langle n_{\sigma} \rangle - \frac{\overline{\widetilde{t}}^2}{(\epsilon \mp n\hbar \widetilde{\omega}_0) - \varepsilon_k - \widetilde{U} \langle n_{\sigma} \rangle} - \widetilde{\widetilde{\Sigma}}^{r(a)} \right]}$$
(6.67)

where 'd' represents the QD (d = 1 for the first QD and d = 2 for second QD) and using Eq. (6.57) we get

$$\bar{\tilde{t}} = t_{12} \langle e^{[g_1(b_1^{\dagger} - b_1) - g_2(b_2^{\dagger} - b_2)]} \rangle = t_{12} e^{-g_i^2}$$
(6.68)

 $\tilde{\tilde{\mathcal{Z}}}^{r(a)}$ is known as the self-energy of the interaction which is calculated as,

$$\tilde{\tilde{\Sigma}}^{r(a)} = \frac{\bar{\tilde{V}}_r e^{-g_i^2}}{[(\epsilon \mp n\hbar \tilde{\omega}_0) - \varepsilon_k]},$$
(6.69)

and the self-energy can be written as,

$$\tilde{\tilde{\Sigma}}^{r(a)}(\epsilon) = \tilde{\Lambda}(\epsilon) + i\tilde{\Gamma}(\epsilon). \tag{6.70}$$

with $\tilde{\Gamma} = 2\pi\rho(0) \left| \overline{\tilde{V}}_r \right|^2 e^{-g_i^2}$ at $(T \to 0)$.

We can write the spectral function (SF) $A(\varepsilon)$ which describes the possible energy excitation in terms of the Keldysh lesser and greater Green functions as

$$A(\varepsilon) = i[G_{dd}^{r}(\varepsilon) - G_{dd}^{a}(\varepsilon)] = i[G_{dd}^{>}(\varepsilon) - G_{dd}^{<}(\varepsilon)], \tag{6.71}$$

and using the Dyson equation of motion method, $\tilde{G}^{>(<)}(\epsilon)$ can be obtained from $\tilde{G}^{r(a)}_{dd}(\epsilon)$ as

$$\tilde{G}^{>(<)}(\varepsilon) = \tilde{G}^{r}_{dd}(\varepsilon) \, \tilde{\Sigma}^{>(<)}(\varepsilon) \, \tilde{G}^{a}_{dd}(\varepsilon). \tag{6.72}$$

Substituting Eq. (6.72) in Eq. (6.71), we calculate the tunnelling current as

$$J_{\sigma} = \frac{e}{2h} \int d\varepsilon \left[\left\{ (f_{S}(\varepsilon)\Gamma_{S} - f_{D}(\varepsilon)\Gamma_{D}) \right\} A(\varepsilon) + (\Gamma_{S} - \Gamma_{D})G^{<}(\varepsilon) \right], \tag{6.73}$$

The lesser and the greater self-energies are defined as,

$$\tilde{\Sigma}^{<}(\varepsilon) = i \, \tilde{\Gamma}[f_S(\varepsilon) + f_D(\varepsilon)],$$
(6.74)

$$\tilde{\Sigma}^{>}(\varepsilon) = -i\,\tilde{\Gamma}\left[2 - (f_{S}(\varepsilon) + f_{D}(\varepsilon))\right],\tag{6.75}$$

where $f_S(\varepsilon)$ and $f_D(\varepsilon)$ are respectively the Fermi distribution functions of S and D and are given by : $f_{S,D}(\varepsilon) = \left(exp[(\mu_{S,D} - \varepsilon)/k_BT] + 1\right)^{-1}$, μ_S and μ_D being the chemical potentials of S and D, and related to the bias-voltage (V_b) and the mid-voltage (V_m) as

$$eV_b = (\mu_S - \mu_D),$$
 (6.76)

$$eV_m = \frac{(\mu_S + \mu_D)}{2},\tag{6.77}$$

 $\tilde{\Gamma} = \Gamma e^{-g_i^2(2N_{ph}+1)}$ with $\Gamma = (\Gamma_S + \Gamma_D)/2$, Γ_S and Γ_D being defined as: $\Gamma_{S,D} = 2\pi \rho_{S,D} |\overline{\tilde{V}}_r|^2 e^{-g_i^2(2N_{ph}+1)}$, where $\rho_{S,D}$ is the density of states of the leads and N_{ph} is the phonon distribution given by $N_{ph} = [exp(\hbar \, \widetilde{\omega}_0/k_B T) - 1]^{-1}$.

We treat the onsite Coulomb interaction strength at the Hartree-Fock mean-field level and evaluate numerically the self-energy self-consistently and hence the tunnelling current J_{σ} . Next we calculate the total differential conductance G which is defined as

$$G = \frac{dJ_{\sigma}}{dV_{h}}. (6.78)$$

and the spin-polarization parameter which is defined as

$$P_{\sigma,-\sigma} = \frac{(J_{\sigma} - J_{-\sigma})}{(J_{\sigma} + J_{-\sigma})}.$$
(6.79)

6.3 Numerical Results

We consider symmetric metallic leads. We also consider that as two QDs have the same EPI strength i.e., $g_1 = g_2 = g$. All the energies are measured in units of the QDs' phonon energy i.e., we consider $\hbar\omega_0 = 1$. We mostly consider the cut-off frequency $\omega_c = 3$, the phonon dissipation $\gamma = 0.02$, onsite Coulomb correlation U = 5 and the gate voltage $eV_g = 0$. The main aim of this work is to study the changes in the spectral function (SF), tunnelling current (J_{σ}) and the differential conductance (G) due to the incorporation of one extra QD in series with the already existing QD in the central region of the single molecular transistor. In Fig.

6.3, the variation of the renormalized SF, $A(\omega)/A_0$ is plotted with respect to ω for different values of the hopping parameter t_{12} . It is observed that as t_{12} increases, the peak height in the SF increases. For each peak, there is a sub-peak and as t_{12} increases the sub-peaks become more prominent. These sub-peaks carry the significance of the second QD.

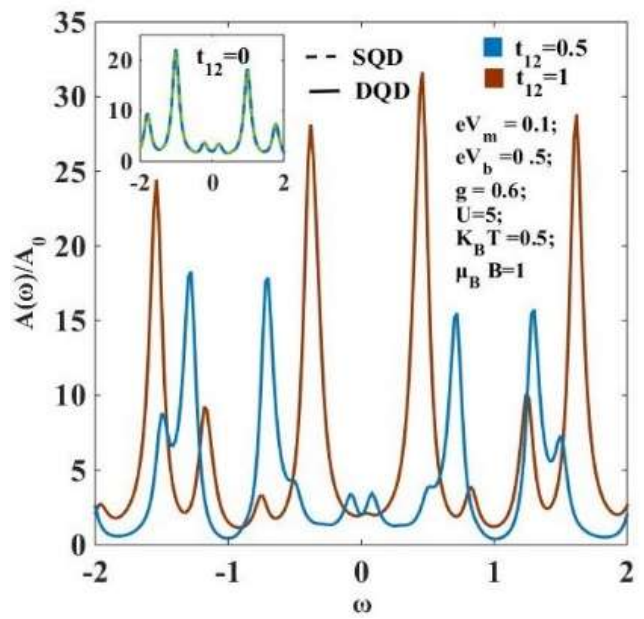


Fig. 6.2: The spectral function $(A(\omega)/A_0)$ with respect to ω for different values of the tunnelling coefficient t_{12} .

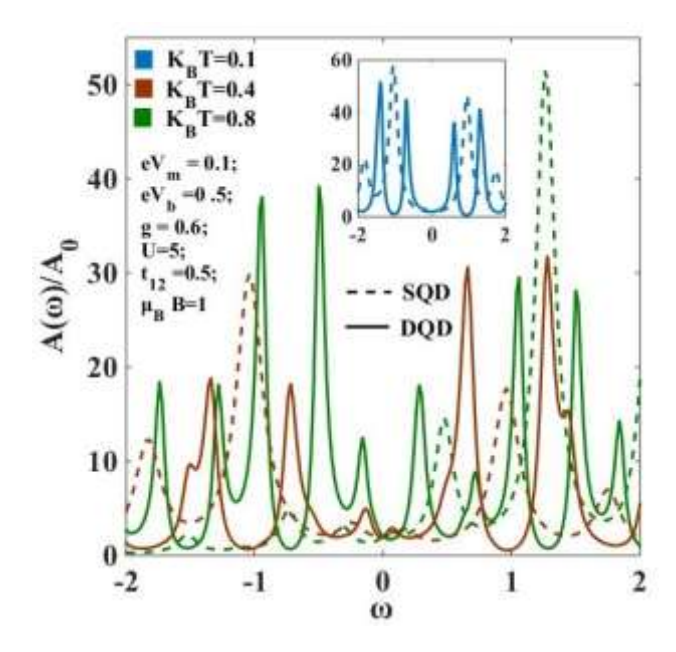


Fig.6.4: The spectral function $(A(\omega)/A_0)$ with respect to ω at different temperature (K_BT) .

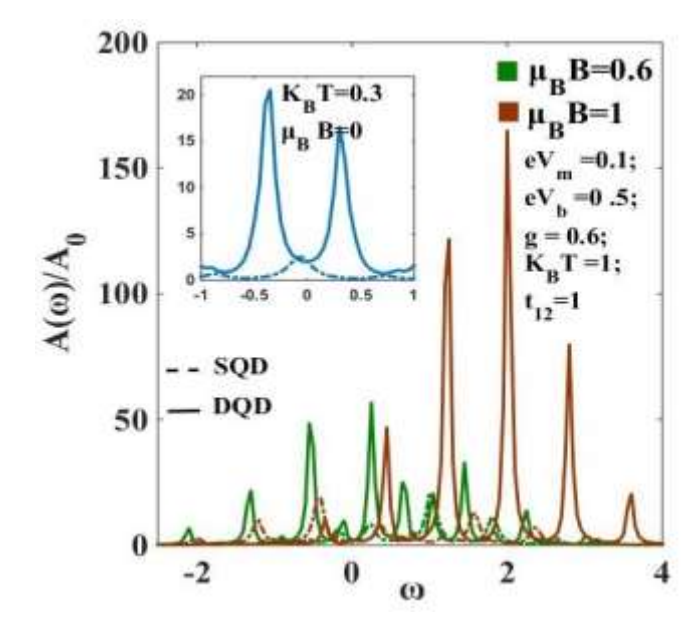


Fig. 6.5: The spectral function $(A(\omega)/A_0)$ with respect to ω for different magnetic fields(B).

In Figs. 6.4 and 6.5, the variations of SF with ω have been studied. In Figs. 6.4, results have been obtained at different temperature while in Fig. 6.5, at different magnetic field. Fig. 6.4 shows that as temperature increases, the number of phonon side-bands and the spectral peak heights increase. The appearance of the side-peaks is due to the phonon excitations, as explained in Ref. [27].

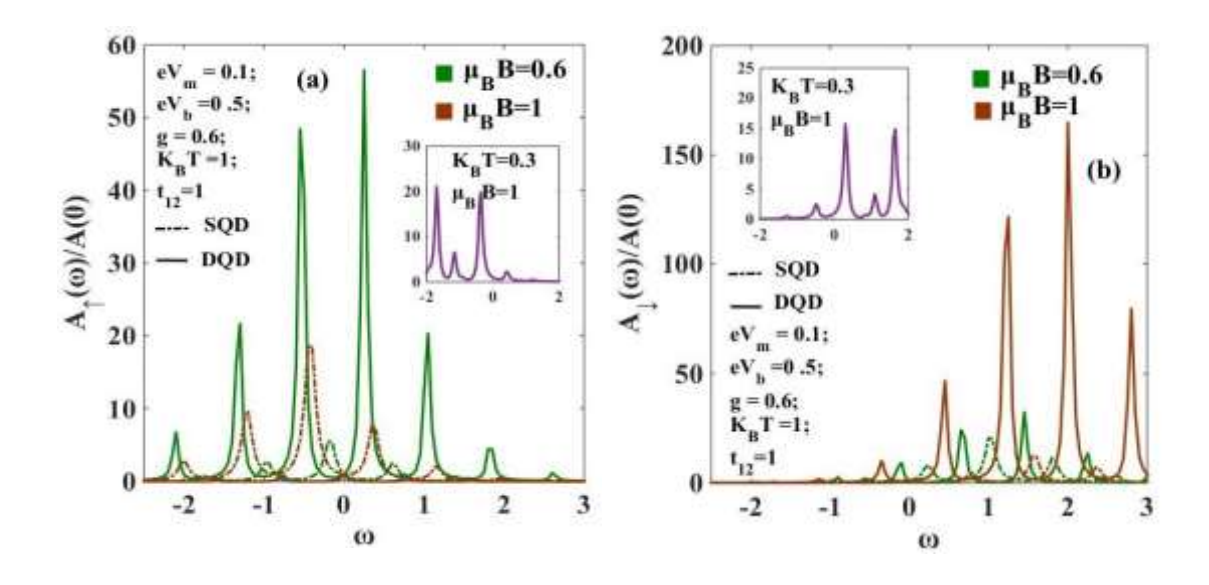


Fig. 6.6: The spectral function (a) $(A_{\uparrow}(\omega)/A_0)$ and (b) $(A_{\downarrow}(\omega)/A_0)$ with respect to ω for different magnetic field (B).

The inset in Fig. 6.5 is plotted in the absence of the magnetic field. Though SMT exhibits only one peak, the double-QD structure in BMT splits the SMT peak into two peaks. As the magnetic field increases, the peaks in SF move towards right and as B increases, the peak heights increase. This behaviour of SF exhibits the spin-filtering effect due to the application of the magnetic field B.

To see how the spin filtering effect changes SF, we plot in Fig. 6.6, the variations of the spin-resolved SF, $A_{\uparrow}(\omega)$ and $A_{\downarrow}(\omega)$ with ω for two values of B. The figures show some interesting behaviour. For the spin-up SF, the peaks shift to the left (negative ω side) as B increases, whereas, for the spin-down SF, the peaks shift towards right. Also, the peaks are higher for $A_{\downarrow}(\omega)$. With increasing B, the spin-up peaks decrease in height, though for the down spin, the SF peaks increase with B. The multi-molecular feature of BMT again shows up through the appearance of the extra sub-peak with each major peak. Thus the number of peaks for BMT is more than a corresponding SMT system.

In Fig. 6.7(a), we study the variations of the spin-current J_{σ} with respect to the tunnelling or QD coupling constant t_{12} at different temperatures. At low temperature, as the coupling between the two QDs increases, the tunnelling current increases (if t_{12} is very large). As T increases, the rate of increase of the tunnelling current with t_{12} decreases. Above a certain T, the current decreases with increasing t_{12} . The reason for this behaviour can be explained from the Fermi distribution (FD) function of the electrons. When T is small, the Fermi level in the metallic leads and the QDs are at comparable energy levels, so the electron can transport from S to D through the QDs. In the low-temperature limit, there is a cross-over region where the J_{σ} value is small for low t_{12} . This may be because when t_{12} and T are both low, the electron does not get sufficient energy to hop from one QD to another. But as T increases, the energy levels shift and the tunnelling current increases even for low t_{12} , or else if the t_{12} is sufficiently high the current is much higher even at low temperature T.

To study the effect of the magnetic field on the current density J_{σ} , we plot Fig. 6.7 (b). As the magnetic field B increases, the spin-splitting of the energy levels in the QDs increases. The energy level due to the spin-up electron goes down and the energy level for the spin-down electron goes up. Therefore, as B is increased, the tunnelling current decreases. This behaviour of BMT is similar to that of SMT. But an interesting behaviour is found for the BMT in the low temperature regime. Here, we observe a competing effect of T and B on

current. As B increases, the current J_{σ} reduces if T is sufficiently high. But if T is low, J_{σ} increases initially, but after a certain value of B, J_{σ} reduces again. It is observed from Figs. 6.7(b) that the tunnelling current is higher in BMT that in SMT in the low temperature and high magnetic field regime.

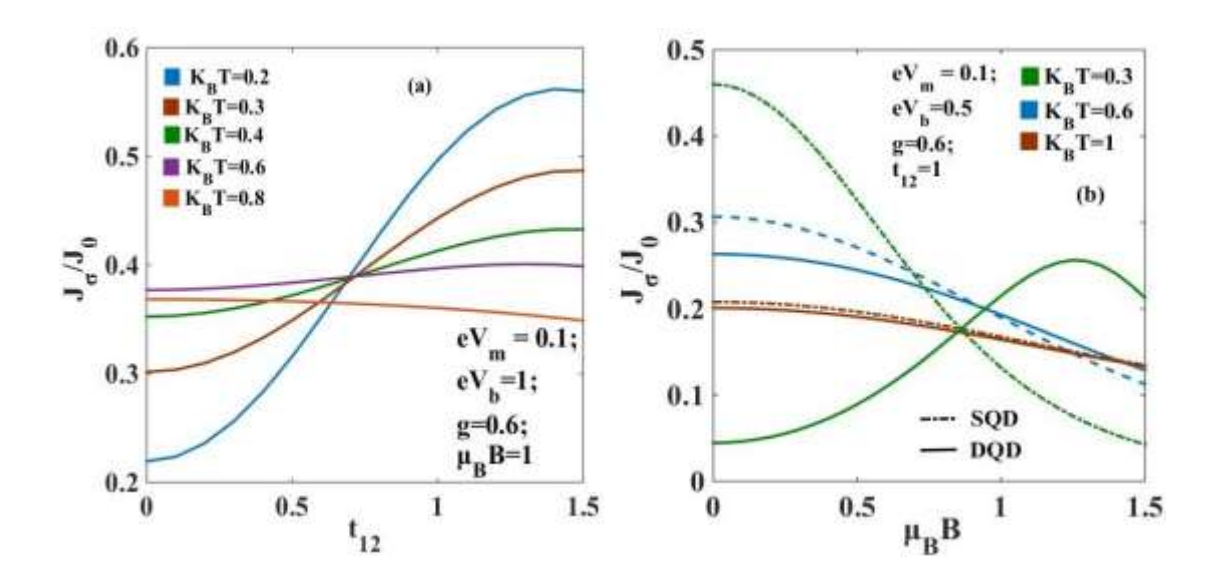


Fig. 6.7: (a) Total tunnelling current (J_{σ}/J_0) with respect to the DQD tunnelling parameter (t_{12}) & (b) J_{σ}/J_0 with respect to the magnetic field $(\mu_B B)$ for different temperatures $(K_B T)$.

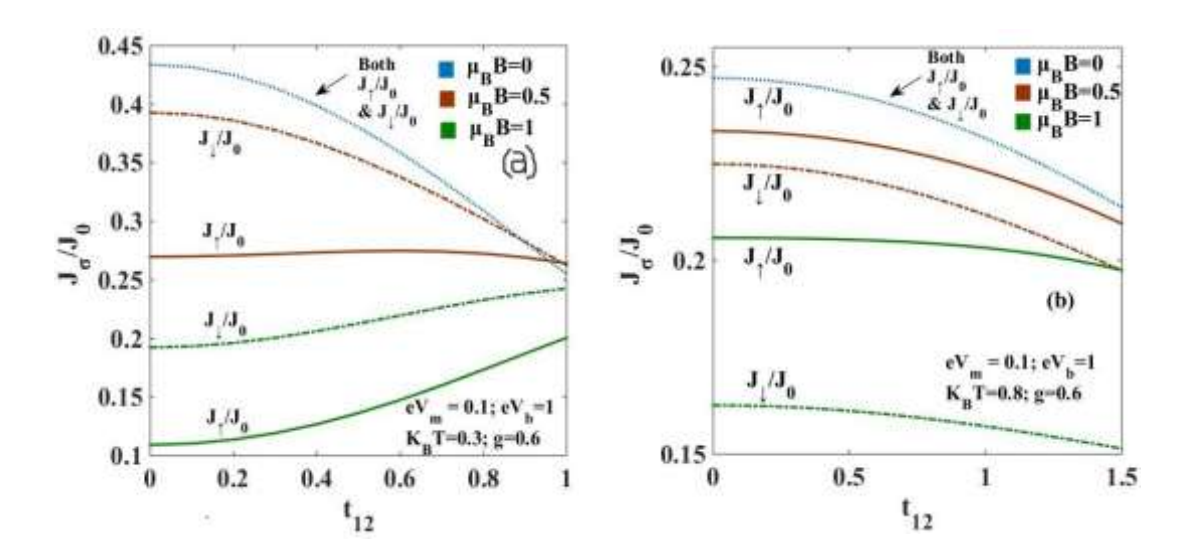


Fig. 6.8: Spin dependent tunnelling current (J_{\uparrow}/J_0) & (J_{\downarrow}/J_0) with respect to the DQD tunnelling parameter (t_{12}) for different values of the magnetic field $(\mu_B B)$ at (a) $K_B T = 0.3$ & (b) $K_B T = 0.8$.

To understand the competing effect of the temperature and the magnetic field, we plot the spin-resolved tunnelling currents J_{\uparrow} and J_{\downarrow} with respect to the QD tunnelling coefficient t_{12} . Fig. 6.8 (a) is plotted for $K_BT=0.3$ (low temperature) and Fig. 6.8 (b) is plotted for $K_BT=0.8$ (high temperature). For $\mu_BB=0$, there is no spin-filtering effect, as is understandable. For $K_BT=0.3$, J_{\uparrow} is lower than J_{\downarrow} , while for $K_BT=0.8$, J_{\uparrow} is higher than J_{\downarrow} . For $K_BT=0.3$, as B increases, difference in currents between J_{\uparrow} and J_{\downarrow} decreases. The opposite effect is observed for $K_BT=0.8$ case i. e., the difference between J_{\uparrow} and J_{\downarrow} increases as B increases.

As the e-p interaction strength increases in each QD, J_{σ} decreases. It is well known that as e-p interaction increases in a QD, the polaron size decreases and the polaron mass increases and the polaron may get trapped in its own potential, which reduces the polaronic transport. Therefore, as the e-p coupling increases in the QDs, the tunnelling current also decreases. In Fig. 6.9 (a) and 6.9 (b), we consider $\mu_B B = 1$ and the variation of J_{σ} with respect to the e-p interaction g is plotted for different values of temperature and phonon dissipation. J_{σ} decreases due to the increase in the polaronic effect as g increases. The increase in temperature also decreases the current as we have explained in Fig. 6.7 (b). Fig. 6.9 (b) shows the effect of dissipation on current. At a certiain value of g, as γ increases, the current increases. This is the effect of phonon dissipation. As the phonon dissipation rate increases, it screens the effect of -p interaction more by reducing the frequency of the QDs.

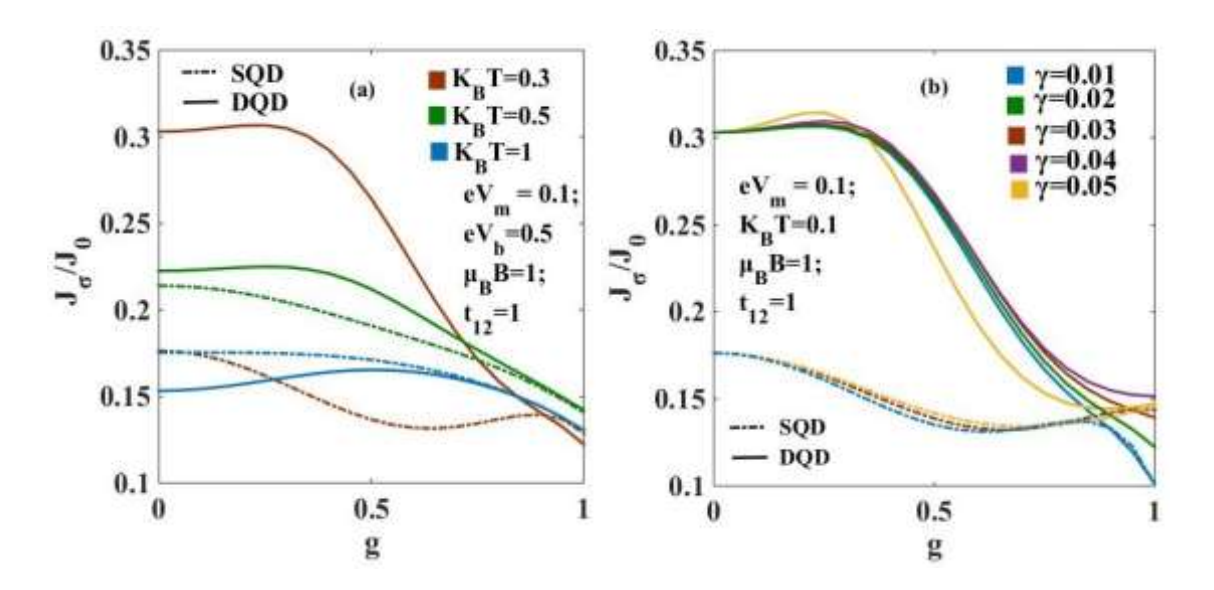


Fig. 6.9: Spin dependent tunnelling current (J_{σ}/J_0) with respect to the EPI coefficient (g) for different values of (a) the magnetic field $(\mu_B B)$ & (b) the phonon dissipation rate (γ) .

With the increase in the bias-voltage eV_b , more electrons can enter from the source to the QDs, which results in the rise in the tunnelling current. In Fig. 6.10 (a), the variation of the tunnelling current with the bias-voltage is studied for different values of the magnetic field. It is found that when the magnetic field is zero, the current J_{σ} in BMT is lower than that in SMT. But, as the magnetic field increases, we find that there exists a certain regime of the bias voltage in which J_{σ} is higher for BMT than for SMT. To see the effect of the magnetic field and the bias-voltage on the spin-polarized tunnelling currents, we plot Fig. 6.10 (b). In the absence of a magnetic field, at a particular bias-voltage V_b , the spin-polarized currents J_{\uparrow} and J_{\downarrow} are equal. But in the presence of a magnetic field, the energy levels in the QDs are split and the spin-up level goes down and the spin-down level goes up. As a result, J_{\downarrow} increases with the magnetic field and J_{\uparrow} decreases as B increases.

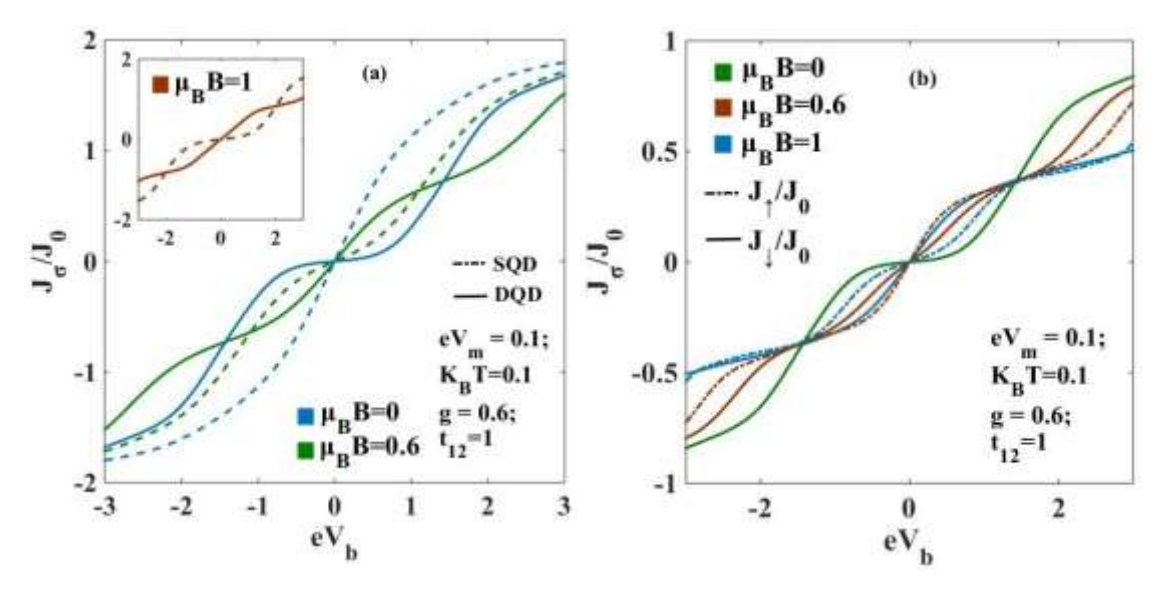


Fig. 6.10: (a) The total tunnelling current (J_{σ}/J_0) and (b) the Spin-resolved tunnelling current J_{\uparrow}/J_0 & J_{\downarrow}/J_0 with respect to the bias-voltage (eV_b) for different values of the magnetic field $(\mu_B B)$.

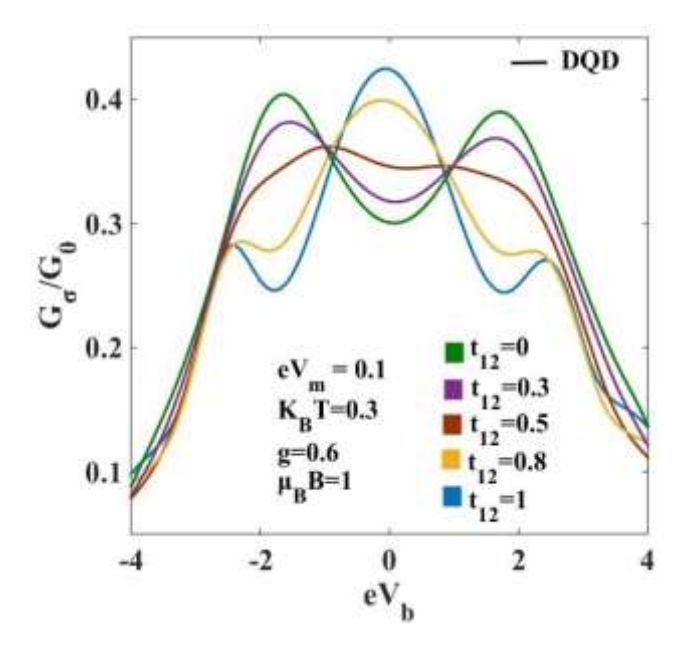


Fig. 6.11: Differential conductance G_{σ}/G_0 with respect to the bias-voltage (eV_b) , for different values of the tunnelling coefficient (t_{12}) .

In Fig. 6.11, we plot the differential conductance G_{σ} with respect to the bias voltage eV_b for different values of the QD tunnelling coefficient t_{12} . As eV_b increases, more electrons can flow from the source to QD, which results in the rise in the tunnelling current as well as in the differential conductance. One can also observe a few side peaks, which occur due to the polaronic fluctuations.

In Fig. 6.12, we plot the differential conductance G_{σ} with respect to the bias voltage eV_b . Fig. 6.12(a) gives results for different values of the magnetic field and Fig. 6.12(b) provides results for different values of temperature. G_{σ} is symmetric about $eV_b = 0$ for all values of B & T. At $K_BT = 0.3$, in the absence of a magnetic field, there is one peak in G_{σ} for SMT, whereas for BMT, the peak splits into two peaks due to the presence of two QDs in the system. But as B is switched on, two peaks appear as the energy levels in the QDs are split. As B increases, G_{σ} decreases which is, of course, an expected behaviour. Fig. 6.12 (b) shows that the effect of temperature on G_{σ} is similar to what we observe in the J_{σ} plot. As T increases more, G_{σ} saturates.

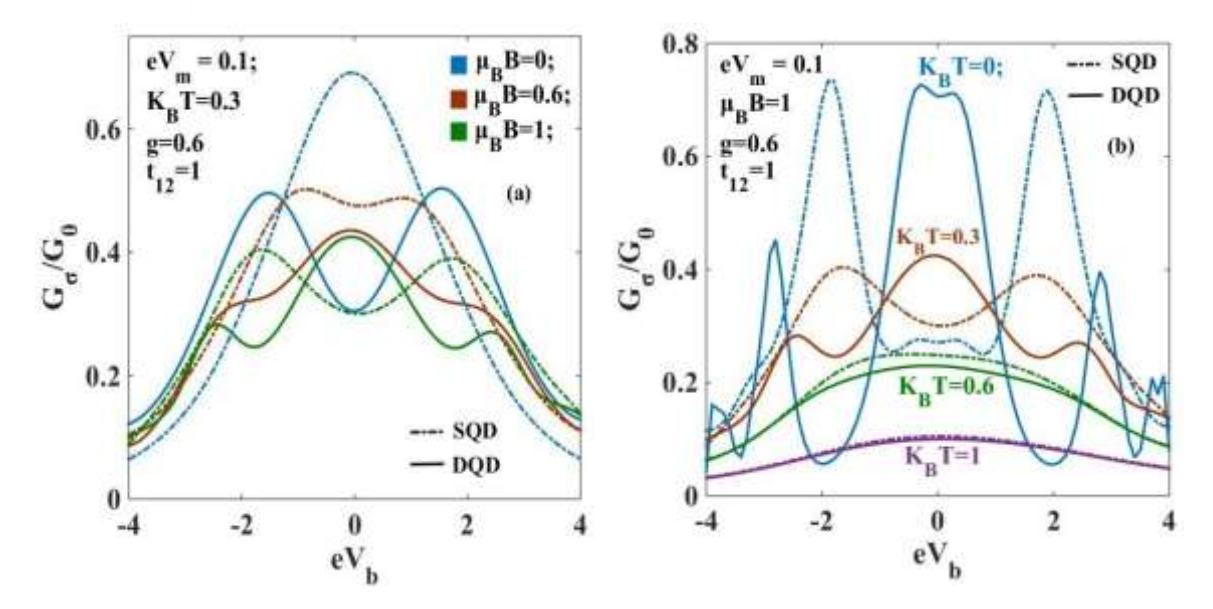


Fig. 6.12: Differential conductance G_{σ}/G_0 with respect to the bias-voltage (eV_b) , for different values of the magnetic field $(\mu_B B)$ & (b) the temperature $(K_B T)$.

To understand how the temperature changes the energy levels in the metallic leads, we have plotted the spin-resolved differential conductance in Fig. 6.13, with respect to the bias voltage for different temperatures. The G_{\uparrow} and G_{\downarrow} are not symmetric with respect to eV_b . The G_{\uparrow} component is shifted to the left and the G_{\downarrow} component is shifted to the right. This behaviour is similar to what we observe in the case of SF.

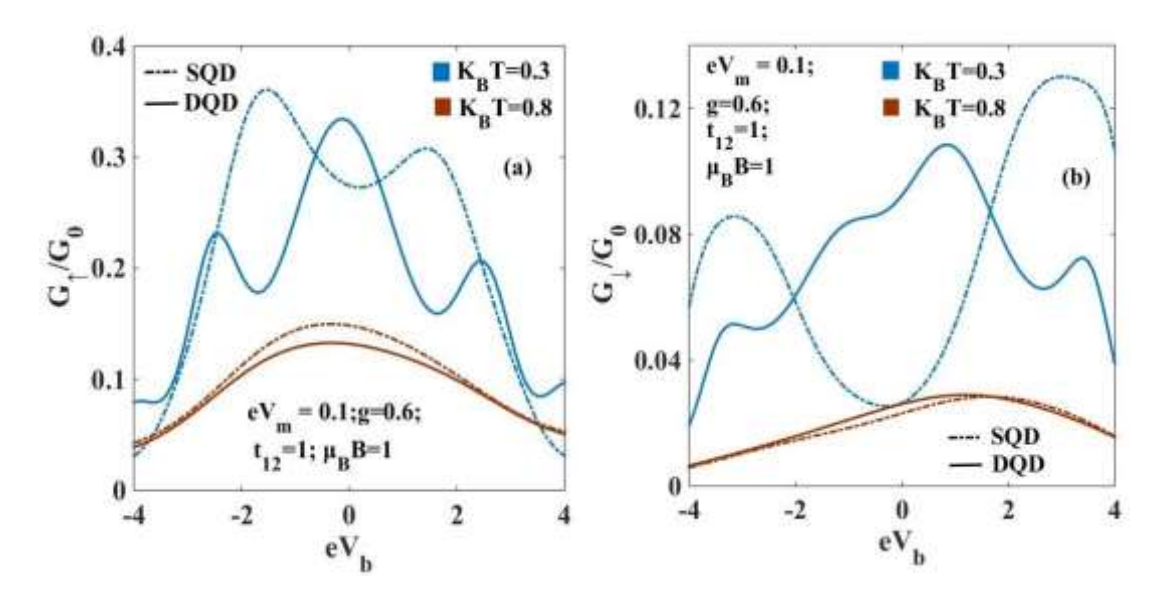


Fig. 6.13: Spin-resolved Differential conductance (a) G_{\uparrow}/G_0 & (b) G_{\downarrow}/G_0 with respect to the bias-voltage (eV_b) for different values of the temperature (K_BT) .

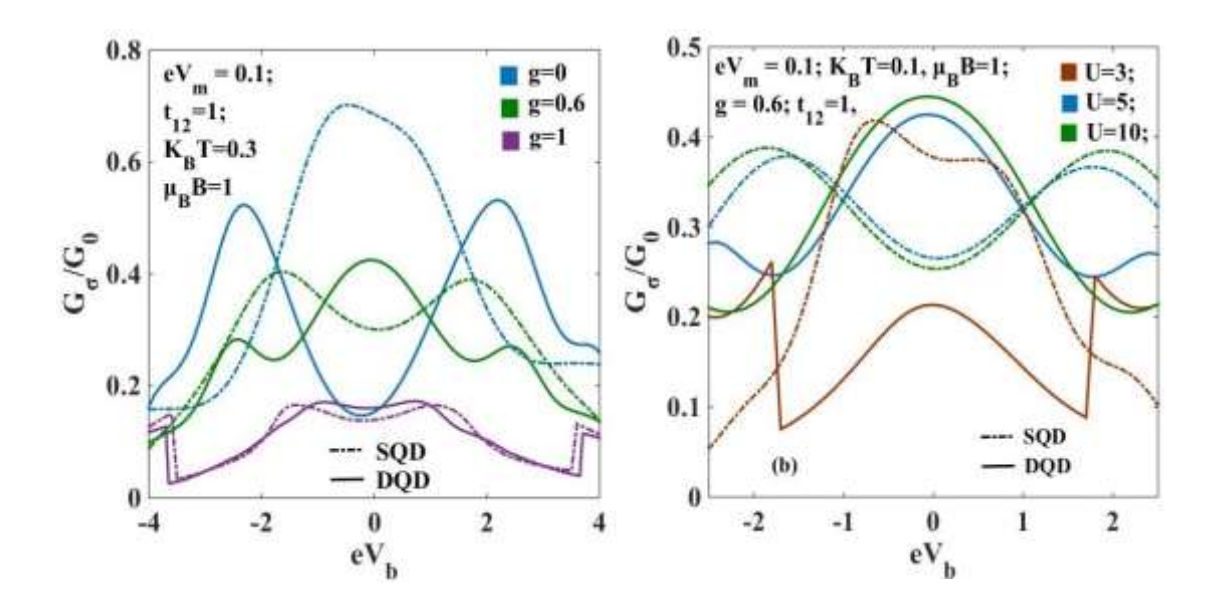


Fig. 6.14: Differential conductance G_{σ}/G_0 with respect to the bias-voltage (eV_b) , for different values of (a) the e-p interaction coefficient (g) & (b) the Coulomb correlation (U).

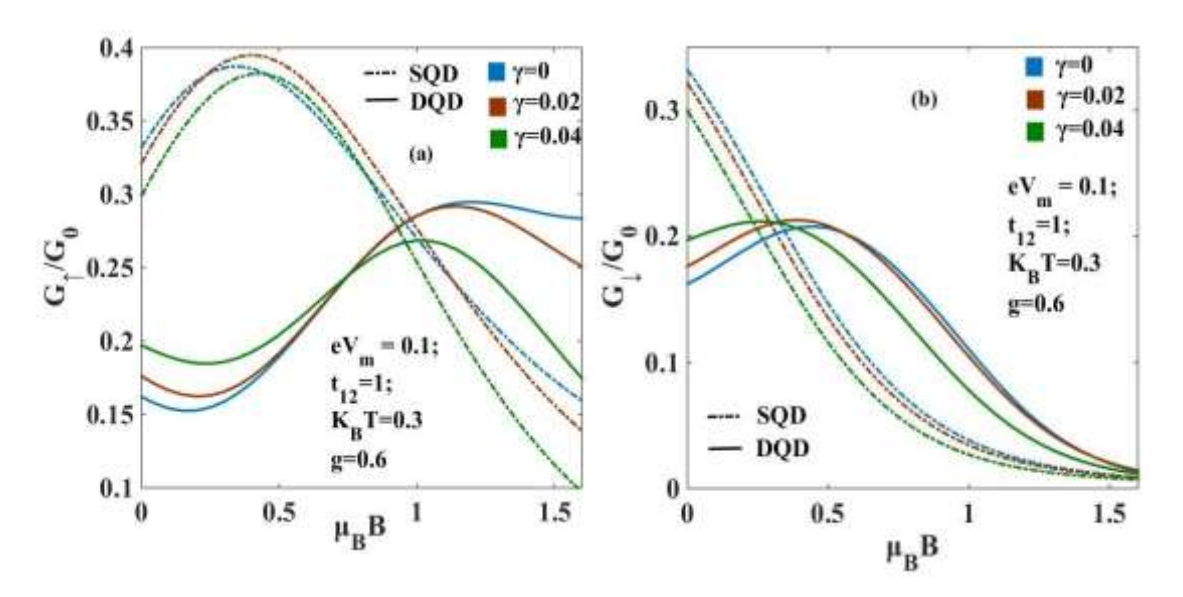


Fig. 6.15: Spin-resolved differential conductance (a) G_{\uparrow}/G_0 & (b) G_{\downarrow}/G_0 with respect to the magnetic field $(\mu_B B)$ for different values of the dissipation constant (γ) .

In Fig. 6.14 (a), the effect of the EPI coefficient g on G_{σ} is studied. We find that as g increases, the differential conductance G_{σ} decreases. As a result, the differential conductance peak also decreases with increasing g. Another very important parameter is the Coulomb correlation U which opposes electrons from coming to the same site. Therefore, as U is

increased, the electrons would like to tunnel from QDs to the drain and the current J_{σ} and differential conductance G_{σ} would increase (Fig. 6.14 (b)).

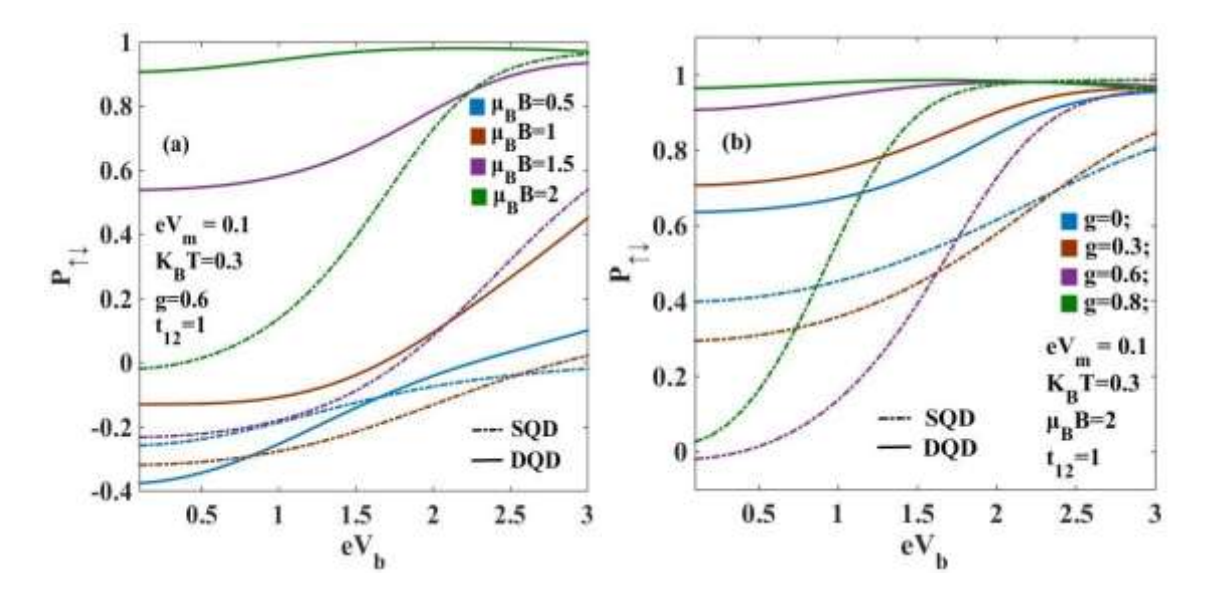


Fig. 6.16: Spin-Polarization $(P_{\uparrow\downarrow})$ with respect to the bias-voltage (eV_b) for different values of (a) the magnetic field $(\mu_B B)$ and (b) the e-p interaction coefficient (g).

The effect of phonon dissipation on G_{σ} is plotted in Fig. 6.15. Here we study the variation of G_{σ} with respect to the magnetic field for different phonon dissipation rates (γ) . The spin-resolved conductances G_{\uparrow} and G_{\downarrow} show a different behaviour, as is understandable. But from both the Figs. 6.15(a) and (b), we find that when the magnetic field is high, the phonon dissipation γ reduces G_{\uparrow} and G_{\downarrow} . But at low values of magnetic field, the conductance increases with dissipation.

Spin polarization $(P_{\uparrow\downarrow})$ is an important parameter in the spin-transport phenomena. In Fig. 6.16(a) we study the effect of magnetic field on spin-polarization. As the magnetic field $(\mu_B B)$ increases, the spin-filtering effect becomes more prominent. Therefore, with the increase in B, the spin-polarization also increases and at a certain B, $P_{\uparrow\downarrow}$ become maximum. From Fig. 6.16(b), we find that e-p interaction also enhances the spin-polarization effect and in the strong coupling limit, $P_{\uparrow\downarrow}$ become 1.

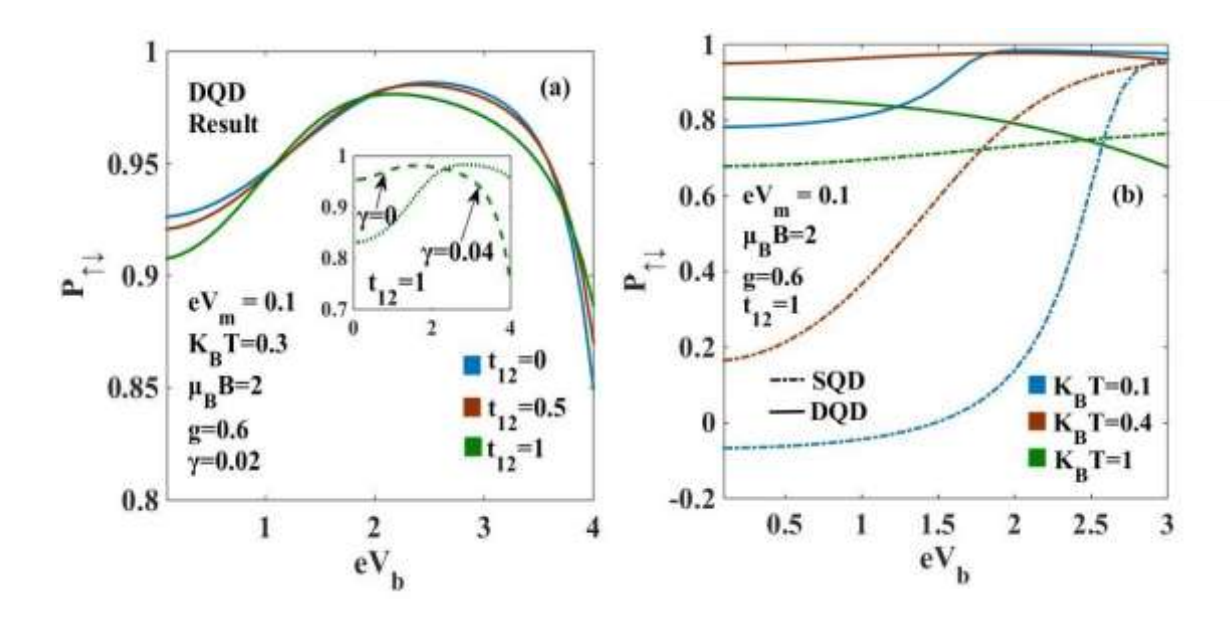


Fig. 6.17: Spin-Polarization $(P_{\uparrow\downarrow})$ with respect to the bias-voltage (eV_b) for different values of the tunnelling coefficient (t_{12}) and (b) temperature (K_BT) .

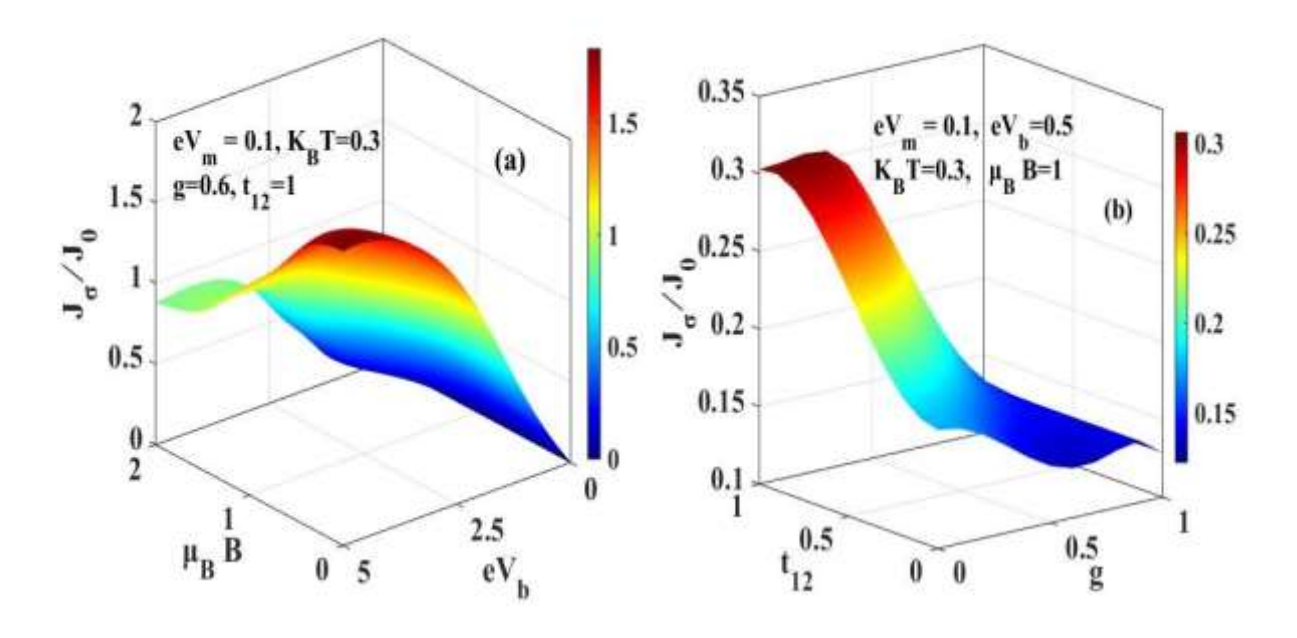


Fig. 6.18: 3D plot of the total tunnelling current (J_{σ}/J_0) (a) with respect to bias-voltage (eV_b) & magnetic field $(\mu_B B)$ with respect to QD tunnelling coefficient (t_{12}) & e-p interaction coefficient (g).

The effect of t_{12} on the spin-polarization $P_{\uparrow\downarrow}$ is studied in Fig. 6.17 (a). We find that as t_{12} increases, $P_{\uparrow\downarrow}$ reduces. The reason for this behaviour is not quite clear. The effect of temperature is interesting on $P_{\uparrow\downarrow}$ in BMT. Fig. 6.17 (b) shows that as T increases, initially the

spin-polarization is elevated due to the shifting in Fermi energy level. At a certain temperature, the system attains the maximum polarization and above that temperature, the spin-polarization starts decreasing. The combined effect of different parameters on the tunnelling current (J_{σ}/J_0) is studied in Fig. 6.18. In Fig. 6.18(a), J_{σ} is plotted with respect to the magnetic field and the bias voltage and the variation is much clearer in the 3D plot. Fig. 6.18(b) shows that J_{σ} increases with t_{12} at $K_BT=0.3$ and B=1 and with the e-p interaction coefficient, J_{σ} reduces.

The variation of differential conductivity G_{σ} is studied with respect to eV_b and t_{12} in a 3D plot in Fig. 6.19. We find that G_{σ} initially increases with the bias-voltage eV_b and after a certain value of eV_b , G_{σ} reduces but with t_{12} , it monotonically increase. The spin-resolved differential conductances G_{\uparrow} and G_{\downarrow} are plotted in Fig. 6.19 with respect to the magnetic field and temperature. Both the spin-resolved conductances are found to be maximum at low temperature and high magnetic field limit.

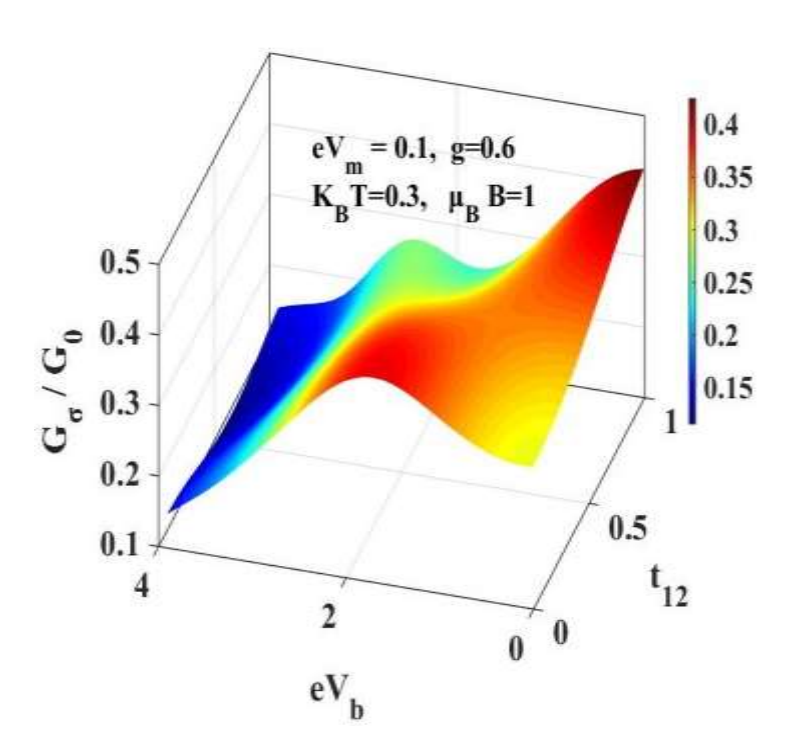


Fig. 6.19: 3D plot of the differential conductance (G_{σ}/G_0) (a) with respect to biasvoltage (eV_b) & the QD tunnelling coefficient (t_{12}) .

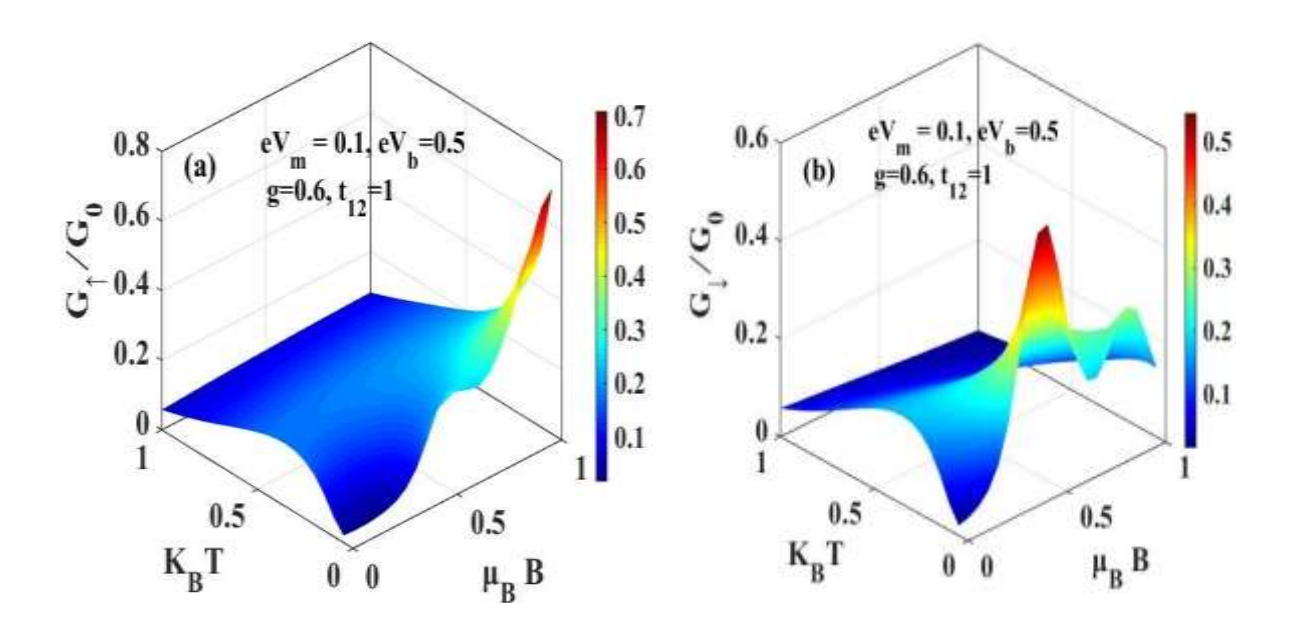


Fig. 6. 20 Spin-resolved differential conductance (a) G_{\uparrow}/G_0 & (b) G_{\downarrow}/G_0 with respect to the magnetic field $(\mu_B B)$ and temperature $(K_B T)$.

6.4 Conclusion

In the present work, two QDs are connected in series and placed between two metallic leads in the presence of an external magnetic field and the whole system is mounted on an insulating substrate which is further attached to a gate. An external bias voltage and a gate voltage is applied to the system. The system has been studied by the Anderson-Holstein-Caldeira-Leggett model and the tunnelling current calculated using the Keldysh non-equilibrium Green function method. The spectral function is studied with respect to the phonon frequency and it has been observed that the spectral function increases as the hopping coefficient between the QDs increases. The external magnetic field splits the spectral function peaks and the polaron side bands are increased with the phonon frequency. The tunnelling current is found to increase with the bias voltage and the QD tunnelling coefficient. The differential conductance is found to be symmetric with respect to the bias voltage, though the spin-resolved quantity is not. It has been found that the tunnelling current and differential conductance are higher in the high-magnetic field and low-temperature regime. The spin-polarization parameter reduces with the QD tunnelling coefficient and at low bias voltage, the spin-polarization increases with the e-p interaction and the magnetic

field. For BMT, we obtain the maximum spin-polarization for a high magnetic field and strong e-p coupling limit.

6.5 References

- [1] Park, H. et al., Nature **407**, 57–60 (2000).
- [2] Liang, W., Shores, M. P., Bockrath, M., Long, J. R. & Park, H., Nature **417**, 725–729 (2002).
- [3] Goldhaber-Gordon, D. et al., Nature **391**, 156–159 (1998).
- [4] Goldhaber-Gordon, D. et al., Phys. Rev. Lett. 81, 5225–5228 (1998).
- [5] L. H. Yu, D. Natelson, Nano Lett. 4, 79–83 (2003).
- [6] Z. Z. Chen, H. Lu, R. Lü, B. F. Zhu, J. Phys.: Condens. Matter 18, 5435–5446 (2006).
- [7] G. Gonzalez, M. N. Leuenberger, E. R. Mucciolo, Phys. Rev. B 78, 054445–12 (2008).
- [8] Pipit, U. V., A. Yasuo, S. Masanori, T. Toshiharu, M. Yutaka, Mater. Res. Express 4, 024004 (2017).
- [9] H. B. Heersche, Z. de Groot, J. A. Folk, H. S. J. van der Zant, C. Romeike, M. R. Wegewijs, L. Zobbi, D. Barreca, E. Tondello and A. Cornia, Phys. Rev. Lett., **96**, 206801 (2006).
- [10] A. S. Zyazin, J. W. G. van den Berg, E. A. Osorio, H. S. J. vander Zant, N. P. Konstantinidis, M. Leijnse, M. R. Wegewijs, F. May, W. Hofstetter, C. Danieli and A. Cornia, Nano Lett., **10**, 3307 (2010).
- [11] E. Burzuri', A. S. Zyazin, A. Cornia and H. S. J. van der Zant, Phys. Rev. Lett., **109**, 147203 (2012).
- [12] Makoto Yamamoto, Yasuo Azuma, Masanori Sakamoto, Toshiharu Teranishi, Hisao Ishii,

Yutaka Majima & Yutaka Noguchi, Sci. Rep. 7, 1589 (2017).

- [13] Abdelghafar, N., Aïmen, B., Bilel, H., Wassim, K. & Adel, K. IEEE Sens. J. 18, 1558 (2018).
- [14] Datta, S. Electronic Transport in Mesoscopic Systems (Cambridge University Press, 1997).
- [15] S. Datta. Quantum Transport Atom to Transistor (Cambridge University Press, Cambridge, 2005).
- [16] Mickael, L. P., Enrique, B. & van der Zant, H. S. J., Chem. Soc. Rev. 44, 902 (2015).

- [17] Huanyan Fu, Xin Zhu, Peihui Li, Mengmeng Li, Lan Yang, Chuancheng Jia and Xuefeng Guo, J. Mater. Chem. C, **10**, 2375 (2022).
- [18] C.S. Lau et al., Nano Lett. 16, 170-176 (2016).
- [19] Y. Li, J. A. Mol, S. C. Benjamin, G. A. Briggs, Sci. Rep. 6, 33686 (2016).
- [20] Z. Zhang, F. Yin, C. Wang, Z. Li, H. Liu, J. Phys. Condensed Matter 33, 235302 (2021).
- [21] N. Roch, S. Florens, V. Bouchiat, W. Wernsdorfer, F. Balestro, Nature 453, 633-637 (2008).
- [22] J. Hwang, M. Pototschnig, R. Lettow, G. Zumofen, A. Renn, S. Gotzinger, V. Sandoghdar, Nature 460, 76-80 (2009).
- [23] S. Richter et. Al., Adv. Mater. 30, 1706941 (2018).
- [24] K. Yoshida, K. Shibata, K. Hirakawa, Phys. Rev. Lett., 115, 138302 (2015).
- [25] K. S. Kwok and J.C. Ellenbogen, Mater. Today 5, 2, 28-37 (2002).
- [26] P. T. Mathew and F. Fang, Engineering 4, 760–771 (2018).
- [27] Jeon, G. S., Park, T. H. & Choi, H. Y., Phys. Rev. B 68, 045106 (2003).
- [28] Z. Z. Chen, R. Lu, B. F. Zhu, Phys. Rev. B. **71**, 165324 (2005).
- [29] Song, J., Sun, Q. F., Gao, J. & Xie, X. C., Phys. Rev B. **75**, 195320 (2007)
- [30] Narasimha Raju, Ch., A. Chatterjee, Sci. Rep. 6, 18511 (2016).
- [31] A. Khedri, T. A. Costi, V. Meden, Phys. Rev. B 96, 195155 (2017).
- [32] A. Khedri, T. A. Costi, V. Meden, Phys. Rev. B 96, 195156 (2017).
- [33] M. Kalla, Narasimha Raju, Ch., A. Chatterjee, Sci. Rep. 9, 16510 (2019).
- [34] Lundin, U., & McKenzie, R. H., Phys. Rev B 66, 075303 (2002).
- [35] M. Kalla, Narasimha Raju, Ch., A. Chatterjee, Sci Rep. 11, 10458 (2021).
- [36] K. Bhattacharyya, M. Kalla, A. Chatterjee (communicated)
- [37] Y. Meir, N. S. Wingreen, P. A. Lee, Phys. Rev. Lett. 70, 2601 (1993).
- [38] N. S. Wingreen, Y. Meir, Phys. Rev. B 49, 11040 (1994).
- [39] A. Mitra, I. Aleiner, A. J. Millis, Phys. Rev. B 69, 245302-21 (2004).
- [40] A. C. Hewson, D. J. Meyer, Phys. Cond. Matter **14**, 427 (2002).
- [41] Song, J., Sun, Q. F., Gao, J. & Xie, X. C. Phys. Rev B. **75**, 195320 (2007).
- [42] Khademhosseini V, Dideban D, Ahmadi MT, Heidari H., Carbon Nanotube and Fullerene. Molecules, **27(1)**:301 (2022).
- [43] F. Abualnaja et al., Phys. Rev. Applied **12**, 064050 (2019).
- [44] E. C. Siqueira, G. G. Cabrera, Journal of Applied Physics 111, 113905 (2012).
- [45] H. K. Sharma, M. Kalla, A. Chatterjee (to be communicated).

- [46] P. W. Anderson, Phys. Rev. 124, 41 (1961).
- [47] T. Holstein, Ann. Phys. (N. Y.) 8, 325 (1959).
- [48] A. O. Caldeira, A. J. Leggett, Physica A 121, 587 (1983).
- [49] A. O. Caldeira, A. J. Leggett, Annals of Physics 149, 374 (1983).
- [50] L. Keldysh, Sov. Phys. JETP 20, 1018 (1965).
- [51] I. G. Lang and Y. A. Firsov, Sov. Phys. JETP 16, 1301 (1962).

"There are very few things that can be proved rigorously in condensed matter physics"... Anthony James Leggett

7

Conclusion

In the present thesis, titled "Electronic and transport properties of the low dimensional systems", we have studied the nature of SDW-CDW transition and the self-trapping transition in a correlated polar system.

In Chapter 1, we have described the basic models and motivations towards the thesis.

In **Chapter 2**, we have studied the SCW-CDW transition in a 1D Holstein-Hubbard model with Gaussian phonon anharmonicity using a more accurate variational calculation than the ones used earlier. Performing a series of canonical transitions followed by a generalized many phonon state, we have obtained an effective electronic Hamiltonian which we have finally solved using the Bethe ansatz technique. Our results suggest a wider metallic phase at the crossover region of the SDW and CDW phases.

In **Chapter 3**, we have considered a 2D Holstein-Hubbard model and examined the nature of the CDW-SDW transition in this model. We have treated the phonon sub-system of this problem in the same way as in Chapter 1. Since the effective electronic Hamiltonian in this case does not admit an exact solution, we have solved the effective electronic problem in the weak correlation regime and the strong correlation regime separately. In the weak Coulomb correlation regime, the effective electronic Hamiltonian has been solved using the mean-field Hartree-Fock method. In the strong correlation regime, the effective electronic Hamiltonian has been first transformed to the t-J model which has then been solved using the Gutzwiller

approximation and the Zubarev technique. Combining the results from two different regimes, we have plotted the phase diagram with respect to the e-e and e-p interaction strengths and obtained the intermediate metallic region. The intervening metallic phase is found to be wider than the result for the corresponding 1D case.

Another phase transition in the Holstein-Hubbard model is the self-trapping (ST) transition. We have studied the nature of the ST transition in the extended Holstein-Hubbard model in 1D in **Chapter 4**. Here we have used same method as in Chapter 2 and have shown that as the e-p interaction is increased, the polaron undergoes a transition from a large polaron to a small polaron in a continuous way.

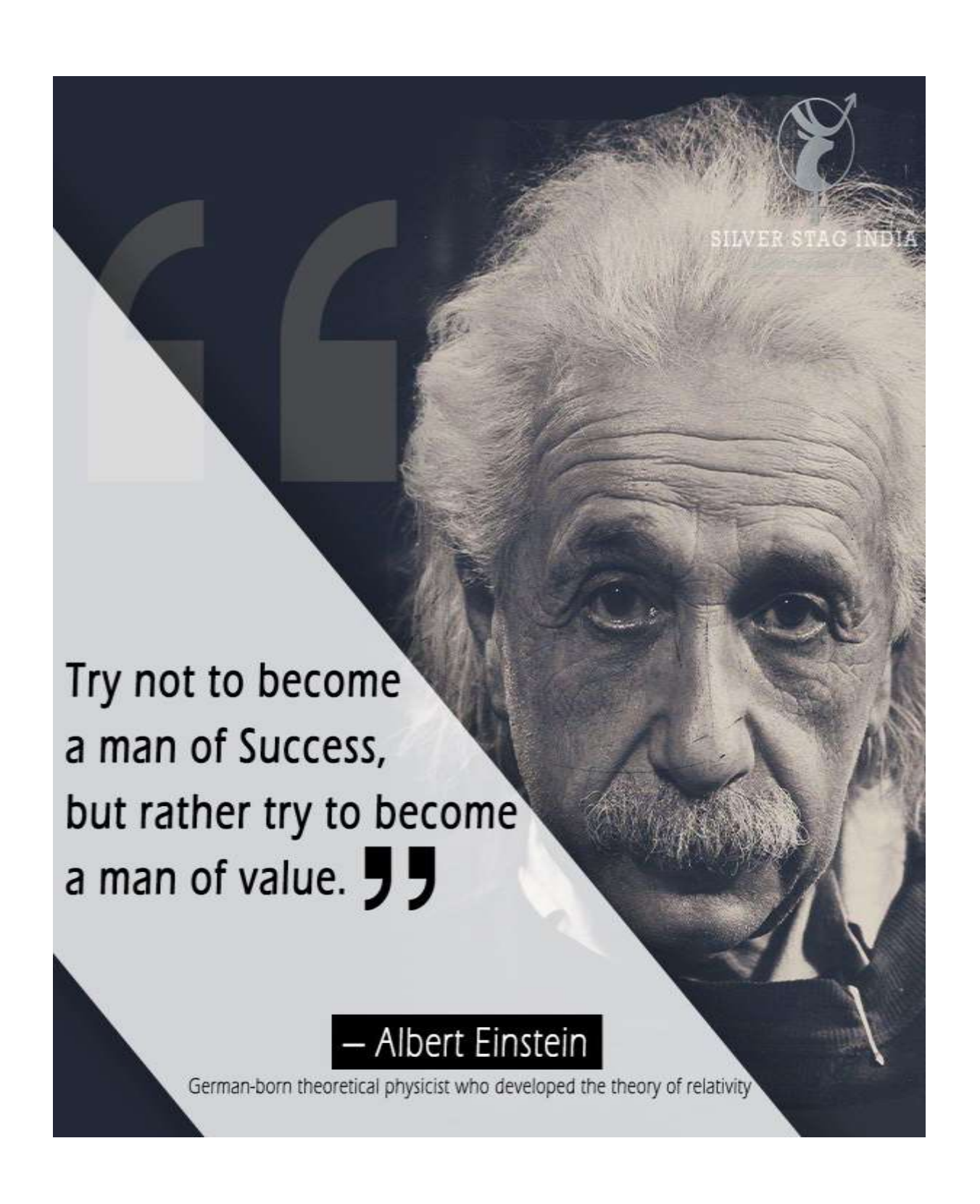
In **Chapter 5**, we have examined the nature of the ST transition in a 2D Holstein-Hubbard model using the same method as used in Chapter 3. We have shown that the ST transition is continuous in the anti-adiabatic regime, but it shows sharp discontinuity for the adiabatic case.

In **Chapter 6**, we have studied temperature dependent magneto-transport in a bi-molecular transistor in the presence of e-e and e-p interactions and quantum dissipation. The system has been modelled by the Anderson-Holstein-Caldeira-Leggett model and the spectral function, tunnelling current and differential conductance are calculated using the non-equilibrium Keldysh Green function technique. Our results show that the tunnelling current in a bi-molecular transistor is higher than that in single molecular transistor in the high magnetic field and low temperature regime.

[&]quot;The physics is theoretical, but the fun is real"... I hope you have enjoyed reading the thesis.

"Physics isn't the most important thing.

Love is"...Richard Feynman



Electronic and Transport Properties of Low Dimensional Systems

by Debika Debnath

Librarian

Indira Gandhi Memorial Library UNIVERSITY OF HYDERABAD

Central University P.O. HYDERABAD-500 046

Submission date: 31-Jan-2023 03:18PM (UTC+0530)

Submission ID: 2003235009

File name: Debika Debnath.pdf (2.49M)

Word count: 30631

Character count: 143672

Electronic and Transport Properties of Low Dimensional Systems

ORIGINALITY REPORT

36% SIMILARITY INDEX

20%

INTERNET SOURCES

35%

PUBLICATIONS

3%

STUDENT PAPERS

PRIMARY SOURCES

Debika Debnath, Kuntal Bhattacharyya, Ashok Chatterjee. "A semi-exact study of self-trapping transition in a one-dimensional Holstein-Hubbard model", Physica B:

Publication

WWW.nature.com percentage is from Internet Source students our publication.

Prof.

9%

Debika Debnath, M. Zahid Malik, Ash Charles of Physical Chatterjee. "A semi exact solution for a metallic phase in a Holstein-Hubbard chain at half filling with Gaussian anharmonic phonons", Scientific Reports, 2021

Prof. ASKON CHATTERIES.
SCHOOL OF PHYSICS
SCHOOL OF THY DECLARATION OF THE SHOP OF THE SHO

Submitted to University of Hyderabad,
Hyderabad
Student Paper

1 %

5 mafiadoc.com
Internet Source

repository. sustech. edu is 36% out of which 29%. The total similarity index is sufficient in Dillications. Thus the student's own publications. Thus the is from the student's own publications which is within the effective similarity index is 7% which is within the effective similarity formissible limit of 10%. It still

Debika Debnath, Ashok Chatterjee. "Mott-Insulator to Peierls Insulator Transition in the Two-Dimensional Holstein-Hubbard Model", Materials Today: Proceedings, 2022

<1%

Publication

M Zahid Malik, Ashok Chatterjee. "An intervening metallic phase at the CDW–SDW transition region in the one-dimensional Holstein-Hubbard model at half filling: a semi-exact solution", Journal of Physics Communications, 2020

<1%

Publication

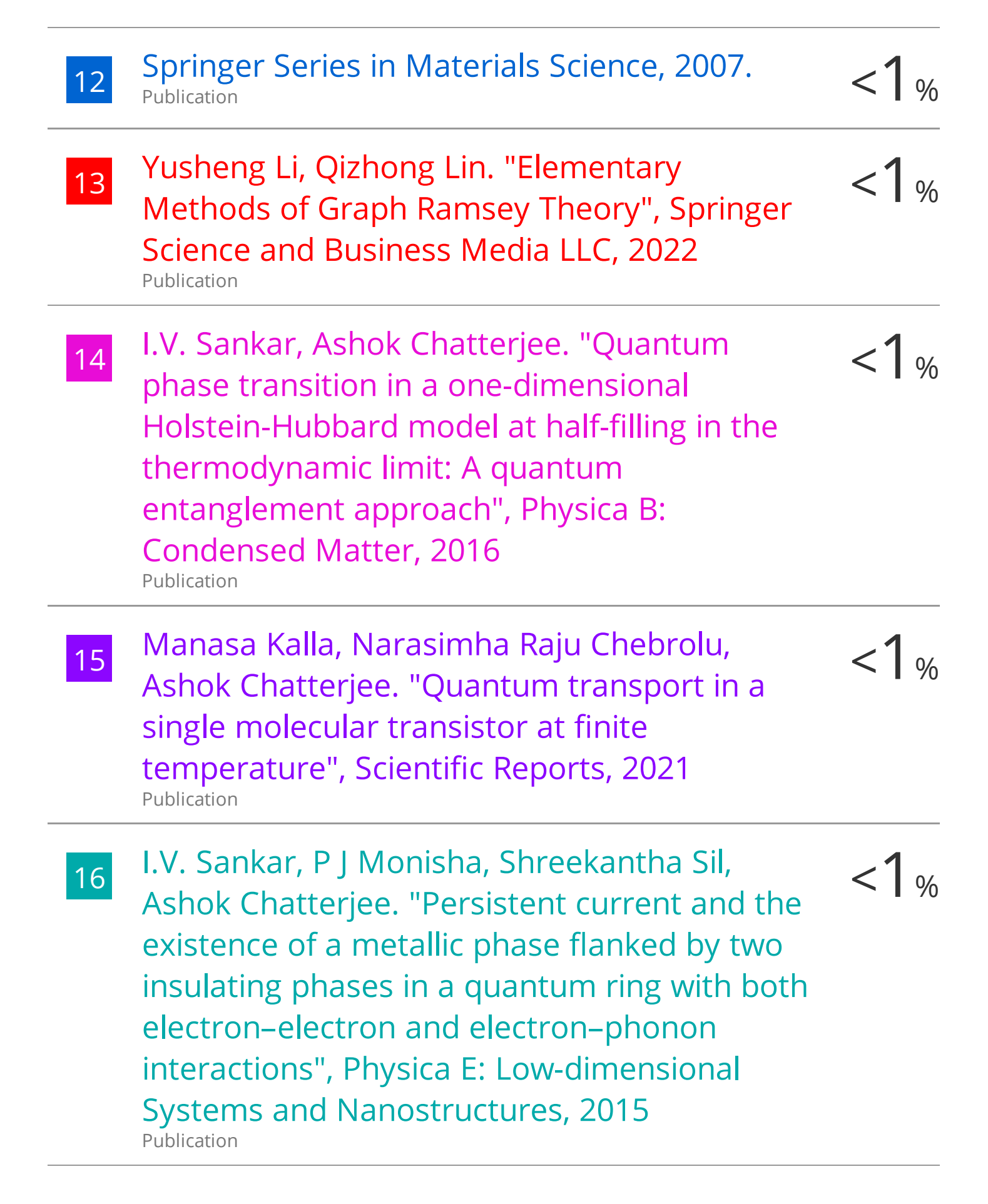
Ashok Chatterjee. "Existence of an Intermediate Metallic Phase at the SDW-CDW Crossover Region in the One-Dimensional Holstein-Hubbard Model at Half-Filling", Advances in Condensed Matter Physics, 2010 Publication

<1%

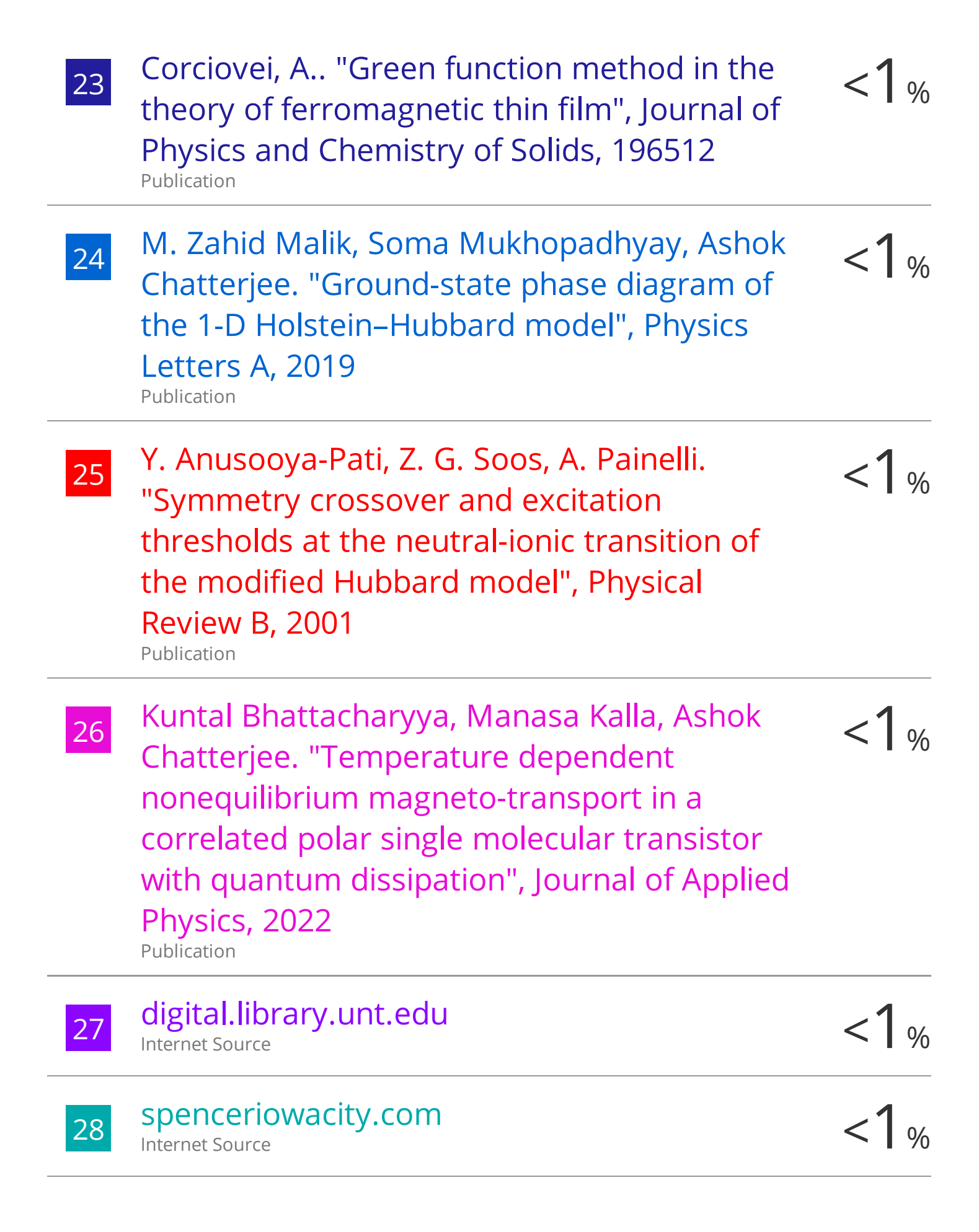
M. Zahid Malik, Ashok Chatterjee. "Quantumentanglement entropy and double occupancy in a 1-D Holstein-Hubbard model at halffilling", Physica E: Low-dimensional Systems and Nanostructures, 2021

<1%

Publication



17	Manasa Kalla, Ch. Narasimha Raju, Ashok Chatterjee. "Magneto-transport properties of a single molecular transistor: Anderson- Holstein-Caldeira-Leggett model", AIP Publishing, 2019	<1%
18	Miodrag L. Kulić. "Interplay of electron- phonon interaction and strong correlations: the possible way to high-temperature superconductivity", Physics Reports, 2000 Publication	<1%
19	irep.ntu.ac.uk Internet Source	<1%
20	Manasa Kalla, Narasimha Raju Chebrolu, Ashok Chatterjee. "Magneto-transport properties of a single molecular transistor in the presence of electron-electron and electron-phonon interactions and quantum dissipation", Scientific Reports, 2019 Publication	<1%
21	T. S. Müller, W. Töws, G. M. Pastor. "Recent Progress in Lattice Density Functional Theory", Computation, 2019	<1%
22	tak.ram.ne.jp Internet Source	<1%



29	Nonequilibrium Physics at Short Time Scales, 2004. Publication	<1%
30	Submitted to University of South Australia Student Paper	<1%
31	Ajay, R.S. Tripathi. "Role of interlayer interactions on transition temperature in high-Tc cuprate superconductors", Physica C: Superconductivity, 1997 Publication	<1%
32	Ch Uma Lavanya, Ashok Chatterjee. "Persistent charge and spin currents in the 1D Holstein-Hubbard ring at half filling and at away from half filling by Bethe-ansatz approach", Physica E: Low-dimensional Systems and Nanostructures, 2021 Publication	<1%
33	I.V. Sankar, Soma Mukhopadhyay, Ashok Chatterjee. "Localization–delocalization transition in a two-dimensional Holstein– Hubbard model", Physica C: Superconductivity, 2012	<1%
34	Submitted to Middle East Technical University Student Paper	<1%
35	Quantum Noise in Mesoscopic Physics, 2003.	<1%



Sander van Smaalen. "Calculations of transfer integrals for tetracyanoquinodimethane salts", Physical Review B, 06/1985

<1%

Publication

Exclude quotes On Exclude matches < 14 words

Exclude bibliography On